THE THERAPEUTIC ROLE OF FOLLISTATIN IN CHRONIC KIDNEY DISEASE

MOLECULAR REGULATION OF FOLLISTATIN BY CAVEOLIN-1 IN GLOMERULAR MESANGIAL CELLS AND ITS THERAPEUTIC POTENTIAL IN CHRONIC KIDNEY DISEASE

By

Neel Mehta, Hon BSc, MSc

A Thesis submitted to the School of Graduate Studies in Partial Fulfillment of the Requirements for the Degree of Doctor of Philosophy

DOCTOR OF PHILOSPOHY (2019) McMaster University

Medical Sciences, Blood and Vasculature Hamilton, Ontario

TITLE: Molecular Regulation of Follistatin by Caveolin-1 in Glomerular Mesangial Cells and its Therapeutic Potential in Chronic Kidney Disease

AUTHOR: Neel Mehta, HBSc (University of Toronto), MSc (University of Toronto)

SUPERVISOR: Dr. Joan Krepinsky, BSc, MSc, MD, FRCPC, Professor, Division of Nephrology, Department of Medicine

SUPERVISORY COMMITTEE: Dr. Thomas Hawke, Dr. Kjetil Ask, Dr. Carl Richards.

NUMBER OF PAGES: xiii, 248

Lay Abstract

Chronic kidney disease results from excessive fibrosis (scarring) within the kidneys. The goal of this thesis is to understand the molecular mechanisms involving the regulation of an antifibrotic protein, follistatin, in glomerular mesangial cells and to identify its therapeutic potential in chronic kidney disease. This thesis has identified that follistatin, an endogenous inhibitor of the profibrotic cytokine activin A, is regulated transcriptionally by Sp1 and post-transcriptionally by microRNA299a-5p. Furthermore, this thesis has demonstrated that exogenous recombinant follistatin administration protects against the progression of chronic kidney disease and that microRNA299a-5p targeting may be an alternative approach to block renal fibrosis. These studies collectively show that follistatin is an effective treatment for the management of chronic kidney disease.

Abstract

Chronic kidney disease (CKD) is a major cause of morbidity and mortality, affecting more than 10% of the world's population. CKD is associated with excessive renal fibrosis, which leads to declining kidney function and eventual kidney failure. In CKD, glomerular mesangial cells (MC), resident fibroblasts and tubular epithelial cells undergo phenotypic activation and transition in response to profibrotic and proinflammatory cytokines such as transforming growth factor β1 (TGFβ1). These activated renal cells excessively produce extracellular matrix (ECM) proteins that replace functional renal tissue and lead to renal fibrosis. Caveolae are small omega-shaped invaginations of the plasma membrane that mediate signaling transduction events. Formation of caveolae require the protein caveolin-1 (cav-1). We have previously shown that the ability of MC to produce matrix proteins is dependent on cav-1 expression. Unfortunately, clinically targeting cav-1 within the kidneys, specifically within MC, is technically challenging and as of yet unfeasible. Thus, to better understand how cav-1 deletion is protective, we carried out a microarray screen comparing cav-1 wild-type (WT) and knockout (KO) MC. Here, we discovered significant up-regulation of a TGFβ superfamily inhibitory protein, follistatin (FST). FST specifically targets and neutralizes activin A (ActA) but not TGFβ1. TGFβ1 and ActA both belong to the TGFβ superfamily of cytokines and growth factors. While TGFβ1 itself is a known key mediator of renal fibrosis, therapies aimed at directly inhibiting TGFβ1 in kidney diseases have not been successful due to opposing profibrotic and anti-inflammatory effects. ActA has been shown to act as a strong profibrotic and proinflammatory agent in various organs,

including the lungs and liver. We along with others have observed elevated levels of ActA within the kidneys and serum of mice and humans with CKD. Functionally, ActA has been shown to contribute to ECM production in the kidneys. Hence, we hypothesized that ActA inhibition through FST could prove beneficial in CKD. In this thesis, our first study elucidated a novel molecular pathway by which cav-1 regulates expression of the FST in MC. Our results indicate that FST is negatively regulated by cav-1 through a PI3K/PKC zeta/Sp1 transcriptional pathway. Our second study expands on these findings and tests whether exogenous FST administration protects against the progression of CKD in a surgical mouse model of CKD. Here, we discovered that FST acts as a reactive oxygen species (ROS) scavenger and that exogenous administration of FST protects against the development of CKD through the inhibition of renal fibrosis and oxidative stress. Lastly, our third study determined whether microRNAs (miRNAs) are implicated in post-transcriptionally regulating FST through cav-1 and whether these FST-targeting miRNAs can be utilized therapeutically to protect against the development and progression of CKD. Here, we determined that a FST-targeting miRNA, microRNA299a-5p, is significantly downregulated in cav-1 deficient MC, upregulated *in vivo* in a mouse model of CKD and that its inhibition, *in vitro* and *in vivo* protects against the accumulation of ECM proteins and renal fibrosis. These studies collectively suggest that FST is an effective therapeutic option for the management of CKD.

Acknowledgments

Firstly, I would like to thank Dr. Joan Krepinsky for providing me with the opportunity and resources to carry out my doctoral studies in her laboratory. Her day-to-day assistance, sound advice, and tremendous knowledge in the field of nephrology allowed me to develop and fine-tune key scientific research skills that will aid me well into the future. I would like to thank the graduate and undergraduates students of the Krepinsky lab for providing me with technical assistance and support while fostering a stimulating and collaborative working environment. I would like to thank all of our collaborators and contributors that have provided us with vital reagents that have allowed us to conduct some of the experiments within this thesis. I sincerely thank Drs. Thomas Hawke, Kjetil Ask and Carl Richards for having genuine interest in serving on my PhD supervisory committee and thoughtfully critiquing and advancing my research. I would also like to thank Dr. Hai-Ying Mary Cheng, my MSc supervisor, who introduced me to basic science research and equipped me with the skills and necessary mindset that enabled me to carry out my doctoral work. Finally, I would like to thank my family for having tremendous patience and the capacity of supporting me throughout this journey.

Preface

This is a “sandwich” style thesis. Chapter 1 is a general introduction that provides an overview of basic concepts that are relevant to this thesis. Chapters 2 and 3 have been published in a peer-reviewed journal. Chapter 4 is presented as manuscript being prepared for submission in a peer-reviewed journal. A preface is presented at the beginning of each chapter. It describes the work performed and the contributions of all authors involved in the study. Chapter 5 is a general discussion that collectively summarizes and analyzes all of the data presented, providing key limitations and future directions.

Table of Contents

Summary of Figures

Summary of Tables

List of Abbreviations

2',7'–dichlorofluorescin diacetate = H_2DCFDA
3' untranslated region = 3'UTR
5/6 nephrectomy = 5/6 Nx

8-OHdG = 8-hydroxy-2' -deoxyguanosine
Activin A = ActA
Activin B = ActB
Activin Type I Receptor = ActRI
Activin Type II Receptor = ActRII
Caveolin-1 = Cav-1
Chronic kidney disease = CKD
Cycloheximide = CHX
Endoplasmic reticulum = ER
End Stage Renal Disease = ESRD
Follistatin = FST
Glomerular Filtration Rate = GFR
Heparin binding sequence = HBS
Hydrogen peroxide = H2O2
Immunoglobulin G = IgG
Knockout = KO
Mesangial cells = MC
microRNA = miRNA
microRNA regulatory element = MRE
NAD(P)H oxidase = Nox
Nuclear localization signal = NLS
Phosphatase and tensin homolog = PTEN
Phosphatidylinositol 3,4,5-trisphosphate = PIP3
Phosphatidylserine = PS
Phosphoinositide 3-kinase = PI3K
Phosphoinositide-dependent protein kinase-1 = PDK-1
Pleckstrin homology = PH
Protein kinase C zeta = PKCζ
Quantitative real-time PCR = qRT-PCR
Reactive oxygen species = ROS
Serine/threonine = ser/thr
Small mothers against decapentaplegic = Smad
Superoxide = SO
Thapsigargin = Tg
Transcription start site = TSS
Transforming growth factor beta = TGFβ
Tryptophan = Trp
Unfolded protein response = UPR
Wheat germ agglutinin = WGA
Wild-type = WT

Chapter 1: Introduction

1.1 Kidney Anatomy and Physiology

The kidneys play a central role in maintaining organismal homeostasis [1]. They carry out several functions that are important for survival [1]. These include but are not limited to producing and excreting waste in the form of urine, reabsorbing key nutrients and ions such as glucose, water and sodium, fine-tuning blood pressure, producing and secreting hormonal and vasoactive compounds such as renin, calcitriol and erythropoietin, and maintaining pH through acid-base homeostasis [1].

Figure 1-1 illustrates the general anatomy of a mammalian kidney. The functional units of the kidneys are the nephrons [2]. In a human kidney, there are approximately one million nephrons [2]. A nephron consist of a renal corpuscle that is attached to the collecting duct and ureter via a tubular system [2]. The renal corpuscle is the blood-filtering component of the nephron [2]. It consists of a tuft of specialized capillaries composed of fenestrated endothelial cells, known as the glomerulus (Fig. 1-2) [2]. Within the renal corpuscle, afferent arterioles arising from the cortical radial arteries at the beginning of a nephron supply blood to the glomerular tufts of the renal corpuscle [2]. Similarly, the efferent arterioles drain the glomeruli [2]. The specific filtration component of the glomerulus consists of visceral epithelial cells known as podocytes and the fenestrated endothelial cells, which are surrounded by a specialized extracellular matrix structure known as the glomerular basement membrane (Fig. 1-2) [3]. The finger-like foot processes of podocytes and the fenestrated endothelium are responsible for charge and size selective filtration of components from the blood (Fig. 1-2) [3]. Finally, the glomerular capsule known as Bowman's capsule feeds the filtered blood, also known as

plasma filtrate or capsular urine, into the tubular system (Fig. 1-2) [2]. The amount of filtrate produced by the glomeruli can be measured and quantified as the glomerular filtration rate (GFR). GFR specifically estimates how much volume of fluid passes through the glomeruli per unit of time and thus is a marker for kidney function.

Lastly, the tubular part of the nephron consists of proximal and distal tubules that are connected by a loop of Henle, which is responsible for further processing and excretion of urine through the collecting duct and ureter [2].

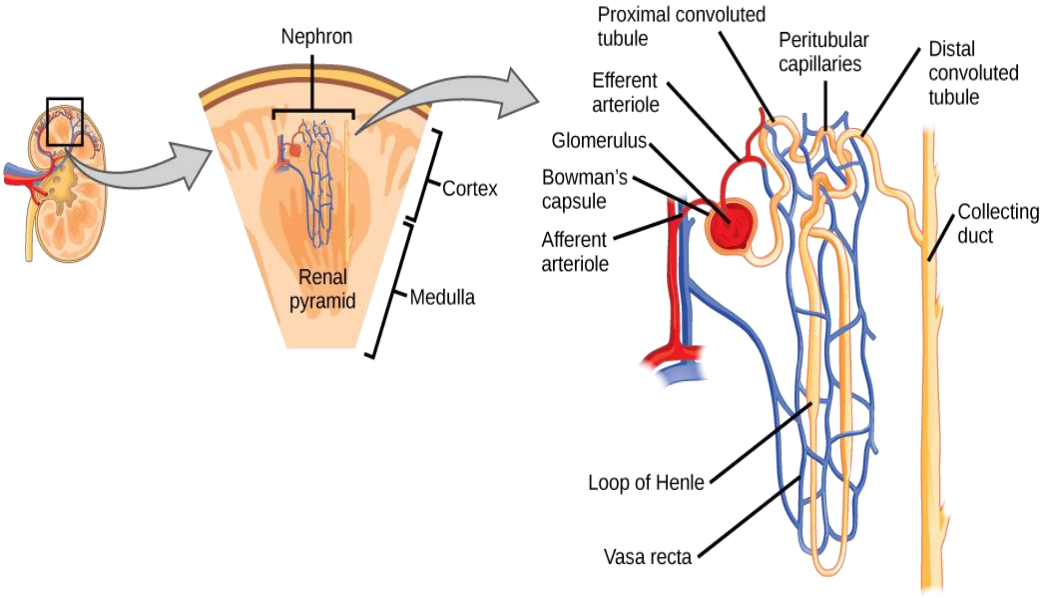

Figure 1-1. General anatomy of the kidneys and the nephron.

Nephrons are the functional units of the kidney. Glomeruli, located with the cortex, are responsible for filtering the blood. The proximal and distal convoluted tubules are involved in the exchange of ions and nutrients from the filtrate, which helps to maintain pH and electrolyte balance in the blood. The loop of Henle further processes the filtrate, primarily exchanging water, along with sodium and chloride ions. The collecting duct reabsorbs solutes and water from the filtrate, forming urine, which is then excreted by the ureter (ureter not shown). Unmodified image taken from http://bio1520.biology.gatech.edu/nutrition-transport-and-homeostasis/animal-ion-and-water-regulation-ii/ https://creativecommons.org/licenses/by-nc-sa/3.0/

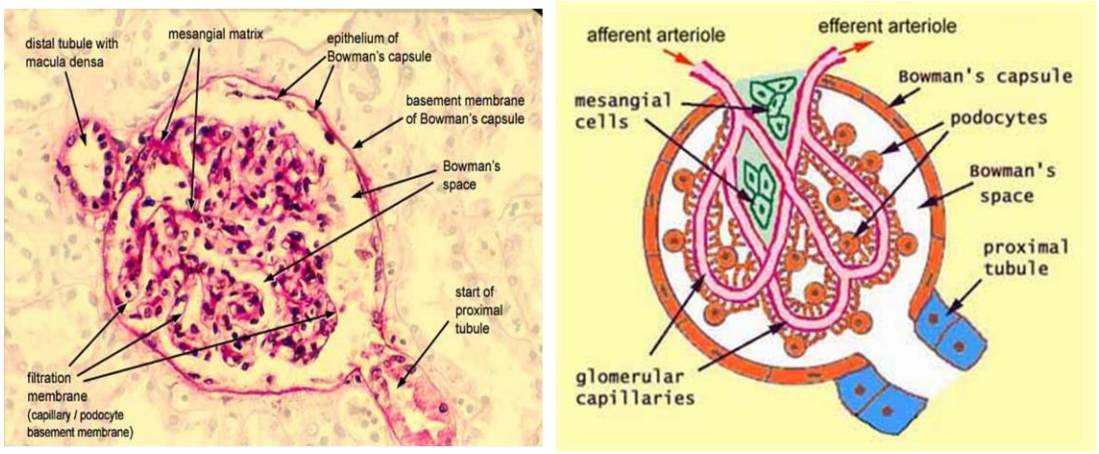

Figure 1-2. General anatomy of the glomerulus and its resident cell types.

Periodic acid–Schiff staining (left) and cartoon (right) of a glomerulus highlighting the localization of the glomerular mesangial cells and their secreted mesangial matrix (shaded as the green area in the cartoon). Podoctyes, the fenestrated endothelium and their common basement membrane make up the filtration membrane. The filtrate collects in the bowman's space on its way through the proximal tubular system of the kidney.

Unmodified images taken from: http://www.siumed.edu/~dking2/index.htm.

1.2 Chronic Kidney Disease

Chronic kidney disease (CKD) affects virtually every organ system in the body [4–7]. It is a major cause of morbidity and mortality [4–7]. CKD is clinically defined by structural and functional abnormalities within the kidneys that persist for more than three months [4–7]. This is associated with an estimated GFR of less than 60 ml/min/1.73m^2 in humans, and/or with the presence kidney damage markers in the urine such as proteins (primarily albumin), which is clinically referred to as albuminuria (Fig. 1-3) [4–7]. CKD is pathologically characterized by excessive renal fibrosis, which over time results in declining kidney function [4–7].

The prevalence of CKD is positively associated with age and with the presence of hypertension and diabetes [4–7]. Worsening CKD has also been positively associated with accelerated risk of cardiovascular disease and mortality [6,8,9]. In CKD, the progressive decay in kidney function ultimately sets the stage for end-stage renal disease (ESRD), a point in time at which dialysis and/or kidney transplantation are the only means of survival [4]. Dialysis and kidney transplantation are not always effective and more importantly are not preventative. They pose substantial healthcare and economic burdens, with current annual costs being estimated to be around $33 billion in the US [10]. CKD is currently reported to affect more than 10% of the world's population [6,9]. By 2030, it is estimated to affect more than 15% of adults in the world [6,9]. Thus, there are pronounced economic and healthcare benefits that can be obtained from the identification of novel therapeutics that can be used to prevent and/or reverse CKD progression.

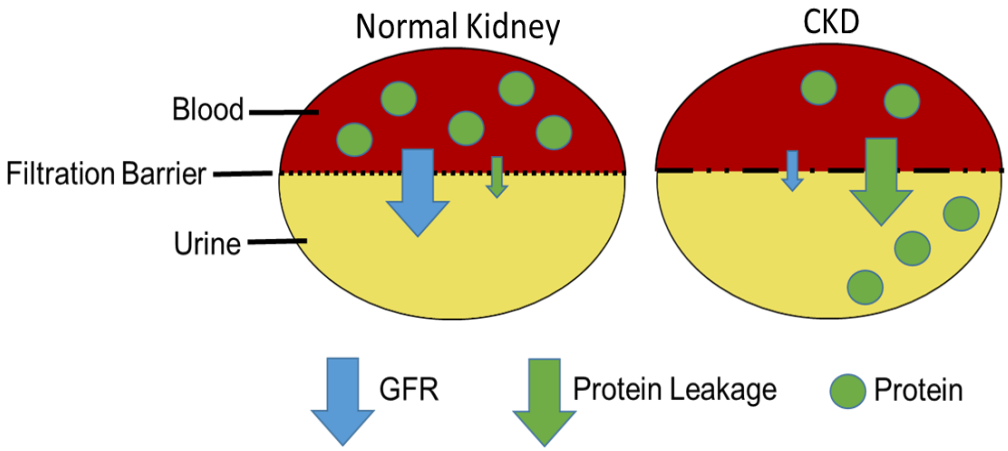

Figure 1-3. GFR and albuminuria in CKD.

CKD is defined by a decrease in GFR, which is the amount or rate of blood that is filtered by the kidneys (blue arrow), and by the presence of proteins (primarily albumin) in the urine (green arrow).

1.2.1 Renal Fibrosis

Renal fibrosis is the final common pathway in CKD and a strong correlate of its progression [11–14]. Renal fibrosis is characterized by the accumulation of extracellular matrix (ECM) proteins such as fibronectin and collagen within the glomerulus, referred to as glomerulosclerosis, and in the tubulointerstitial space, referred to as tubulointerstitial fibrosis (Fig. 1-4) [11–13,15,16]. A multitude of events are involved in the development of renal fibrosis in CKD [4,5]. Primarily, sustained renal injury, coupled with cellular apoptosis, oxidative stress as a result of persistent activation of resident renal cells and immune cells, results in the excessive production of profibrogenic cytokines such as transforming growth factor-β1 (TGFβ1) and activin A (ActA) [17–20]. TGFβ1 has been heavily implicated in the pathogenesis of renal fibrosis [16–20]. In response to TGFβ1, glomerular MC, resident fibroblasts and tubular epithelial cells proliferate and undergo phenotypic activation and in turn excessively synthesize and release ECM proteins that eventually replace functional renal tissue with scar tissue and contribute to the declining renal function that is observed in CKD [11,14,19–21]. The role of ActA in promoting renal fibrosis is not as well established as TGFβ1 but recent research efforts suggest that it is indeed profibrotic and pathologic within the kidneys [22–28].

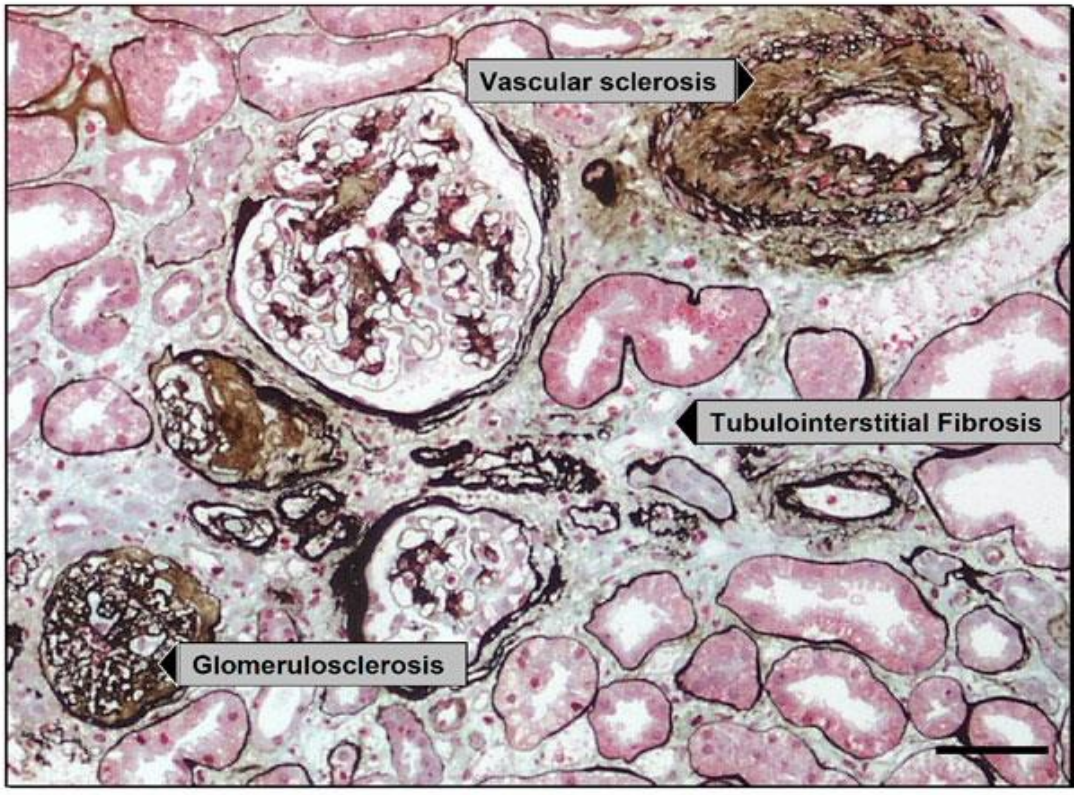

Figure 1-4. Renal fibrosis.

Silver methenamine/Masson trichrome stained kidney cross section illustrating glomerulosclerosis and tubulointerstitial fibrosis in ESRD (scale bar = 50 μm). Unmodified image taken from Hewitson TD (2012) [29].

1.2.2 Glomerular Mesangial Cells

The glomerulus is surrounded by an intercellular substance known as the mesangium [20,30,31]. This mesangial interstitial space is composed of mesangial cells (MC) and extracellular matrix [20,30,31]. Glomerular mesangial cells (MC) are specialized perivascular pericytes that are involved in the production and secretion of the mesangial matrix (Fig. 1-2) [19–21,30,31]. The mesangial matrix is primarily composed of collagens, laminin and fibronectin [19–21,30,31]. The mesangial matrix serves to anchor the MC to the glomerular basement membrane and provide structural support and integrity to the surrounding glomerular capillaries (Fig.1-2) [19–21] . However, activation and transition of MC to a myofibroblastic smooth-muscle-like phenotype has been established to be an early fibrogenic response in CKD [19,20]. Activated MC undergo hypertrophy and proliferation, while upregulating their matrix production [20,32]. This results in mesangial matrix expansion and glomerulosclerosis, which is a prominent finding in CKD (Fig. 1-4) [14,20,21].

Activated MC are also known to possess phagocytic properties similar to monocytes and macrophages, where they play a secretory role and act as a target sites for inflammatory mediators and profibrotic growth factors such as TGFβ1 [20]. MC also possess contractile properties, allowing them contract and relax in order to fine-tune GFR [33]. Here, as part of a negative feedback loop, MC undergo mechanical contraction in response to stretching of the glomerulus during increased intra-glomerular pressure [34–36]. MC also contract and relax in response to vasoactive agents such as angiotensin II and nitric oxide, respectively [34–36]. MC under mechanical stress also produce and

secrete profibrotic growth factors such as TGFβ1 [34–36]. Thus, glomerular MC play a critical role in the pathogenesis of glomerular fibrosis through numerous pathways and are a critical component involved in the loss of renal function in CKD [20,37,38].

1.2.3 Current Clinical Care for CKD

Clinical management of CKD is currently focused on minimizing the renal and cardiovascular risk factors through control of blood pressure, blood glucose and lipids along with emphasizing lifestyle changes through diet and exercise [9,39,40]. Even with proper management and stringent control of these parameters, the residual renal and cardiovascular risks remain high in patients with CKD [9,39,40]. Thus, the likelihood of progression to ESRD along with cardiovascular morbidity and mortality risks associated with CKD remain significantly high due to the relatively small absolute risk reductions along with the occurrence of severe adverse side effects that have been reported with some of these interventions [9,39,40]. No interventions as of now are able to inhibit and/or reverse the progression of CKD through ameliorating renal fibrosis. Thus, novel therapeutic approaches to reverse and/or halt the progression of CKD are needed.

1.3 Transforming Growth Factor Beta (TGFß) Superfamily: Activin A and TGFß1

The TGFβ superfamily consists of highly pleiotropic molecules including TGFβ1, activins, bone morphogenic proteins and growth differentiation factors [41]. They modulate the transcription of genes involved in critical developmental and physiological

processes such as inflammation, fibrosis, cell apoptosis, and proliferation [42–46]. TGFβ1 is the most abundant cytokine that can be produced by resident renal cells [41]. It is highly upregulated in CKD both in human patients and in animal disease models, where it serves as a primary promoter of renal fibrosis [41,42,47,48]. Canonically, active TGFβ1 binds to a constitutively active kinase (type II TGFβ1 receptor), which then recruits the type I TGFβ1 receptor and phosphorylates the downstream receptor-associated small mothers against decapentaplegic (Smad) proteins, Smad2 and Smad3 [41]. Phosphorylated Smad2 and Smad3 form an oligomeric complex with a Smad4, and translocates into the nucleus where it interacts with numerous co-activations and or repressors to regulate the transcription of target Smad-responsive genes [41]. Non-canonically, TGFβ1 also can signal through Smad-independent pathways, including p38, ERK, MAPK, Jun Kinase, Rho-GTPases and integrin linked kinases [41,49]. The importance of TGFβ1 in the development of renal fibrosis in kidney disease is well accepted and strongly supported using *in vivo* and *in vitro* studies [41,42,50]. Accordingly, TGFβ1 inhibition using TGFβ1 neutralizing antibodies, antisense TGFβ1 oligodeoxynucleotides, soluble human TβRII (sTβRII.Fc) and specific inhibitors to TβR kinases (GW788388 and IN-1130) all have been shown to effectively halt the progression of renal fibrosis in a number of experimental kidney disease models [41]. However, in clinical studies in humans with diabetic nephropathy and in patients with steroid-resistant focal segmental glomerulosclerosis, the use of monoclonal TGFβ1 neutralization antibodies have not shown improvements in renal fibrosis or in slowing the progression of kidney disease [51,52]. A major obstacle for specifically blocking TGFβ1 is hypothesized

to be related its anti-inflammatory and anti-tumorigenesis property [41,42,50,51]. Hence, inhibition of alternative TGFβ members might be a more viable and effective therapeutic approach in the treatment of fibrosis in kidney disease.

ActA, belonging to the TGF-ß superfamily of cytokines and growth factors, in addition to stimulating FSH secretion and in turn regulating the reproductive axis, is now being started to be appreciated as an autocrine and paracrine factor that is a prominent contributor to the profibrotic and inflammatory responses within the kidneys, liver and lungs in response to injury [22,45,46,53–58]. ActA are homodimers consisting of two inhibin ßA chains linked by disulphide bonds (Fig. 1-5) [45,56,57]. Similar to canonical TGFβ1 signaling, ActA signals through a heterodimeric complex of serine-threonine receptor kinases, consisting of type-I receptors (ALK4) and type-II receptors (ActRIIA or ActRIIB) with downstream signaling activation of Smad proteins resulting in the transcriptional activation of Smad responsive genes (Fig. 1-6) [45,57].

ActA is an important regulator of normal kidney development [59–61]. ActA expression is not seen in healthy adult kidneys [62,63]. Systemically circulating and renal localized ActA is induced during the early stages of CKD in humans, in rat tubules in response to acute kidney injury where it promotes apoptosis and inhibits tubular cell regeneration and in the glomeruli of diabetic mice, where it activates profibrotic pathways involved in the development of renal fibrosis in an autocrine manner [22,28,54,62–65]. In addition to being prominently involved in the pathogenesis of renal fibrosis and in the activation of apoptotic and inhibition of regeneration pathways within the kidneys during growth or in response to injury, ActA has also been shown to be induced in inflammatory

stress in response to cytokines such as TGFβ1 [54,66–69]. In this regards, ActA has been shown to mediate innate immune responses, stimulate the release of key renal proinflammatory cytokines such as tumor necrosis factor alpha (TNFα), and in some cases be required for and/or augment the pathologic biologic responses of cytokines such as TGFβ1, in particular its profibrotic responses [66–68,70,71].

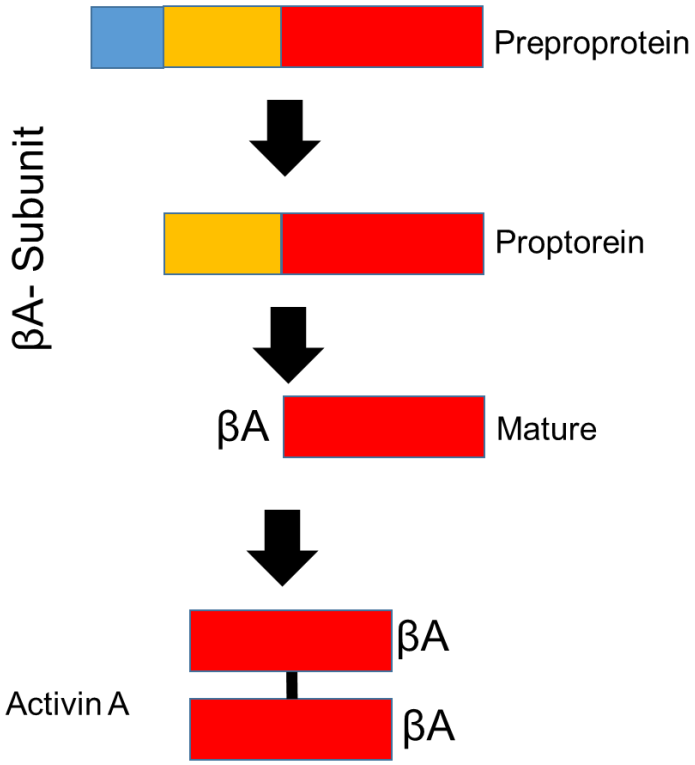

Figure 1-5. Activin A Structure.

ActA is a homodimeric protein consisting of two inhibin ßA chains linked by disulphide bonds. ActA is secreted in an active state containing the N-terminal prodomain that is non-covalently attached to the mature C-terminal domain that is freely disrupted upon receptor binding.

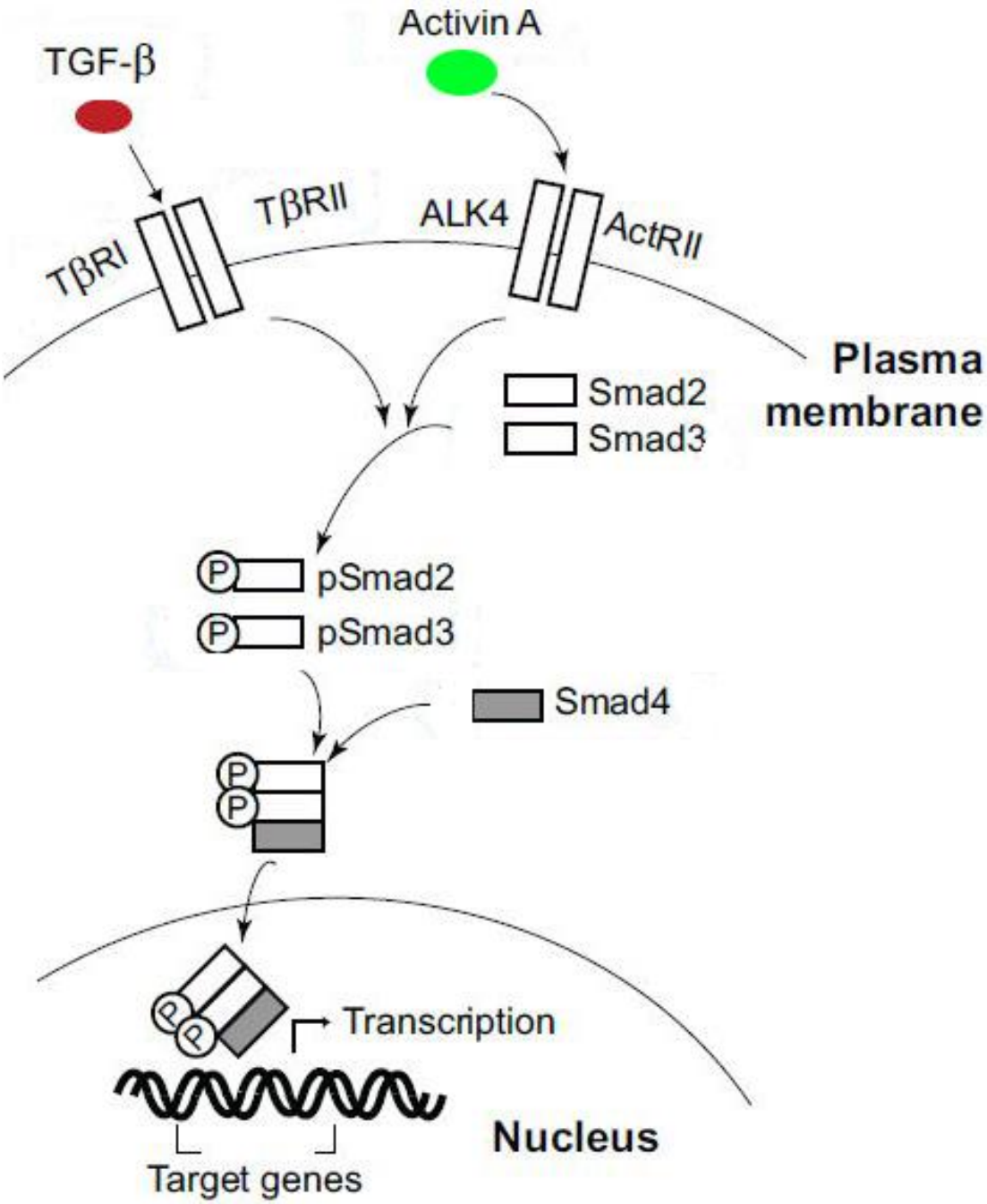
Activin A
TGF-β
TβRII
ALK4
TβRI
ActRII
Plasma membrane
Smad2
Smad3
P
pSmad2
P
pSmad3
Smad4
P
P
P
P
Transcription
Nucleus
Target genes

Figure 1-6. Canonical activin A signaling pathway.

ActA (green ligand) and TGFβ1 (red ligand) both canonically signal through a heterodimeric complex of serine-threonine receptor kinases, consisting of type-I receptors (ALK4) and type-II receptors (ActRIIA or ActRIIB) for ActA and TβRI (ALK1 or ALK5) and TβRII for TGFβ1. Following ligand binding to the type II receptor, the type 1 receptor is recruited and auto-phosphorylated at serine/threonine residues. Phosphorylated type 1 receptor then induces phosphorylation of intracellular Smad proteins, Smad2 and Smad3, which are then translocated into the nucleus in conjunction with Smad4 where they regulate gene transcription. Modified image taken from Borahay MA (2015) [72]. https://doi.org/10.2119/molmed.2014.00053

1.4 Caveolae and Caveolin-1

Caveolae are small (50-100 nm) glycosphingolipid- and cholesterol-enriched omega-shaped invaginations of the plasma membrane that are involved in mediating a wide array of signaling transduction events [73–75]. Through compartmentalization of signaling proteins, caveolae can either positively or negatively mediate signal transduction [73–75]. Caveolae are ubiquitously expressed but predominately found in endothelial cells, epithelial cells, striated and smooth muscle cells and fibroblasts [76]. The caveolin (cav) gene family consists of three proteins, cav-1, cav-2 and cav- 3. Cav-1 and cav-2 are ubiquitously expressed, whereas cav-3 is limited to skeletal muscle, diaphragm, and heart [73–75]. Formation of caveolae requires cav-1, a 21-24 kDa integral membrane protein [73–75].

At the molecular level, caveolae and specifically cav-1 act as chaperones for signaling molecules, such as ligands and receptors, allowing for their delivery and compartmentalization into specific organelles and cellular localizations such as the nucleus, plasma membrane and endosomes [73–76]. Through these actions, cav-1 can either positively or negatively mediate signal transduction events that are critical for normal cellular function [73–76].

Through their interaction with the ECM and integrins, caveolae/cav-1 is involved in the regulation of cell adhesion and migration [76]. In addition, caveolae/cav-1 is involved in mediating the endocytosis and degradation of ECM proteins such as fibronectin [76]. Caveolae also serve as docking points for ligand bound receptors [76]. In the majority of cases, the cellular and molecular effects of these interactions are

inhibitory. For example, activated-ligand bound TGFβ1 receptors are internalized by caveolae in response to phosphorylation of cav-1 at residue Y14, resulting in TGFβ signaling inhibition [76].

We have previously shown that the ability of primary MC to produce ECM proteins both basally and in response to profibrotic stimuli such as TGFβ1, mechanical stress and high glucose is dependent on the presence of cav-1 [77–79] (Fig. 1-7). We have also shown that diabetic mice lacking cav-1 are protected against mesangial matrix expansion and the development of glomerulosclerosis [77]. Thus, cav-1/caveolae are key contributors to the development of kidney fibrosis.

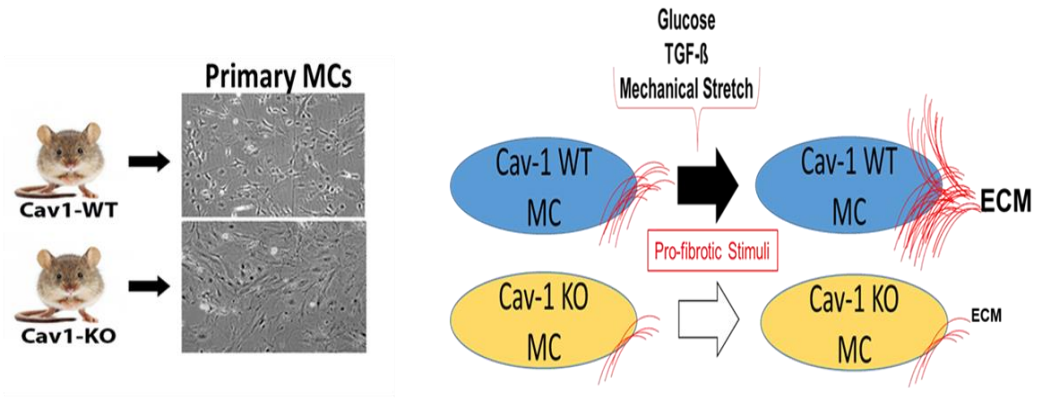

Figure 1-7. Caveolin-1 knockout protects against renal fibrosis.

Primary MC from cav-1 KO mice exhibit reduced basal expression of extracellular matrix proteins and do not respond to profibrotic stimuli such as high glucose, TGFβ1 and mechanical stretch. Cav-KO mice are also protected against renal fibrosis.

1.4.1 Caveolin-1 in Fibrosis

Our previous studies suggest that cav-1 is critical in the regulation of profibrotic signaling events within the kidney [22,77–79]. Expression of cav-1 is induced in several experimental and human renal glomerular diseases and is positively associated with proteinuria and worsening renal phenotypes [75–78,80,81].

We have previously shown that the ability of MC to produce matrix proteins basally and in response to profibrotic stimuli such as TGFβ1, mechanical stress and high glucose is dependent on cav-1 expression (Fig. 1-7) [77–80]. To this end, cav-1 KO mice are viable, kidneys are histologically normal and they are protected against the development of glomerulosclerosis when placed under diabetic stress [75,77]. Interestingly, other organs from the cav-1 KO mouse, such as the skin, heart, and lung, show worsening age related fibrosis [76]. Paradoxically, cav-1 reduction has been associated with worsening fibrosis in several human non-renal fibrotic diseases including idiopathic pulmonary fibrosis, scleroderma, and cardiac fibrosis [76]. These differences are hypothesized to be present due to variation in the organ microenvironment [76]. Thus, the ability of cav-1 to modulate profibrotic signaling pathways has been shown to vary depending on the cell type being examined [76]. However, regardless of localization, the interaction between cav-1 and TGFβ1 is a common pathway by which renal and non-renal fibrotic diseases progress [76]. For example, cav-1 was found to inhibit TGFβ1-induced matrix synthesis in pulmonary fibroblasts, while it was required for dermal fibroblasts to undergo TGFβ1 stimulation [76]. Thus, any studies globally targeting cav-1 or caveolae in CKD will need to be closely monitored for adverse side effects in other organs.

Blocking cav-1 specifically in MC, therapeutically using pharmacologic agents and/or genetically using tools such as Cre/Lox recombination in mice is not feasible due to the lack of MC specific promoters. For this reason, clinically targeting cav-1 specifically in MC is challenging and not yet feasible. Thus, to better understand how cav-1 elimination reduces matrix production in MC and protects against renal fibrosis, and more importantly, to identify novel, feasible therapeutic targets that can be exploited to overcome the difficulties associated with directly targeting cav-1, our lab carried out a microarray analysis to identify potential antifibrotic candidates that are altered in cav-1 deficient MC [22]. Of primary interest, we identified *follistatin* (*fst)*, as the most upregulated gene in MC lacking cav-1, with levels 35-fold higher compared to cav-1 WT MC [22].

1.5 Follistatin

FST is an ubiquitously expressed secreted glycoprotein that binds to and neutralizes the profibrotic and proinflammatory actions of the TGFβ superfamily members [46,57]. FST has the greatest neutralizing activity against the TGFβ superfamily member, ActA [46,57]. FST also antagonizes, with lesser affinity, various other TGFβ superfamily members including myostatin (GDF8), GDF9, TGFβ3 and BMPs 2, 4, 6, and 7 [46,57]. Alternate splicing and protein processing of the *fst* gene results in secretion of two major isoforms containing 288 and 315 amino acids [46,57] (Fig. 1-8). FST-288 is bound to the cell surface via heparan sulfates where it acts to neutralize cell-surface bound activins, allowing for tissue-localized effects [46,57]. On the other hand, in FST-

315, an acidic tail blocks this cell-surface binding, effectively causing the release of FST-315 into circulation where it can scavenge and neutralize activins [46,57]. Mechanistically, two FST molecules bind one activin dimer and in turn sterically hinder its receptor binding sites [46,57,82]. Both forms of FST act to clear activin from circulation by attachment to the cell surface and consequent internalization and targeting for lysosomal degradation [46,57] (Fig. 1-9). The neutralizing effect of FST-288 is reported to be 8-10x greater than that of FST-315 [46,57]. We have also previously shown the ability of exogenously administered FST to be deposited within the kidneys where it can have localized effects [22]. In MC lacking cav-1, we have previously found significant upregulation of FST at the transcript and protein level [22]. This increase in FST has been linked to the renoprotective effects of cav-1 deficiency in response to high glucose and TGFβ [22]. If FST expression in cav-1 KO MC is decreased to that of cav-1 WT levels, then these FST-deficient cav-1 KO MC are no longer protected against the profibrotic stimuli [22]. Thus, FST is an important contributor to the protective antifibrotic phenotype that is observed in cav-1 KO MC. How cav-1 regulates expression of FST at the molecular level in MC has not been identified. **The first aim of this thesis is to examine how cav-1 is involved in the molecular regulation of FST in MC.**

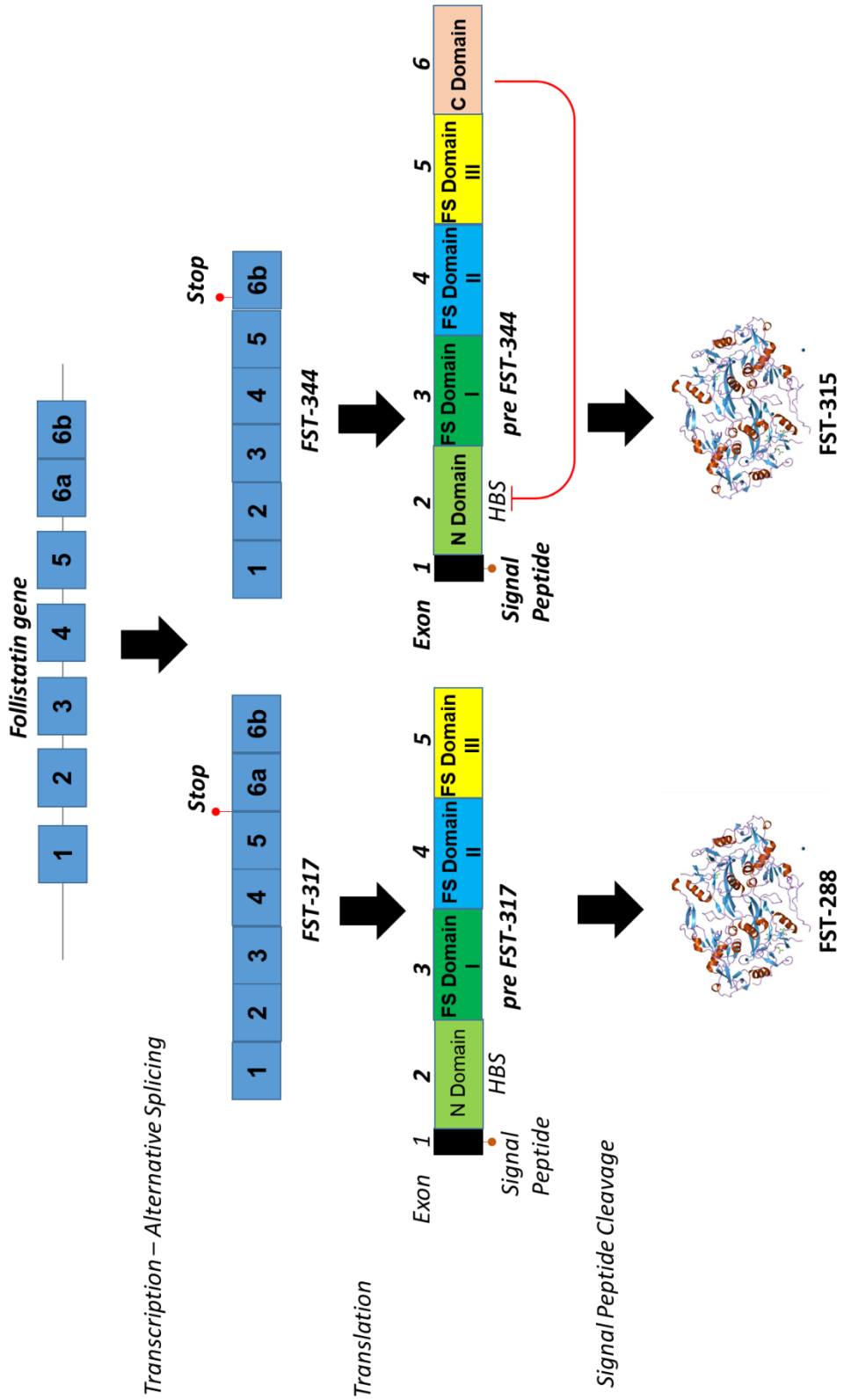
Follistatin gene
1
2
3
4
5
6a
6b
Transcription – Alternative Splicing
Stop
FST-317
FST-344
Translation
Exon
Signal Peptide
HBS
pre FST-317
pre FST-344
N Domain
FS Domain I
FS Domain II
FS Domain III
C Domain
Signal Peptide Cleavage
FST-288
FST-315

Figure 1-8. Follistatin isoforms.

Alternate splicing and protein processing of the *fst* gene results in production and secretion of two major isoforms containing 288 and 315 amino acids. FST contains a heparin binding sequence (HBS) that enables it bind to proteoglycans on the cell surface. FST-288 is bound to the cell surface via heparan sulfates whereas an acidic tail at the C-terminal in FST-315 blocks this cell-surface binding, causing the release of FST-315 into circulation.

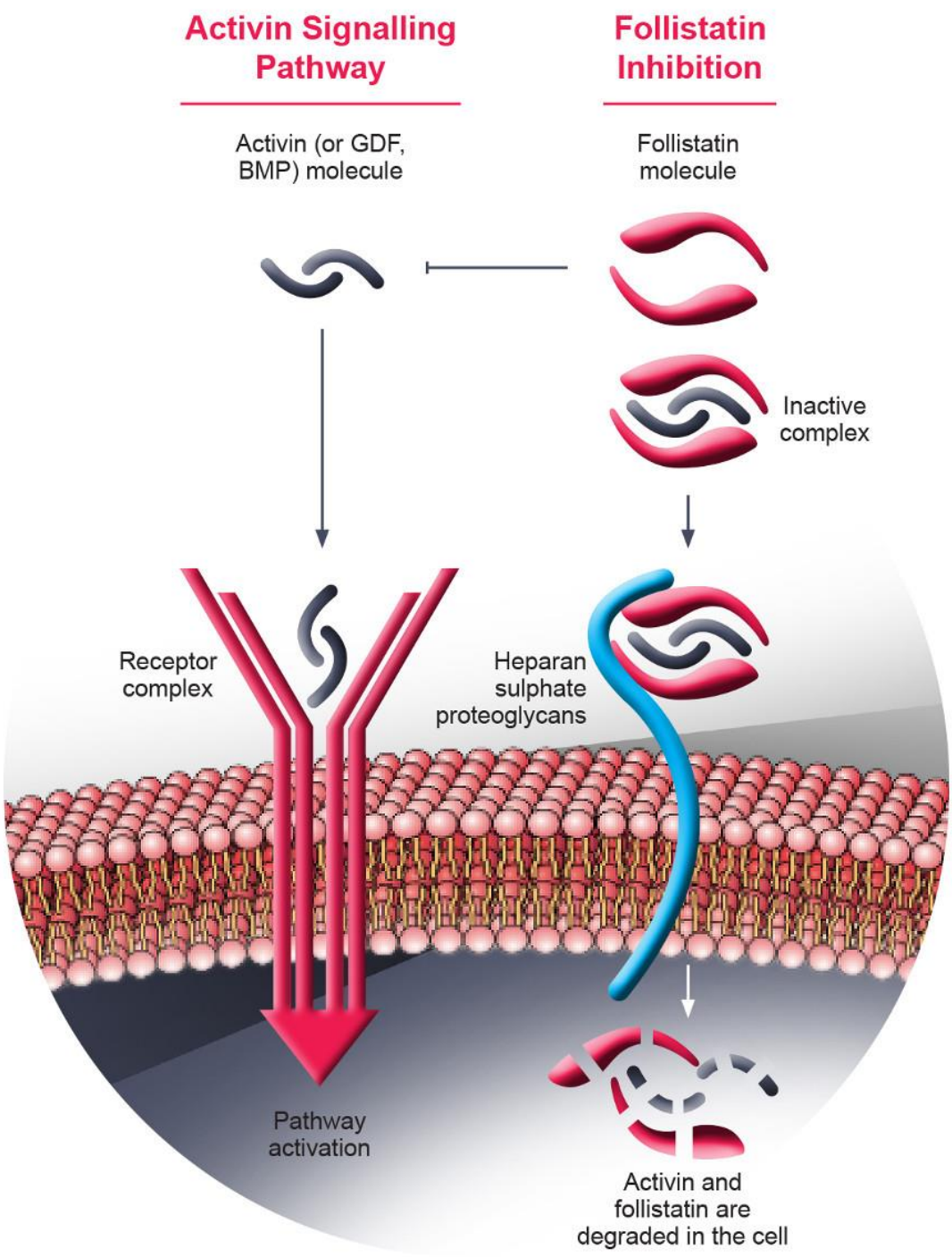
Activin Signalling Pathway
Follistatin Inhibition
Activin (or GDF, BMP) molecule
Follistatin molecule
Inactive complex
Receptor complex
Heparan sulphate proteoglycans
Pathway activation
Activin and follistatin are degraded in the cell

Figure 1-9. FST neutralization of Activin A.

FST binds and block the biologic effects of TGFß cytokines, primarily activins. Two FST molecules bind one activin dimer, either in circulation (FST-315) or at the cell surface (FST-288). This interaction sterically hinders the receptor binding sites on ActA. The FST-ActA complex is consequently internalized and targeted for degradation via the lysosomal pathway. Unmodified image taken with permission from: https://www.parantabio.com/site/therapy/about-pb01.

1.5.1 Follistatin and Cellular Stress

In CKD, MC oxidative stress, through an impairment in the balance of free radical production and clearance, is known to be an important pathogenic contributor to CKD that has been correlated with progressive glomerulosclerosis and albuminuria [38,83,84]. This oxidative stressed environment has been shown to induce apoptosis in several renal cell types including MC, with loss of these resident renal cells being an important driver of CKD to kidney failure [37,38,84,85]. Unfortunately, directed treatments specifically targeted to modulate oxidative stress in a CKD setting have not been very effective and thus need to be better established. Furthermore, endoplasmic reticulum (ER) stress is an established important factor in CKD pathogenesis [86–88]. ER stress has been shown to drive apoptosis in renal cells, including MC, through chronic activation of the unfolded protein response (UPR) [86–92]. ER stress also induces cellular death through promoting oxidative stress in numerous cell types [90,92]. Whether renal MC apoptosis is mediated through oxidative stress and reactive oxygen species (ROS) has not as yet been clearly established. However, some data suggest that in MC, at least in response to high glucose, MC through oxidative stress undergo activation of an apoptotic death program [93]. Recently, ActA has been shown to induce ROS production and mediate apoptosis in several cell types [94–96]. We and others have shown increased expression of serum and kidney ActA in mice with CKD [25]. Activins are most effectively neutralized through the ubiquitously expressed secreted glycoprotein FST [46,57]. Recent work has shown a protective role of FST against ROS production and apoptosis in several settings both *in vitro* and *in vivo* [97]. This has been thought to be due to neutralization of ActA in some

cases, although in others the role of activins has been less clear. **Thus, this thesis examines whether FST can protect against oxidative stress and apoptosis *in vitro* in MC and *in vivo* in mice with CKD.**

1.6 microRNAs (miRNAs)

microRNAs (miRNAs) are small single-stranded noncoding RNAs (~22bp) in length that regulate gene expression [98,99]. miRNAs, through their fully or partially complementary "seed sequence" (2-8bp) bind to a specific miRNA regulatory element (MRE) localized within the 3' untranslated region (UTR) of the target mRNA [98,99]. Depending on binding complementary, the miRNA targets the mRNA for degradation or translational repression [98,99]. miRNAs are involved in the regulation of critical cellular processes [98–103]. Consequently, their dysregulation has been linked to progression of various diseases, including kidney disease [100–103]. Experiments involving overexpression and inhibition of miRNAs are now routinely being used to assess their functions in diseases [100,102,104]. As a result, numerous studies have been carried out to assess the therapeutic potential of inhibiting or overexpressing these specific miRNAs in protecting against renal fibrosis [100,102,104].

To identify the role of miRNAs in regulating expression of the antifibrotic protein FST, we carried out a miRNA screen to determine differentially expressed FST-targeting miRNAs in cav-1 WT and KO MC (Fig. 1-10). As a part of this thesis, in screening for miRNAs targeting FST that are differentially expressed in cav-1 KO MC, we discovered miR299a-5p as an important regulator of FST expression.

miR-299a-5p is a member of the miR-154 family which is found in the second largest miRNA cluster in the human genome on chromosome 14q32. This cluster is highly conserved between rodents and humans. Recent studies have implicated members of this family in pulmonary and cardiac fibrosis [105]. For example, in lungs affected by idiopathic fibrosis, several miR-154 cluster members were found to be altered, including an increase in miR-299a-5p [105]. Increased miR-299a-5p has also been found in fibrotic liver from patients with primary biliary cirrhosis [106]. The role of miR-299a-5p in the development of renal fibrosis through regulation of FST has not yet been investigated. **Thus, this thesis examines whether miR299a-5p is pathologic in CKD through repression of FST and whether its inhibition is protective against renal fibrosis.**

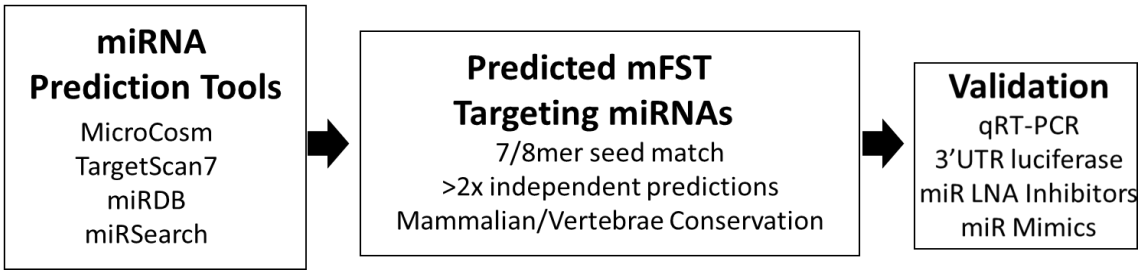

Figure 1-10. miRNA screen.

miRNAs targeting the 3'UTR of FST are first determined using four miRNA prediction software, MircoCosm, TargetScan7, miRDB and miRSearch. Predicted miRNAs targeting FST are screened and selected based on a 7/8mer seed match with the FST 3'UTR, along with at least 2 independent predictions conserved amongst mammals and vertebrae. The expression of FST-targeting miRNAs are then assessed using qRT-PCR to identify and select for significantly down-regulated miRNAs in cav-1 KO MC. Resulting target(s) are functionally validated using 3'UTR and miRNA regulatory element (MRE) luciferase assays. Functional assays using miRNA mimics and LNA inhibitors are then used to determine the biological roles of the predicted miRNA(s).

1.7 The Interplay between Follistatin, TGFß1, Activin A in Renal Fibrosis

Renal profibrotic cytokines ActA and TGFβ1 are involved in a positive feedback loop [57]. TGFβ1 has been shown to stimulate ActA expression [54,57,71,107]. On the other hand, ActA has also been shown to upregulate TGFβ1 and be required for the profibrotic actions of TGFβ1 in MC and various other cell types such as lung, hepatic stellate cells and renal fibroblasts (Fig. 1-11) [54,57,71,107,108]. Furthermore, FST, a potent activin inhibitor, while not capable of directly binding and neutralizing TGFβ1, has been shown to inhibit the TGFβ1-induced profibrotic response [54,57]. We have also shown that FST protects against both basal and glucose-induced matrix production through ActA inhibition [22]. These findings suggest that TGFβ1 and ActA are involved in a positive feedback loop, where ActA is stimulated by TGFβ1 and serves as an intermediator of the profibrotic effects of TGFβ1 and that FST is an antifibrotic factor that inhibits the actions of both ActA and TGFβ1 (Fig.1-11). Based on its ability to neutralize the profibrotic factors ActA and TGFβ1, FST has been shown to act as a strong antifibrotic agent in various organs [22,23,107,109]. Exogenous administration of FST to CCl_4-treated or bleomycin-treated rats attenuated the formation of liver fibrosis and pulmonary fibrosis, respectively[107,109]. Furthermore, FST was also effective in attenuating tubulointerstitial fibrosis in a rat model of obstructive kidney damage [23]. In a recent study in our laboratory using the Akita type 1 diabetic mouse model, we have demonstrated that the administration of exogenous FST has therapeutic potential in protecting against the progression of early diabetic kidney disease, characterized by glomerular hyper-filtration, albuminuria and glomerulosclerosis [22]. Whether exogenous

FST is protective against the progression of renal fibrosis in CKD has not been studied. Based on its potent ability to neutralize the profibrotic effects of both ActA and TGFβ1 (Fig.1-11), we hypothesize that the use of exogenous FST is an effective therapeutic approach to block and/or reverse the progression of renal fibrosis in CKD. **Thus, this thesis examines whether blockade of ActA via exogenous administration of FST can attenuate the development and progression of renal fibrosis in a 5/6 nephrectomy (5/6 Nx) surgical mouse model of CKD** [110,111] (Fig. 1-12).

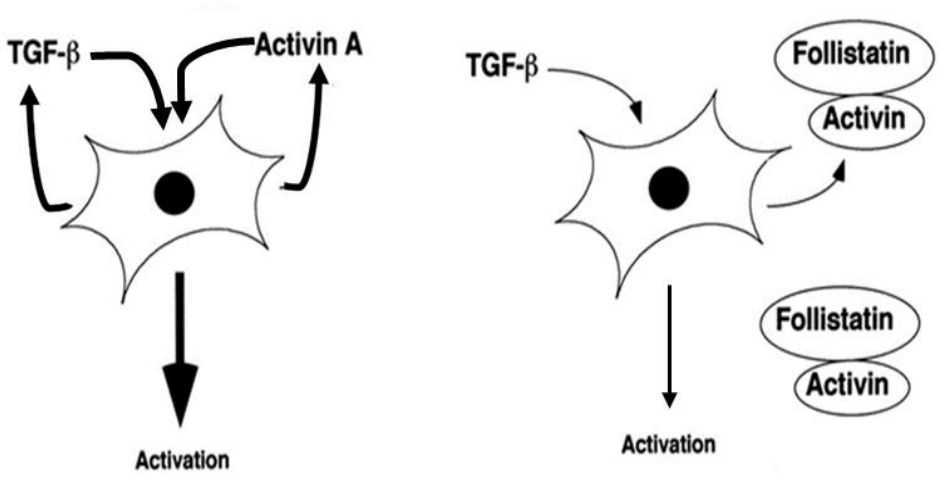

Figure 1-11. Interplay between TGFβ1, Activin A in promoting fibrosis and the protective role of FST.

Left: Positive feedback loop between ActA and TGFβ1 where ActA serves as an intermediator of the profibrotic effects of TGFβ1 actions. TGFβ1 stimulates ActA production with ActA being required for the profibrotic actions of TGFβ1. Right: FST acts as an antifibrotic factor by inhibiting the profibrotic actions of both ActA and in turn, indirectly, TGFβ1. *Arrow thickness represents magnitude of response.* License and permission obtained - Modified image taken from Wada W (2004)[71]. https://doi.org/10.1210/en.2003-1663.

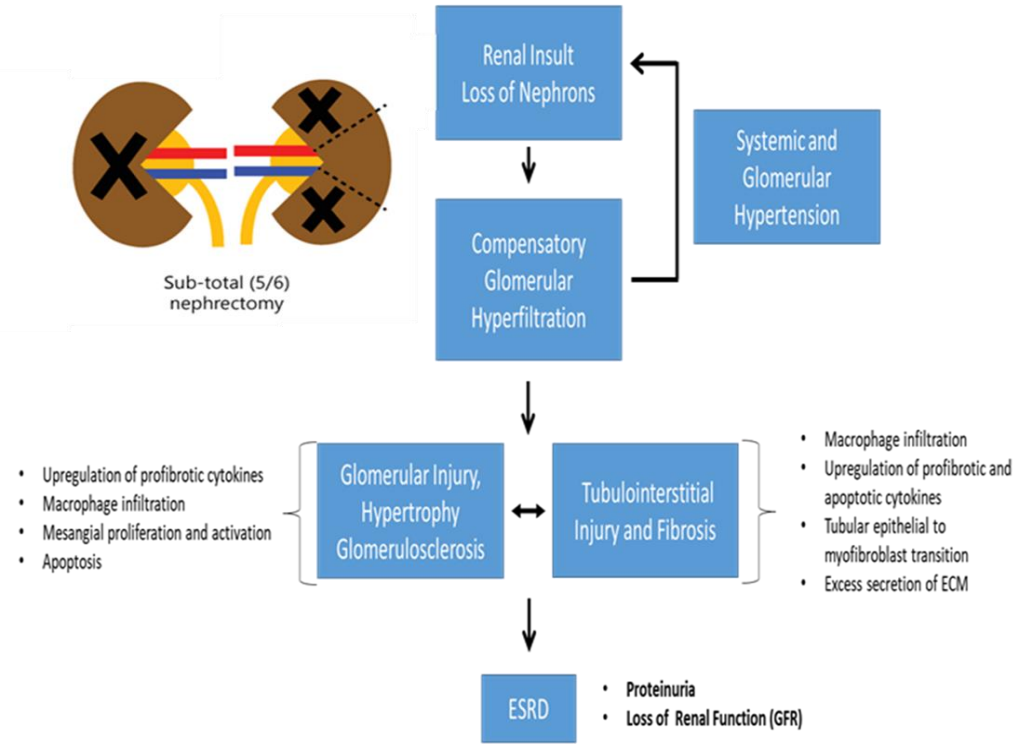

Figure 1-12. 5/6 nephrectomy mouse model of CKD.

CKD is achieved using surgical renal mass reduction in male CD1 mice. The 5/6 nephrectomy (Nx) consists of a resection of the upper and lower poles of the left kidney followed by a right kidney nephrectomy. Surgical renal mass reduction results in the development of CKD that closely mimics the progression of CKD to ESRD in humans. In this model, excessive compensatory glomerular hyperfiltration leads to systemic and glomerular hypertension. Over time, chronic activation of proinflammatory and fibrotic pathway results in glomerulosclerosis and tubulointerstitial fibrosis. A sharp decrease in glomerular filtration rate is observed. Overt renal damage results in albuminuria. This gradual loss of renal function eventually leads to kidney failure.

1.8 Main Objectives

The main objectives of this thesis are to determine the molecular mechanisms via which cav-1 deficiency in MC leads to up-regulation of FST and determine whether FST is a potential novel therapeutic agent for CKD.

1.8.1 Research Aims

1) Determine the molecular mechanism by which cav-1 deletion leads to upregulation of the antifibrotic protein FST.
2) Determine the therapeutic potential of FST using a mouse model of CKD.
3) A) Screen and validate FST-targeting miRNAs that are differentially expressed in cav-1 KO MC and B) determine whether miR299a-5p inhibition protects against the progression of CKD.

1.8.2 Overall Hypothesis

Increased renal FST through direct exogenous recombinant FST administration or post-transcriptionally through miR299a-5p inhibition will protect against the development of renal fibrosis and slow the progression of CKD.

1.8.3 Summary of Research Findings

1) Absence of cav-1 transcriptionally increased FST expression through elevated Sp1 activity via augmentation of phosphoinositide 3-kinase and protein kinase C zeta (PKCζ) signaling.
2) Exogenous recombinant FST treatment alleviated renal oxidative stress, reduced renal fibrosis and albuminuria while improving kidney function in mice with CKD.
3) miR299a-5p expression was downregulated in cav-1 KO MC and elevated in mice with CKD. miR299a-5p post-transcriptionally repressed FST and augmented profibrotic responses. miR299a-5p inhibition ameliorated renal fibrosis in mice with CKD.

Chapter 2: Caveolin-1 regulation of Sp1 controls production of the antifibrotic protein follistatin in kidney mesangial cells

Title: Caveolin-1 regulation of Sp1 controls production of the antifibrotic protein follistatin in kidney mesangial cells

Authors: Neel Mehta, Dan Zhang, Renzhong Li, Tony Wang, Agata Gava, Pavithra Parthasarathy, Bo Gao and Joan C. Krepinsky

Corresponding Author: Dr. Joan C. Krepinsky, Department of Nephrology, St. Joseph Hospital, 50 Charlton Ave E, Room T3311, Hamilton, Ontario L8N 4A6, Canada, Telephone: (905) 522-1155 x 34991; FAX: (905) 540-6589; Email: krepinj@mcmaster.ca

Citation: Mehta, N. *et al.* Caveolin-1 regulation of Sp1 controls production of the antifibrotic protein follistatin in kidney mesangial cells. *Cell Commun. Signal.* 17, 37 (2019).

2.1 Preface

Significance to thesis: Previously, we observed that cav-1 KO mice and caveolin-1 deficient MC are protected against several profibrotic stimuli and against the development of glomerulosclerosis. In cav-1 KO MC, we identified significant upregulation of the antifibrotic protein FST. The purpose of this study was to determine the molecular mechanism through which FST is upregulated in cav-1 deficient MC. Our results identified Sp1 as the critical transcription factor regulating activation of the FST promoter. Absence of cav-1 was found to increase Sp1 transcriptional activity through activation of phosphoinositide 3-kinase and protein kinase C zeta. These findings describe a novel transcriptional mechanism regulated by cav-1, which functions to repress the expression of FST. These findings shed novel mechanistic insight towards the development of antifibrotic treatment strategies for CKD through the use of FST.

Author's contribution: NM, DZ, RL, TW, AG, PP performed experiments and analysed data. NM wrote the manuscript. NM and JCK conceived the ideas. JCK edited the manuscript. BG assisted with animal studies. All authors read and approved the final manuscript.

- RL and PP assisted in the preparation of FST promoter deletion constructs.
- DZ and BG assisted in the processing of mouse kidneys for IHC analysis.
- RL, PP, TW and AG assisted with luciferase promoter assays in Figures 2 and 3.

2.2 Abstract

Background: We previously showed that caveolin-1 (cav-1), an integral membrane protein, is required for the synthesis of matrix proteins by glomerular mesangial cells (MC). In a previous study to understand how cav-1 is involved in regulating matrix production, we had identified significant upregulation of the antifibrotic protein follistatin in cav-1 knockout MC. Follistatin inhibits the profibrotic effects of several members of the transforming growth factor beta superfamily, in particular the activins. Here, we characterize the molecular mechanism through which cav-1 regulates the expression of follistatin. *Methods:* Kidneys from cav-1 wild type and knockout (KO) mice were analyzed and primary cultures of MC from cav-1 wild-type and KO mice were utilized. FST promoter deletion constructs were generated to determine the region of the promoter important for mediating FST upregulation in cav-1 KO MC. siRNA-mediated down-regulation and overexpression of Sp1 in conjunction with luciferase activity assays, immunoprecipitation, western blotting and ChiP was used to assess the role of Sp1 in transcriptionally regulating FST expression. Pharmacologic kinase inhibitors and specific siRNA were used to determine the post-translational mechanism through which cav-1 affects Sp1 activity. *Results:* Our results establish that follistatin upregulation occurs at the transcript level. We identified Sp1 as the critical transcription factor regulating activation of the FST promoter in cav-1 KO MC through binding to a region within 123 bp of the transcription start site. We further determined that the lack of cav-1 increases Sp1 nuclear levels and transcriptional activity. This occurred through increased

phosphoinositide 3-kinase (PI3K) activity and downstream protein kinase C (PKC) zeta-mediated phosphorylation and activation of Sp1. *Conclusions:* These findings shed light on the transcriptional mechanism by which cav-1 represses the expression of a major antifibrotic protein, and can inform the development of novel antifibrotic treatment strategies.

2.3 Background

Mesangial cells (MC) are specialized pericytes involved in the production and secretion of mesangial matrix within glomeruli of kidneys [19–21]. The mesangial matrix serves to anchor MC and provide structural support and integrity to the surrounding glomerular capillaries [19–21]. Under homeostatic conditions, MC secrete matrix that is composed of collagens, laminin and fibronectin [19,31,35,112]. The activation and transition of MC to a more secretory myofibroblastic phenotype has been established to be an early fibrogenic response in kidney disease of varying etiology, including that due to diabetes and hypertension [14,19–21,31,35,112].

Caveolae are small (50-100 nm) glycosphingolipid- and cholesterol-enriched omega-shaped invaginations of the plasma membrane that are involved in mediating a wide array of signaling transduction events [73–75]. Through compartmentalization of signaling proteins, caveolae can either positively or negatively mediate signal transduction [73–75]. The caveolin (cav) gene family consists of three proteins, cav-1, cav-2 and cav- 3. Cav-1 and cav-2 are ubiquitously expressed, whereas cav-3 is limited to skeletal muscle, diaphragm, and heart [73–75]. Formation of caveolae requires cav-1, a

21-24 kDa integral membrane protein [73–75]. We have previously shown that the ability of MC to produce matrix proteins both basally and in response to profibrotic stimuli such as transforming growth factor beta 1 (TGFβ1), mechanical stress, and high glucose is dependent on cav-1 expression [77–79]. Importantly, diabetic mice lacking cav-1 are protected against mesangial matrix expansion and the development of glomerular sclerosis [77]. Strong upregulation of cav-1 has also been demonstrated in rodent models of chronic kidney disease and diabetic nephropathy [75,81]. These studies support a profibrotic role for cav-1/caveolae in kidney fibrosis.

Clinically targeting cav-1 in vivo is challenging [75]. Thus, to better understand how cav-1 elimination reduces matrix production in MC, and more importantly, to identify potential novel therapeutically applicable targets that can be exploited to overcome the difficulties associated with directly targeting cav-1, our lab previously identified and measured the expression of potential antifibrotic candidates that are altered in cav-1 deficient MC. Of primary interest, we identified significant upregulation of follistatin (FST), an antifibrotic factor, in MC lacking cav-1.

FST is an ubiquitously expressed and secreted glycoprotein that binds to and neutralizes the profibrotic and proinflammatory actions of several TGFβ superfamily members, with greatest activity against activins [46,57]. We and others have shown that FST acts as a strong antifibrotic agent in various organs, including the kidneys in models of obstructive kidney damage and diabetic nephropathy [22,23,107,109]

The molecular mechanism through which FST is regulated by cav-1 in glomerular MC is as yet unknown. Here, we show that signaling through the phosphoinositide 3-

kinase (PI3K), protein kinase C zeta (PKCζ) and Sp1 signaling pathway is augmented in cav-1 deficient MC to increase the transcriptional regulation of FST. These findings shed insight into the molecular mechanism through which cav-1 regulates the expression of FST and provide important knowledge that can inform the development of antifibrotic treatment strategies for chronic kidney disease.

2.4 Materials and Methods

Cell Culture

Primary mouse MC were isolated from cav-1 wild-type (WT) and cav-1 knockout (KO) B6129SF1/J mice (Jackson Laboratory) using Dynabeads (Invitrogen). Briefly, mice were perfused with magnetic Dynabeads, kidneys were harvested and digested by collagenase and glomeruli were collected using a magnet. Isolated glomeruli were washed with HBSS, resuspended in Dulbecco's modified Eagle's medium supplemented with 20% fetal bovine serum (Invitrogen), penicillin (100µg/ml) and streptomycin (100µg/ml) at 37˚C in 95% O_2, 5% CO_2. MC were grown out, with passages 7-14 used for experiments. MC were serum deprived in 0.5% FBS 24h prior to all treatments unless otherwise stated. Drugs/reagents used in the study are provided in table 2-1.

Transfection

MC at 60%-70% confluence were transfected (0.5µg luciferase plasmid with 0.05µg β-galactosidase or 1-2µg protein expression plasmid) using Effectene (Qiagen) as per the manufacturer's recommendation. siRNA-mediated knockdown was achieved

using RNAiMAX (Thermo Fisher Scientific) as per the manufacturer's recommendation. Plasmids and siRNA used in the study are provided in table 2-2.

Luciferase Assay

MC lysis was achieved using Reporter Lysis Buffer (Promega) as per the manufacturer's recommendation. Luciferase activity was measured on clarified cell lysate using the Luciferase Assay System (Promega) with a luminometer (Junior LB 9509, Berthold). β-galactosidase activity, used to normalize for transfection efficiency, was measured in clarified cell lysates using the β-Galactosidase Enzyme Assay System (Promega) with a plate reader absorbance set at 420nm (SpectraMax Plus 384 Microplate Reader, Molecular Devices).

Protein Extraction, Immunoprecipitation and Immunoblotting

MC cell lysis and protein extraction were carried out as described previously [113]. Briefly, cell lysates were centrifuged (15,000 rpm, 10min, 4^{o}C), supernatant was collected and protein concentration quantified. For immunoprecipitation experiments, cells were lysed, clarified and equal amounts of lysate were immunoprecipitated using 1μg primary antibody (18h, 4°C), followed by incubation with protein-G–agarose slurry (2h, 4°C). Cell protein lysates (10μg-50μg) and immunoprecipitated products (total yield) were separated on SDS-PAGE for subsequent immunoblotting. Antibodies used in the study are provided in table 2-3.

Quantitative-real time PCR

RNA from MC was extracted using Ribozol RNA Extraction Reagent (Amresco) as per the manufacturer's recommendation, with 1µg of RNA reverse transcribed into cDNA using qScript cDNA SuperMix Reagent (Quanta Biosciences). Quantitative real-time PCR was carried out using the Power SYBR Green PCR Master Mix (Thermo Fisher Scientific) on the Applied Biosystems ViiA 7 Real-Time PCR System (Thermo Fisher Scientific). mRNA expression and fold changes were calculated using the $\Delta\Delta C_T$ method, where 18S was used as the endogenous control. Primer sequences used in the study are provided in table 2-4.

ChIP

At endpoint, MC were cross-linked using formaldehyde (10 min, RT), neutralized using 1M glycine (pH 2.2) (5min, RT), resuspended in ice-cold PBS containing protease inhibitors and centrifuged (13,000 rpm, 5 min, 4^{o}C). The cell pellet was resuspended in nuclear extraction buffer (20 mM HEPES pH7.9, 25% glycerol, 420mM NaCl,1.5mM MgCl2,0.2mM EDTA, protease inhibitors), incubated on ice (20min) and centrifuged (13,000 rpm, 10min, 4^{o}C). The resulting nuclear pellet was resuspended in Breaking Buffer (50mM Tris-HCl pH8.0, 1mM EDTA, 150mM NaCl, 1% SDS, 2% Triton X-100, protease inhibitors), sonicated 6x3s, and Triton Buffer added (50mM Tris-HCl pH8.0, 1mM EDTA, 150mM NaCl, 0.1% Triton X-100). 10% of the original aliquot was collected (input) and the rest used for immunoprecipitation for Sp1 and mouse IgG (as described above). Immunoprecipitated samples were washed 3x in Triton Buffer. SDS

Buffer was then added (62.5mM Tris HCl pH6.8, 200mM NaCl, 2% SDS, 10mM DTT, 2µl of proteinase K (40mg/ml)) and samples incubated (18h, 65^{o}C) to reverse crosslinking. DNA was isolated using phenol/chloroform extraction and resuspended in dH2O. qRT-PCR was used, as described above, to amplify the purified DNA using primers specific to the Sp1 binding site located within -123bp of the mouse FST (mFST) promoter. Ct values were evaluated across multiple replicate experiments using the %input method, where $\%input=100*2^{(Adjusted\ input - Ct\ (IP))}$.

Cloning

The full-length mouse FST luciferase (-luc) construct, mFST4-FL-luc, (obtained from Dr. Jeong Yoon) containing the mouse FST promoter with exon 1 and intron 1 was digested with KpnI and NheI. The resulting product was inserted into a linearized pGL3-luc vector in order to generate a construct which lacks intron 1 and most of exon 1 (+20bp is included, where transcription start site = +1). The resulting plasmid hereafter is referred to as mFST4-luc. mFST4-luc was used to generate mFST promoter deletion constructs using the primer sequences listed in table 2-5.

Two Sp1 binding sites (CCGCCC) localized within the mFST4-123bp promoter were deleted in order to generate mFST4Δintron1-123ΔSp1-luc. Briefly, oligonucleotides coding the FST-123 promoter sequence lacking the two Sp1 binding sites along with the KpnI (5') and NheI(3') digestion sites were synthesized, annealed, and ligated into pGL3-Basic luc. All sequences synthesized for cloning are listed in table 2-5. All generated constructs were confirmed by sequencing (Mobix Lab, McMaster University).

PI3K activity assay

A plasmid encoding a Venus-tagged pleckstrin homology (PH) domain of Akt (PH-Akt-Venus), a gift from Dr. Narasimhan Gautam (Addgene plasmid # 85223), was transfected into MC. Plasma membrane localization of the PH domain of Akt was used as a live phosphatidylinositol 3,4,5-trisphosphate (PIP3) sensor for assessing PI3K activity [114]. Briefly, 24h following transfection, cav-1 WT and KO MC were incubated with wheat germ agglutinin (WGA) Alexa Fluor-594 Conjugate (Thermo Scientific) in HBSS (2μg/ml, 10min, 37^{o}C) to delineate the plasma membrane. After plasma membrane labeling, MC were washed and images were taken using a fluorescein (ex490nm/em525nm) and rhodamine (ex550nm/em620nm) filter sets (EVOS FL Cell Imaging System, Thermo Fisher Scientific). Image J, in conjunction with the co-localization finder plugin (https://imagej.nih.gov/ij/plugins/colocalization-finder.html), was used to create colocalization masks and quantify the percent localization of PH-Akt-Venus to the cell membrane.

Immunohistochemistry/Immunocytochemistry

Cav-1 WT and KO B6129SF1/J mice were sacrificed and perfused with cold PBS in accordance with principles of laboratory animal care and McMaster University and Canadian Council on Animal Care guidelines. For immunohistochemistry, 4μm FFPE

kidney sections were deparaffinized, endogenous peroxidase activity was blocked, and heat-induced epitope retrieval was carried out for immunohistological staining. Briefly, tissues were blocked with 5% horse serum and incubated in primary antibody overnight at 4°C. Tissues were then incubated with biotinylated secondary antibodies (Vector Labs) (30 minutes, room temperature) and then incubated with streptavidin/peroxidase (30 minutes, room temperature) (Vector Labs). Chromogenic color development was carried out using Nova Red (Vector Labs), followed by counterstaining using Gill's hematoxylin (Sigma), and mounting in a xylene based mounting media (Permount; Thermo Scientific). All micrographs were captured at x200 and x400 magnification using the BX41 Olympus microscope. The total percentage of positive area (signal) within the kidneys was measured using ImageJ. Briefly, 10-20 micrographs were captured, percentage of positive area quantified and averaged per mouse. This was repeated for the indicated '*n'* number of mice, with final average and standard error calculated from the individual averages obtained from each mouse.

Serum deprived MC plated in an 8-well chamber slide were used for ICC. Cells were fixed in 4% paraformaldehyde, permeabilized in 0.2% Triton X-100, blocked in 1% BSA/3% donkey serum, and incubated with primary antibodies overnight at 4°C. Cells were then incubated with Alex-Fluor (Thermo Scientific) conjugated secondary antibodies (30 minutes, room temperature, dark), and mounted and counterstained using a DAPI-containing fluorescent mounting media (Vector Labs). All ICC micrographs were captured using the fluorescein (ex490nm/em525nm) and DAPI (ex350nm/em470nm) filter sets (EVOS FL Cell Imaging System, Thermo Fisher Scientific). Mean fluorescence

intensity within the nucleus, delineated using DAPI and/or total cellular expression examined under the appropriate fluorescence filter sets was measured using ImageJ.

Statistical Analysis

Statistical analyses were performed using GraphPad Prism 6. A Student's *t*-test or one-way ANOVA was used to determine statistical significance between two or more groups, respectively. *Post hoc* significance of pairwise comparisons was assessed using Tukey's HSD. A p-value <0.05 (two-tailed) was considered significant. Data are presented as mean±SEM. The number of experimental repetitions (*n*) is indicated in the figure captions.

2.5 Results

Cav-1 regulation of FST occurs at the transcript level in MC

We have identified FST as a significantly upregulated gene in cav-1 deficient MC compared to their wild-type (WT) counterparts. Fig. 2-1 shows elevated FST expression at the mRNA (Fig. 2-1A) and protein level (Fig. 2-1B) in cultured primary cav-1 KO MC. It should be noted that the FST antibody detects two main bands in MC. Using FST siRNA, we confirm that these are both FST (Fig. 2-1C). This is likely due to the presence of different isoforms and/or differentially glycosylated forms of the protein [115–118]. Increased FST expression is also seen in the kidneys of mice lacking cav-1 compared to WT mice (Fig. 2-1D). Confirming the antifibrotic properties of FST in MC, TGFβ1-mediated extracellular matrix protein (ECM) production was blunted by the addition of

recombinant FST in cav-1 WT MC (Fig. 2-8; Supplemental Fig. 1A). Conversely, FST downregulation using siRNA significantly augmented TGFβ1-medited ECM production in cav-1 KO MC (Fig. 2-8; Supplemental Fig. 1B). These results confirm that FST inhibits TGFβ1-induced ECM production in MC.

To identify potential avenues by which cav-1 regulates FST expression, we began by examining stability of the FST transcript in cav-1 WT and KO MC. Using actinomycin D to stop de novo transcription, we observed that FST mRNA has a half-life of about 4 hours which was unaffected by cav-1 expression (Fig. 2-1E). We next assessed whether FST protein stability was affected by cav-1. Using cycloheximide to prevent de novo protein synthesis, we determined that FST has a rapid turnover rate, which is also unaffected by cav-1 expression (Fig. 2-1F). The increased transcript and protein levels seen in cav-1 KO MC are thus not a result of increased post-transcriptional mRNA stability or post-translational protein stability.

We next sought to determine whether cav-1 regulates FST expression at the transcriptional level. The mouse FST promoter has been previously characterized [119]. Using a mouse FST promoter luciferase reporter construct, we assessed whether FST promoter activity was differentially regulated in cav-1 WT and KO MC. Here, we found significantly elevated transcriptional activity in cav-1 KO MC of both mFST4-FL-luc, which also contains intron 1 and exon 1 of FST, and mFST4-luc in which these are removed (Fig. 2-2A and B). Since removal of intron 1 and exon 1 did not affect cav-1 KO upregulation of FST promoter activity, we used mFST4-luc as a template to generate promoter deletion constructs ranging from -1840bp to -123bp upstream of the

transcription start site (TSS) (Fig. 2-2C). Here, we surprisingly found significantly elevated transcriptional activity of all promoter deletion constructs in cav-1 KO MC (Fig. 2-2D). These data illustrate that transcriptional regulatory elements residing between -123bp and the TSS of the mouse FST promoter are critical for the upregulation of FST that is observed in cav-1 KO MC. Next, using siRNA-mediated cav-1 downregulation in cav-1 WT MC, we confirmed that cav-1 was directly involved in the regulation of FST promoter activity (Fig. 2-2E) and protein expression (Fig. 2-2F). However, the relative increase in FST transcription and expression upon cav-1 downregulation with siRNA was not as effective in comparison to the elevation seen in cav-1 KO MC. This is likely due to differences in the degree of cav-1 suppression between these two approaches.

Cav-1 transcriptionally regulates FST through Sp1

Having established a transcriptional effect of cav-1 on the -123bp FST promoter, we next screened for transcription factor regulatory element(s) located within this region. Putative transcription factor binding sites within the mFST promoter were identified using MatInspector and PROMO [120]. Interestingly, we identified two Sp1 binding sites (CCGCCC) in this region (Fig. 2-3A), with Sp1 having been shown to regulate FST promoter activity in intestinal epithelial cells [121]. We thus assessed its role in mediating FST upregulation in cav-1 KO MC. We first determined whether Sp1 levels are altered in these cells. To this end, we found elevated Sp1 expression in cav-1 KO MC (Fig. 2-3B). This was associated with increased Sp1 nuclear presence, as assessed by immunoblotting (Fig. 2-3C) and immunofluorescence (Fig. 2-3D), as well as increased transcriptional

activity as measured using a Sp1-target sequence binding luciferase (Fig. 2-3E). Similar increases of Sp1 expression and nuclear localization were seen in both glomeruli and tubules of cav-1 KO mice (Fig. 2-3F). Next, using siRNA-mediated cav-1 downregulation in WT MC, we confirmed the regulation of Sp1 activity by cav-1 (Fig. 2-3G).

Our next studies aimed to determine whether Sp1 is a major regulator of FST transcription in cav-1 KO MC. We first assessed if Sp1 overexpression can increase the transcriptional activity of the -123bp mouse FST promoter. Fig. 2-4A shows that the overexpressed Sp1 is functionally active, effectively increasing Sp1 transcriptional activity. In cav-1 WT MC, Sp1 overexpression also significantly increased FST promoter transcriptional activity (Fig. 2-4B), showing a prominent role for Sp1 in FST promoter regulation. We then downregulated Sp1 using siRNA to assess whether it is essential for the increased FST seen in cav-1 KO MC. Fig. 2-4C confirms the successful knockdown of Sp1. As we hypothesized, Sp1 knockdown reduced FST promoter transcriptional activity in KO MC to levels seen in WT cells (Fig. 2-4D). FST mRNA and protein expression were similarly reduced (Fig. 2-4E, F). A smaller decrease in protein levels was also observed in cav-1 WT cells, demonstrating the importance of Sp1 to basal FST regulation.

We next wished to confirm that Sp1 binds to the FST -123 promoter region. Using ChIP coupled with qRT-PCR, we quantified the amount of Sp1 binding to the putative Sp1 binding sites localized within the -123bp promoter region of FST. As seen in Fig. 2-4G, Sp1 binding in this region was significantly more abundant in cav-1 KO compared to WT MC. To confirm that this is required for transcriptional regulation of FST, we deleted

the two identified Sp1 binding sites within the -123bp region of the FST promoter (Fig. 2-4H). Deletion of both of these resulted in a significant decrease in FST promoter activity in both cav-1 WT and KO MC. Importantly, the elevated FST promoter activity observed in cav-1 KO compared with WT MC was abolished, highlighting the central role for Sp1 in FST transcriptional regulation by cav-1 (Fig. 2-4I). The decrease seen in WT MC additionally illustrates the importance of Sp1 to basal FST regulation. Taken together, these data show an important regulatory role for cav-1 in Sp1 expression and transcriptional activity, which leads to a significant upregulation of FST in cav-1 KO cells.

Cav-1 regulates Sp1 activity through PI3K and PKCζ

The regulation of Sp1 by cav-1 has not previously been described. We thus wanted to determine the mechanism underlying this observation. It is well known that Sp1 activity is under tight regulation via phosphorylation, which can either positively or negatively influence the activity and binding of Sp1 to its downstream targets [122]. Since serine/threonine (ser/thr) phosphorylation of Sp1 by various kinases was shown to be an important stimulator of Sp1activity, we compared baseline Sp1 ser/thr phosphorylation between cav-1 KO and WT cells. After Sp1 was immunoprecipitated from total cell lysate, immunoblotting for phosphorylated ser/thr sites showed a greater degree of Sp1 ser/thr phosphorylation in cav-1 KO MC (Fig. 2-5A).

Next, we sought to identify the kinase responsible for increased Sp1 phosphorylation in cav-1 KO MC. Using various inhibitors, we screened kinases known

to phosphorylate Sp1 at ser/thr residues and thereby enhance Sp1 activity. Fig. 2-5B shows that in cav-1 KO MC, glycogen synthase kinase 3 beta (GSKβ) (using LiCl), c-Jun N-terminal kinase (JNK) (using SP600125) and p38 mitogen-activated protein kinase (MAPK) (using SB203580) inhibition significantly upregulated Sp1 activity, while mitogen-activated protein kinase kinase (MEK) inhibition (using U0126) did not affect Sp1 activity. None of these kinases are thus responsible for the upregulation of Sp1 activity in cav-1 KO MC.

We next assessed the role of protein kinase C zeta (PKCζ), which has been shown in numerous cell types to phosphorylate and positively regulate Sp1 activity [123]. We found that PKCζ inhibition using a PKCζ pseudosubstrate reduced the increased activity of Sp1 in cav-1 KO MC to WT levels (Fig. 2-5C). We then questioned whether the expression of PKCζ is altered in cav-1 deficient MC. Interestingly, both PKCζ mRNA (Fig. 2-5D) and protein (Fig. 2-5E) were significantly increased in cav-1 KO MC. Upregulation of PKCζ expression was also observed in the glomeruli and tubules of cav-1 KO mice (Fig. 2-5F). To further confirm the role of PKCζ as an upstream regulator of the increased Sp1 activity seen in cav-1 KO cells, we downregulated PKCζ using siRNA. Fig. 2-5G shows effective PKCζ knockdown in cav-1 WT and KO MC. Similar to pharmacologic inhibition, this reduced Sp1 activity in cav-1 KO MC to levels seen in WT cells (Fig. 2-5H). Accompanying decreases in FST protein expression were also seen (Fig. 2-5I).

PI3K was shown to be an important promoter of PKCζ activity in numerous cell types [123]. To assess the importance of PI3K-mediated activation of PKCζ in Sp1

activation and thereby FST regulation in cav-1 KO MC, we examined the effects of two distinct PI3K inhibitors. Both of these (wortmannin and LY294002) significantly reduced Sp1 activity in cav-1 KO MC to that seen in WT cells (Fig. 2-6A), although LY249002 was more efficacious than wortmannin in this regard. This may be due to the greater stability of LY294002 in solution [124]. Akt is a ser/thr kinase well-known to be activated by PI3K [125]. However, the Akt inhibitor VIII did not reduce Sp1 activity in KO cells. This is in keeping with a known role for the enzyme phosphoinositide-dependent protein kinase-1 (PDK-1) and not Akt as the kinase downstream of PI3K which phosphorylates and activates PKCζ [126].

We next tested the effects of PI3K inhibition on FST mRNA and protein expression. PI3K inhibition significantly reduced FST mRNA expression in cav-1 KO MC (Fig. 2-6B). Fig. 2-6C similarly shows that, in cav-1 KO MC, PI3K inhibition reduced FST protein expression to levels seen in WT cells. Last, we assessed whether cav-1 KO MC have increased PI3K activity. Here, we transfected cav-1 WT and KO MC with a fluorescent biosensor (Ph-Akt-Venus) for phosphatidylinositol 3,4,5-trisphosphate (PIP3) [114]. Class I PI3Ks are responsible for the production of PIP3 at the plasma membrane. Thus, the translocation of the pleckstrin homology (Ph) domain of Akt to the plasma membrane is indicative of PIP3 generation and can serve as a readout of enzymatic PI3K activity. A fluorophore-labeled wheat germ agglutinin (WGA) was used to label the plasma membrane to confirm localization. Fig. 2-6D shows a pronounced increase in PI3K activity in cav-1 KO MC, identified by colocalization of Ph-Akt-VENUS and WGA and highlighted using a colocalization mask (seen in white).

Quantification of the colocalization mask is shown in the accompanying graph. Collectively, as summarized in Fig. 2-7, our results show that cav-1 deficient MC exhibit increased activity of PI3K, an upstream regulator of PKCζ activity. Increased PKCζ activity results in elevated Sp1 activation which augments FST transcription.

2.6 Discussion

Our previous studies have identified a critical role for cav-1 in the ability of MC to produce extracellular matrix proteins and profibrotic cytokines, both basally and in response to profibrotic stimuli [77–79]. Increased cav-1 expression has been observed in several fibrotic kidney diseases in both animal models and humans [81,127–129]. Furthermore, studies using cav-1 knockout mice and cav-1 deficient cells have shown that the elimination of cav-1 can protect against fibrosis both *in vivo* and *in vitro*, while having no adverse effects on blood pressure and renal function [75,77,79,130]. As of now, targeting cav-1 via therapeutic approaches has not been feasible. In our efforts to better understand how cav-1 deficient MC are protected against the profibrotic effects of several stimuli relevant to chronic kidney disease such as high glucose, TGFβ1 and mechanical stress [77–79], we identified significant upregulation of the antifibrotic protein FST in mouse MC lacking cav-1. Functionally, we show that inhibiting the expression of FST in cav-1 KO MC restored matrix production both basally and in response to profibrotic stimuli and that supplementing exogenous FST in cav-1 WT MC protected against matrix protein production. We also identified the mechanism by which cav-1 deficiency led to FST upregulation. Our data now identify a novel role for cav-1 in controlling activity of

the transcription factor Sp1, a critical regulator of FST transcription in MC. We further provide mechanistic insight into Sp1 regulation by cav-1, showing that this occurs at the post-translational level through control of PI3K-PKCζ signaling. Figure 2-7 highlights our proposed molecular mechanism through which cav-1 regulates expression of the antifibrotic protein FST in glomerular mesangial cells. These findings carry important implications for the potential use of therapies targeting this pathway in the treatment of chronic kidney disease, as discussed below.

Interestingly, a related follistatin-domain containing protein, follistatin-like 3 (FSTL-3), has been shown to protect against matrix production in MC exposed to high glucose [131]. FSTL-3 functions similarly to FST, binding and neutralizing similar TGFβ superfamily family members. However, it is distinct from FST due to the absence of a heparin binding motif, preventing its binding to cell surface heparan-sulfate proteoglycans as occurs with FST [132,133]. Thus, difference in *in vivo* biologic activities between FSTL-3 and FST likely exist. We did not find any differences in FSTL-3 transcript expression in cav-1 WT and KO MC (Fig. 2-9; Supplemental Fig. 2), thus excluding a major contribution of FSTL-3 to the antifibrotic phenotype we observed in cav-1 KO MC.

Several transcription factors have thus far been found to regulate FST expression in different cell types, including CREB, Smad3 and β-catenin [121,134–136]. Sp1, a ubiquitously expressed transcription factor, was also noted to activate the FST promoter in intestinal epithelial cells [121]. Our findings in MC support an important role for Sp1 in regulation of the FST promoter, and further identify elevated Sp1 activity as the mechanism by which cav-1 deletion leads to FST upregulation. Interestingly, we found

that only a very short segment (123bp) of the proximal promoter, containing two Sp1 binding sites, regulates FST promoter activity both basally and in response to cav-1 deletion. Concurrent with our findings, a region 262bp upstream of the translation start site was previously shown to be critical for the regulation of FST expression in a manner reflecting endogenous mRNA expression [119].

How Sp1 activity is regulated by cav-1 is not as yet understood. It is well known, however, that it is under tight regulation via numerous post-translational modifications such as phosphorylation, acetylation, sumoylation, ubiquitylation, and glycosylation [122]. These can positively or negatively influence Sp1 DNA binding and activity [122]. Since cav-1 is a well-known regulator of a wide variety of intracellular signaling cascades, we initially assessed whether cav-1 deficiency altered Sp1 phosphorylation, the most well described Sp1 post-translational modification. Our results now reveal novel regulation of Sp1 ser/thr phosphorylation, and hence activation, by cav-1. In seeking to identify the mechanism behind this increased phosphorylation, we further identified augmented activity of PI3K-PKCζ signaling in cav-1 deficient MC as a mediator of this increased Sp1 phosphorylation.

PI3K is a lipid kinase that catalyzes the formation of a family of phosphoinositides, including PIP3, with an important role in cell growth and transformation [137,138]. Our studies illustrate that cav-1 deficient MC exhibit basally elevated PI3K activity and signaling compared to cav-1 WT cells. Although a few studies have assessed the regulation of PI3K by cav-1, these show discordant effects, likely dependent on cell type. Thus, in cancer cells (HeLa), cav-1 overexpression increased

PI3K activity [139], while in fibroblasts the opposite effects were observed [140]. In some studies, while PI3K activity was not assessed directly, downstream signaling was found to be regulated by cav-1. For example, in hepatoma cells, increased cav-1 expression induced by plasmalogens was associated with decreased Akt activity, suggesting inhibitory effects of cav-1 on PI3K [141]. The inhibitory association of cav-1 with p85, the regulatory subunit of PI3K, was suggested to mediate this effect [140]. However, inhibition of PI3K signaling by cav-1 may also occur through an indirect mechanism by augmenting activity of PTEN (phosphatase and tensin homolog). This lipid phosphatase acts as the primary suppressor of PI3K signaling by dephosphorylating PIP3 [142]. Xia et al demonstrated that cav-1 deficient fibroblasts have lower PTEN activity than their WT counterparts. Cav-1 reconstitution increased PTEN membrane localization and activity, and this was associated with a reduction in signaling downstream of PI3K (Akt activity) [143]. Like PI3K, PTEN was also found to physically interact with cav-1 [143]. These data thus suggest both direct and indirect regulation of PI3K by cav-1, and support our findings that cav-1 represses PI3K activity.

The most well studied mediator of PI3K signaling is the ser/thr kinase Akt. Our data, however, excluded a role for Akt in FST regulation by cav-1. Instead, we identified PKCζ, also known to function downstream of PI3K, as the effector for Sp1 activation and FST upregulation in cav-1 deficient MC. PKCζ is a ser/thr kinase which activates Sp1 through phosphorylation of residues in its zinc region [122,144,145]. Unlike most other PKC isoforms, PKCζ is activated without the need for calcium and/or diacylglycerol [146]. Secondary messenger lipids including PIP3 recruit PKCζ from cytosol to the

membrane through binding to its regulatory domain. They can also induce a conformational change that removes auto-inhibition of PKCζ catalytic activity [146,147]. At the membrane, the PI3K-dependent kinase PDK-1 can activate PKCζ through phosphorylation on its activation loop [126]. Similar to several other, but not all, PKC isoforms, PKCζ was shown to interact with the cav-1 scaffolding domain, a region of cav-1 that mediates its interaction with numerous other proteins [148,149]. This interaction was also found to inhibit PKCζ autophosphorylation and kinase activity [148]. Furthermore, PDK1 interaction with cav-1, which reduced its kinase activity, was also found [150]. Cav-1/caveolae thus function at several levels to inhibit PKCζ activation. In disagreement with this, however, PKCζ localization to caveolae was associated with increased activity in response to the lipid metabolite ceramide, highlighting stimulus specificity for the role of cav-1/caveolae in PKCζ activation [151]. Finally, it should be noted that we also observed elevated PKCζ transcript levels in cav-1 deficient MC. The mechanism underlying this will be defined in future studies.

Interestingly, while pharmacologic PI3K and PKCζ inhibition blunted Sp1 activity, GSK, JNK and p38 inhibition in our studies was found to promote Sp1 activity. In agreement with these findings, these kinases have been individually shown to negatively regulate components of the PI3K/PKCζ pathways, which converge to modulate Sp1 activity. For example, in murine microglia cells GSK3 inhibition increased nuclear Sp1 expression and activity along with increased IL-10 production through elevated PI3K activity [152]. In chondrocytes, p38 was shown to bind the regulatory domain of PKCζ, preventing its autophosphorylation and thereby inhibiting its activity [153]. Finally, in

human lung cancer cells, JNK inhibited Sp1 and thereby its downstream target genes that regulate cell growth [154]. However, in some settings, positive regulation of PI3K/PKCζ/Sp1 by JNK has been found. For example, in lung epithelial cells JNK increased Sp1 phosphorylation and activity in repose to oxidative stress [155]. In another study, JNK was found to positively regulate PKCζ through affecting its localization to podosomes [156]. These differences could be attributed to differences in the cell type and stimulus being investigated. Nonetheless, it is likely that these kinases function through modulation of PI3K/PKCζ to affect Sp1 transcriptional activity.

Collectively, our data have thus identified novel regulation of FST transcription by cav-1/caveolae through suppression of PI3K/PKCζ/Sp1 signaling. It is noteworthy that in several fibrotic kidney diseases in both rodent models and humans, renal cav-1 expression is elevated [81,127–129]. This would be expected to attenuate FST expression, thereby inhibiting its protective antifibrotic effect. Therapies to increase activity of Sp1 or its upstream mediators would thus seem to be of potential therapeutic interest. However, activation of PI3K, PKCζ and Sp1 have all also been associated with renal profibrotic effects [157–159]. Indeed, Sp1 was shown to activate the transcription of several profibrotic and matrix protein genes including PAI-1,TGFβ1, fibronectin, PDGF-BB, α-SMA and collagen in various cell types [157,160–162]. Sp1 was also shown to act synergistically with profibrotic signaling molecules such as Smad3 in response to TGFβ1 to promote matrix production [163]. Furthermore, inhibition of Sp1 activity using ring-type Sp1 decoy oligonucleotides attenuated kidney fibrosis in the unilateral obstruction model [164]. While these data support a profibrotic role for Sp1, it should be noted that

Sp1 also regulates a concurrent protective response to limit the extent of fibrosis. Thus, Sp1 mediates induction of the antifibrotic protein Smad7 by TGFβ1 [165], and as our data show, of the antifibrotic protein FST.

Taken together, our data show a novel role for cav-1 in the post-translational regulation of Sp1 through PI3K/PKCζ signaling. Importantly, we established that Sp1, which has thus far been identified as a profibrotic factor in kidney disease, is a critical transcriptional regulator for the antifibrotic protein FST. Thus, therapeutically targeting enhanced activity of PI3K/PKCζ/Sp1 is not a viable option for the treatment of kidney disease due to potential unwanted profibrotic effects. Future studies should further address the therapeutic potential of FST administration in the treatment of fibrotic kidney disease.

2.7 Conclusion

Our results identified Sp1 as the critical transcription factor regulating activation of the FST promoter in MC lacking cav-1 through binding to a region within 123bp of the transcription start site. Absence of cav-1 increases Sp1 transcriptional activity through augmented activation of phosphoinositide 3-kinase (PI3K) and its downstream mediator protein kinase C (PKC) zeta. In turn, PKC zeta phosphorylates and activates Sp1. These findings describe a novel transcriptional mechanism regulated by cav-1 which functions to repress the expression of FST, a major antifibrotic protein. These findings provide important knowledge that will inform the development of antifibrotic treatment strategies for chronic kidney disease.

Declarations:

Acknowledgements: We acknowledge the support of St. Joseph's Healthcare for nephrology research. We thank Dr. J. Yoon for providing mFST4-FL luciferase construct, Dr. P. Di for providing 3xmt Sp1 luciferase construct, Dr. J. Clifford for providing CMV-GST-Sp1-HA construct and Dr. N. Gautam (Addgene plasmid # 85223) for providing PH Akt-Venus construct.

Funding: This work was supported by the Canadian Institutes of Health Research (CIHR) (JCK), MOP 136868 and Kidney Foundation of Canada (JCK), KFOC160011. NM is the recipient of a studentship award from the Research Institute of St. Joe's Hamilton.

Availability of data and materials: All data generated or analyzed during this study are included in this published article.

Authors' contributions: NM, DZ, RL, TW, AG, PP performed experiments and analysed data. NM wrote the manuscript. NM and JCK conceived the ideas. JCK edited the manuscript. BG assisted with animal studies.

All authors read and approved the final manuscript.

Ethics approval and consent to participate: N/A.

Competing interests: The authors declare that they have no competing financial interests.

2.8 Figures

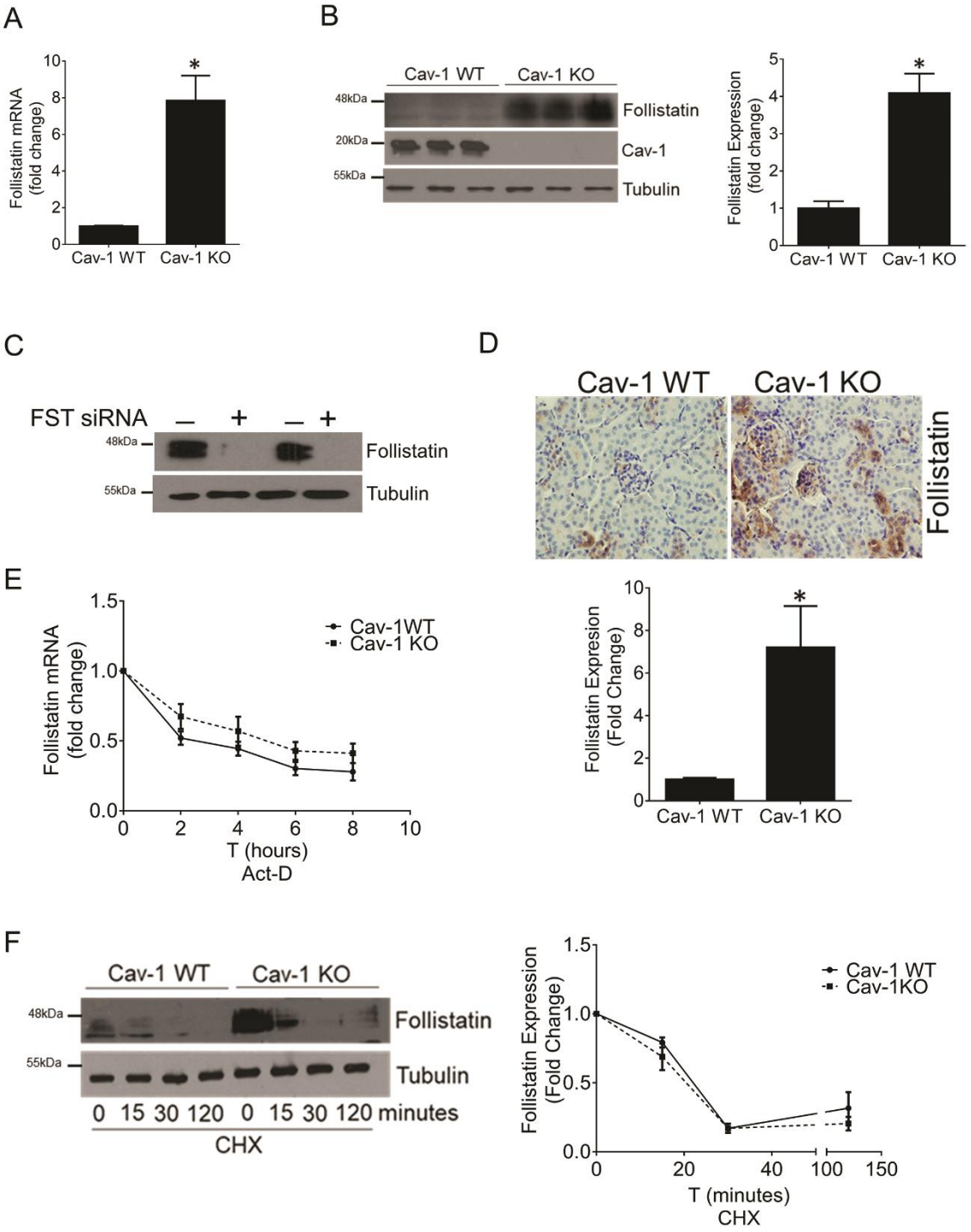
A
Follistatin mRNA (fold change)
Cav-1 WT
Cav-1 KO
B
Cav-1 WT
Cav-1 KO
48kDa
Follistatin
20kDa
Cav-1
55kDa
Tubulin
Follistatin Expression (fold change)
C
FST siRNA – + – +
48kDa
Follistatin
55kDa
Tubulin
D
Cav-1 WT
Cav-1 KO
Follistatin
Follistatin Expresion (Fold Change)
E
Follistatin mRNA (fold change)
Cav-1WT
Cav-1 KO
T (hours)
Act-D
F
Cav-1 WT
Cav-1 KO
48kDa
Follistatin
55kDa
Tubulin
0 15 30 120 0 15 30 120 minutes
CHX
Follistatin Expression (Fold Change)
Cav-1 WT
Cav-1KO
T (minutes)
CHX

Figure 2-1. Cav-1 transcriptionally represses FST.

In primary cav-1 KO MC, FST expression was increased at both the transcript level (n=12, *p<0.05) (A) and protein level (n=9, *p<0.05) (B). (C) Immunoblotting after FST downregulation with siRNA showed the specificity of the FST antibody in cav-1 KO MC (n=2). (D) FST was elevated in the kidneys of cav-1 KO mice (n=4 mice, *p<0.05, representative micrographs shown). (E) MC were treated with the transcriptional inhibitor actinomycin D (1µg/ml), and FST transcript assessed at the indicated times. FST mRNA stability did not differ between cav-1 WT and KO MC (n=5). (F) Cav-1 WT and KO MC were treated with the translational inhibitor cycloheximide (10µg/ml), and FST protein assessed at the indicated times. FST protein stability was not altered by cav-1 KO (n=3).

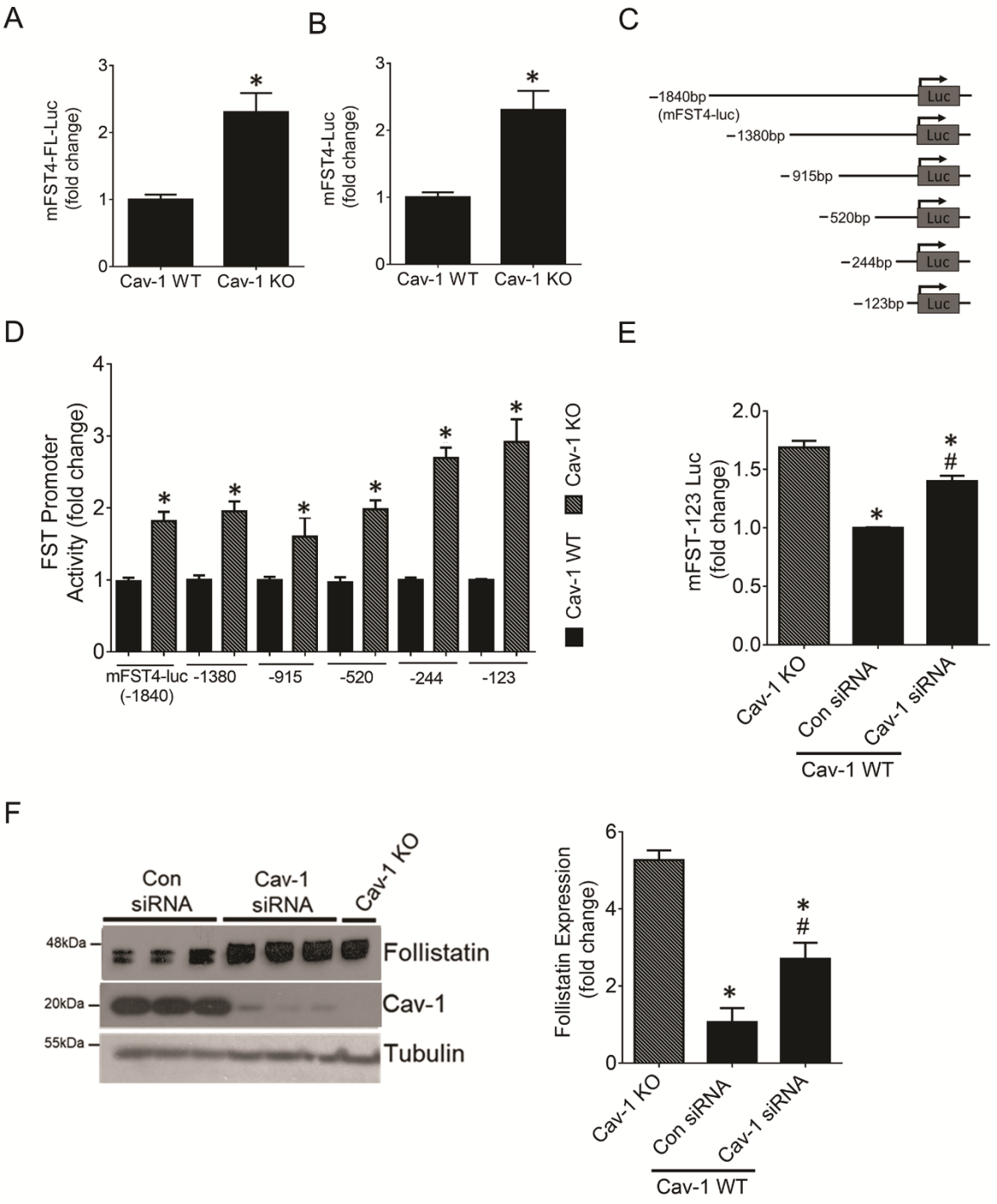
A
mFST4-FL-Luc (fold change)
Cav-1 WT
Cav-1 KO
B
mFST4-Luc (fold change)
Cav-1 WT
Cav-1 KO
C
−1840bp (mFST4-luc)
−1380bp
−915bp
−520bp
−244bp
−123bp
Luc
D
FST Promoter Activity (fold change)
Cav-1 KO
Cav-1 WT
mFST4-luc (-1840)
-1380
-915
-520
-244
-123
E
mFST-123 Luc (fold change)
Cav-1 KO
Con siRNA
Cav-1 siRNA
Cav-1 WT
F
Con siRNA
Cav-1 siRNA
Cav-1 KO
48kDa
Follistatin
20kDa
Cav-1
55kDa
Tubulin
Follistatin Expression (fold change)
Cav-1 KO
Con siRNA
Cav-1 siRNA
Cav-1 WT

Figure 2-2. Cav-1 regulates activity of the FST promoter.

Cav-1 WT and KO MC were transfected with (A) the full-length FST promoter luciferase construct or (B) the full-length FST promoter luciferase construct lacking intron 1 and exon 1. KO MC exhibited significantly elevated transcriptional activity of both constructs (n=6, *$p<0.05$). (C) Graphical representation of the synthesized FST promoter deletion constructs. (D) Cav-1 WT and KO MC were transfected with the FST promoter deletion constructs shown in (C). Transcriptional activation of all constructs was elevated in cav-1 KO MC (n=6-20, *$p<0.05$ vs WT for each construct). (E, F) Cav-1 knockdown in WT MC significantly increased the transcriptional activation of the -123bp FST promoter (E) and FST protein expression (F) compared with control siRNA-transfected KO MC (for both, n=6, *vs KO, #vs WT con siRNA, $p<0.05$).

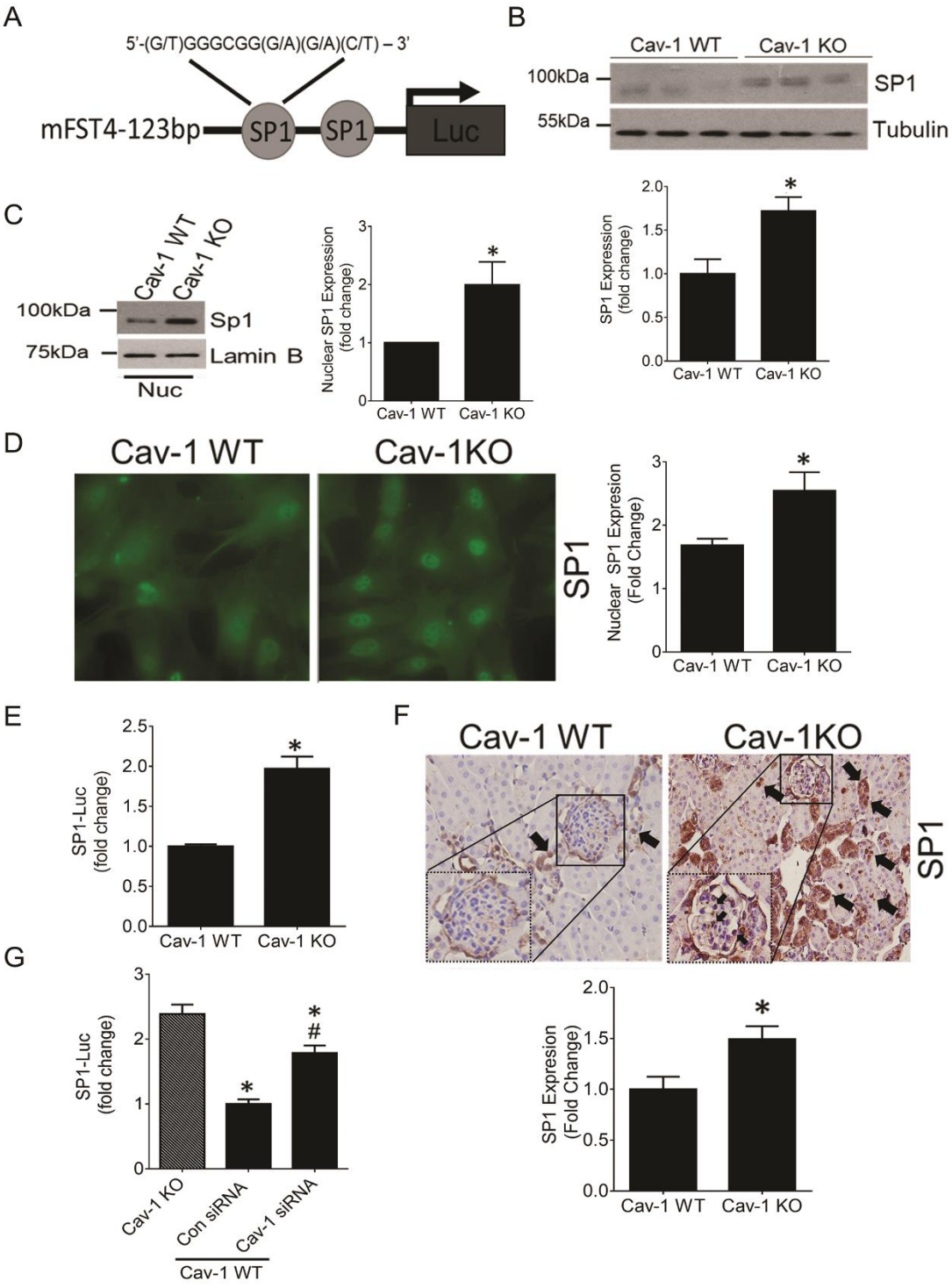
A
5'-(G/T)GGGCGG(G/A)(G/A)(C/T) – 3'
mFST4-123bp
SP1
SP1
Luc
B
Cav-1 WT
Cav-1 KO
100kDa
55kDa
SP1
Tubulin
C
Cav-1 WT
Cav-1 KO
100kDa
Sp1
75kDa
Lamin B
Nuc
Nuclear SP1 Expression (fold change)
Cav-1 WT
Cav-1 KO
SP1 Expression (fold change)
Cav-1 WT
Cav-1 KO
D
Cav-1 WT
Cav-1KO
SP1
Nuclear SP1 Expresion (Fold Change)
Cav-1 WT
Cav-1 KO
E
SP1-Luc (fold change)
Cav-1 WT
Cav-1 KO
F
Cav-1 WT
Cav-1KO
SP1
SP1 Expresion (Fold Change)
Cav-1 WT
Cav-1 KO
G
SP1-Luc (fold change)
Cav-1 KO
Con siRNA
Cav-1 siRNA
Cav-1 WT

Figure 2-3. Sp1 expression and activity are elevated by cav-1 deletion.

(A) Predicted Sp1 transcription factor binding sites within the -123bp region of the FST promoter are shown. Sp1 protein expression was significantly increased in cav-1 KO compared to WT MC as assessed by western blotting of total cell lysate (n=12, *$p<0.05$) (B) and nucleus (n=5, *$p<0.05$) (C), as well as by immunofluorescence microscopy (n=5, *$p<0.05$, representative micrographs shown) (D). (E) Sp1 activity, as assessed by the Sp1 reporter construct Sp1-luc, was elevated in cav-1 KO MC (n=16, *$p<0.05$). (F) Sp1 expression and nuclear localization (arrows) were elevated in the kidneys of cav-1 KO mice, seen in both glomeruli (magnified glomerular area shown within dotted box) and tubules (n=3 mice, *$p<0.05$, representative micrographs shown). (G) Cav-1 knockdown in WT MC significantly increased Sp1 activity compared with control siRNA-transfected KO MC (n=6, *vs KO, #vs WT con siRNA, $p<0.05$).

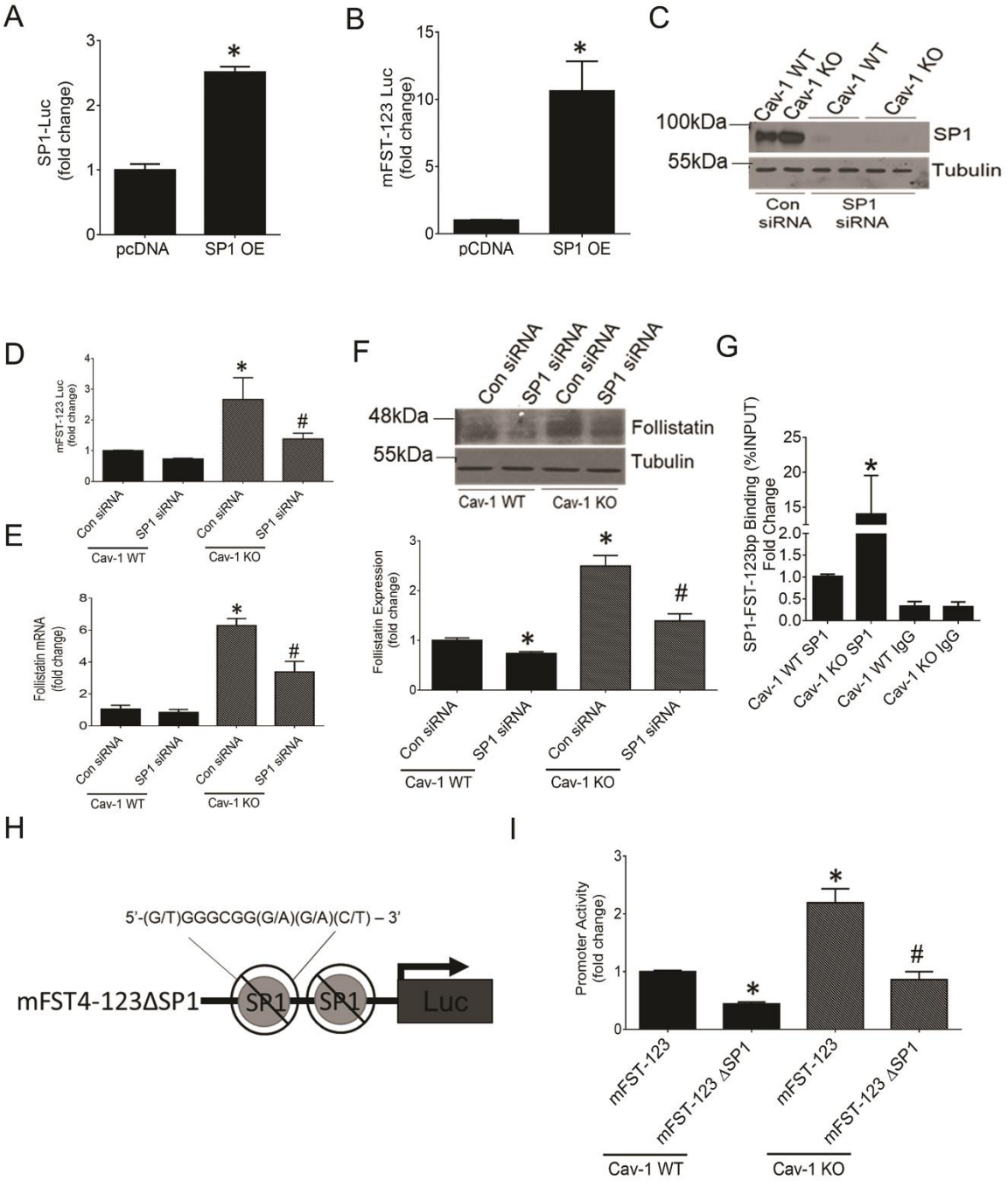
A
SP1-Luc (fold change)
pcDNA
SP1 OE
B
mFST-123 Luc (fold change)
pCDNA
SP1 OE
C
Cav-1 WT
Cav-1 KO
Cav-1 WT
Cav-1 KO
100kDa
55kDa
SP1
Tubulin
Con siRNA
SP1 siRNA
D
mFST-123 Luc (fold change)
Con siRNA
SP1 siRNA
Con siRNA
SP1 siRNA
Cav-1 WT
Cav-1 KO
E
Follistatin mRNA (fold change)
F
Con siRNA
SP1 siRNA
Con siRNA
SP1 siRNA
48kDa
55kDa
Follistatin
Tubulin
Cav-1 WT
Cav-1 KO
Follistatin Expression (fold change)
G
SP1-FST-123bp Binding (%INPUT) Fold Change
Cav-1 WT SP1
Cav-1 KO SP1
Cav-1 WT IgG
Cav-1 KO IgG
H
5'-(G/T)GGGCGG(G/A)(G/A)(C/T) – 3'
mFST4-123ΔSP1
SP1
SP1
Luc
I
Promoter Activity (fold change)
mFST-123
mFST-123 ΔSP1
mFST-123
mFST-123 ΔSP1
Cav-1 WT
Cav-1 KO

Figure 2-4. Sp1 binds the -123bp region of the FST promoter to regulate its activity. Expression of constitutively active Sp1 in cav-1 WT MC increased activity of both the Sp1 reporter construct (A) (n=3, *$p<0.05$) and mFST-123-luc (B) (n=6, *$p<0.05$). (C) Effective siRNA-mediated Sp1 knockdown in cav-1 WT and KO MC was confirmed by immunoblotting. (D) Sp1 knockdown abolished the increased transcriptional activity of the -123bp FST promoter in cav-1 KO MC, with little effect in WT cells (n=6, *vs WT con siRNA, #vs KO con siRNA, $p<0.05$). (E) Sp1 knockdown repressed the elevation in FST mRNA expression in cav-1 KO MC (n=3, *vs WT con siRNA, #vs KO con siRNA, $p<0.05$). (F) Similar effects of Sp1 knockdown on FST protein expression were seen (n=4, *vs WT con siRNA, #vs KO con siRNA, $p<0.05$). (G) Sp1 binding within the -123bp region of the FST promoter at the predicted Sp1 binding sites was significantly elevated in cav-1 KO MC as assessed by ChIP (n=14, $p<0.05$). (H) Graphical representation of the deletion of the two predicted Sp1 binding sites within the -123bp promoter region of FST (mFST4-123ΔSp1-luc). (I) Deletion of the two Sp1 binding sites attenuated transcriptional activity of mFST4-123-luc in cav-1 WT and normalized activity in cav-1 KO MC to levels seen in WT cells (n=9, *vs WT mFST-123-luc, #vs KO mFST-123-luc, $p<0.05$).

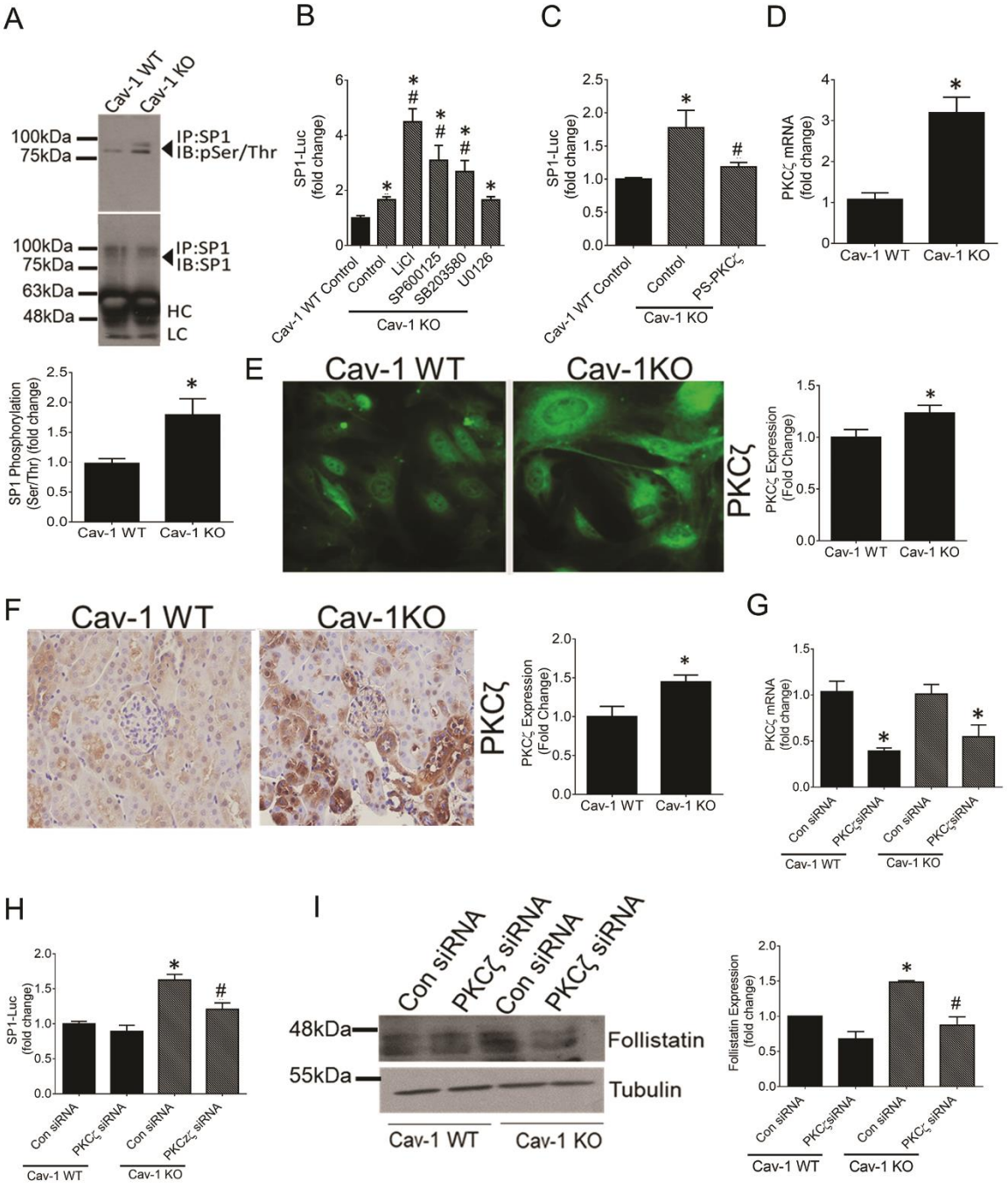
A
Cav-1 WT
Cav-1 KO
100kDa
75kDa
IP:SP1
IB:pSer/Thr
100kDa
75kDa
63kDa
48kDa
IP:SP1
IB:SP1
HC
LC
SP1 Phosphorylation (Ser/Thr) (fold change)
Cav-1 WT
Cav-1 KO
B
SP1-Luc (fold change)
Cav-1 WT Control
Control
LiCl
SP600125
SB203580
U0126
Cav-1 KO
C
SP1-Luc (fold change)
Cav-1 WT Control
Control
PS-PKCζ
Cav-1 KO
D
PKCζ mRNA (fold change)
Cav-1 WT
Cav-1 KO
E
Cav-1 WT
Cav-1KO
PKCζ
PKCζ Expression (Fold Change)
Cav-1 WT
Cav-1 KO
F
Cav-1 WT
Cav-1KO
PKCζ
PKCζ Expression (Fold Change)
Cav-1 WT
Cav-1 KO
G
PKCζ mRNA (fold change)
Con siRNA
PKCζ siRNA
Con siRNA
PKCζ siRNA
Cav-1 WT
Cav-1 KO
H
SP1-Luc (fold change)
Con siRNA
PKCζ siRNA
Con siRNA
PKCζ siRNA
Cav-1 WT
Cav-1 KO
I
Con siRNA
PKCζ siRNA
Con siRNA
PKCζ siRNA
48kDa
Follistatin
55kDa
Tubulin
Cav-1 WT
Cav-1 KO
Follistatin Expression (fold change)
Con siRNA
PKCζ siRNA
Con siRNA
PKCζ siRNA
Cav-1 WT
Cav-1 KO

Figure 2-5. Increased PKCζ induces Sp1 activity to upregulate FST in cav-1 KO MC. (A) Sp1 was immunoprecipitated from cav-1 WT and KO MC and immunoblotted for serine/threonine phosphorylation. Elevated phosphorylation was seen in KO cells (n=3, representative blots shown). (B) None of the following kinase inhibitors reduced Sp1 activity, assessed using the Sp1 reporter construct, to that seen in WT cells: GSK3β inhibitor LiCl (10mM), JNK inhibitor SP600125 (20μM), p38 inhibitor SB203580 (5μM) or MEK/Erk inhibitor U0126 (10μM) for 24h. (n=3-6, *vs WT, #vs KO control, $p<0.05$). (C) PKCζ inhibition with a pseudo-substrate inhibitor peptide (PS-PKCζ) (10μM, 24h) abolished the increased Sp1 activity in cav-1 KO MC (n=9, *vs WT, # vs KO control, $p<0.05$). (D) PKCζ mRNA (n=3, *$p<0.05$) and (E) protein expression (n=2, *$p<0.05$, representative micrographs shown) was significantly elevated in cav-1 KO MC. (F) PKCζ expression was elevated in the kidneys of cav-1 KO mice in both tubules and glomeruli (n=3 mice, *$p<0.05$, representative micrographs shown). (G) Effective siRNA-mediated PKCζ knockdown was confirmed by qRT-PCR in cav-1 WT and KO MC (n=3,*$p<0.05$ vs con siRNA for both WT and KO MC normalized to their own controls). (H, I) PKCζ knockdown reduced both the increased Sp1 activity (H) and FST protein expression (I) in KO MC to levels seen in WT cells (G: n=9, *vs WT con siRNA, # vs KO con siRNA, $p<0.05$; H: n=3, *vs WT con siRNA, #vs KO con siRNA, $p<0.05$).

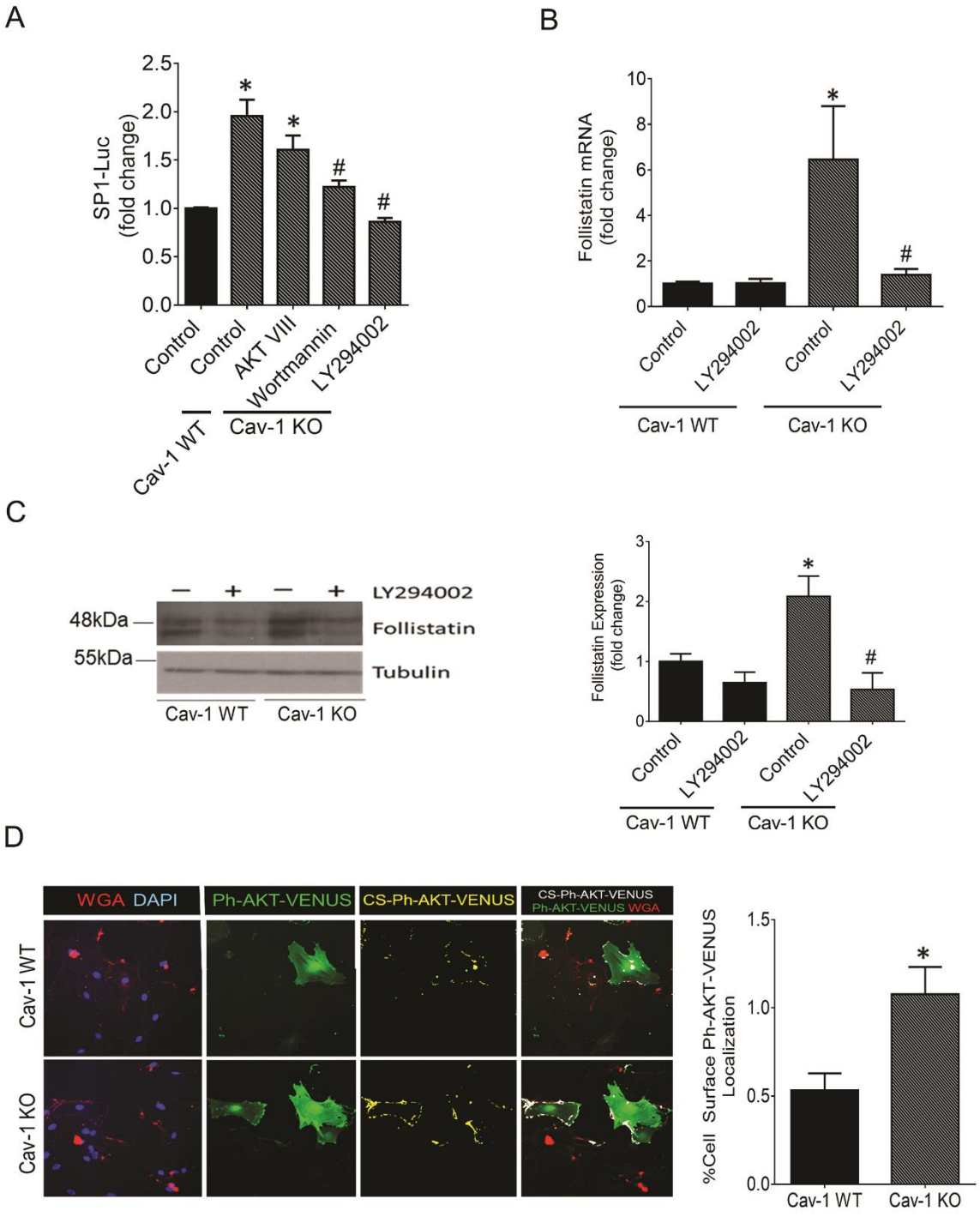
A
SP1-Luc (fold change)
2.5
2.0
1.5
1.0
0.5
0.0
*
*
#
#
Control
Control
AKT VIII
Wortmannin
LY294002
Cav-1 WT
Cav-1 KO
B
Follistatin mRNA (fold change)
10
8
6
4
2
0
*
#
Control
LY294002
Control
LY294002
Cav-1 WT
Cav-1 KO
C
— + — + LY294002
48kDa
Follistatin
55kDa
Tubulin
Cav-1 WT
Cav-1 KO
Follistatin Expression (fold change)
3
2
1
0
*
#
Control
LY294002
Control
LY294002
Cav-1 WT
Cav-1 KO
D
WGA DAPI
Ph-AKT-VENUS
CS-Ph-AKT-VENUS
CS-Ph-AKT-VENUS Ph-AKT-VENUS WGA
Cav-1 WT
Cav-1 KO
%Cell Surface Ph-AKT-VENUS Localization
1.5
1.0
0.5
0.0
*
Cav-1 WT
Cav-1 KO

Figure 2-6. PI3K is a caveolin-1-regulated mediator of PKCζ required for FST upregulation in cav-1 KO MC.

(A) The Akt inhibitor Akt VIII (20 μM) or the PI3K inhibitors wortmannin (500nM) or LY294002 (20 μM) for 24h abolished the increased Sp1 activity observed in cav-1 KO vs WT MC (n=6, *vs WT, # vs KO control, $p<0.05$). (B) PI3K inhibition prevented the increase in FST mRNA expression observed in cav-1 KO MC (n=5, *vs WT, #vs KO control, $p<0.05$). (C) PI3K inhibition also abolished the increased FST protein expression observed in cav-1 KO vs WT MC (n=4, *vs WT, #vs KO control, $p<0.05$). (D) Cav-1 WT and KO MC were transfected with the fluorescent PIP3 biosensor PH AKT-Venus (green). Elevated basal PI3K activity, as observed by increased PIP3 production at the plasma membrane, delineated by WGA (red), was seen in cav-1 KO MC. This is highlighted by the white co-localization mask (n=3, 21 micrographs quantified, with representative micrographs shown).

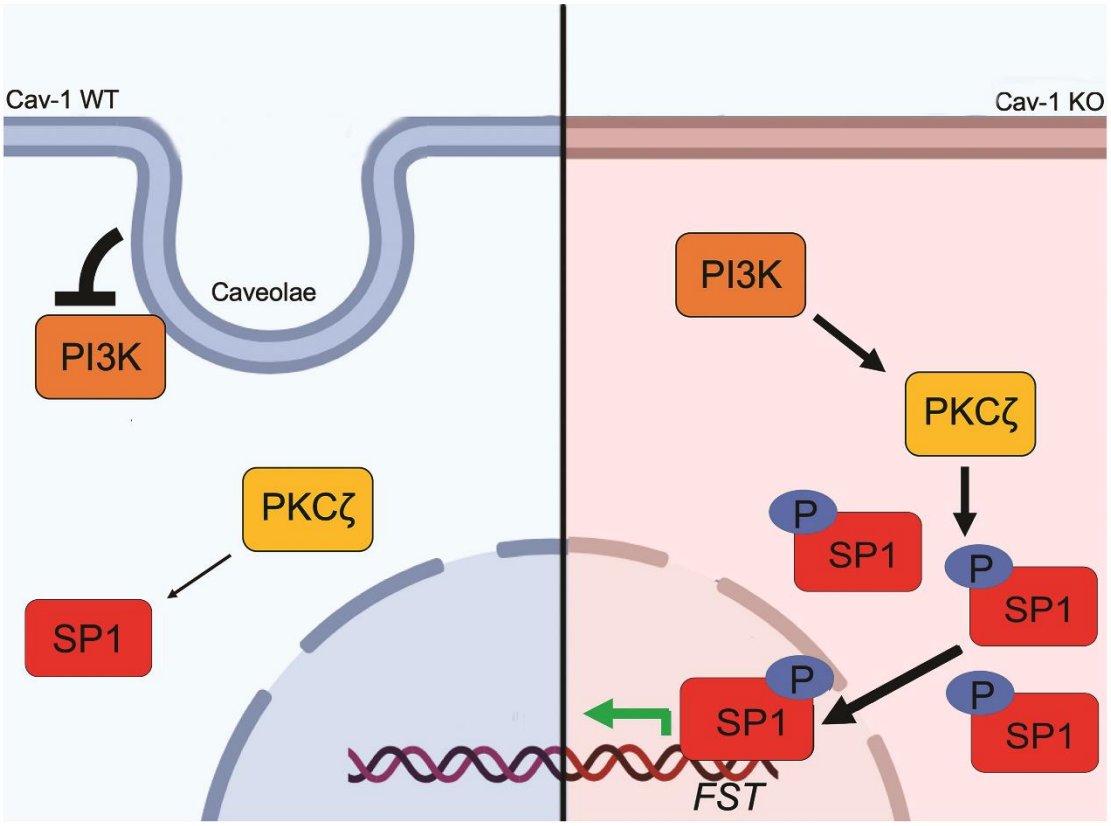

Figure 2-7. Proposed molecular mechanism for the regulation of FST by cav-1.

In the absence of cav-1/caveolae, enhanced PI3K activity activates PKCζ which augments Sp1 phosphorylation, nuclear accumulation and activity. This increases Sp1 binding to the -123bp region of the FST promoter, resulting in elevated FST transcriptional activation and protein expression.

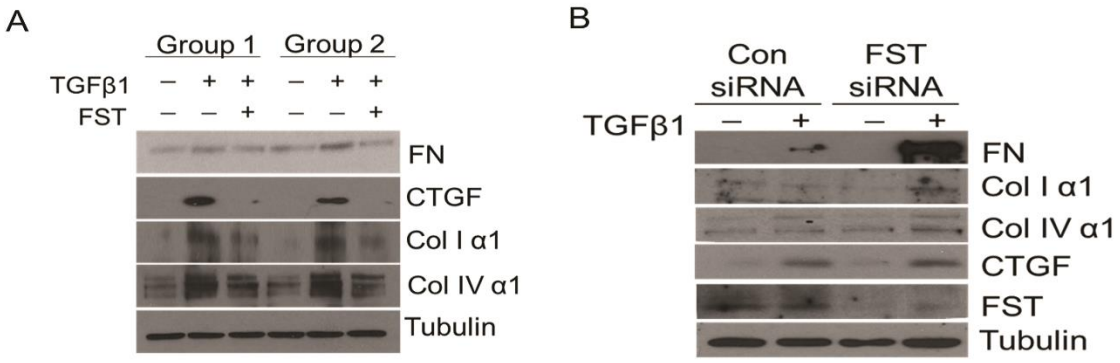

Figure 2-8. Supplemental Figure 1.

(A) Exogenous recombinant FST (1μg/ml) protects against TGFβ1 (0.5ng, 24h)-induced extracellular matrix (ECM) production in cav-1 WT MC (n=2). (B) siRNA (50nM)-mediated FST downregulation augments TGFβ1 (0.5ng, 24h)-induced ECM production in cav-1 KO MC (n=2).

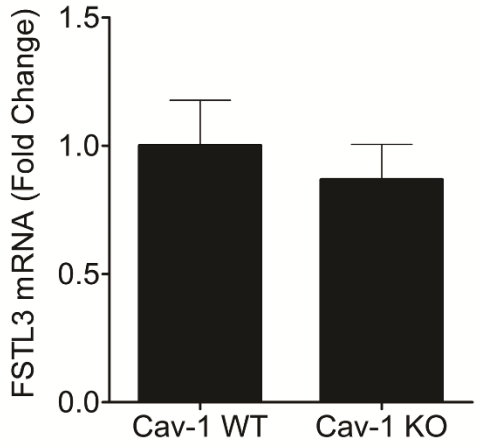

Figure 2-9. Supplemental Figure 2.

The mRNA expression of FSTL-3 is not significantly different between cav-1 WT and KO MC (n=6).

Table 2-1. Drugs

Drug	***Dose***	***Source***
Cycloheximide	10µg/ml	Sigma
Actinomycin D	1µg/ml	Sigma
PS-PKC ζ (pseudosubstrate)	10µM	Tocris
Wortmannin	500nM	Sigma
LY-294002	20µM	Sigma
LiCl	10mM	Sigma
AKT VIII	20µM	EMD
U0126	10µM	Promega
SB203580	5µM	Sigma
SP600125	20µM	EMD
Follistatin	1µg/ml	R&D Systems

Table 2-2. Plasmids and siRNA.

siRNA or Plasmid	***Amount***	***Source***
Mouse Sp1 ON Target Smart Pool siRNA	50nM	Dharmacon
Mouse PKCζ ON Target Smart Pool siRNA	100nM	Dharmacon
Mouse Cav-1 Silencer Select SiRNA	150nM	Life Tech
Mouse Follistatin Silencer Select SiRNA	50nM	Life Tech
On-target plus siCONTROL non-targeting siRNA	50nM	Dharmacon
Control Silencer Select SiRNA	50nM	Life Tech
mFST4-FL Luciferase		Dr. Jeong Yoon
mFST4Δintron1-1840 (mFST-4 Luciferase)		Generated in lab
mFST4Δintron1-1380		Generated in lab
mFST4Δintron1-915		Generated in lab
mFST4Δintron1-520		Generated in lab
mFST4Δintron1-244		Generated in lab
mFST4Δintron1-123		Generated in lab
mFST4Δintron1-123 ΔSp1		Generated in lab
3xmt Sp1 Luciferase		Dr. Peter Di
pCMV β-galactosidase		Clonetech
CMV-GST-Sp1-HA		Dr. Jane Clifford
PH Akt-Venus		Dr. Narasimhan Gautam (Addgene plasmid # 85223)
pcDNA3.1(+) (plasmid)		Thermo Scientific

Table 2-3. Antibodies.

Antibody	***Application***	***Dilution/Amount***	***Source***
Caveolin-1	WB	1:1,000	BD Biosciences; 610059
Follistatin	WB	1:1,000	Santa Cruz; sc-30194
Follistatin	IHC	1:100	Proteintech ; 60060-1-Ig
Sp1	WB	1:1,000	Pierce; 82406
Sp1	CHIP/IP and IHC/IF	1µg and 1:500	Abcam; ab13370
Mouse IgG	IP	1µg	Millipore; 12371
pSerine/threonine	WB	1:1000	BD Transduction; 612548
PKCζ	IHC and IF	1:100 and 1:50	Santa Cruz; sc-393218
α-Tubulin	WB	1:10,000	Sigma; T6074

Table 2-4. qPCR Primers.

Gene	***Forward***	***Reverse***
FST	AAAACCTACCGCAACGAATG	GGTCTGATCCACCACACAAG
Sp1–FST-123bp (CHIP)	TCACCTGATTCACACTGAAC	TTCAATGGACGTCAGAAGCC
PKCζ	GCCTCCCTTCCAGCCCCAGA	CACGGACTCCTCAGCAGACAGCA
FSTL3	ACTCTGTGGCAACAACAACG	TTCTCTTCCTCCTCTGCTGG
18s	GCCGCTAGAGGTGAAATTCTTG	CATTCTTGGCAAATGCTTTCG

Table 2-5. Cloning Sequences.

Construct	***Forward***	***Reverse***
mFST4 Δintron1 -1840	CATGGTACCAGATTAAGAAGGATGTGAAG	CATGCTAGCCGCGCGATTCAATGGACGTC
mFST4 Δintron1 -1380	CATGGTACCGGGCTAGAGAAGAAGGGCGA	CATGCTAGCCGCGCGATTCAATGGACGTC
mFST4 Δintron1 -915	CATGGTACCGCGACGAAGTGAAAGGGGAG	CATGCTAGCCGCGCGATTCAATGGACGTC
mFST4 Δintron1-520	CATGGTACCAGAGGTGCTGGGGACCCAT	CATGCTAGCCGCGCGATTCAATGGACGTC
mFST4 Δintron1-244	CATGGTACCGCCGCTTTGATTTCGGGCAC	CATGCTAGCCGCGCGATTCAATGGACGTC
mFST4 Δintron1-123	CATGGTACCTCGGTCGCGGCCGCCCT	CATGCTAGCCGCGCGATTCAATGGACGTC

mFST4Δintron1-123ΔSp1 *(deleted Sp1 binding sites are underlined)*

Forward Strand/Sense	***Reverse Strand/Anti-Sense***
CTCGGTCGCGG<u>CCGCCC</u>TCCCACAGCCCCACACACTGGGAGA<u>CCGCCC</u>ACCGCAAACCTCGGAGACCCCCGTCTAGATTTAAAGCGCGGCTGCGCCCGGCTTCTGACGTCCATTGAATCGCGCG	CTAGCGCGCGATTCAATGGACGTCAGAAGCCGGGCGCAGCCGCGCTTTAAATCTAGACGGGGGTCTCCGAGGTTTGCGGT<u>G</u><u>GGCGG</u>TCTCCCAGTGTGTGGGGCTGTGGGA<u>GGGCGG</u>CCGCGACCGAGGTAC

Chapter 3: Follistatin Protects against Glomerular Mesangial Cell Apoptosis and Oxidative Stress to Ameliorate Chronic Kidney Disease

Title: Follistatin Protects against Glomerular Mesangial Cell Apoptosis and Oxidative Stress to Ameliorate Chronic Kidney Disease

Authors: Neel Mehta, Agata L. Gava, Dan Zhang, Bo Gao, Joan C. Krepinsky

Corresponding Author: Dr. Joan C. Krepinsky, Department of Nephrology, St. Joseph Hospital, 50 Charlton Ave E, Room T3311, Hamilton, Ontario L8N 4A6, Canada, Telephone: (905) 522-1155 x 34991; FAX: (905) 540-6589; Email: krepinj@mcmaster.ca

Citation: Mehta, N., Gava, A. L., Zhang, D., Gao, B. & Krepinsky, J. Follistatin Protects against Glomerular Mesangial Cell Apoptosis and Oxidative Stress to Ameliorate Chronic Kidney Disease. Antioxid. Redox Signal. ars.2018.7684 (2019). doi:10.1089/ars.2018.7684

3.1 Preface

Significance to thesis: Therapeutic interventions to inhibit the progression of renal fibrosis in CKD are not well established. The purpose of this study was to investigate the therapeutic potential of a TGFβ superfamily neutralizing protein, FST, in the progression of CKD through assessing its role in modulating apoptosis and oxidative stress in glomerular mesangial cells and in *in vivo* in mice with CKD. Out study identified FST as a potent inhibitor of apoptosis through neutralization of reactive oxygen species independent of activin neutralization. *In vivo* administration of FST to mice with CKD protected against renal cell apoptosis and oxidative stress while ameliorating renal fibrosis and improving kidney function. These findings suggest that follistatin is a novel therapeutic agent for delaying the progression of CKD.

Author's contribution: NM and AG performed experiments and analysed data, DZ performed experiments, NM wrote the manuscript, AG, NM and JCK conceived the ideas, BG assisted with animal studies, all authors read and approved the final manuscript.

- DZ and BG assisted with mouse handling and tissue/specimen collection.
- DZ and AG assisted with western blotting experiments in Figures 1 and 2.

3.2 Abstract

Aims: Interventions to inhibit oxidative stress and apoptosis, important pathogenic contributors towards the progression of chronic kidney disease (CKD), are not well established. Here, we investigated the role of a TGFβ superfamily neutralizing protein, follistatin (FST), in the regulation of apoptosis and oxidative stress in glomerular mesangial cells (MC) and in the progression of CKD.

Results: The ER stress inducer thapsigargin (Tg), known to cause MC apoptosis, led to a post-translational increase in the expression of FST. Recombinant FST protected, while FST down-regulation augmented, Tg-induced apoptosis without affecting Ca^{2+} release or ER stress induction. Although activins are the primary ligands neutralized by FST, their inhibition with neutralizing antibodies did not affect Tg-induced apoptosis. Instead, FST protected against Tg-induced apoptosis through neutralization of reactive oxygen species (ROS) independently of its ability to neutralize activins. Importantly, administration of FST to mice with CKD protected against renal cell apoptosis and oxidative stress. This was associated with improved kidney function, reduced albuminuria and attenuation of fibrosis.

Innovation and Conclusion: Independent of its activin neutralizing ability, FST protected against Tg-induced apoptosis through neutralization of ROS and consequent suppression of oxidative stress, seen both *in vitro* and *in vivo*. Importantly, FST also ameliorated fibrosis and improved kidney function in CKD. FST is thus a novel potential therapeutic agent for delaying the progression of CKD.

3.3 Introduction

Chronic kidney disease (CKD) is a major cause of morbidity and mortality, affecting more than 10% of the world's population [6]. It is characterized by an excess of profibrotic and inflammatory cytokines, most notably transforming growth factor beta (TGFβ) and its family members, that lead to cellular stresses including endoplasmic reticulum (ER) stress and oxidative stress. These result in renal cell injury and fibrosis that lead to progressively worsening renal dysfunction and eventually kidney failure [38,86–88]. Although oxidative stress and apoptosis occur in several renal cell types, these processes in glomerular mesangial cells (MC) play a major role in glomerular fibrosis and consequent loss of renal function in CKD of varying etiology [20,37,38].

Oxidative stress is an important pathogenic contributor to CKD. The accumulation of excessive reactive oxygen species (ROS) occurs from impaired balance of free radical production and clearance [84,166–168]. ROS arise from the metabolism of oxygen and include small reactive molecules such as superoxide (SO), hydrogen peroxide (H_2O_2), peroxynitrite ($ONOO^-$), hydroxyl radicals (HO), nitric oxide (NO) and the peroxy radical (ROO). Under physiologic conditions, ROS maintain redox homeostasis, act as vital intracellular second messengers and mediate the activation of genes important in processes ranging from cell proliferation to differentiation and growth [166,167]. Excess oxidative stress, however, has been shown to induce apoptosis in several renal cell types including glomerular MC, and is recognized as an important factor in the pathogenesis of CKD of varying etiology [37,84,93].

ER stress is also an established contributor to CKD pathogenesis, with its inhibition reducing the progression of CKD in several studies [86–88]. ER stress was shown to induce apoptosis in renal cells, including MC, through chronic activation of the unfolded protein response (UPR) [86–89,91]. It also induces cellular death by promoting oxidative stress [90,92]. Thus, both oxidative stress and apoptosis are important contributors to the progression of CKD to end-stage renal disease, and interventions that can protect against these stressors would provide important therapeutic benefit [83,169].

Recent work has shown a protective therapeutic role for the secreted glycoprotein follistatin (FST) against ROS production and apoptosis in non-renal cells [97]. FST is an endogenous inhibitor of members of the TGFβ superfamily, with greatest potency against activins. Once activins are bound by FST, they are cleared by internalization of the complex followed by lysosomal degradation [46,57]. Activin A (ActA) has been shown to induce ROS production and mediate apoptosis in several cell types [94–96], and interestingly, elevated serum and kidney ActA was recently found in a mouse CKD model [25]. Although the use of a ligand trap to inhibit ActA signaling attenuated fibrosis in this model, neither ROS nor apoptosis were studied [25].

In the present study, we thus sought to determine whether FST can protect against oxidative stress and apoptosis induced by ER stress in renal MC, and inhibit the progression of CKD *in vivo*. We show for the first time that FST protects against both oxidative stress and apoptosis, and that this occurs through neutralization of ROS in a manner that is independent of activins. *In vivo,* FST alleviated renal oxidative stress,

protected against the development of renal fibrosis, and improved kidney function in a mouse model of CKD.

3.4 Results

The ER stress inducer thapsigargin causes mesangial cell apoptosis and post-translationally increases the expression of follistatin.

The ER-stress inducer thapsigargin (Tg), a non-competitive inhibitor of the sarco/endoplasmic reticulum (ER) Ca^{2+} Mg^{2+}-ATPase (SERCA), is a potent activator of apoptosis in several cell types, including MC [89–92,170]. We first confirmed that Tg promoted apoptosis in cultured primary mouse MCs. Apoptosis was assessed by quantifying the exposure of phosphatidylserine (PS) on the outer leaflet of the plasma membrane using a luminescent Annexin V binding assay. Tg significantly increased PS-Annexin V binding as compared to vehicle-treated cells (Fig. 3-1A). Effector caspases 3 and 7 are members of the cysteine aspartic acid-specific protease family that, once activated through cleavage, irreversibly mark the cell's entry into the apoptotic signaling pathway [83]. Tg significantly increased the enzymatic activity of caspase 3 and 7 (Fig. 3-1B) and led to increased cleavage of caspase 3 (Fig. 3-1C). These results confirm that Tg promotes MC apoptosis.

Although FST has been described to serve as a protective stress responsive protein under several stressors [97,171,172], whether it is regulated by ER stress is unknown. Thus, we first examined the effect of Tg on the expression of FST. Fig. 3-1D shows that Tg time-dependently increased FST protein expression. To determine whether this was

mediated by increased transcription, the effects of Tg on a full-length mouse FST promoter luciferase construct were assessed. Contrary to expectations, FST promoter activity was significantly repressed by Tg (Fig. 3-1E). FST mRNA levels, as assessed by quantitative real-time PCR (qRT-PCR), were also decreased by Tg (Fig. 3-1F). These results show that the increase in FST seen in response to Tg is not mediated by increased transcriptional activity. We next studied the effects of Tg on FST post-translational regulation. To assess whether Tg affects FST protein stability, cycloheximide (CHX) was used to block *de novo* protein synthesis after Tg treatment for 8h. Fig. 3-1G shows that FST protein is normally rapidly degraded, with Tg leading to significant stabilization. Thus, Tg post-translationally increases FST expression through enhancing its protein stability.

Follistatin protects against thapsigargin-induced mesangial cell apoptosis.

Since FST has been shown to function as an anti-apoptotic protein, we hypothesized that the increase in FST in response to Tg may also serve to protect against apoptosis [97,171,172]. We first assessed whether FST down-regulation using siRNA augments Tg-induced apoptosis. Fig. 3-2A confirms downregulation of FST and shows that this exacerbates Tg-induced apoptosis as measured by cleavage of caspase 3, as well as by caspase 3/7 enzymatic activity (Fig. 3-2B). We next assessed the efficacy of exogenous recombinant FST in protecting against Tg-induced apoptosis. Fig. 3-2C shows that FST significantly reduced Tg-induced apoptosis, as assessed by PS-Annexin V binding, caspase 3/7 enzymatic activity (Fig. 3-2D) and caspase 3 cleavage (Fig. 3-2E).

Finally, we assessed the effects of FST overexpression on Tg-induced apoptosis. We transfected MC with myc-tagged wild-type FST or the FSTΔNLS mutant [171]. The FSTΔNLS vector encodes a mutated FST protein that lacks a nuclear localization signal (NLS) [171], with FST nuclear import shown to be important for the protection of cancer cells against apoptosis [171]. We first confirmed that Tg upregulated the expression of both transfected proteins (Fig. 3-2F). We next determined whether Tg promotes nuclear FST localization using immunoblotting of cytosolic/nuclear preparations. While we did find basal nuclear expression of wild-type FST, its localization within the nucleus was not increased by Tg. Nuclear exclusion of the FSTΔNLS mutant protein was also confirmed (Fig 3-10; Supplemental Fig. 1A). Furthermore, our results show that both wild-type FST and FSTΔNLS were equally effective against reducing Tg-induced apoptosis, as measured by caspase 3 cleavage (Fig. 3-2F) and caspase 3/7 enzymatic activity (Fig. 3-2G). These results show that FST protects against Tg-induced apoptosis, and that this occurs independently of its ability to localize within the nucleus.

Finally, FST is canonically known to be a secreted protein [46,97]. Based on our findings that the addition of exogenous FST was effective in decreasing Tg-induced apoptosis (Fig. 3-2C, D, E), we questioned whether wild-type FST and FSTΔNLS were both secreted into the medium in MCs in response to Tg. Fig 3-10; Supplemental Fig.1B shows the basal secretion of both forms of overexpressed FST proteins without augmentation by Tg. Taken together, these data show that FST protects against Tg-induced apoptosis and that this protection is independent of its ability to localize to the nucleus.

Follistatin does not inhibit thapsigargin-induced Ca^{2+} release or ER stress.

We next sought to determine how FST attenuates Tg-induced MC apoptosis. Since Tg promotes apoptosis through depletion of ER Ca^{2+} with concurrent accumulation of cytosolic Ca^{2+} [89], we examined whether FST alters Tg-induced Ca^{2+} release. Cytosolic Ca^{2+} levels were assessed using the ratiometric intracellular calcium indicator, Fura-2 and spectrofluorometry. We found that the addition of recombinant FST did not affect Tg-induced cytosolic Ca^{2+} influx (Fig. 3-3A).

Based on its ability to deplete ER Ca^{2+} stores, Tg also leads to ER stress and activation of the ER stress-mediated apoptotic pathway [86,173]. Thus, we investigated whether FST inhibits ER stress. We found that Tg-induced ER stress, as measured by the up-regulation of GRP78 and CHOP and the phosphorylation of eIF2α, was not affected by the addition of recombinant FST (Fig. 3-3B). Similarly, overexpression of wild-type FST (Fig. 3-3C) or siRNA-mediated downregulation of FST (Fig. 3-3D) did not affect Tg-induced ER stress. These results suggest that FST protects against Tg-induced MC apoptosis independently of Ca^{2+} regulation and ER stress induction.

Follistatin protects against thapsigargin-induced mesangial cell apoptosis by inhibiting ROS.

Tg has been shown to induce oxidative stress in numerous cell types by promoting ectopic cytosolic Ca^{2+} accumulation [90,92]. Furthermore, ROS are known to play an important role in the induction of apoptosis, including that effected by Tg [90,174].

Interestingly, FST was shown to be an oxidative stress responsive protein that is effective at inhibiting ROS in several cell types [175,176]. We thus sought to determine whether FST inhibits Tg-induced apoptosis through attenuation of ROS production. A proprietary ROS/Superoxide detection cocktail (ROS-ID Total ROS/Superoxide Kit) was used to concurrently assess and differentiate SO from other intracellular ROS species including H_2O_2, $ONOO^-$, HO, NO, and ROO. In this study, superoxides are abbreviated as 'SO', while ROS collectively refers to species including hydrogen peroxide (H_2O_2), peroxynitrite ($ONOO^-$), hydroxyl radicals (HO), nitric oxide (NO) and the peroxy radical (ROO), unless other specified. We first assessed ROS and SO production after Tg exposure to confirm that this can be seen in MC. Fig. 3-4A shows that Tg led to an accumulation of ROS in MCs which was attenuated by the hydrogen peroxide scavenger PEGylated-catalase. Tg did not affect SO production. Spectrofluorometric quantification confirmed the inhibitory effects of PEGylated-catalase on Tg-induced ROS production (Fig. 3-4B, C). Catalase also significantly blocked Tg-induced apoptosis, as assessed by PS-Annexin V binding (Fig. 3-4D) and caspase 3/7 enzymatic activity (Fig. 3-4E). We next assessed whether FST can inhibit Tg-induced ROS production. Interestingly, the addition of recombinant FST drastically reduced the accumulation of intracellular ROS (Fig. 3-4F), which was confirmed with spectrofluorometric quantification (Fig. 3-4G, H). Interestingly, incubation of MC with the SO scavengers superoxide dismutase (SOD) and TEMPOL effectively blunted Tg-induced apoptosis in MC (Fig. 3-4I). Since Tg did not increase intracellular SO, we questioned whether SO scavengers could deplete basal SO

levels in MC which could explain these protective anti-apoptotic effects. Indeed, basal depletion of SO was confirmed (Fig. 3-11; Supplemental Fig. 2).

These data collectively illustrate that FST inhibits intracellular ROS, and that inhibition of basal SO or Tg-induced ROS production protects against Tg-induced apoptosis. This raised the question of the mechanism by which FST can inhibit intracellular ROS.

Activins A and B do not mediate thapsigargin-induced apoptosis and ROS production.

FST has greatest neutralizing potency against activins [46,57]. Secreted activins act in an autocrine manner through cell surface receptor binding and activation of downstream signaling events [177]. While the role of activin B (ActB) is unclear, ActA has been shown to induce ROS production and initiate apoptosis in several cell types [94–96,177–179]. We thus investigated whether activin production and secretion is regulated by Tg in MC. Fig. 3-5A shows that Tg did not increase the cellular protein expression of activins A or B. The secretion of ActA into the medium was also not increased, as assessed by ELISA, although the expected decrease with FST was seen (Fig. 3-5B). Thus, Tg does not increase ActA or ActB.

Since FST functions as a potent activin antagonist, we next investigated whether FST protects against Tg-induced ROS production and apoptosis through neutralization of basally present activins [46,97]. We used ActA and/or ActB neutralizing antibodies. To first confirm their efficacy in neutralizing activins, we tested Smad3 activation downstream of activins using the $CAGA_{12}$ reporter luciferase assay, which contains 11

repeats of the Smad3 consensus binding site. Fig. 3-12; Supplemental Fig. 3 confirms that both antibodies inhibit signaling of their targeted activin. However, neither antibody alone or in combination inhibited Tg-induced ROS production in MCs (Fig. 3-5C), with spectrofluorometric quantification shown in Fig. 3-5D, E. Tg-induced apoptosis, as assessed by caspase 3/7 enzymatic activity, was similarly unaffected by ActA and/or ActB neutralization (Fig. 3-5F). These results suggest that the ability of FST to protect against Tg-induced ROS production and apoptosis in MCs is independent of its neutralization of activins A/B.

To determine whether activins can exacerbate Tg-induced ROS accumulation and apoptosis in MCs, we treated cells with Tg in combination with either activin. The addition of recombinant ActA or ActB did not promote intracellular ROS or SO accumulation, nor did it augment ROS production in response to Tg (Fig. 3-5G). Spectrofluorometric quantification is shown in Fig. 3-5H and I. Similarly, ActA or ActB did not promote apoptosis, as assessed by caspase 3/7 enzymatic activity (Fig. 3-5J). These data demonstrate that activins do not contribute to Tg-induced ROS production and apoptosis in MCs, and that FST is protective independently of its activin neutralizing activity.

Follistatin acts as a ROS scavenger

Since we observed that FST attenuates ROS detection, we next sought to determine whether FST could act as a ROS scavenger. Here, we evaluated the effects of FST on oxidative stress induced using a general oxidative stress agent, pyocyanin, a

cytotoxic pigment secreted by *Pseudomonas aeruginosa* which induces production of various ROS species [180]. As expected, pyocyanin led to the accumulation of both ROS and SO in MCs after 1h, and this was effectively inhibited by FST (Fig. 3-6A). Notably, FST inhibited the production of both general ROS species and SO, with effects on SO production similar to that seen by SOD, an enzyme that is well-established to play a role in the breakdown and degradation of SO (Fig. 3-6A). Spectrofluorometric quantification confirmed the inhibitory effects of FST and SOD on pyocyanin-induced ROS and SO production (Fig. 3-6B, C). It should also be noted here that we observed a small, but significant decrease in ROS by SOD. This is consistent with the known spontaneous conversion of SO to more reactive species such as peroxynitrite, such that SOD reduction of SO would also reduce these other ROS species [181]. This effect might also contribute to the anti-apoptotic effect of SOD seen in Fig. 3-4I, despite the absence of significant SO induction by Tg.

Next, we tested the effects of FST on H_2O_2-induced DCF oxidation using MC loaded with 2',7'–dichlorofluorescin diacetate (H_2DCFDA). Here, MCs treated with H_2O_2 were co-incubated with either recombinant FST or catalase, an enzyme which catalyzes the decomposition of H_2O_2. Fig. 3-6D shows that FST significantly suppressed H_2O_2-induced DCF oxidation, with potency somewhat greater than that seen with catalase. The specificity of FST in reducing ROS and SO was confirmed using immunoglobulin G (IgG), one of the most abundant proteins found in serum. Mouse IgG, unlike FST, was unable to neutralize pyocyanin-induced ROS and SO production (Fig. 3-13; Supplemental Fig. 4A,B,C).

Last, we utilized cell-free assays to determine whether FST can directly scavenge ROS. Firstly, to assess the ability of FST to neutralize H_2O_2 in a cell free system and to assess whether FST has peroxidase activity, we utilized a non-fluorescent ADHP (10-Acetyl-3, 7-dihydroxyphenoxazine) probe that reacts with H_2O_2 and is oxidized in the presence of peroxidase activity to form a highly fluorescent compound, resorufin. Using this assay, we first found that recombinant FST did not possess endogenous peroxidase activity when compared to the positive control horseradish peroxidase (HRP) (Fig. 3-6E). However, FST incubation with H_2O_2 significantly decreased H_2O_2 availability to HRP, indicating its ability to scavenge this ROS species (Fig. 3-6F). In MC treated with H_2O_2, this scavenging effect was dose-dependent, seen to increase from 25ng/ml to 1000ng/ml of FST (Fig. 3-14; Supplemental Fig. 5A). Furthermore, FST scavenging of H_2O_2 protected MC against H_2O_2-induced apoptosis (Fig. 3-6G) and dose-dependently against Tg-induced apoptosis (Fig. 3-14; Supplemental Fig 5B). In a separate cell-free assay, we examined the effects of FST on xanthine oxidase-generated SO. Here, we found that FST decreased the presence of detectable SO by 20% (0.5µg FST) and 29% (1 µg FST), in comparison to an 81% percent decrease with SOD (Fig. 3-6H).Thus, FST has the ability to dose-dependently scavenge ROS, which would at least in part contribute to the effects seen on intracellular ROS and its anti-apoptotic effects.

To address the mechanism by which exogenous FST administration could attenuate intracellular ROS detection (Fig. 3-4F, 3-6A), we wished to determine whether recombinant FST could be internalized in the short timeframe we used for treatment in our studies. We thus incubated MC with FST for 30min, and assessed intracellular levels

by immunoblotting total cell lysate. Fig. 3-14; Supplemental Fig. 5C shows that FST indeed dose-dependently enters cells. Since FST internalization is known to occur after its binding to activins [182], we then assessed whether neutralization of ActA would attenuate its internalization. As seen in Fig. 3-14; Supplemental Fig. 5C FST internalization was only prevented at low doses of FST (25ng). Interestingly, at higher doses of FST (1000ng), which are required for FST to fully exert its protective anti-apoptotic effects, internalization was not blunted by ActA neutralization. Thus, exogenous FST is rapidly internalized, partially via ActA and partially via an alternate and as yet undescribed mechanism, to attenuate intracellular oxidative species.

Follistatin inhibits NOX4 upregulation

With longer-term incubation, FST was shown to inhibit upregulation of NAD(P)H oxidase subunits Nox1/5 by silica particles in human lung epithelial cells [176]. We thus sought to determine whether Tg upregulated the expression of Nox subunits and whether these responses were regulated by FST. Nox4 specifically has been shown to be an important generator of intracellular H_2O_2 in numerous cell types, including MC [183,184]. Fig. 3-7A, B show that Tg led to a pronounced and transient increase in NOX4 transcript at 4h, which was diminished by 8h. Nox1 and Nox2, which are primarily SO generating enzymes, were not affected by Tg (Fig. 3-7A). Nox3 transcript was not detected in MC (data not shown). Next, since Nox4 is constitutively active, we assessed whether FST could inhibit Tg-induced Nox4 production and in turn activity. Here, we found that Tg-induced Nox4 protein expression was prevented by the addition of

exogenous recombinant FST (Fig. 3-7C). Since oxidative stress and the ERK pathway were shown to be an important regulator of Nox4 expression [185], we also tested whether Tg-induced Nox4 induction and its repression by FST is mediated through effects on ERK activation and reduction in oxidative stress. As seen in Fig. 3-7D, ERK activation, assessed by its phosphorylation, was inhibited by FST and the ROS scavenger catalase, and as expected by inhibition of its upstream kinase MEK with U0126. These all also effectively blocked the induction of Nox4 expression by Tg (Fig. 3-7E), suggesting that follistatin inhibits Nox4 induction by Tg through attenuation of ROS-induced ERK activation.

Collectively, these results demonstrate that Tg-induced apoptosis is mediated at least in part through oxidative species and that the protective anti-apoptotic effects of FST may be attributed to its potent ability to inhibit oxidative stress through both direct and indirect mechanisms.

FST protects against apoptosis and oxidative stress in vivo in CKD

ER stress is a known important contributor to the progression of fibrosis and kidney dysfunction in rodent and human CKD [88,186]. The production of ROS has also been implicated in the pathogenesis of CKD [38,84,187]. Furthermore, oxidative stress and apoptosis have been correlated with worsening kidney function [83], with several studies showing beneficial effects of inhibiting apoptosis and ROS on limiting CKD progression [85,188,189]. Since we have shown that FST is effective at inhibiting ER stress-induced apoptosis and ROS accumulation in cultured MCs, we next examined

whether FST administration is protective *in vivo*. We used a well-established 5/6 nephrectomy (5/6 Nx) model of CKD due to reduced renal mass in which ER stress, ROS production and renal cell apoptosis are known to occur [88,111,186,190]. Mice were treated with one of 2 doses of recombinant FST for 9 weeks prior to analysis of renal oxidative stress. IHC demonstrated a dose-dependent increase in kidney FST after treatment, suggesting its successful targeting to the kidney (Fig. 3-15; Supplemental Fig. 6).

We first analyzed mouse kidneys for the expression of nitrotyrosine, a commonly used marker for peroxynitrite formation and oxidative stress *in vivo*. As expected, global protein nitrotyrosination within the glomeruli and tubules of CKD mice was dose-dependently inhibited by FST (Fig. 3-8A). Secondly, within nuclear and mitochondrial DNA, the presence of oxidized deoxyguanosine molecules, or 8-hydroxy-2' -deoxyguanosine (8-OHdG) is a well-established biomarker of oxidative stress. As expected, we observed prominent expression of 8-OHdG within the nuclei of tubular and glomerular cells in CKD mice treated with vehicle, with staining significantly reduced by FST (Fig. 3-8B). The release of multiple oxidized guanine species into the urine also serves as a strong indicator of renal oxidative stress *in vivo*. We assessed this by ELISA, which measures the major oxidative damage DNA/RNA markers 8-OHdG, 8-hydroxyguanosine and 8-hydroxyguanine (8-OHG). This also demonstrated increased oxidative stress in CKD, which was inhibited by FST in a dose-dependent manner (Fig. 3-8C). Last, we assessed apoptosis by cleavage of caspase 3 and PARP. The increased apoptosis clearly seen in kidneys of mice with CKD was inhibited by FST (Fig. 3-8D).

Thus, FST is also effective at inhibiting oxidative stress and apoptosis *in vivo* in mice with CKD.

FST preserves kidney function and protects against renal fibrosis in mice with CKD

Having seen a prominent reduction in oxidative stress and apoptosis in CKD mice treated with FST, we next assessed whether these mice are protected against the progression of CKD. The 5/6 Nx mouse model of CKD is characterized by progressive decline in kidney function, albuminuria, and glomerular and tubulointerstitial fibrosis [110,111]. We found that CKD mice treated with 5µg FST had a higher glomerular filtration rate (GFR), showing protection against the decline in kidney function (Fig. 3-9A). FST (5µg) also reduced albuminuria in these mice (Fig. 3-9B).

Next, we carried out an RNA screen using Nanostring to assess for changes in the renal expression of profibrotic and extracellular matrix (ECM) genes involved in fibrosis in CKD. Fig. 3-9C shows an agglomerative clustered heat-map of kidney RNA expression profiles from CKD mice treated with FST. These data demonstrate a reduction of profibrotic and ECM markers by 5µg of FST which was confirmed by immunoblotting as shown in Fig. 3-9D. Glomerular and tubulointerstitial fibrosis was also histologically assessed using Picrosirius Red and trichrome staining, both of which mark the deposition of collagens, as well as with IHC staining for fibronectin. Fig. 3-9E shows both glomerular and tubulointerstitial fibrosis in vehicle-treated CKD mice which were significantly attenuated by 5µg FST. Thus, in addition to protecting against renal oxidative stress, apoptosis and kidney function, FST also reduced renal fibrosis in CKD.

Interestingly, our data illustrate that while a higher dose of FST (10μg) provides a greater reduction in renal oxidative stress, this does not directly correlate with a further improvement in kidney function and renal fibrosis. Potential mechanisms are discussed below.

3.5 Discussion

Interventions to inhibit chronic oxidative stress and renal cell apoptosis are essential towards halting the progression of CKD to kidney failure. We investigated a potential protective role of FST, a TGFβ superfamily neutralizing protein which primarily neutralizes activins, in the regulation of renal cell apoptosis and oxidative stress. Recent work has shown that FST protects against ROS production and apoptosis in several settings, both *in vitro* and *in vivo* [97]. This has been thought to be due to neutralization of ActA in some cases, although in others, the role of activins has been less clear. For example, FST protection against glucose deprivation-induced apoptosis in cancer cells required its nuclear localization and attenuation of rRNA synthesis [171]. Herein we found that FST functioned as a cellular stress responsive protein. Importantly, in cultured MC and when administered systemically to mice with CKD, FST protected against apoptosis, reduced renal fibrosis and improved kidney function. This was associated with its direct and potent ability to inhibit ROS as a scavenger and thereby to repress oxidative stress, independent of its ability to neutralize activins. Our data thus identify a novel, activin-independent, role for FST in attenuating oxidative stress and apoptosis. Together

with its antifibrotic properties, FST may be a highly effective novel therapeutic agent for renal protection in a CKD setting.

In keeping with our findings, a protective role of FST against apoptosis has also been demonstrated in several other settings. For example, in pulmonary epithelial cells, FST protected against silica-induced oxidative stress and cell death [176]. Conversely, siRNA-mediated downregulation of FST significantly augmented apoptosis in bovine granulosa cells [172]. While these and our studies show an increase in FST expression by various cell stressors, the mechanism by which this increase occurs markedly differs between settings. For example, silica nanoparticles in epithelial cells induce the transcriptional activation of FST [176], while glucose starvation in cancer cells induces FST mRNA stabilization [191]. In our studies, the increased expression of FST in response to Tg was specifically attributed to a post-translational increase in protein stability. How FST is post-translationally stabilized in response to MC stress requires further investigation.

ER stress is an important pathogenic contributor not only to CKD, but also to numerous other chronic diseases [86,192]. Our data show a novel protective role for FST against ER-stress induced apoptosis, effected in our studies by Tg. This is a non-competitive inhibitor of the sarco/endoplasmic reticulum Ca^{2+} Mg^{2+}-ATPase [90–92,170]. Interestingly, FST attenuated apoptosis without affecting the induction of ER stress by Tg. This may be through its effects on inhibition of oxidative stress, since ROS scavengers inhibited Tg-induced apoptosis in our studies. Indeed, apoptotic induction by

Tg in other cells such as cortical neurons and hepatocytes could be alleviated by inhibition of oxidative stress [90,92].

How FST may function to prevent oxidative stress is not as yet completely understood. Alternate splicing and processing of the FST gene results in extracellular secretion of two major isoforms containing 288 and 315 amino acids [57]. These differ in their localization. FST-288 is bound to the cell surface via heparan sulfates [57]. In FST-315, an acidic tail blocks this cell-surface binding site, causing its release into the circulation [57]. FST most potently neutralizes activins, but can also inhibit several other TGFβ family members, including myostatin, GDF9, TGFβ3, and BMPs 2, 4, 6, and 7, albeit with much lower affinity [57]. Interestingly, FST-targeted cytokines, through Smad3-dependent and -independent signaling pathways, have been shown to promote ROS production and apoptosis in numerous cell types [94–96,193]. The role of the primary FST-targeted cytokine, activin, in promoting oxidative stress and apoptosis in MC has not been previously examined. While activins were shown to induce apoptosis in other cells such as hepatic stellate cells, hepatocytes and myeloma cells [94,194–197], our data show that neither ActA nor ActB promote oxidative stress or apoptosis, and that their inhibition is not protective against Tg-induced apoptosis and ROS induction in MC. However, other ligands targeted by FST, namely myostatin and BMP4, have also been shown to promote apoptosis and/or oxidative stress in other settings [175,193,198]. Whether these other ligands neutralized by FST could contribute to its protective effects against ROS induction and apoptosis in MC remains to be determined.

Reactive species can be produced intracellularly by the NAD(P)H oxidase (Nox) enzyme system. A recent study showed that FST inhibits expression of the subunits Nox1 and Nox5 in human pulmonary epithelial cells [176]. It was also shown to reduce ActA-induced Nox2 upregulation in endothelial cells [199]. We thus assessed the effects of FST on the expression of Nox4, a constitutively active enzyme expressed by MC that is involved in the intracellular production of H_2O_2 and free radicals such as SO [184,200]. We found that Tg-induced Nox4 upregulation was suppressed by FST. However, it should be noted that the role of Nox4 in CKD is not entirely clear. In some studies Nox4 is shown to be protective, while in others it promotes cell apoptosis, inflammation and fibrosis [200,201]. Nonetheless, these and our findings support the notion that FST protects against oxidative stress by affecting the expression and/or activity of intracellular Noxs.

How FST might regulate the expression of Nox4 is as yet unknown. FST was shown to localize to the nucleus and regulate RNA synthesis in glucose-deprived cancer cells [171]. Our studies with a mutant FST protein which is unable to enter the nucleus, however, clearly demonstrated that nuclear localization is not required for its ability to protect against ROS generation and apoptosis. Although endogenous nuclear FST in MC may have contributed, this role would likely be minor. Our data also do not support a role for activin-mediated Nox4 induction by Tg given that we did not find any effect of activin neutralization on ROS production. Furthermore, although Smad3 activation by TGFβ1 regulated Nox4 expression in kidney myofibroblasts [202], we also did not observe Smad3 activation by Tg in MC (not shown). Similarly, activation of Smad1, a mediator of

BMP signaling, was also unaffected by FST (not shown), suggesting that secretion of TGFβ1 family ligands is not involved in the induction of Nox4 by Tg. Interestingly, however, as found in endothelial cells [185], we identified that Nox4 induction by Tg was mediated by ROS-dependent activation of the ERK1/2 kinases. The ability of FST to scavenge ROS appears critical to its inhibition of ERK1/2-Nox4 induction.

Oxidative species, including H_2O_2 and SO can also be generated and regulated extracellularly through cell-surface bound Noxs and SODs, where they have been shown to exert deleterious effects in CKD [181,203]. SO are generally short lived and not readily permeable through cell membranes [181]. On the other hand, H_2O_2 is uncharged, highly stable and cell membrane permeant [181]. Thus, we questioned whether FST selectively inhibits ROS intra- or extra-cellularly. FST is a secreted glycoprotein that functions extracellularly to neutralize its ligands [57], after which the ligand-FST complex is internalized by endocytosis and cleared by the lysosomal degradation pathway [182]. Using cell-free assays, our data show that FST is able to directly scavenge reactive oxygen species in cell-free conditions, suggesting ability to scavenge both intra- and extracellularly located ROS. These results are the first to show that FST is able to directly neutralize SO and H_2O_2. However, treatment with FST quite rapidly also decreased intracellular ROS generation, as assessed by ROS-specific immunofluorescent dyes, in a dose dependent manner. We thus tested whether this could be explained by internalization of the exogenously administered FST. Surprisingly, we found that MC are able to rapidly internalize extracellular FST, and that this occurs in the presence of ActA. However,

when FST is administered at higher doses (≥100ng), internalization was also found to be independent of ActA. How this occurs is not understood and requires further research.

Since we found that FST is able to scavenge ROS, but does not have endogenous peroxidase activity, we examined its amino acid composition for characteristic features of a ROS scavenger. Either free reduced cysteine (cys) or methionine (met) residues, such as the free reduced Cys34 in human serum albumin, can be readily oxidized and thus act as an endogenous antioxidant [204–206]. FST is highly enriched in cys (n=36, 11.3%) and met (n=5, 1.5%) residues [207]. However, all of the 36 cys residues in FST are disulfide bonded and thus lacking in free reactive sites that can be readily oxidized [208]. On the other hand, the met residues in FST are available for oxidation by H_2O_2 and met modification does not affect the ability of FST to bind and neutralize activins [207]. Interestingly, however, oxidation of tryptophan (trp) in FST was shown to almost completely inhibit activin binding [207]. Thus, it is likely that FST can act as a sink for ROS through oxidation of its met and trp residues, and with the latter this is associated with loss of activin neutralizing activity. Further studies are needed to test this hypothesis.

Oxidative stress and apoptosis are critical contributors to the pathogenesis of CKD of varying etiology [83,84,209]. These stressors induce renal fibrosis, and therapies that reduce renal oxidative stress have been shown to reduce fibrosis and improve renal function [210,211]. ER stress has also been identified in both human and rodent CKD, including in mice with 5/6 nephrectomy as used in our studies [88,111,186,190]. Our *in vivo* data confirm the relevance of our *in vitro* findings. Indeed, in our mice with experimentally-induced CKD, FST was highly protective against both oxidative stress

and renal cell apoptosis. Our data are also consistent with the reported attenuation of hepatocyte apoptosis by FST in a model of liver fibrosis (although oxidative stress was not examined here) [109]. At the 5µg FST dose, these protective effects were associated with improvement in renal function, a decrease in urinary albumin excretion and a significant reduction in renal fibrosis. Indeed FST has been shown to act as an antifibrotic agent in various organs [23,107,109]. Interestingly, this antifibrotic effect was thought to be predominantly due to attenuation of ActA signaling. Our data support an additional and potent antioxidative property of FST that contributes to its *in vivo* efficacy.

Why the higher dose of FST (10µg), while further reducing oxidative stress, did not improve kidney function and renal fibrosis in our studies is not yet clearly understood. Interestingly, administration of heavily oxidized albumin or tyrosine to animals at high doses over time was shown to induce kidney or liver fibrosis [212,213]. These findings may explain why a higher dose of FST in our *in vivo* study, while reducing global renal oxidative stress, did not linearly result in improvements in kidney function and fibrosis when compared to the lower efficacious dose. Alternatively, it is also plausible that excessive reduction of ROS such as H_2O_2, which at physiologic basal levels serve as important homeostatic cell signaling regulators, contributes to worsening disease progression. Future studies will aim to better understand this finding.

Taken together, our data support a novel role for the antifibrotic protein FST as a ROS scavenger with protective effects both *in vitro* and *in vivo* in CKD. Future studies will focus on understanding the pharmacokinetic and pharmacodynamic profile of FST as a step towards therapeutic implementation.

Innovation: ROS generation and apoptosis are key pathophysiologic contributors to CKD which are not as yet effectively targeted with current therapies. We present novel data demonstrating that the glycoprotein FST, best known for its ability to neutralize TGFβ family members called activins, has potent anti-apoptotic and anti-oxidant effects in CKD through its ability to scavenge ROS and in turn therapeutically protects against the progression of CKD through improving kidney function and reducing renal fibrosis

3.6 Materials and Methods

Cell Culture

Primary mouse mesangial cells (MCs) were isolated from B6129SF1/J mice (Jackson Laboratory) using Dynabeads (Invitrogen). They were cultured in Dulbecco's modified Eagle's medium (DMEM) supplemented with 20% fetal bovine serum (Invitrogen), penicillin (100 μg/ml) and streptomycin (100 μg/ml) at 37˚C in 95% O_2, 5% CO_2. Passages 7-14 were used. MCs were serum deprived in 0.5% FBS 24h prior to treatment unless otherwise stated. Drugs/reagents used in the study are provided in table 3-1.

Transfection

Transient expression of plasmids was achieved using electroporation with the ECM 830 Square Wave Electroporation System (Harvard Bioscience). Briefly, MCs resuspended in electroporation buffer containing the appropriate plasmids (0.5μg

luciferase plasmid with 0.05µg β-Galactosidase or 10µg protein expression plasmid) were electroporated using a single square pulse set at 200V for 35 msec. siRNA-mediated (50nM) knockdown was achieved using RNAiMAX (Thermo Fisher Scientific) as per the manufacturer's recommendation. MCs were serum deprived 24h following transfection prior to treatment and harvest. Plasmids and siRNA used in the study are provided in table 3-2 and 3-3.

Luciferase Assay

MC lysis was achieved using Reporter Lysis Buffer (Promega) as per the manufacturer's recommendation. Luciferase activity was measured on clarified cell lysate using the Luciferase Assay System (Promega) with a luminometer (Junior LB 9509, Berthold). β-galactosidase activity, used to normalize for transfection efficiency, was measured in clarified cell lysates using the β-Galactosidase Enzyme Assay System (Promega) with a plate reader absorbance set at 420nm (SpectraMax Plus 384 Microplate Reader, Molecular Devices).

Protein Extraction and Immunoblotting

MC cell lysis and total cellular protein extraction was carried out using a buffer containing 20mM Tris-HCl (pH 7.5), 150mM NaCl, 1% Triton X-100, 1mM EDTA, 1mM EGTA, 2.5mM sodium pyrophosphate, 1mM /β-glycerophosphate, 2mM DTT, 1mM sodium vanadate, 1mM phenylmethylsulfonyl fluoride, 1µg/ml leupeptin, and 2 µg/ml aprotinin. Cell lysates were centrifuged (15,000 rpm, 10min, 4^{o}C), supernatant was

collected, protein concentration quantified and sample boiled in SDS-PAGE sample loading buffer containing 250mM Tris HCl (pH 6.8), 10% SDS, 30% (v/v) Glycerol, 10mM DTT, 0.05% (w/v) bromophenol blue (5 min, 100 ^{o}C).

Secreted proteins were isolated and concentrated from cell culture media using trichloroacetic acid and acetone precipitation. Briefly, 1 volume of trichloroacetic acid was added to 4 volumes of cell culture media and incubated (10 min, 4^{o}C). Samples were centrifuged (15,000 rpm, 10min, 4^{o}C) and the resulting pellet was washed in cold acetone 3 times, then air-dried and resuspended and boiled in SDS-PAGE sample loading buffer.

MC cell lysis and cytoplasmic/nucleus protein extraction was carried out using hypotonic lysis buffer containing 20mM HEPES (pH 7.6), 20% glycerol, 10mM NaCl, 1.5mM $MgCl_2$, 0.2 mM EDTA, 0.1% NP40, 2mM DTT, 1mM sodium vanadate, 1mM phenylmethylsulfonyl fluoride, 1 µg/ml leupeptin, and 2 µg/ml aprotinin. Cell lysates were centrifuged (500rpm, 10min, 4^{o}C), the pellet containing nucleus was suspended in buffer and sonicated, and supernatant (cytoplasmic extract) was collected, protein concentration quantified, and boiled in SDS-PAGE sample loading buffer.

Total, nuclear and/or cytoplasmic protein lysates (10µg-50µg) and secreted protein lysates (total yield) were separated on SDS-PAGE for subsequent immunoblotting. Densitometric analysis was carried out using ImageJ. (https://imagej.nih.gov/ij/plugins/colocalization-finder.html)). Tubulin or GAPDH was used as loading controls. Primary antibodies used in the study are provided in table 3-4.

Quantitative real-time PCR

RNA from MCs was extracted using Ribozol RNA Extraction Reagent (Amresco) as per the manufacturer's recommendation, with 1µg of RNA reverse transcribed into cDNA using qScript cDNA SuperMix Reagent (Quanta Biosciences). Quantitative real-time PCR was carried out using the Power SYBR Green PCR Master Mix (Thermo Fisher Scientific) on the Applied Biosystems ViiA 7 Real-Time PCR System (Thermo Fisher Scientific). mRNA expression and fold changes were calculated using the $\Delta\Delta C_T$ method, where 18S was used as the endogenous control. Primers sequences used in the study are provided in table 3-5.

Activin A ELISA

At endpoint, secreted ActA was quantified from clarified (15,000 rpm, 10min, 4^{o}C) MC culture media using the ActA Quantikine ELISA Kit (R&D Systems).

Apoptosis Assays

Caspase-Glo 3/7 Assay (Promega) was used to assess the enzymatic activity of executioner caspases 3 and 7. Briefly, at endpoint, MCs seeded in an opaque-walled clear bottom 96-well plate were washed in PBS and incubated with freshly prepared Caspase-Glo 3/7 reagent (45min, RT). Following incubation, luminescence readings, indicative of caspase 3/7 enzymatic activity, were obtained with a microplate reader (LUMIstar Galaxy, BMG Labtech). RealTime-Glo Annexin V Apoptosis Assay (Promega) was used to measure apoptosis in real-time in live cells. Briefly, MCs seeded in an opaque white-

walled clear bottom 96-well plate were loaded with freshly prepared Annexin V Detection Reagent in DMEM supplemented with 1% BSA (1h, 37ºC). Immediately after loading, treatment was initiated (18h, 37ºC). At endpoint, luminescence readings, indicative of cell surface phosphatidylserine-annexin V binding were obtained with a microplate reader (LUMIstar Galaxy, BMG Labtech).

Intracellular Calcium Assessment

Cell-permeant Fura-2 AM (Thermo Fisher Scientific) was used to measure the intracellular concentration of Ca^{2+} in real-time in live cells. Briefly, MCs seeded in an opaque black-walled, clear bottom 96-well plate were loaded with Fura-2 AM in Ca^{2+} free HBSS (5µM, 45 min, RT, dark). Immediately after loading, baseline fluorescence readings (ex340/em510 nm and ex380/em510nm) were taken every minute for 5 minutes using a temperature-controlled fluorescent microplate reader at the indicated time points (Gemini EM Spectra Max, Molecular Devices). Experimental drugs/treatments were then introduced and fluorescence readings were taken every minute thereafter for 30 minutes (37°C). Intracellular Ca^{2+} concentrations were calculated by quantifying the ratio of fluorescence signal obtained at 340nm and 380nm (F_{340nm}/F_{380nm}).

ROS and SO Detection

ROS-ID Total ROS/Superoxide detection kit (Enzo Life Sciences) and H_2DCFDA (Thermo Fisher Scientific) were used for the assessment of oxidative stress. To assess ROS generation through DCF oxidation, MCs seeded in an opaque black-walled, clear

bottom 96-well plate were loaded with H_2DCFDA in the dark (20μM, 45 min, 37ºC). Immediately after loading, cells were treated and ROS generation was assessed by measuring fluorescence emissions using a temperature-controlled fluorescent microplate reader set at 37°C (ex490nm/em525nm, Gemini EM Spectra Max, Molecular Devices). To simultaneously assess and differentiate between specific ROS species (H_2O_2, $ONOO^-$, HO, NO, and ROO) and SO, MCs seeded in an opaque black-walled, clear bottom 96-well plate were loaded with a cocktail of Oxidative Stress Detection Reagent and Superoxide Detection Reagent (ROS/SO cocktail, 5μM each, 45 min, 37ºC, dark). Immediately after loading, cells were treated and ROS and SO generation were assessed by measuring fluorescence emissions using a temperature-controlled fluorescent microplate reader set at 37°C (ex490nm/em525nm for ROS and ex550nm/em620nm for SO, Gemini EM Spectra Max, Molecular Devices). For some experiments, ROS-ID Total ROS/Superoxide detection kit (Enzo Life Sciences) was used for fluorescence imaging of intracellular ROS and SO accumulation. Briefly, MCs seeded in an 8-well chamber slide were treated and then loaded with the ROS/SO cocktail (5μM each, 45 min, 37ºC, dark). Immediately after loading, slides were cover-slipped and images were taken using a fluorescein filter set (ex490nm/em525nm) for ROS detection and a rhodamine filter set (ex550nm/em620nm) for SO detection (EVOS FL Cell Imaging System, Thermo Fisher Scientific).

ROS and SO Scavenging Assays

A Colorimetric OxiSelect Superoxide Dismutase Activity Assay Kit (Cell Biolabs) was used to measure the ability of FST to neutralize SO. Briefly, SO was generated using the xanthine/xanthine oxidase complex in an opaque-walled clear bottom 96-well plate. A chromogen which produces a water-soluble formazan dye upon reduction by SO anions was used to quantify the amount of SO. The chromogenic reaction was measured using a plate reader absorbance set at 490nm (SpectraMax Plus 384 Microplate Reader, Molecular Devices).

A Fluorometric OxiSelect Hydrogen Peroxide/Peroxidase Assay Kit (Cell Biolabs) was used to measure the ability of FST to neutralize H_2O_2 and to assess whether FST has peroxidase activity. Non-fluorescent ADHP (10-Acetyl-3, 7-dihydroxyphenoxazine) was added and allowed to react with H_2O_2, which is oxidized in the presence of peroxidase activity to form a highly florescent compound, resorufin. Fluorescent emissions are proportional to the amount of H_2O_2. Fluoresce emissions were measured using a plate reader (ex530nm/em590nm, Gemini EM Spectra Max, Molecular Devices).

Animal Studies

Animal studies were carried out in accordance with principles of laboratory animal care and McMaster University and Canadian Council on Animal Care guidelines. Male CD1 mice were obtained from Charles River Laboratories. CKD was achieved using the 5/6 nephrectomy (5/6 Nx) renal mass reduction model. Briefly, at 6-7 weeks of

age, anesthetized mice underwent resection of the upper and lower poles of the left kidney. After a one-week recovery period, anesthetized mice underwent a right nephrectomy. Sham mice were anesthetized and the kidney manipulated without resection. Resected kidney weights were divided by the nephrectomized right kidney weight (Nx ratio) and mice were placed into 6 groups, with the Nx groups containing mice with roughly equal Nx ratios: Sham-Vehicle (n=5), Sham-FST- 5μg (n=5), Sham-FST-10μg (n=5), 5/6 Nx-Vehicle (n=5), and 5/6 Nx-FST-5μg (n=5), and 5/6 Nx-FST-10μg (n=7). Following completion of the 5/6 nephrectomy, vehicle-treated mice were injected (IP) every other day with vehicle (20mM $NaPO_4$, 500mM NaCl, pH 7). FST-treated mice were injected (IP) every other day with human recombinant FST-288, provided by Paranta Biosciences Ltd and followed for 9 weeks.

At study endpoint, urine was collected and albumin-to-creatinine ratio measured according to manufacturer's instructions (Albuwell M, Exocell for urine albumin and Crystal Chem for creatinine). To assess DNA/RNA oxidative damage by ELISA, urine samples were centrifuged (3000 rpm, 5min, 4^{o}C), diluted 500 fold in ELISA buffer and assessed using a DNA/RNA Oxidative Damage ELISA kit (Cayman Chemicals). This kit measures major oxidative damage markers 8-hydroxy-2'-deoxyguanosine, 8-hydroxyguanosine, and 8-hydroxyguanine. Obtained concentrations (pg/ml) were normalized against urinary creatinine values, measured using a kit (Exocell).

Glomerular filtration rate (GFR) was assessed in conscious mice by measuring the clearance of fluorescein isothiocyanate (FITC)-labeled sinistrin (Fresenius Kabi Linz, Austria). Briefly, a 5% FITC-sinistrin solution was injected retro-orbitally, after which

blood was collected from the saphenous vein at 7, 15, 30, 60, 90 and 120 mins. Plasma fluorescence was assessed using a fluorometer (Gemini EM, Molecular Devices) at 485 nm excitation and 538nm emission. Following GFR assessment, mice were perfused with cold PBS. Kidney portions (renal cortex) were snap-frozen in liquid nitrogen for RNA or protein analysis or fixed in formalin for immunohistochemistry (IHC).

RNA was isolated using Trizol (Invitrogen). Nanostring analysis on the extracted RNA was carried out at the Farncombe Metagenomics Facility at McMaster University. Data were analyzed using nSolver 4.0. Samples were normalized using background subtraction with the negative control, and the geometric means of the housekeeping genes (actin, gusb, pgk1, and pp1a). For protein analysis, cortex was sonicated in lysis buffer, centrifuged (15 min, 13,000 rpm, 4°C) and supernatant separated on a SDS-PAGE for subsequent immunoblotting. Protein expression was normalized against GAPDH.

Formalin-fixed sections (4μm) were stained with trichrome or picrosirius red (PSR). For fibronectin immunohistochemistry, 4μm FFPE kidney sections were deparaffinized, endogenous peroxidase activity was blocked, tissues were blocked with 5% horse serum and incubated in primary antibody (overnight, 4°C). Tissues were incubated with biotinylated secondary antibodies (Vector Labs) (30 minutes, room temperature) and then with streptavidin/peroxidase (30 minutes, room temperature) (Vector Labs). Chromogenic color development was carried out using Nova Red (Vector Labs), followed by counterstaining using Gill's hematoxylin (Sigma) and mounting (Permount; Thermo Scientific). Images were quantified by measuring the percentage of positive area examined under transmitted light using ImageJ. All micrographs were

captured at x200 and x400 magnification using the BX41 Olympus microscope. Briefly, 10-20 micrographs were captured, percentage of positive area quantified and averaged per mouse. This was repeated for the indicated '*n'* number of mice, with final average and standard error calculated from the individual averages obtained from each mouse.

Statistical Analysis

Statistical analyses were performed using GraphPad Prism 6. A Student's *t*-test or one-way ANOVA was used to determine statistical significance between two or more groups of data, respectively. *Post hoc* significance of pairwise comparisons was assessed using Tukey's HSD. Statistical significance between two categorical independent variables was assessed using a two-way ANOVA, with Bonferroni's multiple comparisons test. A p-value <0.05 (two-tailed) was considered significant. Data are presented as mean±SEM. The number of experimental repetitions (*n*) is indicated in the figure captions.

Declarations:

Acknowledgements: We acknowledge the support of St. Joseph's Healthcare for nephrology research. We thank Dr. M. Bilandzic (Prince Henry's Institute, Australia) for providing pGL3-CAGA$_{12}$-luc, Dr. J. Yoon (Maine Medical Center Research Institute, USA) for providing mFST-luc, Dr. X. Gao (Institute of Environmental Medicine, China) for providing the WT-FST and ΔNLS-FST over-expression constructs. We thank Paranta Biosciences Limited (Australia) for providing human recombinant FST-288 for animal administration.

Contributions: NM and AG performed experiments and analysed data, DZ performed experiments, NM wrote the manuscript, AG, NM and JCK conceived the ideas, BG assisted with animal studies, all authors read and approved the final manuscript.

Competing interests: The authors declare that they have no competing financial interests.

Funding: This work was supported by the Canadian Institutes of Health Research (CIHR) (JCK), MOP 136868 and Kidney Foundation of Canada (JCK), KFOC160011. NM is the recipient of a studentship award from the Research Institute of St. Joe's Hamilton.

3.7 Figures

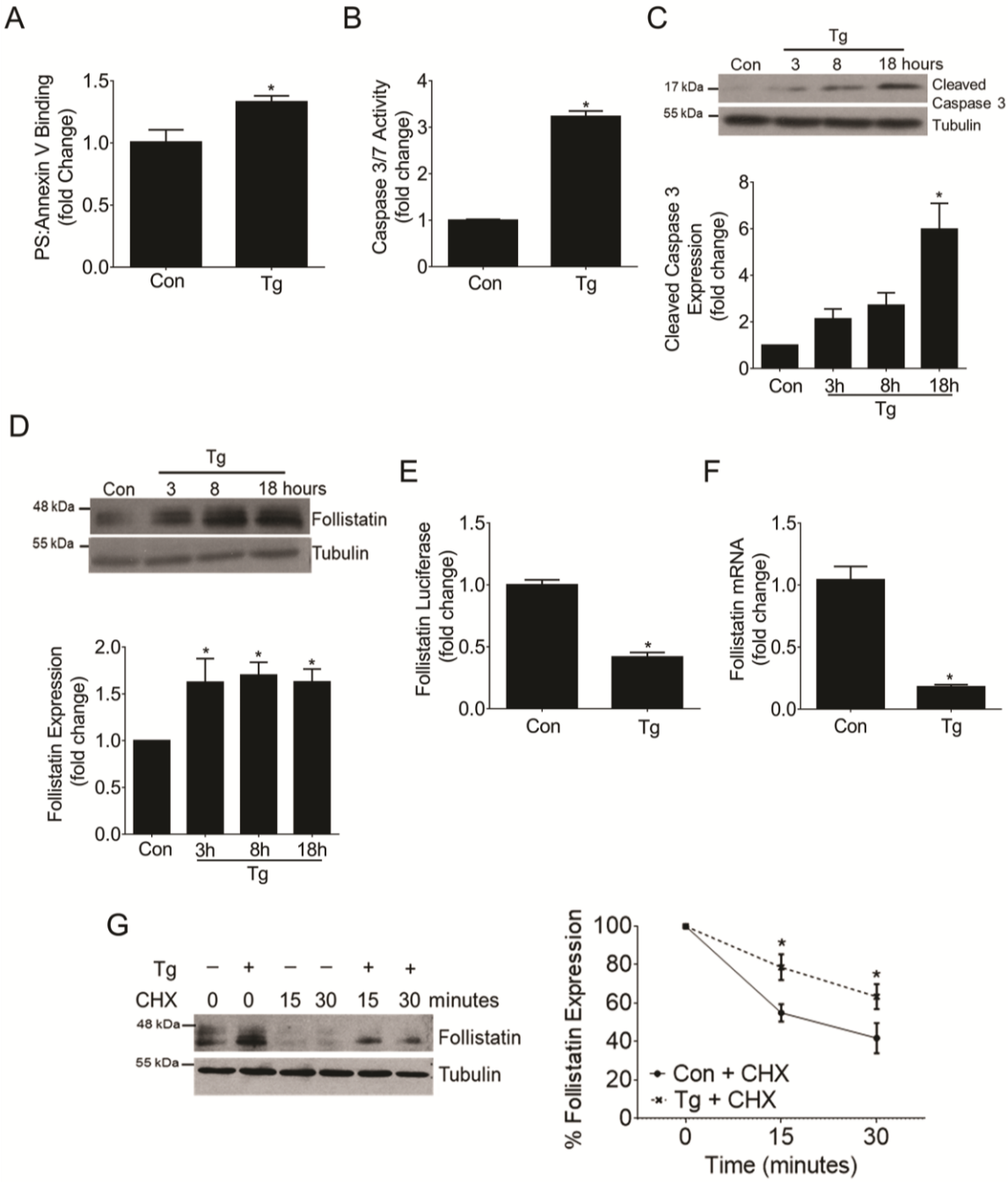
A
PS:Annexin V Binding (fold Change)
1.5
1.0
0.5
0.0
Con
Tg
B
Caspase 3/7 Activity (fold change)
4
3
2
1
0
Con
Tg
C
Tg
Con 3 8 18 hours
17 kDa
55 kDa
Cleaved Caspase 3
Tubulin
Cleaved Caspase 3 Expression (fold change)
8
6
4
2
0
Con 3h 8h 18h
Tg
D
Tg
Con 3 8 18 hours
48 kDa
55 kDa
Follistatin
Tubulin
Follistatin Expression (fold change)
2.0
1.5
1.0
0.5
0.0
Con 3h 8h 18h
Tg
E
Follistatin Luciferase (fold change)
1.5
1.0
0.5
0.0
Con
Tg
F
Follistatin mRNA (fold change)
1.5
1.0
0.5
0.0
Con
Tg
G
Tg – + – – + +
CHX 0 0 15 30 15 30 minutes
48 kDa
55 kDa
Follistatin
Tubulin
% Follistatin Expression
100
80
60
40
20
0
Con + CHX
Tg + CHX
0 15 30
Time (minutes)

Figure 3-1. Tg causes MC apoptosis and post-translationally increases the expression of follistatin.
Tg (200nM, 18h) led to MC apoptosis, as assessed by increased: (A) cell surface phosphatidylserine-annexin V binding (n=6, *p<0.05), (B) caspase 3/7 enzymatic activity (n=6, *p<0.05), and (C) cleavage of caspase 3 (n=6, *p<0.05). (D) Tg (200nM) induced the protein expression of FST (n=8, *p<0.05). (E) MC were transfected with a full-length mouse FST promoter luciferase construct. Tg (200nM, 18h) blunted the transcriptional activation of FST (n=12, *p<0.05). (F) Tg (200nM, 18h) reduced FST transcript mRNA expression, as assessed by qRT-PCR (n=8, *p<0.05). (G) MC were treated with Tg (200nM, 8h) followed by co-incubation with the translation inhibitor cycloheximide (10µg/ml) for the indicated durations. Tg significantly increased FST protein stability (n=4, *p<0.05).

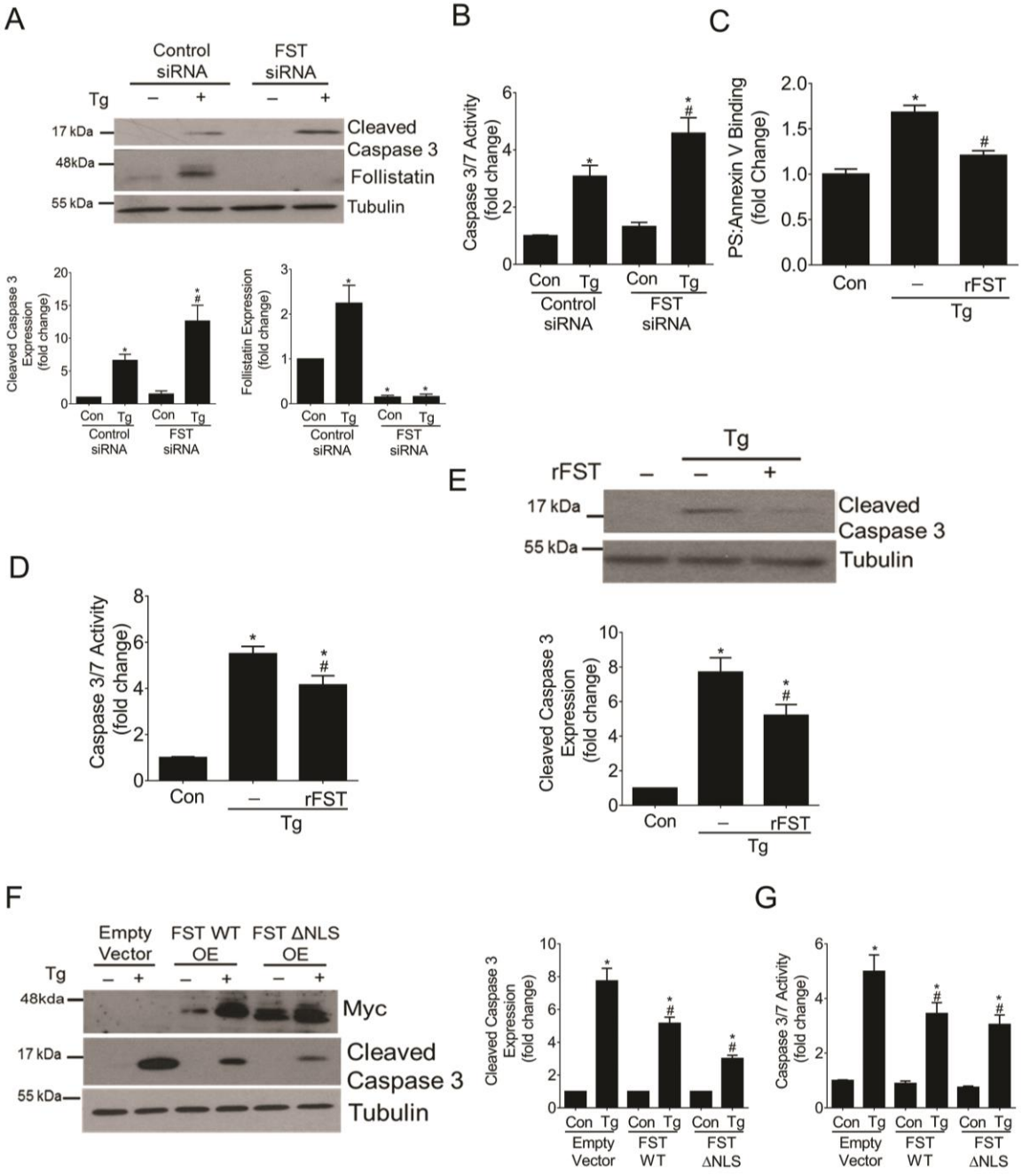
A
Control siRNA
FST siRNA
Tg
17 kDa
48kDa
55 kDa
Cleaved Caspase 3
Follistatin
Tubulin
Cleaved Caspase 3 Expression (fold change)
Follistatin Expression (fold change)
Con
Tg
Control siRNA
FST siRNA
B
Caspase 3/7 Activity (fold change)
C
PS:Annexin V Binding (fold Change)
rFST
D
E
F
Empty Vector
FST WT OE
FST ΔNLS OE
Myc
G

Figure 3-2. Follistatin protects against Tg-induced MC apoptosis.

(A) FST was downregulated using siRNA (50nM). siRNA-mediated FST downregulation augmented Tg (200nM, 18h)-induced MC apoptosis, as assessed by increased: (A) cleavage of caspase 3 (n=4, *vs control, # vs Tg control siRNA, $p<0.05$), and (B) caspase 3/7 enzymatic activity (n=9, *vs control, #vs Tg control siRNA, $p<0.05$). Recombinant FST (1µg/ml, 30 min pre-treat) protected against Tg (200nM, 18h)-induced MC apoptosis, as assessed by decreased: (C) cell surface phosphatidylserine-annexin V binding (n=5, *vs control, #vs Tg, $p<0.05$), (D) caspase 3/7 enzymatic activity (n=6, *vs control, #vs Tg, $p<0.05$), and (E) cleavage of caspase 3 (n=10, *vs control, #vs Tg, $p<0.05$). MC were transfected with myc-tagged wild-type FST or FSTΔNLS mutant, which prevents nuclear localization of FST. (F) Tg (200nM, 18h) increased the expression of wild-type FST and FSTΔNLS (n=3, representative blots shown). Over-expression (OE) of wild-type FST or FSTΔNLS both protect against Tg (200nM, 18h)-induced MC apoptosis, as assessed by decreased: (F) cleavage of caspase 3 (n=3, *vs empty vector control, #vs empty vector Tg, $p<0.05$) and (G) caspase 3/7 enzymatic activity (n=13, *vs empty vector control, #vs empty vector Tg, $p<0.05$).

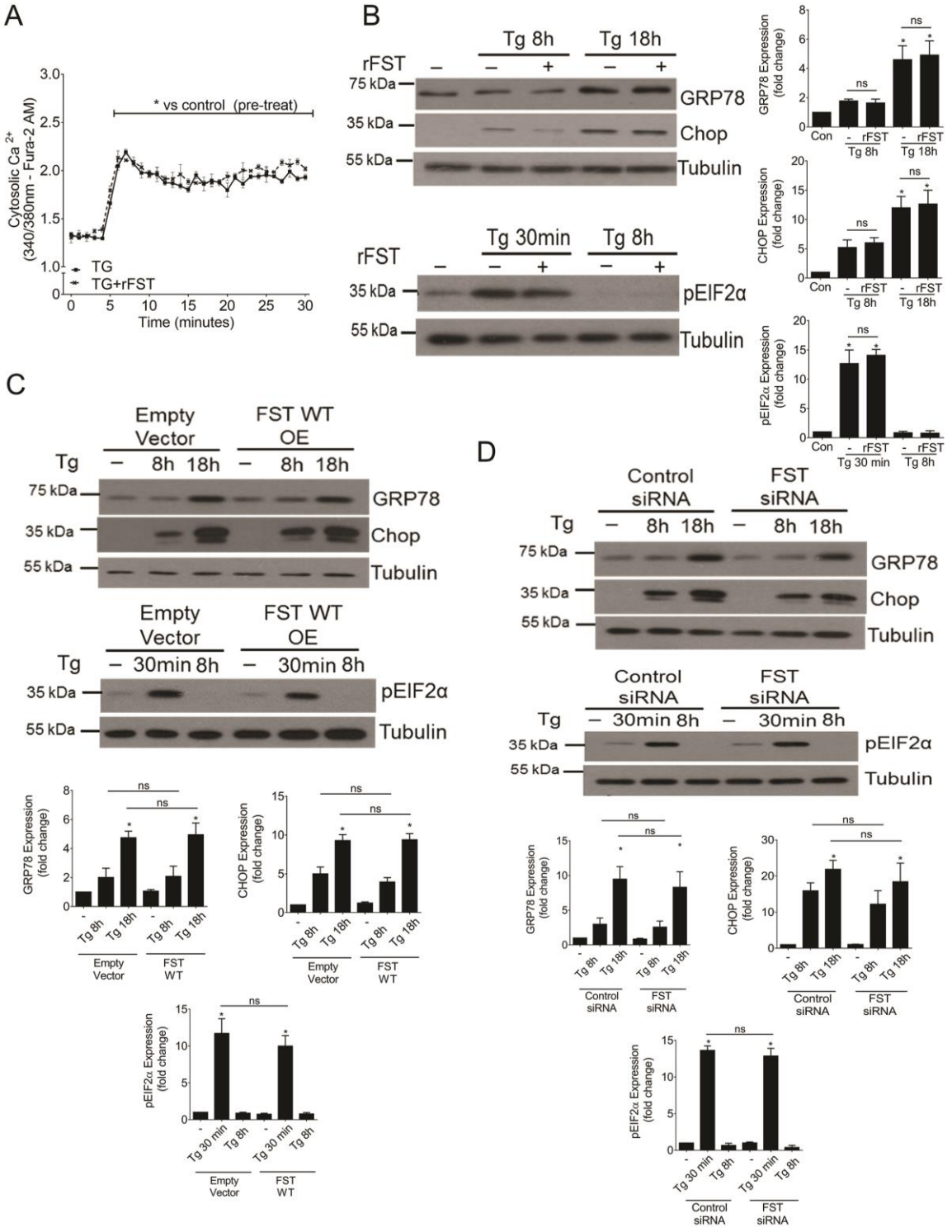
A
Cytosolic Ca2+ (340/380nm - Fura-2 AM)
* vs control (pre-treat)
TG
TG+rFST
Time (minutes)
B
Tg 8h
Tg 18h
rFST
75 kDa
GRP78
35 kDa
Chop
55 kDa
Tubulin
Tg 30min
Tg 8h
pEIF2α
GRP78 Expression (fold change)
CHOP Expression (fold change)
pEIF2α Expression (fold change)
Con
Tg 30 min
C
Empty Vector
FST WT OE
Tg
30min
D
Control siRNA
FST siRNA

Figure 3-3. Follistatin does not affect Tg-induced cytosolic Ca2+ release or ER stress. (A) MC were loaded with the ratiometric intracellular Ca^{2+} indicator Fura-2 AM. The arrow indicates addition of Tg (200nM) 5 minutes after loading. Tg caused a rapid increase in cytosolic [Ca^{2+}]. Recombinant FST (1µg/ml, 30 min pre-Tg) had no significant effect on Tg-induced intracellular [Ca^{2+}] influx (n=4, representative experiment shown). (B) Recombinant FST (1µg/ml, 30 min pre-treat), (C) overexpression (OE) of wild-type FST or (D) siRNA (50nM)-mediated FST downregulation did not affect Tg (200nM)-induced ER stress, as assessed by measuring the expression of canonical ER stress markers GRP78, CHOP, and phosphorylated eIF2α (peIF2α) (n=3, * vs control/empty vector or control siRNA, $p<0.05$).

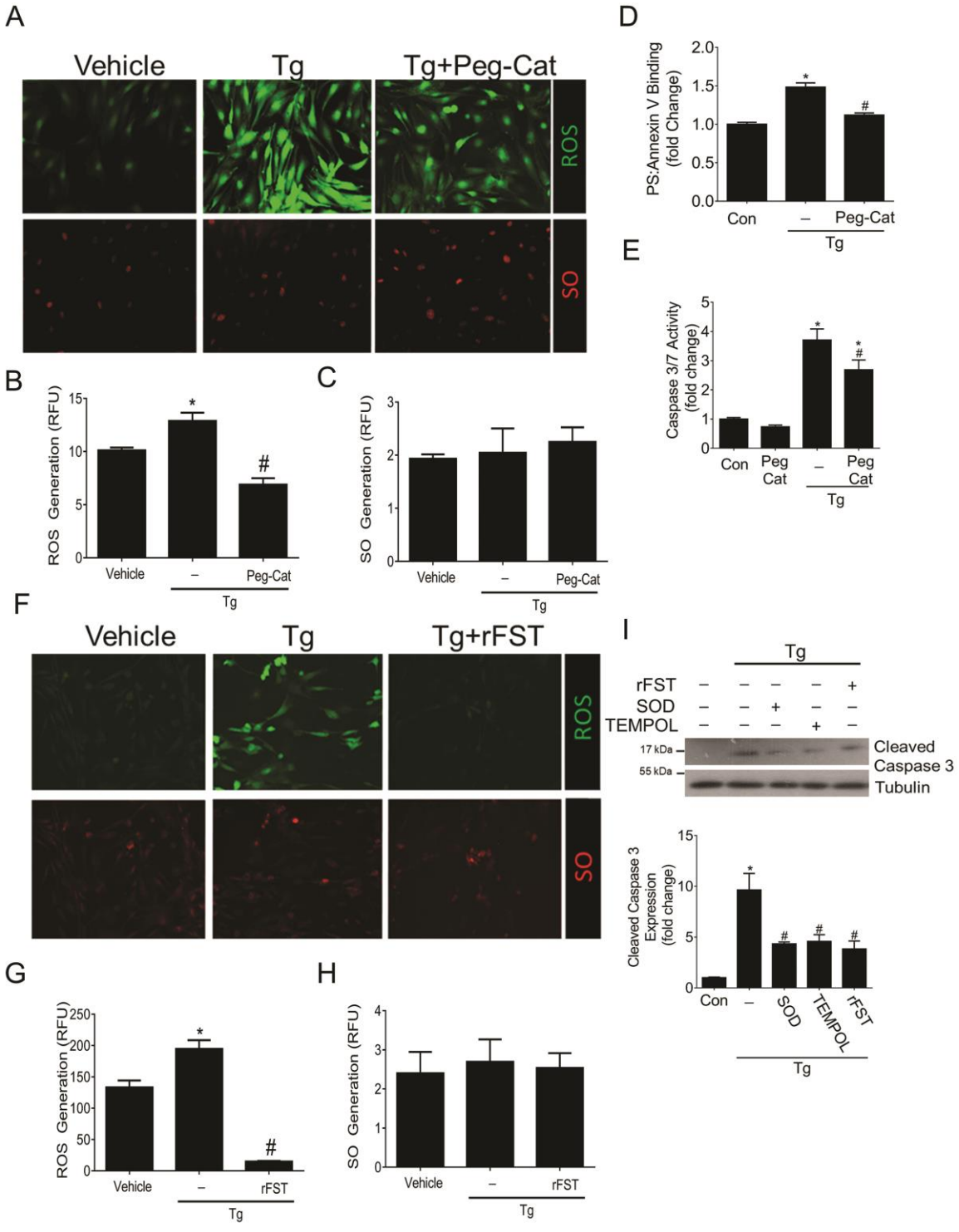
A
Vehicle
Tg
Tg+Peg-Cat
ROS
SO
B
ROS Generation (RFU)
Vehicle
–
Peg-Cat
Tg
C
SO Generation (RFU)
Vehicle
–
Peg-Cat
Tg
D
PS:Annexin V Binding (fold Change)
Con
–
Peg-Cat
Tg
E
Caspase 3/7 Activity (fold change)
Con
Peg Cat
–
Peg Cat
Tg
F
Vehicle
Tg
Tg+rFST
ROS
SO
G
ROS Generation (RFU)
Vehicle
–
rFST
Tg
H
SO Generation (RFU)
Vehicle
–
rFST
Tg
I
Tg
rFST
SOD
TEMPOL
17 kDa
55 kDa
Cleaved Caspase 3
Tubulin
Cleaved Caspase 3 Expression (fold change)
Con
–
SOD
TEMPOL
rFST
Tg

Figure 3-4. FST protects against Tg-induced apoptosis through blocking ROS generation. (A) MC were treated with vehicle (0.1%BSA/PBS, 30 min) or PEGylated-catalase (500U/ml, 30 min), followed by Tg (1µM, 8h) prior to loading with ROS/SO cocktail. Tg significantly increased the accumulation of intracellular ROS, but not SO, and this was reduced by catalase (n=4, representative micrographs shown). (B,C) MC were treated as above and quantitatively assessed using fluorescence spectrofluorometry. Tg-induced intracellular ROS (B) was inhibited by PEGylated-catalase, while SO (C) was not affected (n=3, *vs control, #vs Tg, $p<0.05$).

ROS inhibition using catalase (500U/ml) also significantly blunted Tg (200nM, 18h)-induced apoptosis, as assessed by decreased (D) cell surface phosphatidylserine-annexin V binding (n=6, *vs control, #vs Tg, $p<0.05$), and (E) caspase 3/7 enzymatic activity (n=9, *vs control, #vs Tg, $p<0.05$). (F) MC were treated with vehicle or recombinant FST (1µg/ml, 30 min) and then loaded with ROS/SO cocktail containing Tg (1µM, 8h). FST blocked the accumulation of intracellular ROS by Tg (n=6, representative micrographs shown). (G, H) MC were treated as above and quantitatively assessed using fluorescence spectrofluorometry. Tg-induced intracellular ROS (G) was most effectively inhibited by FST, while SO (H) was not affected (n=3, *vs control, #vs Tg, $p<0.05$). (I) SOD (5U) and TEMPOL (5mM) significantly blunted Tg (200nM, 18h)-induced apoptosis, similar to recombinant FST (1µg/ml) as assessed by cleavage of caspase 3 (n=3, *vs control, #vs Tg, $p<0.05$).

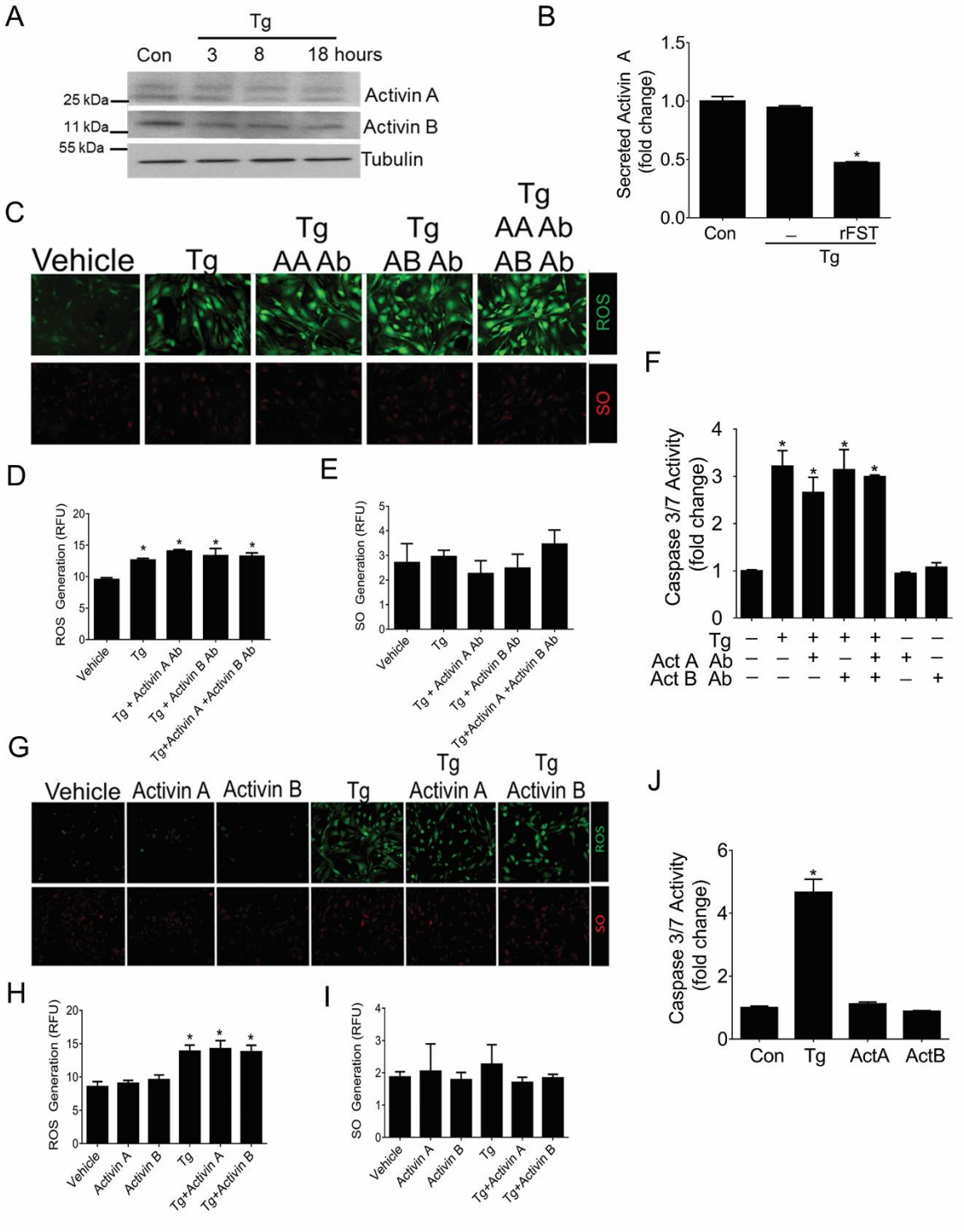
A
Tg
Con
3
8
18 hours
25 kDa
11 kDa
55 kDa
Activin A
Activin B
Tubulin
B
Secreted Activin A (fold change)
1.5
1.0
0.5
0.0
Con
–
rFST
Tg
C
Vehicle
Tg
Tg AA Ab
Tg AB Ab
Tg AA Ab AB Ab
ROS
SO
D
ROS Generation (RFU)
Vehicle
Tg
Tg + Activin A Ab
Tg + Activin B Ab
Tg+Activin A +Activin B Ab
E
SO Generation (RFU)
Vehicle
Tg
Tg + Activin A Ab
Tg + Activin B Ab
Tg+Activin A +Activin B Ab
F
Caspase 3/7 Activity (fold change)
Tg
Act A Ab
Act B Ab
G
Vehicle
Activin A
Activin B
Tg
Tg Activin A
Tg Activin B
ROS
SO
H
ROS Generation (RFU)
Vehicle
Activin A
Activin B
Tg
Tg+Activin A
Tg+Activin B
I
SO Generation (RFU)
Vehicle
Activin A
Activin B
Tg
Tg+Activin A
Tg+Activin B
J
Caspase 3/7 Activity (fold change)
Con
Tg
ActA
ActB

Figure 3-5. Tg-induced ROS production and apoptosis is not mediated by activin A or activin B.

(A) Tg (200nM) did not alter the protein expression of ActA or ActB (n=3, representative blots shown). (B) Tg (200nM, 8h) did not increase ActA secretion as assessed by ELISA. Recombinant FST (1µg/ml, 30 min), however, significantly decreased detectable ActA in the medium (n=2, *$p<0.05$). (C) MC were treated with either mouse IgG1 antibody (vehicle) (1ug/ml, 30 min), ActA neutralizing antibody (0.1µg/ml, 30 min), and/or ActB neutralizing antibody (1µg/ml, 30 min), followed by Tg (1µM, 8h) and then loaded with ROS/SO cocktail. ActA or ActB neutralization alone or in combination did not affect Tg-induced intracellular ROS and SO accumulation (n=3, representative micrographs shown). (D, E) MC were treated as above and quantitatively assessed using fluorescence spectrofluorometry. Tg-induced intracellular ROS (D) and SO (E) was not affected by activin neutralization (n=3, *vs control, $p<0.05$). (F) ActA antibody (0.1µg/ml) and/or ActB antibody (1µg/ml) did not significantly alter Tg (200nM, 18h)-induced MC apoptosis, as assessed by caspase 3/7 enzymatic activity (n=6, *vs control, $p<0.05$). (G) MC were treated with vehicle (0.1%BSA/PBS, 8h), recombinant ActA (5ng/ml, 8h), or recombinant ActB (5ng/ml, 8h), with or without Tg (1µM, 8h) and then loaded with ROS/SO cocktail. Neither ActA or ActB affected basal or Tg-induced intracellular ROS and SO accumulation (n=4, representative micrographs shown). (H, I) MC were treated as above and quantitatively assessed using fluorescence spectrofluorometry. Tg-induced intracellular ROS (H) and SO (I) was not affected by exogenous recombinant activin (n=3, *vs control, #vs Tg, $p<0.05$). (J) Neither ActA (5ng/ml, 18h) nor ActB (5ng/ml,

18h) promoted MC apoptosis, as assessed by caspase 3/7 enzymatic activity (n=9, *vs control, $p<0.05$).

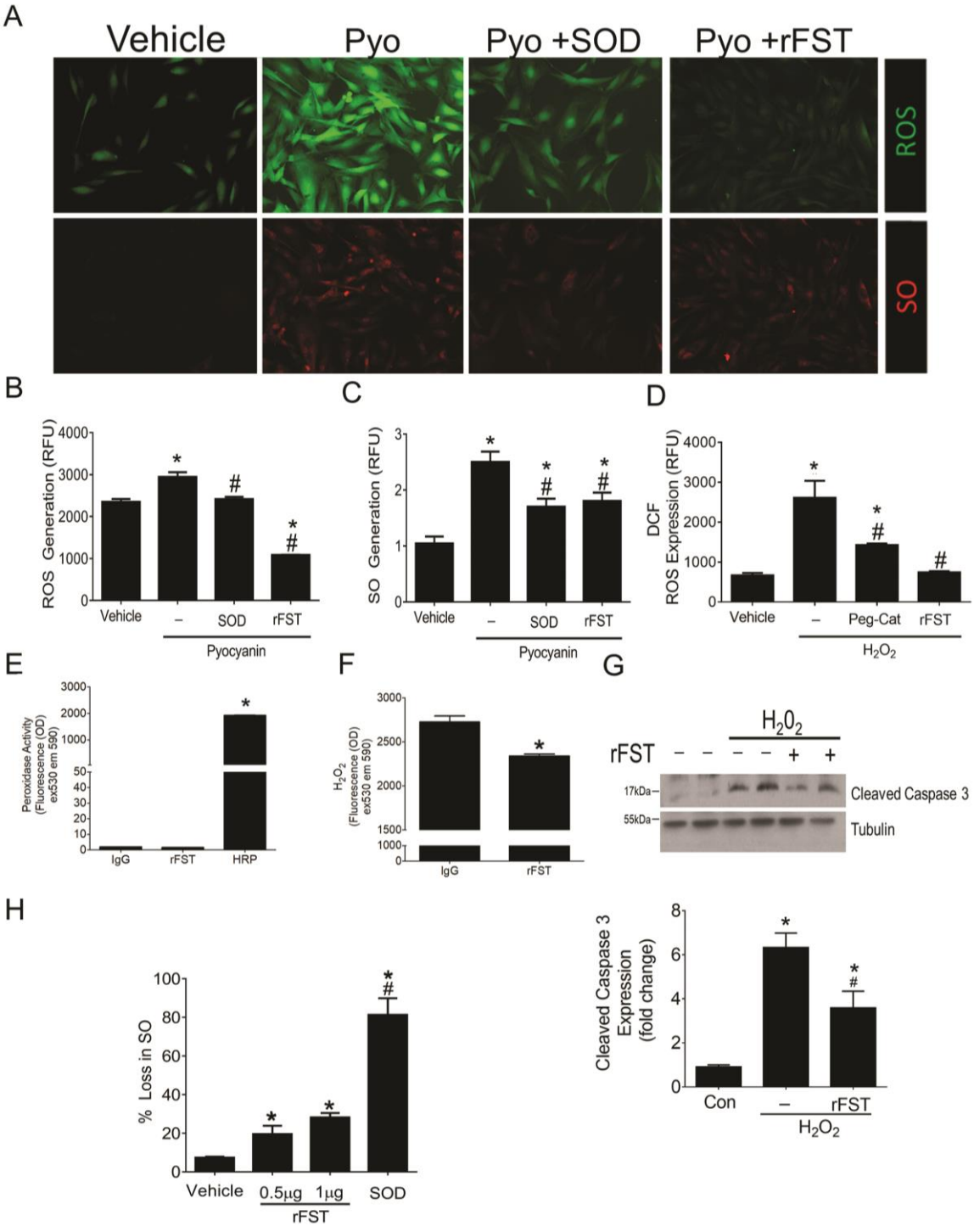
A
Vehicle
Pyo
Pyo +SOD
Pyo +rFST
ROS
SO
B
ROS Generation (RFU)
Vehicle
–
SOD
rFST
Pyocyanin
C
SO Generation (RFU)
Vehicle
–
SOD
rFST
Pyocyanin
D
DCF
ROS Expression (RFU)
Vehicle
–
Peg-Cat
rFST
H2O2
E
Peroxidase Activity (Fluorescence (OD) ex530 em 590)
IgG
rFST
HRP
F
H2O2 (Fluorescence (OD) ex530 em 590)
IgG
rFST
G
H2O2
rFST
17kDa
55kDa
Cleaved Caspase 3
Tubulin
H
% Loss in SO
Vehicle
0.5µg
1µg
SOD
rFST
Cleaved Caspase 3 Expression (fold change)
Con
–
rFST
H2O2

Figure 3-6. FST scavenges H2O2 and SO and protects against apoptosis.

(A) MC were treated with vehicle (0.1%BSA/PBS, 30 min), recombinant FST (1µg/ml, 30 min) or SOD (5U, 30 min), then loaded with ROS/SO cocktail prior to treatment with pyocyanin (50µM, 1h). Pyocyanin promoted a pronounced increase in the intracellular accumulation of ROS and SO which were suppressed by both FST and SOD (n=4, representative micrographs shown). (B, C) MC were treated as above and quantitatively assessed using fluorescence spectrofluorometry. Pyocyanin-induced intracellular ROS (B) was most effectively inhibited by FST, and SO (C) was significantly inhibited by both FST and SOD (n=3, *vs control, #vs pyocyanin, $p<0.05$). (D) MC were treated with vehicle (0.1%BSA/PBS, 30 min), PEGylated-catalase (500U/ml, 30 min) or recombinant FST (1µg/ml, 30 min), then loaded with H_2DCFDA prior to treatment with H_2O_2 (100µM, 8h). ROS detection in live MC, as assessed via spectrofluorometry, was significantly blunted by FST and catalase (n=6, *vs control, #vs H_2O_2, $p<0.05$). (E) Mouse IgG1 (1µg/ml) or recombinant FST (1µg/ml) was incubated with H_2O_2 (100µM, 30 min) and then introduced to ADHP (100µM, 30min). HRP (0.25U) was used as a positive control. FST did not exhibit any endogenous peroxidase activity (n=2, *vs IgG, $p<0.05$) (F) Mouse IgG1 (1µg/ml) or recombinant FST (1µg/ml) was incubated with H_2O_2 (25µM) and HRP (0.25U) for 1h and then introduced to ADHP (100µM, 30min). FST significantly decreased the amount of free H_2O_2 (n=6, *$p<0.05$). (G) Recombinant FST (1µg/ml, 30 min pre-treat) protected against H_2O_2 (100µM, 8h)-induced MC apoptosis, as assessed by decreased cleavage of caspase 3 (n=3, *vs control, #vs H_2O_2, $p<0.05$). (H) Xanthine/xanthine oxidase was used to generate SO in combination with mouse IgG1

(1µg/ml), recombinant FST (0.5µg/ml or 1µg/ml) or SOD (5U). FST significantly decreased detectable SO as compared to IgG, but was less effective when compared to SOD (n=4, *vs control, #vs FST, $p<0.05$).

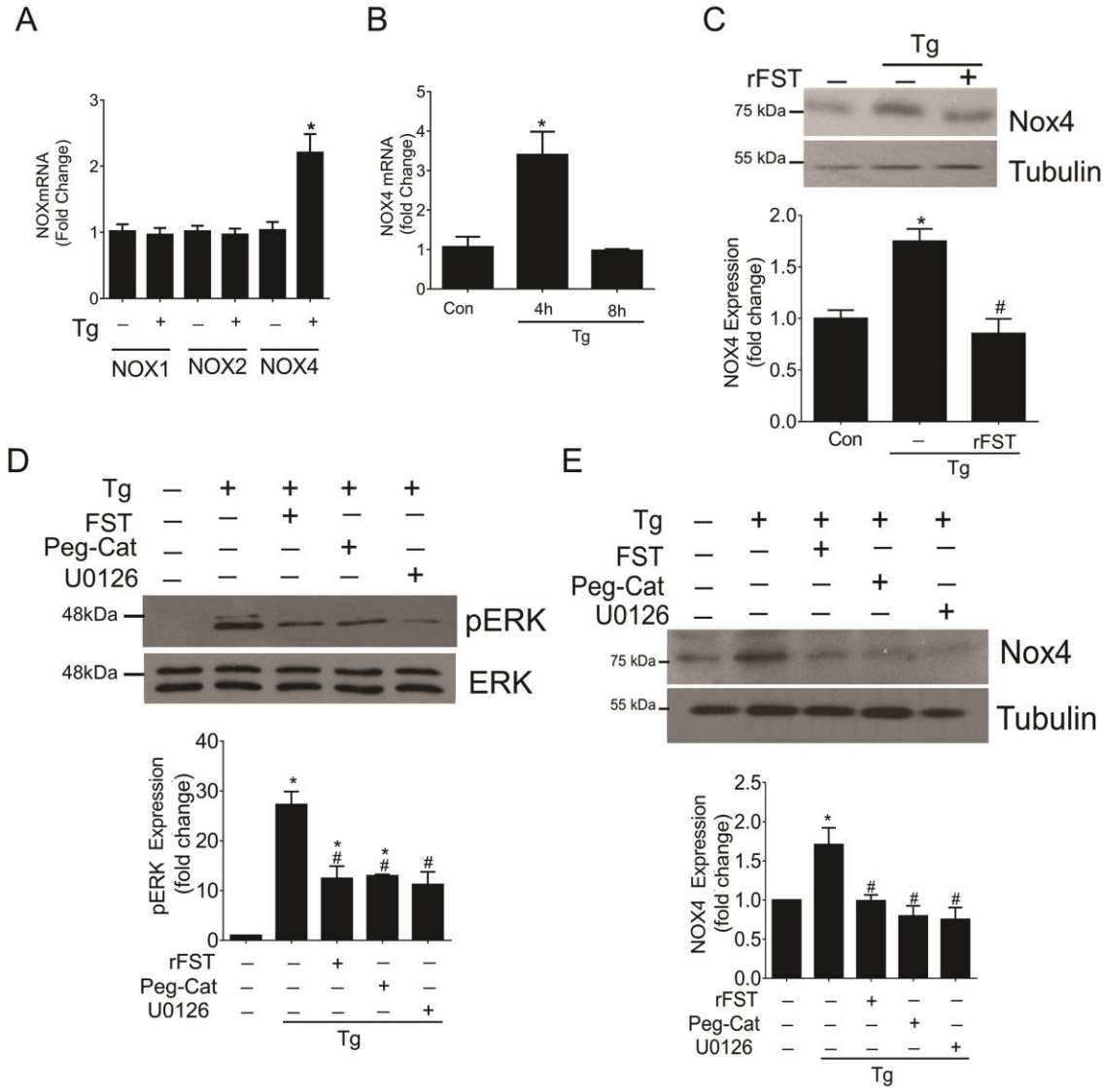
A
NOXmRNA (Fold Change)
Tg
NOX1
NOX2
NOX4
B
NOX4 mRNA (fold Change)
Con
4h
8h
Tg
C
Tg
rFST
75 kDa
Nox4
55 kDa
Tubulin
NOX4 Expression (fold change)
Con
rFST
Tg
D
Tg
FST
Peg-Cat
U0126
48kDa
pERK
48kDa
ERK
pERK Expression (fold change)
rFST
Peg-Cat
U0126
Tg
E
Tg
FST
Peg-Cat
U0126
75 kDa
Nox4
55 kDa
Tubulin
NOX4 Expression (fold change)
rFST
Peg-Cat
U0126
Tg

Figure 3-7. FST blocks Tg-induced NOX4 expression.

(A) Tg (200nM, 4h) led to significantly increased *nox4* transcript mRNA expression, but not *nox1* and *2*, as assessed by qRT-PCR (n=5, *vs control, $p<0.05$). (B) Tg (200nM) led to significantly increased *nox4* transcript mRNA expression at 4h, but not 8h, as assessed by qRT-PCR (n=4, *vs control, $p<0.05$). (C) Tg (200nM, 4h) led to significantly increased Nox4 protein expression, which was blunted by recombinant FST (1µg/ml, 30 min pre-treat) (n=5, *vs control, #vs Tg, $p<0.05$). (D) Tg (200nM, 30min) induced phosphorylation of ERK, which was inhibited by pre-treatment with recombinant FST (1µg/ml, 30 min), PEGylated-catalase (500U/ml, 30 min). The MEK inhibitor U0126 (10µM, 30 min) was used as a positive control for effective ERK inhibition (n=3, *vs control, #vs Tg, $p<0.05$). (E) Pre-treatment with recombinant FST (1µg/ml, 30 min), PEGylated-catalase (500U/ml, 30 min), or U0126 (10µM, 30 min) significantly blunted Tg (200nM, 4h)- induced Nox4 expression (n=4, *vs control, #vs Tg, $p<0.05$).

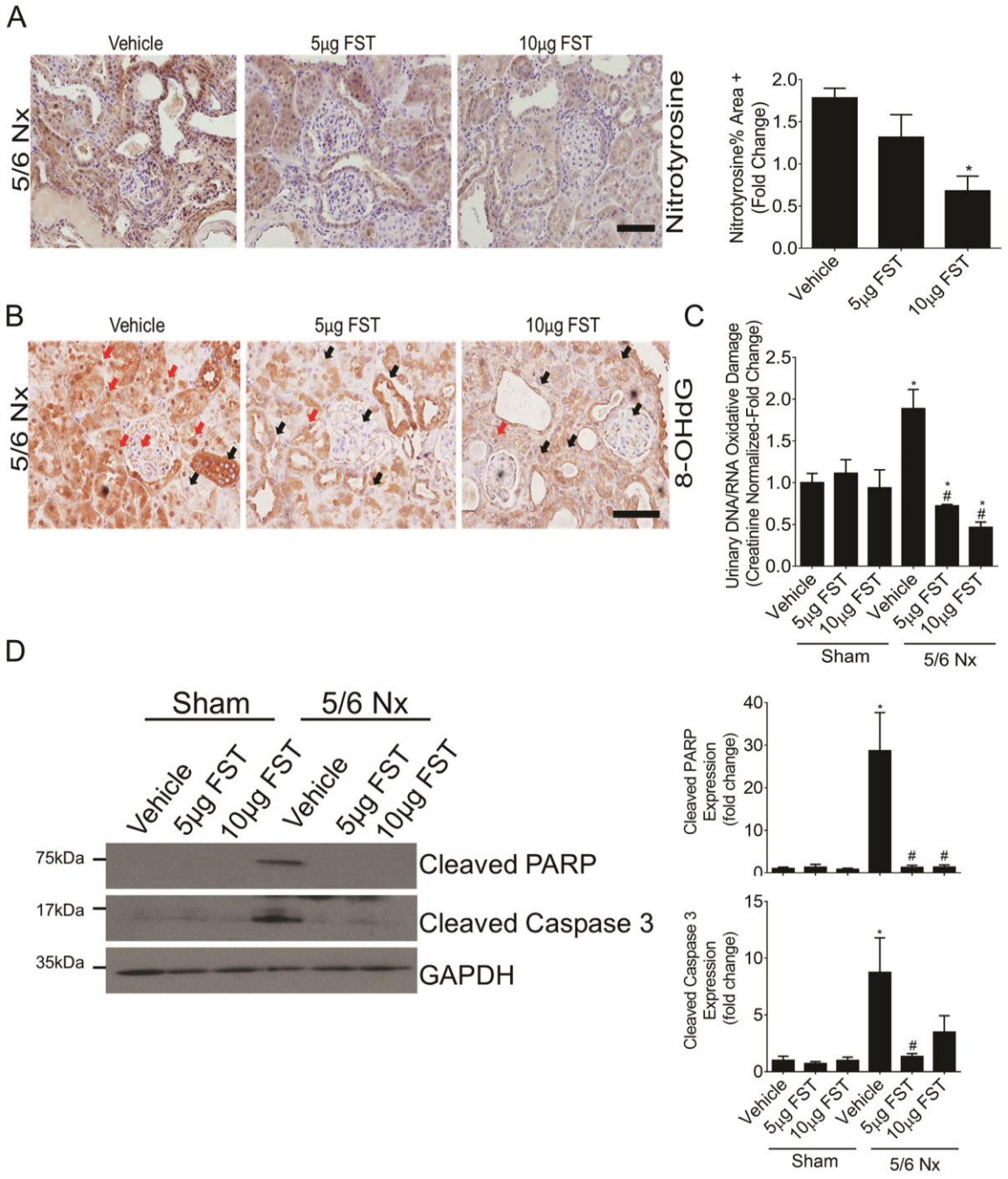
A
Vehicle
5µg FST
10µg FST
5/6 Nx
Nitrotyrosine
Nitrotyrosine% Area + (Fold Change)
2.0
1.5
1.0
0.5
0.0
Vehicle
5µg FST
10µg FST
B
Vehicle
5µg FST
10µg FST
5/6 Nx
8-OHdG
C
Urinary DNA/RNA Oxidative Damage (Creatinine Normalized-Fold Change)
2.5
2.0
1.5
1.0
0.5
0.0
Vehicle
5µg FST
10µg FST
Vehicle
5µg FST
10µg FST
Sham
5/6 Nx
D
Sham
5/6 Nx
Vehicle
5µg FST
10µg FST
Vehicle
5µg FST
10µg FST
75kDa
Cleaved PARP
17kDa
Cleaved Caspase 3
35kDa
GAPDH
Cleaved PARP Expression (fold change)
40
30
20
10
0
Cleaved Caspase 3 Expression (fold change)
15
10
5
0
Vehicle
5µg FST
10µg FST
Vehicle
5µg FST
10µg FST
Sham
5/6 Nx

Figure 3-8. FST treatment reduces oxidative stress and protects against apoptosis in kidneys of mice with CKD.

(A) Oxidative stress observed in the kidneys of mice with CKD, assessed by the expression of nitrotyrosinated proteins, was significantly reduced with 10µg FST administration (*vs Nx-Veh, $p<0.05$, scale bar =200µm). (B) DNA damage, assessed by the nuclear localization of 8-OHdG, was reduced by FST in CKD kidneys (red arrows indicate 8-OHdG positive nuclei, black arrows indicate 8-OHdG negative nuclei) (representative micrographs shown, scale bar =100µm). (C) Urinary expression of DNA/RNA damage markers were elevated in mice with CKD and significantly reduced in CKD mice treated with FST (*vs Sham Veh, #vs Nx-Veh, $p<0.05$). (D) Apoptosis was prominently inhibited in the kidneys of CKD mice treated with FST, as assessed by examining the cleavage of caspase 3 and PARP (*vs Sham Veh, #vs Nx-Veh, $p<0.05$).

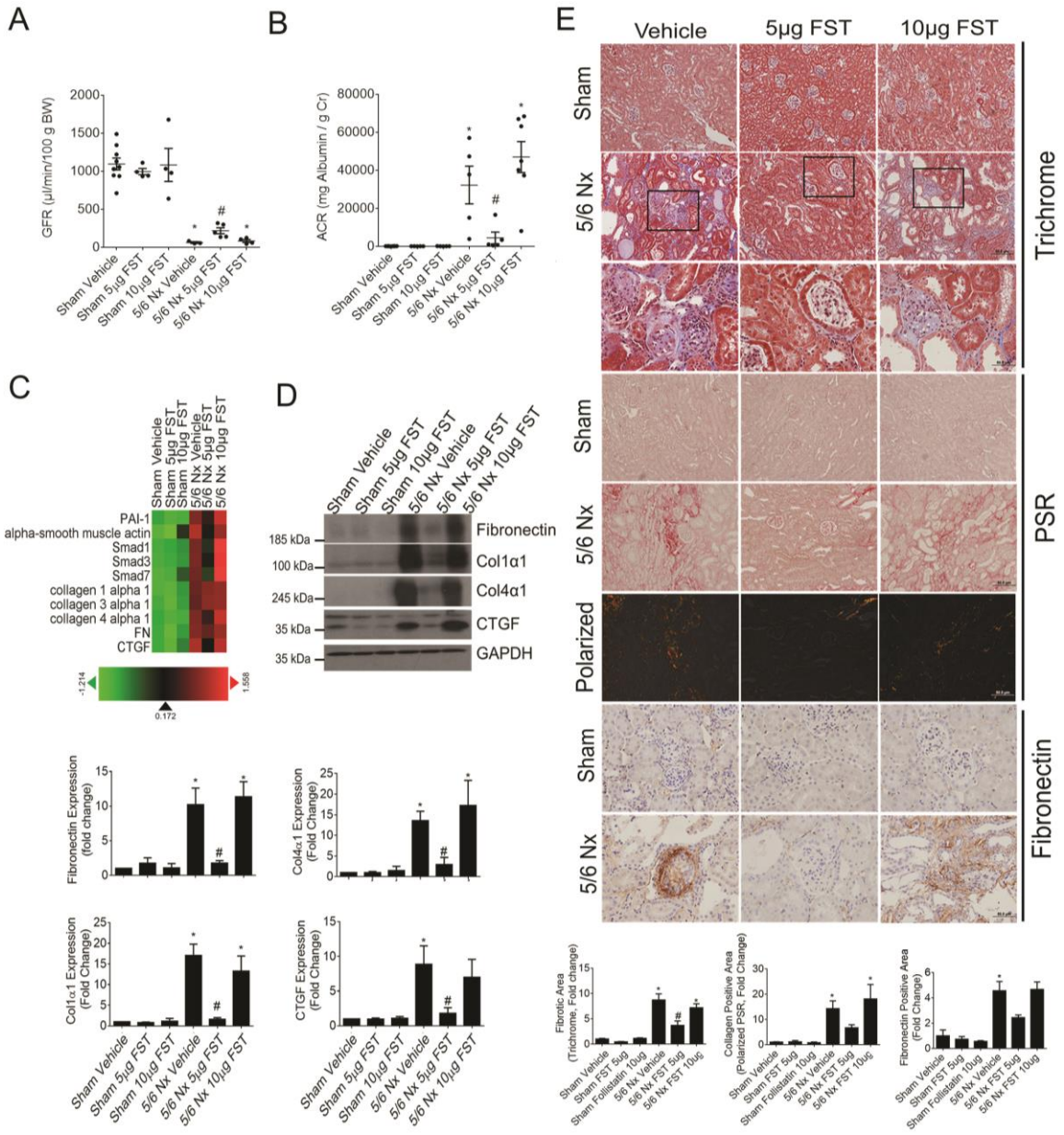
A
GFR (µl/min/100 g BW)
Sham Vehicle
Sham 5µg FST
Sham 10µg FST
5/6 Nx Vehicle
5/6 Nx 5µg FST
5/6 Nx 10µg FST
B
ACR (mg Albumin / g Cr)
C
PAI-1
alpha-smooth muscle actin
Smad1
Smad3
Smad7
collagen 1 alpha 1
collagen 3 alpha 1
collagen 4 alpha 1
FN
CTGF
Fibronectin Expression (fold change)
Col4α1 Expression (Fold Change)
Col1α1 Expression (Fold Change)
CTGF Expression (Fold Change)
D
185 kDa
100 kDa
245 kDa
35 kDa
35 kDa
Fibronectin
Col1α1
Col4α1
CTGF
GAPDH
E
Vehicle
5µg FST
10µg FST
Sham
5/6 Nx
Polarized
Trichrome
PSR
Fibronectin
Fibrotic Area (Trichrome, Fold change)
Collagen Positive Area (Polarized PSR, Fold Change)
Fibronectin Positive Area (Fold Change)
Sham Vehicle
Sham FST 5ug
Sham Follistatin 10ug
5/6 Nx Vehicle
5/6 Nx FST 5ug
5/6 Nx FST 10ug

Figure 3-9. FST treatment improves kidney function and protects against renal fibrosis in mice with CKD.

(A) The drastically diminished glomerular filtration rate (GFR) in CKD mice injected with vehicle was significantly improved with 5μg FST administration (*vs Sham-Veh, #vs Nx-Veh, $p<0.05$). (B) Albuminuria, as measured by the urinary albumin to creatinine ratio (ACR) was elevated in CKD mice and significantly improved with 5μg FST (*vs Sham-Veh, #vs Nx-Veh, $p<0.05$). (C) Agglomerative clustered heat-map analysis of kidney mRNA expression data obtained using Nanostring. Elevated mRNA expression profiles of profibrotic and ECM markers within the kidneys of CKD mice injected with vehicle was observed, with decreases seen with 5μg FST. (D) The increased expression of ECM proteins fibronectin, collagen Iα1 and collagen IVα1, along with profibrotic CTGF in CKD mice injected with vehicle was significantly decreased by 5μg FST (*vs Sham-Veh, #vs Nx-Veh, $p<0.05$). (E) Trichrome to assess fibrosis (boxed regions are magnified below), picrosirius red (PSR) to assess collagen deposition (polarized images provided below) and fibronectin IHC were used to analyse fibrosis. CKD mice injected with vehicle exhibited extensive glomerular sclerosis, tubular dilatation and tublulointerstitial fibrosis, which was significantly improved by 5μg FST (*vs Sham-Veh, #vs Nx-Veh, $p<0.05$, scale bar =200μm (trichrome and PSR), 50μm (magnified trichrome), 100μm (fibronectin)).

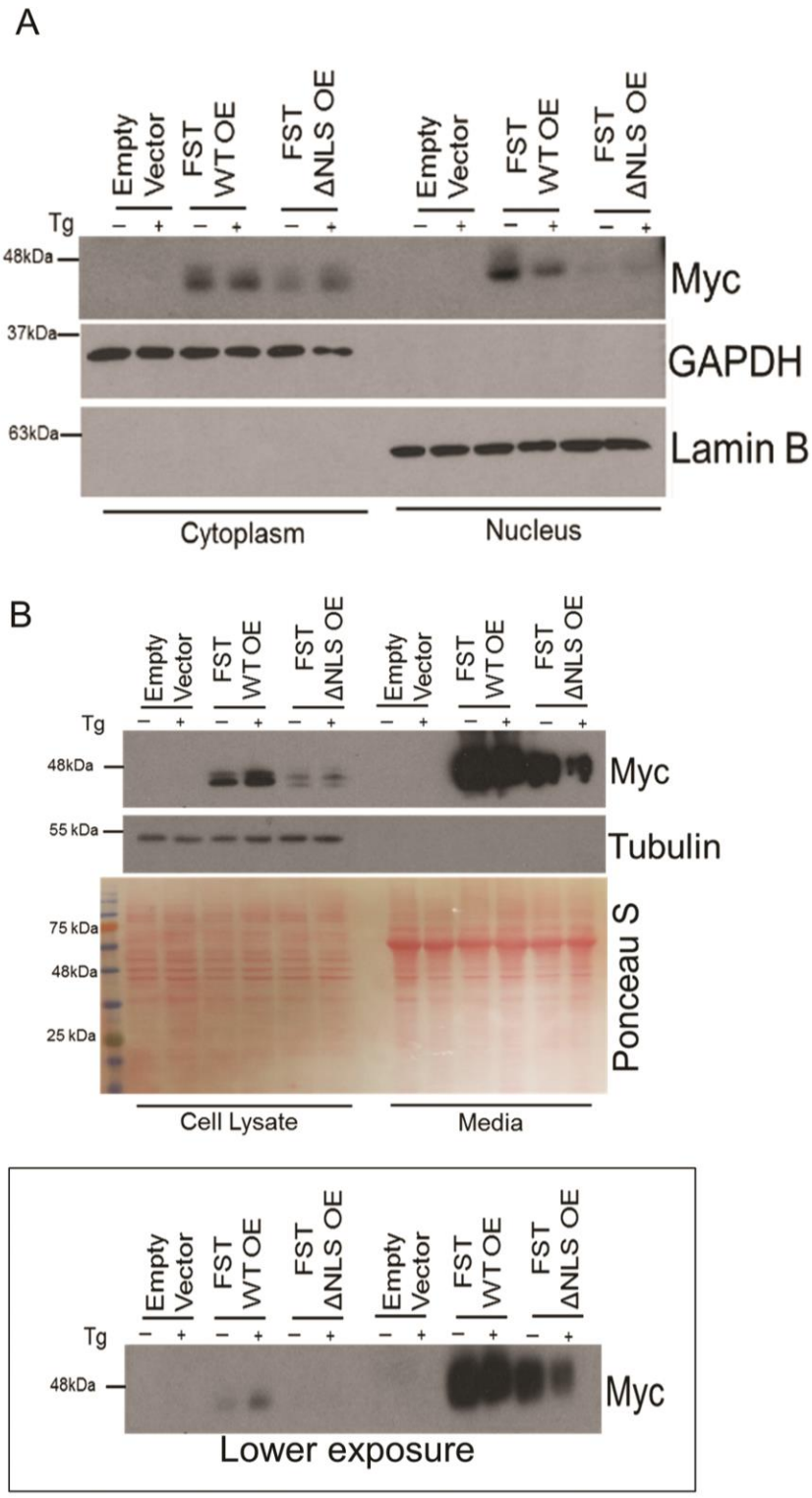
A
Empty Vector
FST WT OE
FST ΔNLS OE
Empty Vector
FST WT OE
FST ΔNLS OE
Tg
– + – + – + – + – + – +
48kDa
Myc
37kDa
GAPDH
63kDa
Lamin B
Cytoplasm
Nucleus
B
Empty Vector
FST WT OE
FST ΔNLS OE
Empty Vector
FST WT OE
FST ΔNLS OE
Tg
– + – + – + – + – + – +
48kDa
Myc
55 kDa
Tubulin
75 kDa
48kDa
25 kDa
Ponceau S
Cell Lysate
Media
Empty Vector
FST WT OE
FST ΔNLS OE
Empty Vector
FST WT OE
FST ΔNLS OE
Tg
– + – + – + – + – + – +
48kDa
Myc
Lower exposure

Figure 3-10. Supplemental Figure 1.

(A) Tg (200nM, 18h) did not increase the nuclear localization of wild-type FST. FSTΔNLS mutant is excluded from the nucleus. Nuclear and cytoplasmic separation and equal loading were confirmed using lamin B and GAPDH, respectively. (n=2, representative blots shown). (B) Tg (200nM, 18h) did not alter secretion of wild-type FST or FSTΔNLS mutant. Ponceau S staining confirms equal loading of proteins isolated from MC media (n=2, representative blots shown). [Lower exposure of blot shown in outlined box].

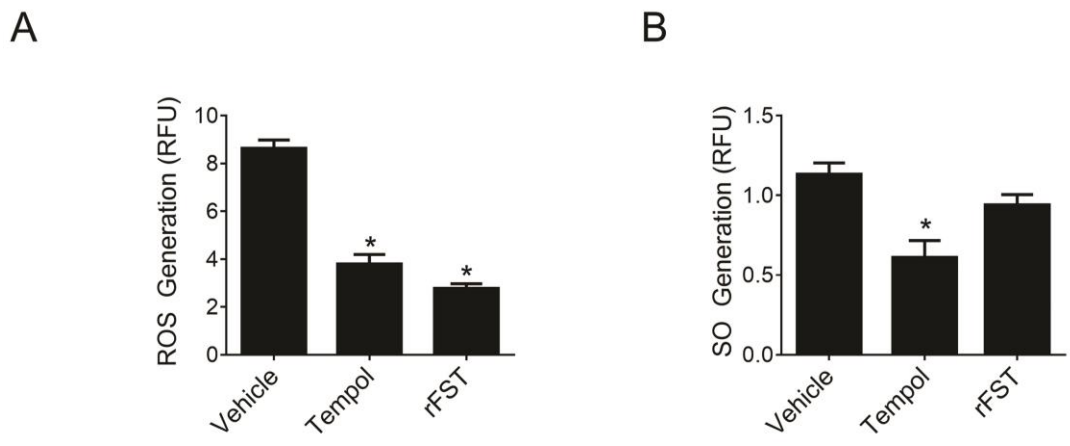

Figure 3-11. Supplemental Figure 2.

(A, B) MC were treated with vehicle (0.1%BSA/PBS, 30 min), TEMPOL (5mM, 30 min) or rFST (1μg/ml, 30 min), then loaded with ROS/SO cocktail and quantitatively assessed using fluorescence spectrofluorometry. TEMPOL significantly repressed basal intracellular ROS and SO expression, while FST significantly repressed ROS (n=3, *vs control, $p<0.05$).

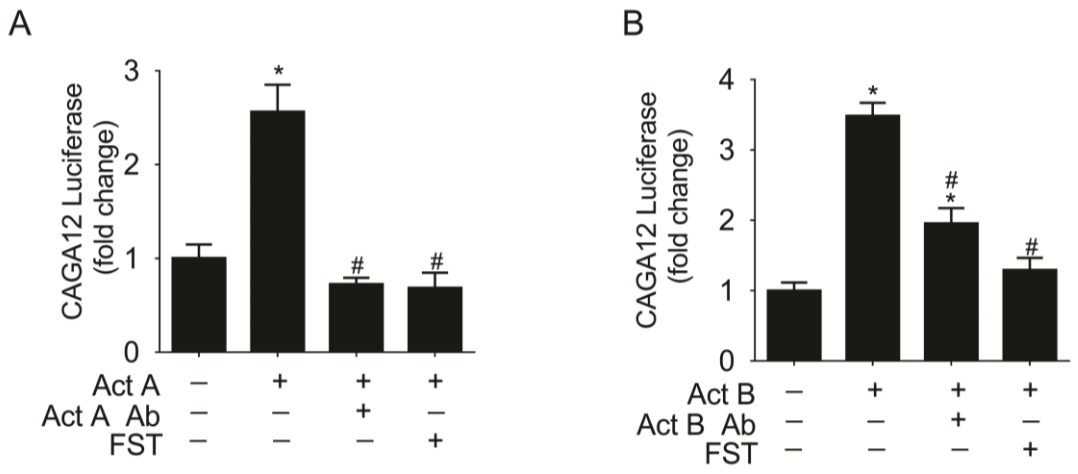

Figure 3-12. Supplemental Figure 3.

(A) ActA antibody (Ab) (0.1µg/ml, 30 min pre-treat) and recombinant FST (1µg/ml, 30 min pre-treat) significantly neutralize ActA (5ng, 8h)-mediated Smad3 signaling, assessed by activation of the Smad3-responsive CAGA12-luciferase (n=3, *vs control, #vs Tg+Act-A, $p<0.05$). (B) ActB Ab (1µg/ml, 30 min pre-treat) and recombinant FST (1µg/ml, 30 min pre-treat) significantly neutralize ActB (5ng, 8h)-mediated Smad3 signaling (n=3, *vs control, #vs Tg+Act-B, $p<0.05$).

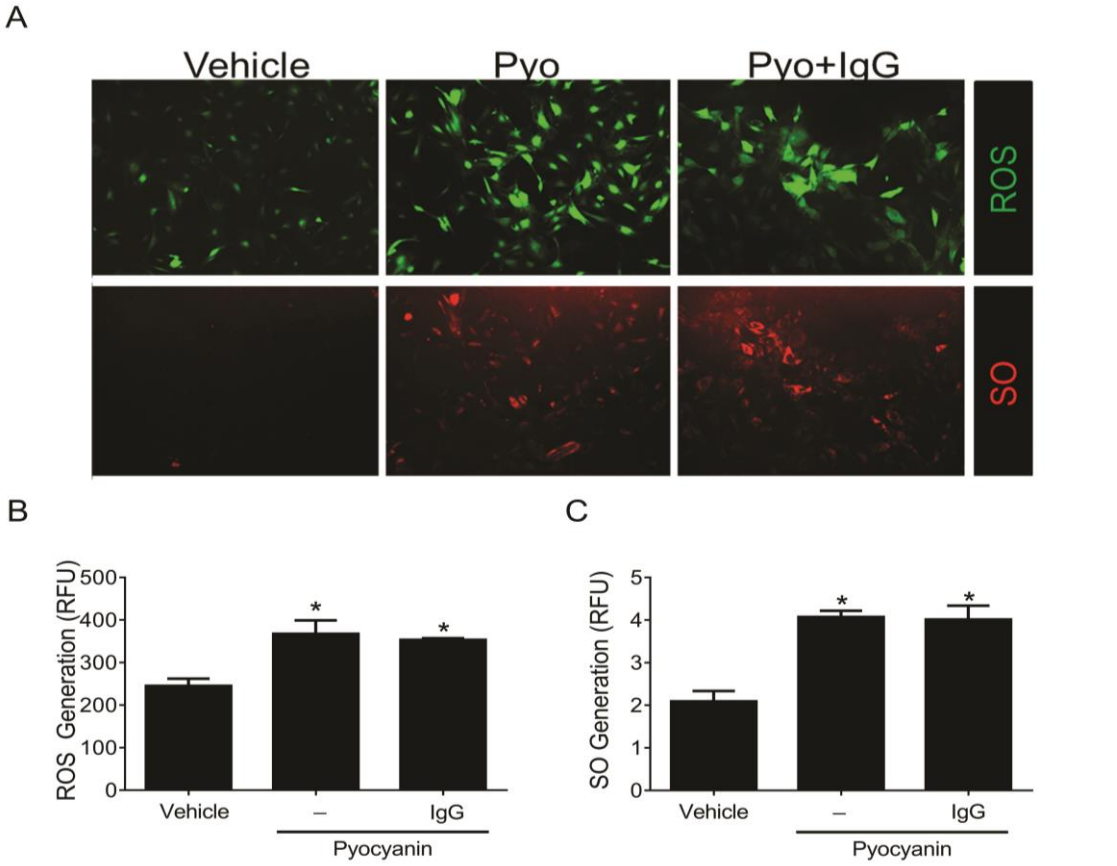

Figure 3-13. Supplemental Figure 4.

A) MC were treated with vehicle (0.1%BSA/PBS, 30 min) or mouse IgG1 (1µg/ml, 30 min) then loaded with ROS/SO cocktail prior to treatment with pyocyanin (pyo, 50µM, 1h). IgG did not affect pyocyanin-induced SO and ROS production (n=2, representative micrographs shown). (B, C) MC were treated as above and quantitatively assessed using fluorescence spectrofluorometry. Pyocyanin-induced intracellular ROS (B) and SO (C) generation in live MC was not affected by IgG (n=3, *vs control, #vs pyocyanin, $p<0.05$). (n=3, *vs control, #vs pyocyanin, $p<0.05$).

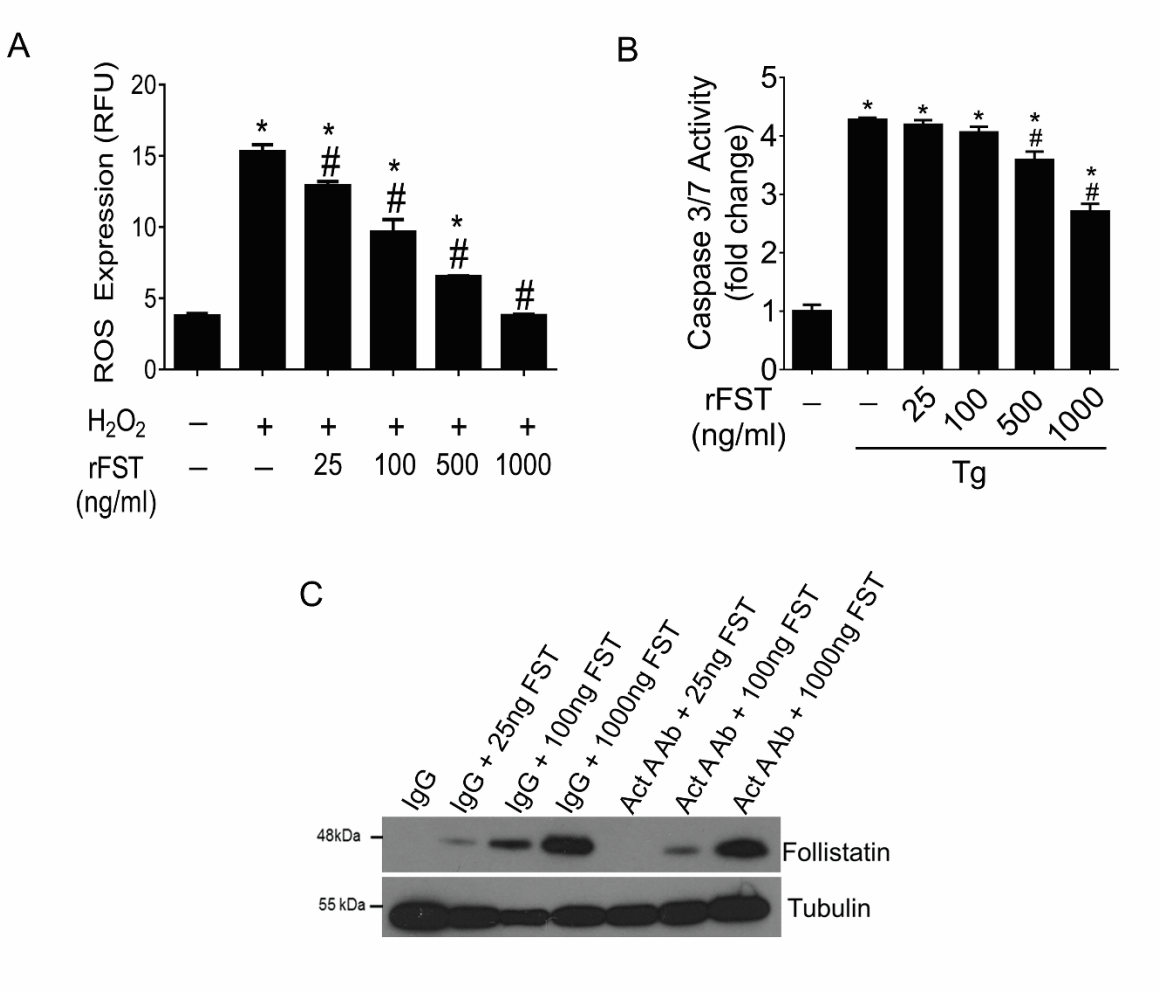
A
ROS Expression (RFU)
20
15
10
5
0
H2O2 – + + + + +
rFST – – 25 100 500 1000
(ng/ml)
B
Caspase 3/7 Activity
(fold change)
5
4
3
2
1
0
rFST – – 25 100 500 1000
(ng/ml)
Tg
C
IgG
IgG + 25ng FST
IgG + 100ng FST
IgG + 1000ng FST
Act A Ab + 25ng FST
Act A Ab + 100ng FST
Act A Ab + 1000ng FST
48kDa
Follistatin
55 kDa
Tubulin

Figure 3-14. Supplemental Figure 5.

(A) MC were treated with vehicle (0.1%BSA/PBS, 30 min) or recombinant FST ranging from 25 to 1000ng/ml (30 min), then loaded with ROS/SO cocktail prior to treatment with H_2O_2 (50μM, 1h) and quantitatively assessed using fluorescence spectrofluorometry. Recombinant FST dose dependently repressed detectable H_2O_2 (n=3, * vs control, # vs H_2O_2, $p<0.05$). **(B)** Recombinant FST (25 to 1000ng/ml, 30 min pre-treat) dose-dependently protected against Tg (200nM, 18h)-induced MC apoptosis, as assessed by decreased caspase 3/7 enzymatic activity (n=3, *vs control, #vs Tg, $p<0.05$). **(C)** Exogenous recombinant FST administered up to 1000ng was dose-dependently internalized by MC. However, ActA neutralization using a neutralizing antibody (5μg/ml, 30 min pre-treat) was only effective at blocking FST internalization at doses up to 100ng (n=4, representative blots shown).

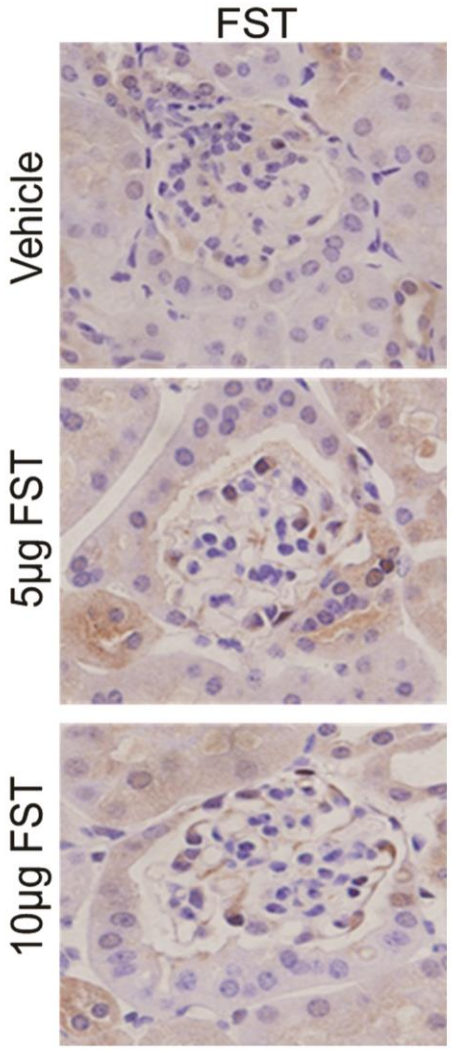

Figure 3-15. Supplemental Figure 6.

Exogenous FST administration results in increased FST identified in mouse kidneys.

Table 3-1. Drugs and recombinant proteins.

Drugs and Recombinant Proteins	***Working Concentration***	***Source***
Cycloheximide	10µg/ml	Sigma; 01810
Thapsigargin	200nM-1µM	Sigma; T9033
H_2O_2	100µM	Sigma; H1009
PEGylated Catalase	500U	Sigma; C4963
PEGylated SOD	5U	Sigma; S9549
TEMPOL	5mM	Sigma; 581500
Pyocyanin	50µM	Enzo; ENZ-53001-C001
U0126	10µM	Promega; V1121
Recomb. Mouse Activin A	5ng/ml	R&D Systems; 338-AC
Recomb. Mouse Activin B	5ng/ml	R&D Systems; 8260-AB
Recomb. Mouse Follistatin 244	25ng-1µg/ml (*in vitro*)	R&D Systems; 769-FS
Recomb. Human Follistatin 244	5-10µg (*in vivo)*	Paranta Biosciences

Table 3-2. siRNA.

siRNA	***Working Concentration***	***Source***
Mouse Follistatin Silencer Select siRNA	50nM	Life Tech; 4390771
Control Silencer Select siRNA	50nM	Life Tech; 4390844

Table 3-3. Plasmids.

Plasmids	***Source***
mFST4 Luciferase	Dr. Jeong Yoon
hFST-WT-myc	Dr. Xiangwei Gao
hFST-ΔNLS-myc	Dr. Xiangwei Gao
CAGA12 Luciferase	Dr. Maree Bilandzic
pcDNA3.1(+)	Thermo Scientific
pCMV β-galactosidase	Clonetech

Table 3-4. Antibodies.

Antibody	***Application***	***Working Concentration***	***Source***
Follistatin	WB	1:1,000	Santa Cruz; sc-30194
Follistatin	IHC	1:100	Proteintech ; 60060-1-lg
Activin A	IHC and WB	1:200 and 1:1,000	R&D Systems; AF338
Activin A	Neutralization	0.1µg/ml-5µg/ml	R&D Systems; MAB3381
Activin B	IHC and WB	1:200 and 1:1,000	R&D Systems; MAB659
Activin B	Neutralization	1µg /ml	R&D Systems; MAB659
Collagen Iα1	WB	1:4,000	Novus; NB600-408
Collagen IVα1	WB	1:4,000	Novus; NB120-6586
Fibronectin	WB and IHC	1:1,000 and 1:200	Sigma; F3648
CTGF	WB	1:1,000	Santa Cruz; sc-14939
Phospho-p44/42 MAPK	WB	1:1000	CST; 9106
p44/42 MAPK	WB	1:1000	CST; 9102
NOX4	WB	1:1,000	Novus; NB110-5885
8-OHdG	IHC	1:100	Novus; NB600-1508
Nitrotyrosine	IHC	1:1,000	Millipore; 06-284
Mouse IgG1	Neutralization	1µg /ml	R&D Systems; MAB002
α-Tubulin	WB	1:10,000	Sigma; T6074
GAPDH	WB	1:10,000	CST; 2118

Table 3-5. qPCR Primers.

Gene	***Forward***	***Reverse***
Mouse FST	AAAACCTACCGCAACGAATG	GGTCTGATCCACCACACAAG
Mouse Nox1	AATGCCCAGGATCGAGGT	GATGGAAGCAAAGGGAGTGA
Mouse Nox2	CCCTTTGGTACAGCCAGTGAAGAT	CAATCCCGGCTCCCACTAACATCA
Mouse Nox3	CGACGAATTCAAGCAGATTGC	AAGAGTCTTTGACATTGCTTTGG
Mouse Nox4	GGATCACAGAAGGTCCCTAGCAG	GCGGCTACATGCACACCTGAGAA
Mouse 18s	GCCGCTAGAGGTGAAATTCTTG	CATTCTTGGCAAATGCTTTCG

Chapter 4: miR299a-5p Promotes Renal Fibrosis Through Suppression of Antifibrotic Follistatin in Chronic Kidney Disease

Title: miR299a-5p Promotes Renal Fibrosis Through Suppression of Antifibrotic Follistatin in Chronic Kidney Disease

Authors: Neel Mehta, Dan Zhang, Juehua He, Bo Gao, Joan C. Krepinsky

Corresponding Author: Dr. Joan C. Krepinsky, Department of Nephrology, St. Joseph Hospital, 50 Charlton Ave E, Room T3311, Hamilton, Ontario L8N 4A6, Canada, Telephone: (905) 522-1155 x 34991; FAX: (905) 540-6589; Email: krepinj@mcmaster.ca

Citation: *Manuscript in preparation for submission.*

4.1 Preface

Significance to thesis: Previously, we observed that cav-1 knockout KO mice and cav-1 deficient glomerular MC are protected against the development of glomerulosclerosis. In chapter 2, we established a novel transcriptional mechanism regulated by cav1 that functions to repress the expression of the antifibrotic protein FST. 3'UTR analysis of the FST promoter suggested that cav-1 KO MC exhibit 3'UTR stabilization. Post-transcriptional regulation of FST by cav-1 via miRNA could thus be another mechanism via which the expression of FST is regulated in CKD. In this project, a FST targeting miRNA, miR299a-5p, was identified to be downregulated in cav-1 deficient MC and involved in post-transcriptionally regulating the expression of FST. miR299a-5p was found to be stimulated by TGFß1 and be involved in augmenting the profibrotic responses of TGFß1 through the inhibition of FST. Its expression was elevated in the kidneys of mice with CKD and its inhibition was efficacious in ameliorating renal fibrosis. This chapter has identified a novel therapeutically targetable miRNA, miR299a-5p, that is involved in the development of renal fibrosis CKD.

Author's contribution: NM performed experiments and analysed data, DZ, HJ and BG performed experiments, NM wrote the manuscript, NM and JCK conceived the ideas, BG assisted with animal studies, all authors read and approved the final manuscript.

- DZ and BG assisted with mouse handling and tissue/specimen collection.
- DZ and HJ assisted with western blotting experiments in Figures 2,3 and 4.

4.2 Abstract

Caveolin-1 (cav-1), an integral membrane protein, is required for the synthesis of matrix proteins by glomerular mesangial cells (MC). The antifibrotic protein follistatin (FST) is 35-fold upregulated in cav-1 knockout MC. Follistatin inhibits the profibrotic effects of several members of the TGFß superfamily. In addition to its regulation at the transcriptional level, as we've previously shown (chapter 2), here, we performed a screen to identify differences in expression of FST-targeting microRNA (miRNA) profiles between cav-1 WT and KO MC to identity novel post-transcriptional regulators of FST. We found that the expression of miR-299a-5p was significantly suppressed in cav-1 KO MC. This was associated with stabilization of the 3'UTR of FST in cav-1 KO MC. Overexpression and inhibition studies in primary cultured MC confirmed the role of miR299a-5p in regulating the expression of FST. TGFß was found to stimulate the expression of miR299a-5p and in turn down-regulate FST. Through downregulation of the antifibrotic protein FST, miR299a-5p was found to augment TGFß-induced extracellular matrix production by MC. Inhibition of miR299a-5p in cav-1 WT MC was found to diminish TGFß profibrotic responses, while overexpression was found to re-enable the ability of cav-1 KO MC to respond to TGFß and produce extracellular matrix proteins. Lastly, miR299a-5p was upregulated in the kidneys of mice with hypertensive CKD that had undergone 5/6 nephrectomy. Our data collectively suggest miR299-5p is pathogenic via the inhibition of FST and that its inhibition could be a viable therapeutic approach for ameliorating renal fibrosis in CKD.

4.3 Introduction

Chronic kidney disease (CKD) is a major cause of morbidity and mortality that is pathologically characterized by excessive renal fibrosis, which over time results in declining kidney function and ultimately end-stage renal disease [4–6]. Renal fibrosis encompasses both glomerulosclerosis and tubulointerstitial fibrosis, with the latter known to be a strong correlate of CKD progression [11–16]. Treatments specifically targeted at reversing or slowing renal fibrosis in CKD are not well established.

Mesangial cells (MC) are specialized pericytes that are involved in the production and secretion of mesangial matrix within the glomerulus [19–21]. Under homeostatic conditions, MC secrete matrix that is composed of collagens, laminin and fibronectin [19,31,35,112]. In a CKD setting, the activation and transition of MC to a myofibroblastic smooth-muscle-like phenotype has been established to be an early fibrogenic response [19,20]. Activated MC undergo hypertrophy and proliferation and increase their matrix production [20,32]. Expansion of the mesangial matrix is a prominent finding in CKD [14,20,21].

Caveolae are ubiquitous small (50-100 nm) glycosphingolipid and cholesterol enriched omega-shaped invaginations of the plasma membrane . Through compartmentalization of signaling proteins, they can either positively or negatively mediate signal transduction events [73–75]. The caveolin family consists of three proteins, cav-1, cav-2 and cav- 3. Our lab has shown a role for cav-1 in the ability of MC to produce matrix proteins both basally and in response to profibrotic stimuli such as TGFβ1, mechanical stress, and high glucose [77–80]. We further identified significant

upregulation of the antifibrotic protein follistatin (FST) in cav-1 deficient MC, and showed it to be important in the reduced glucose and TGFβ-induced profibrotic responses of these cells [22,214]. FST is an ubiquitously expressed secreted glycoprotein that binds to and neutralizes the profibrotic and proinflammatory actions of several TGFβ superfamily members, with greatest potency against the activins [46,57]. Our work further showed an important role for activin A (ActA) in the glucose-induced profibrotic response in MC.

Therapeutically, our recent studies have shown promising antifibrotic and kidney function preserving effects of routine, frequent exogenous FST administration in mouse models of diabetic nephropathy and hypertensive CKD [22,214]. However, a rapid half-life of FST necessitates frequent dosing which is not clinically practical [214]. Thus, alternative approaches that can more efficiently and stably upregulate FST *in vivo* may potentially improve the clinical ability to harness the endogenous antifibrotic properties of FST to protect against renal fibrosis.

We have recently shown that increased expression of FST in cav-1 knockout (KO) MC is seen at the transcript level, at least in part through promoter activation by heightened activity of the transcription factor Sp1 [214]. To further identify the mechanisms for FST upregulation in cav-1 KO MC, here we tested the potential role of microRNAs (miRNAs). These are small single-stranded noncoding RNAs (~22bp) that bind to a specific 2-8bp miRNA regulatory element (MRE) localized within the 3' untranslated region (UTR) of the target mRNAs through their fully or partially complementary “seed sequence” [98,99]. Depending on binding complementarity, the

miRNA targets the mRNA for degradation or translational repression [98,99]. Despite their multiple targets, mature miRNAs have distinct features that are favorable for their potential therapeutic and biomarker use, including their short sequence and high homology across species [103,104,215,216]. Indeed, therapeutically targeting miRNAs using LNA technology has become a highly investigated area with both overexpression and inhibition being used depending on the miRNA and its function in disease [100,102–104,215,216]. As a result, numerous studies have been carried out to assess the therapeutic potential of inhibiting or overexpressing these specific miRNAs in protecting against fibrosis in the kidneys [100,102,104].

In screening for miRNAs targeting FST and which are differentially expressed in cav-1 KO MC, we discovered miR299a-5p as an important inhibitor of FST expression, which was significantly decreased in cav-1 KO MC. We show that miR299a-5p is profibrotic through its potent ability to repress the expression of FST. In a mouse model of CKD, miR299a-5p expression was increased and its inhibition protected against the progression of CKD through reducing fibrosis and albuminuria along with improving kidney function and blood pressure. Targeting miR299a-5p is therapeutically beneficially for protecting against renal fibrosis in CKD.

4.4 Materials and Methods

Cell Culture

Primary mouse mesangial cells (MCs) were isolated from cav-1 wild-type (WT) and cav-1 KO B6129SF1/J mice (Jackson Laboratory), as described previously[214]. MCs were grown in Dulbecco's modified Eagle's medium (DMEM) supplemented with 20% fetal bovine serum (Invitrogen), penicillin (100 μg/ml) and streptomycin (100 μg/ml) at 37˚C in 95% O_2, 5% CO_2. Passages 7-14 were used. MCs were serum deprived in 0.5% FBS 24h prior to treatment unless otherwise stated. Drugs/reagents used in the study are provided in table 4-1.

Transfection

Transient expression of plasmids was achieved using electroporation with the ECM 830 Square Wave Electroporation System (Harvard Bioscience). Briefly, MCs resuspended in electroporation buffer containing the appropriate plasmids (0.5μg luciferase plasmid with 0.05μg β-Galactosidase or 10μg protein expression plasmid) were electroporated using a single square pulse set at 200V for 35 msec. Effective transfection of miR inhibitor and over-expression clones was confirmed by observing mCherry (ex550nm/em620nm) and GFP (ex490nm/em525nm) immunofluorescence, respectively (EVOS FL Cell Imaging System, Thermo Fisher Scientific). SiRNA-mediated (50nM) knockdown was achieved using RNAiMAX (Thermo Fisher Scientific) as per the manufacturer's recommendation. MCs were serum deprived 24h following transfection prior to treatment and harvest. Plasmids and siRNA used in the study are provided in table 4-2 and 4-3.

Luciferase Assay

MC lysis was achieved using Reporter Lysis Buffer (Promega) as per the manufacturer's recommendation. Luciferase (luc) activity was measured on clarified cell lysate using the Luciferase Assay System (Promega) with a luminometer (Junior LB 9509, Berthold). β-galactosidase activity, used to normalize for transfection efficiency, was measured in clarified cell lysates using the β-Galactosidase Enzyme Assay System (Promega) with a plate reader absorbance set at 420nm (SpectraMax Plus 384 Microplate Reader, Molecular Devices).

Protein Extraction and Immunoblotting

MC cell lysis and protein extraction were carried out as described previously[113]. Briefly, cell lysates were centrifuged (15,000 rpm, 10min, 4^{o}C), supernatant was collected and protein concentration quantified. Cell protein lysates (10μg-50μg) were separated on SDS-PAGE for subsequent immunoblotting. Primary antibodies used in the study are provided in table 4-4.

mRNA and miRNA Extraction and Quantitative-real time PCR

RNA from MCs was extracted using Ribozol RNA Extraction Reagent (Amresco) as per the manufacturer's recommendation, with 1μg of RNA reverse transcribed into cDNA using qScript cDNA SuperMix Reagent (Quanta Biosciences). miRNA-enriched cDNA was generated using the qScript microRNA Quantification System (Quanta Biosciences). Quantitative real-time PCR was carried out using the Power SYBR Green PCR Master

Mix (Thermo Fisher Scientific) on the Applied Biosystems ViiA 7 Real-Time PCR System (Thermo Fisher Scientific). mRNA and miRNA expression and fold changes were calculated using the $\Delta\Delta C_T$ method, where 18S was used as a control for mRNA and U6 snRNA as a control for miRNA. Primers sequences used in the study are provided in table 4-5.

Cloning

miR299a-5p regulatory element (MRE) luc was generated in order to measure miR299a-5p activity. Briefly, a 5'-phosphorylated oligonucleotide encoding a 67-bp region within the FST 3'UTR that includes the mir299a-5p 8mer MRE was synthesized. No other miRNA MRE completely localized and /or overlapped within this region. This oligonucleotide was inserted into a XbaI digested pGL3 control construct. All sequences synthesized for cloning are listed in table 4-6. All generated constructs were confirmed by sequencing (Mobix Lab, McMaster University).

Animal Studies

Animal studies were carried out in accordance with the principles of laboratory animal care and McMaster University and Canadian Council on Animal Care guidelines. Male CD1 mice were obtained from Charles River Laboratories. CKD was achieved using the 5/6 nephrectomy (5/6 Nx) renal mass reduction model. Briefly, at 6-7 weeks, anesthetized mice underwent resection of the upper and lower poles of the left kidney. After a one-week recovery period, anesthetized mice underwent a right nephrectomy. Sham mice

were anesthetized and the kidney manipulated without resection. Resected kidney weights were divided by the nephrectomized right kidney weight (Nx ratio) and mice were placed into 4 groups, with the Nx groups containing mice with roughly equal Nx ratios: Sham-con-LNA (n=5), Sham-mir299a-5p-LNA (n=5), 5/6 Nx-con-LNA (n=10), and 5/6 Nx-miR-299a-5p-LNA (n=10). Mice were injected subcutaneously (SC) once 24h before right nephrectomy, and then with 2mg/kg scrambled control (con) con-LNA or 2mg/kg miR299a-5p LNA twice a week for the entire study duration. At study endpoint (week 9), blood pressures were measured in conscious mice using tail-cuff volume pressure recordings with the Coda non-invasive blood pressure monitoring system (Kent Scientific), as done previously [22]. At study endpoint (week 9), urine was collected and albumin-to-creatinine ratio measured according to manufacturer's instructions (Albuwell M, Exocell for urine albumin and Crystal Chem for creatinine). Glomerular filtration rate (GFR) was assessed in conscious mice by measuring the clearance of fluorescein isothiocyanate (FITC)-labeled sinistrin (Fresenius Kabi Linz, Austria). Briefly, a 5% FITC-sinistrin solution was injected retro-orbitally, after which blood was collected from the saphenous vein at 7, 15, 30, 60, 90 and 120 mins. Plasma fluorescence was assessed using a fluorometer (Gemini EM, Molecular Devices) at 485 nm excitation and 538nm emission. Following GFR assessment, mice were perfused with cold PBS. Kidney portions were fixed in formalin. Trichrome (Sigma) and PSR (Sigma) staining was done on 4μm FFPE kidney sections following deparaffinization and heat-induced epitope retrieval was carried out for immunohistological staining. Primary antibodies used in the study are provided in table 4-4. Images were quantified by measuring the percentage of

positive area examined under transmitted light using ImageJ. All micrographs were captured at x200 and x400 magnification using the BX41 Olympus microscope. Briefly, 10-20 micrographs were captured, percentage of positive area quantified and averaged per mouse. This was repeated for the indicated '*n'* number of mice, with final average and standard error calculated from the individual averages obtained from each mouse.

miRNA In situ hybridization (ISH)

4µm FFPE kidney sections were treated with proteinase K (10 min, 37 °C), followed by fixation in 4%PFA (10 min, RT). Subsequently sections were incubated in hybridization buffer (1hr, 52°C) and then incubated with DIG labeled miRCURY LNA detection probes targeting miR-299a and U6 snRNA probes (positive control) (18h, 52°C). Probe details are provided in table 4-2. Stringency washes were carried out exactly as described [217]. Sections were blocked in 1x Casein Solution (Vector labs) (1h, RT) and incubated with anti-Digoxigenin-AP Fab fragment (1:100, 18h, 4°C). Chromogenic reaction was carried out using NBT/BCIP (dark, RT, 4h-6h) (Vector labs). Slides were counterstained with nuclear fast red and then mounted with Vectamount (Vector labs) and examined using light microscopy (BX41 Olympus). All micrographs were captured at x200 and x400 magnification.

Statistical Analysis

Statistical analyses were performed using GraphPad Prism 6. A Student's *t*-test or one-way were used to determine statistical significance between two or more groups of data,

respectively. *Post hoc* significance of pairwise comparisons was assessed using Tukey's HSD. A p-value <0.05 (two-tailed) was considered significant. Data are presented as mean±SEM. The number of experimental repetitions (*n*) is indicated in the figure captions.

4.5 Results

miR299a-5p expression and activity is downregulated in cav-1 deficient MC

We previously identified FST as the most upregulated gene in cav-1 deficient MC compared to WT MC [22,214]. Here, we first confirmed elevated FST expression at the protein level (Fig. 4-1A) in cav-1 KO MC. Our previous data showed that cav-1 transcriptionally regulates FST through Sp1 [214]. To determine whether cav-1 is also involved in post-transcriptional regulation of FST, we examined stability of the FST 3'UTR. We observed that cav-1 elimination resulted in a significant stabilization of the 3'UTR of FST (Fig. 4-1B).

The 3'UTR of a gene can be regulated by numerous factors including microRNAs (miRNAs) [218]. miRNAs bind to a complementary target mRNA sequence in the 3'UTR and effectively silence the gene by targeting it for degradation and/or inhibiting its translation into protein [98]. Hypothesizing that cav-1 might destabilize the 3'UTR of FST through altered miRNA expression, we performed a bioinformatics screen to identify potential candidate miRNAs that target the 3'UTR of mouse FST, with candidate miRNAs selected based on the most number of hits that were present in several miRNA

target prediction algorithms including TargetScan, MicroCosm, mirRDB and miRSearch V3.0. As seen in Fig. 4-1C, of the 14 miRNAs identified, miR299a-5p was the most reduced in cav-1 KO vs WT MC. Its 8-mer miRNA regulator element (MRE) within the FST 3'UTR is shown in Fig. 4-1D, with 100% homology between mouse and human in this region. To functionally validate that miR299a-5p is downregulated in cav-1 KO MC, we generated a construct with the miR299a-5p MRE downstream of luciferase. Consequently, stability of the luciferase is indicative of miR299a-5p expression and activity. As expected given the decreased miR299a-5p expression, the miR299a-5p MRE-luc is stabilized in cav-1 KO compared to cav-1 WT MC (Fig. 4-1E). These results suggest that the increased FST 3'UTR stability seen in cav-1 KO MC may be mediated by suppressed miR299a-5p expression.

miR299a-5p destabilizes the 3'UTR of FST to attenuate its protein expression

To directly validate the role of miR299a-5p in destabilizing the FST 3'UTR, we tested the effects of miR299a-5p inhibition and overexpression. Inhibition was achieved using a miR299a-5p inhibitor construct which upon transfection and post-transcriptional processing results in the formation of an entrapping structure that attracts and binds to two miR299a-5p molecules, thus preventing the binding of endogenous mir299a-5p to target mRNAs and its inhibiting its downstream regulatory effects on target gene expression. A miR299a-5p precursor construct was used for miR299a-5p overexpression. Briefly, upon transfection, precursor miR-299-5p in constitutively overexpressed, which is then maturated using the endogenous cellular miRNA processing machinery. These constructs

additionally constitutively produce mCherry and GFP proteins with the inhibitor or precursor, respectively. Thus, effective transfection could be confirmed by observing mCherry and GFP immunofluorescence (Fig. 4-2A). Functionality of the miR299a-5p inhibitor was confirmed by observing significantly increased miR299a-5p MRE-luc stability (Fig. 4-2B). miR-299a-5p overexpression was confirmed by PCR which showed significantly increased transcript levels of miR299a-5p (Fig. 4-2C).

As hypothesized, miR299a-5p inhibition significantly increased stability of the FST 3'UTR in cav-1 WT MC (Fig. 4-2D) and in turn also increased the protein expression of FST (Fig. 4-2E). Conversely, miR299a-5p overexpression significantly destabilized the FST 3'UTR in both cav-1 KO and WT MC, although effects in KO cells were much greater, likely due to their lower basal levels of this miRNA (Fig. 4-2F). Overexpression of miR299a-5p also significantly reduced FST protein expression in cav-1 KO MC (Fig. 4-2G), with effects also observed in cav-1 WT MC (Fig. 4-6; Supplemental Fig. S1A). These results clearly shown a direct role for miR299a-5p in post-transcriptionally regulating the expression of FST.

TGFβ1 dependent repression of FST is mediated through miR299a-5p

TGFβ1 is a major profibrotic factor in the development and progression of CKD [42,50,219,220]. FST binds to and neutralizes the actions of numerous TGFβ family members, including activins. While not directly capable of binding and neutralizing TGFβ1, FST was shown to inhibit the TGFβ1-induced profibrotic response in numerous cell types, including MC [57,214]. These findings suggest that TGFβ1 and activins are

involved in a positive feedback loop, with activins potentially serving as a mediator of the profibrotic effects of TGFβ1. miR299a-5p is a member of the miR-154 family [221,222]. Based on recent evidence showing smad3-dependent induction of miR-154a in response to TGFβ1, we questioned whether TGFβ1 also increases the expression of miR299a-5p in MC [105,106,223]. Indeed, we observed that TGFβ1 prominently increased the miR299a-5p transcript (Fig. 4-3A). This was associated with significant destabilization of the 3'UTR (Fig. 4-3B) as well as decreased FST transcript (Fig. 4-3C) and protein expression (Fig. 4-3D). We next determined whether miR299a-5p induction was mediated through FST downregulation in response to TGFβ1. As predicted, inhibition of miR299a-5p activity attenuated the downregulation of FST by TGFβ1 (Fig. 4-3E). These results illustrate that TGFβ1-induced miR299a-5p expression leads to FST downregulation.

miR299a-5p augments the profibrotic effects of TGFβ1 through FST downregulation

Given our findings that TGFβ1 reduces the expression of FST through miR299a-5p upregulation, and the known ability of FST to inhibit TGFβ1 profibrotic effects [57,71,107,108], we hypothesized that miR299a-5p contributes to the TGFβ1 profibrotic response in MC. We first inhibited miR299a-5p expression in cav-1 WT MC, and observed that this significantly blunted the ability of TGFβ1 to induce extracellular matrix (ECM) and the profibrotic cytokine connective tissue growth factor (CTGF) (Fig. 4-4A). To determine whether this protective effect was due to increased FST expression, we inhibited both miR299a-5p and FST, the latter using siRNA. The downregulation of FST enabled TGFβ1 induction of ECM protein and CTGF production (Fig. 4-4B). These

results show that miR299a-5p mediates TGFβ1 profibrotic responses through repression of FST.

We previously showed that cav-1 KO MC exhibit decreased basal ECM expression and are protected against numerous profibrotic stimuli, including TGFβ1[77–80]. We recently showed that the elevated expression of FST by these cells is a key mediator of these findings [22]. Since we now demonstrate that cav-1 KO cells also have significantly decreased miR299a-5p expression and activity (Fig. 4-1C and 4-1E), we assessed whether this contributes to their antifibrotic phenotype. We thus overexpressed miR299a-5p in cav-1 KO MC, and showed that this augmented their ability to respond to TGFβ1. Basal matrix production was also augmented (Fig. 4-4C). An augmentation of basal and TGFβ1-induced profibrotic signals was also observed when miR299a-5p was overexpressed in cav-1 WT MC (Fig. 4-6; Supplemental Fig. S1B).

miR299a-5p expression is increased in mice with CKD

The expression of miR299a-5p is increased in mouse models of pulmonary and cardiac fibrosis and in patients with primary biliary cirrhosis [105,106,223]. Furthermore, in a model of myocardial infarction, increased miR299a-5p was found to correlate inversely with cardiac function, where therapeutic inhibition of a related family member miR-154 protected against cardiac dysfunction and fibrosis [223]. TGFβ1 is well established to be increased in the kidneys and serum of mice with CKD [42,50,219,220]. Since our *in vitro* data show that TGFβ1 upregulation of miR299a-5p mediates its profibrotic responses, we examined whether miR299a-5p expression is elevated in the

kidneys of mice with hypertensive CKD. CKD was induced using a surgical renal mass reduction model of CKD, where 5/6 of the kidney mass is removed (5/6 nephrectomy; 5/6 Nx). Using both qRT-PCR (Fig. 4-5A) and miRNA *in-situ* hybridization (ISH) (Fig. 4-5B), we show that the expression of miR299a-5p is elevated in both glomeruli and tubules of mice with CKD. This suggests that miR299a-5p may contribute to fibrosis in CKD.

miR299a-5p inhibition protects against renal fibrosis in mice with CKD

We sought to determine the therapeutic potential of miR299a-5p inhibition in mice with CKD. Here, we assessed whether miR299-5p inhibition using Locked Nucleic Acid (LNA) technology is an effective strategy for blocking renal fibrosis in the 5/6 Nx mouse model of CKD. The efficacy and functionality of the inhibitor was initially tested *in vitro* in MC and confirmed to effectively stabilize the mir299a-5p MRE (Fig. 4-5C) and FST 3'UTR luciferases (Fig. 4-5D). After confirming the efficacy and specificity of the miR299a-5p LNA**,** mice were treated with the *in vivo* grade miRNA LNA inhibitor targeting miR299a-5p for 9 weeks after induction of CKD as shown in Fig. 4-5E.

First, we assessed renal FST expression to determine whether miR299a-5p inhibition was functional in the kidneys of mice with CKD. As expected, miR-299a-5p inhibition in CKD mice led to significantly upregulated FST expression in the tubules and glomeruli when compared the sham control LNA treated mice (Fig. 4-6). Based on the protective roles of FST that have been previously observed within the kidneys, we assessed whether miR299a-5p inhibition through FST upregulation protects against the progression of CKD [22,23,224]. Mice with 5/6 Nx mouse exhibit progressive decline in

kidney function, albuminuria along with glomerular and tubulointerstitial fibrosis and systemic hypertension [110,111] **.** Although not statistically significant, we observed that CKD mice treated with the miR299a-5p LNA had a higher glomerular filtration rate (GFR) compared to the CKD mice treated with the control LNA, suggesting that miR299a-5p is protective against the decline in kidney function in CKD (Fig. 4-7A). Similarly, a modest reduction in albuminuria was also observed in these mice (Fig. 4-7B). Mice with CKD had significantly elevated systolic (Fig. 4-7C) and diastolic blood pressures (Fig. 4-7D), which were normalized in response to miR299a-5p inhibition. Lastly, these mice were also modestly protected against the development of glomerulosclerosis and tubulointerstitial fibrosis as assessed through decreased accumulation of extracellular collagen using trichrome (Fig. 4-8A) and PSR staining (Fig. 4-8B). Thus, miR299a-5p inhibition is protective against the progression of CKD by ameliorating renal fibrosis.

4.6 Discussion

microRNAs (miRNAs) have been implicated in the regulation of a wide range of fundamental cellular processes and normal renal physiology. These miRNAs have also been linked to progression of various diseases including kidney disease. Indeed, therapeutically targeting miRNAs using LNA technology has become a highly investigated area with both overexpression and inhibition being used depending on the miRNA and its function in disease. For example, several miRNAs are highly expressed in the kidney, such as miR192, 194, 21, 200a, 204 where they play an important role in

regulating renal fibrosis [100,102,104]. These miRNAs are often found to be either inhibited (e.g. miR-29) or upregulated by TGFβ1 (e.g. miR-192 and miR-21), through which they can augment the profibrotic effects of TGFβ1 [100,102,104]. The synthesis of some of these miRNAs has been shown to be regulated by the Smad proteins involved in the TGFβ1 signaling cascade [100,102,104]. As a result, numerous studies have been carried out to assess the therapeutic potential of inhibiting or overexpressing these specific miRNAs in protecting against renal fibrosis [100,102,104].

Here, we have showed that the 3'UTR of FST is also differentially post-transcriptionally stabilized by cav-1. We began our analysis of cav-1 mediated regulation of the FST 3'UTR by examining miRNAs. miRNAs are short RNA sequences that bind to complimentary target sequences within the 3'UTR of a gene and act as silencers of gene expression or translational repressors [98]. Using bioinformatics tools, we identified numerous miRNAs that can target the FST 3'UTR. Here, we determined that cav-1 deficiency is involved in downregulating the expression of some of these FST-targeting miRNAs, particularly miR299a-5p. miR299a-5p is localized to chromosome 14q32.31 cluster containing >40 intergenic miRNAs, belonging to the miR-154 family [221,222]. miR299a-5p expression and activity was confirmed to be decreased in cav-1 deficient MC. It is predicted to target >150 genes involved in a wide variety of cellular process and signaling pathways, involving apoptosis, autophagy and fibrosis [221–223]. Using transient miR299a-5p inhibition and overexpression, we have validated a functional role of miR299a-5p in binding the 8-mer MRE within the 3'UTR of FST and in turn

downregulating its transcript and protein expression. Furthermore, our results show that miR299a-5p is induced by the profibrotic cytokine TGFß1. These results are in line with the literature showing upregulation of the miR-154 family member miRNAs, including miR-154 [105].

While miR-154 was shown to be upregulated through Smad3, our experiments do not provide a mechanism through which the expression of miR299a-5p is upregulated by TGFß1 [105]. Nonetheless, these results might help explain why cav-1 deficient MC, which are protected against TGFß1-induced profibrotic responses, have decreased miR299-5p expression when compared with cav-1 WT MC.

Interestingly, we also observed that TGFβ1 inhibits FST expression. While other groups have shown the ability of TGFβ1 to upregulate FST in differentiating bovine granulosa cells [225], TGFβ1-mediated depression of FST has not yet been described. In assessing the molecular avenues via which TGFβ1 represses FST expression in MC, our data show that TGFβ1 post-transcriptionally decreases the stability of the 3'UTR of FST. Mechanistically, we identified that TGFß1 downregulated FST through increasing miR299a-5p. This was confirmed using miR299a-5p inhibition. Here, when miR299a-5p was inhibited, TGFß1 was not able to downregulate FST. These results suggest that miR299a-5p promotes the profibrotic effects of TGFß1 through the repression of FST. Indeed, when miR299a-5p was inhibited, TGFß1 was not able to repress the expression of FST, and consequently TGFß1-induced matrix production was blunted. We have previously shown that cav-1 KO MC are protected against basal and profibrotic stimuli-induced matrix production [75,77,78]. Here, we have identified that upregulating the

expression of miR299a-5p in cav-1 KO MC to the levels observed in WT MC is sufficient in restoring the ability of TGFß1 to promote the production of matrix proteins such as fibronectin, collagen Iα1, collagen IVα1, and profibrotic cytokines such as CTGF in these cells. These results clearly show that miR299a-5p through FST downregulation plays an important pathogenic role in promoting ECM production.

Until now, miR299a-5p has not been studied in MC and in the regulation of kidney function. miR299a-5p is upregulated following MI and cardiac fibrosis and is inversely correlated with cardiac function[59]. Recent studies have shown that the expression of miR299a-5p is increased in mouse models of pulmonary and cardiac fibrosis and in patients with primary biliary cirrhosis [105,106,223]. Since TGFß1 is a prominent upregulated profibrotic cytokine in CKD, we assessed the role of TGFß1-mediated miR299a-5p upregulation *in vivo.* Here, we showed that miR299a-5p is also upregulated in the glomeruli and tubules of mice with CKD. Thus, we assessed whether inhibition of miR299a-5 *in vivo* using LNA can protect against the progression of CKD through inhibiting renal fibrosis. Indeed, we found that as expected, miR299a-5p inhibition increased the expression of FST in the kidneys of mice with CKD and this was associated with protection against fibrosis. In accordance with decreases in renal fibrosis, we saw slight improvements in albuminuria and GFR, along with significant reduction in blood pressure. These results are in line with numerous other studies showing the benefit of FST upregulation in protecting against renal fibrosis in several models of kidney disease and injury [22,23,224].

For the first time we report a novel profibrotic role of miR299a-5p in MC in response to TGFß1 through the repression of the antifibrotic protein FST. Importantly, we also provide pre-clinical data suggesting that miR299a-5p inhibition could be a novel therapeutic approach for protecting against renal fibrosis in CKD.

Declarations:

Acknowledgements: We acknowledge the support of St. Joseph's Healthcare for nephrology research. We thank Dr. Zhengping Xu for providing us with the FST 3´UTR Luciferase construct.

Contributions: NM performed experiments and analysed data, DZ, HJ and BG performed experiments, NM wrote the manuscript, NM and JCK conceived the ideas, BG assisted with animal studies, all authors read and approved the final manuscript.

Competing interests: The authors declare that they have no competing financial interests.

Funding: This work was supported by the Canadian Institutes of Health Research (CIHR) (JCK), MOP 136868 and Kidney Foundation of Canada (JCK and NM), NM is the recipient of a studentship award from the Research Institute of St. Joe's Hamilton.

4.7 Figures

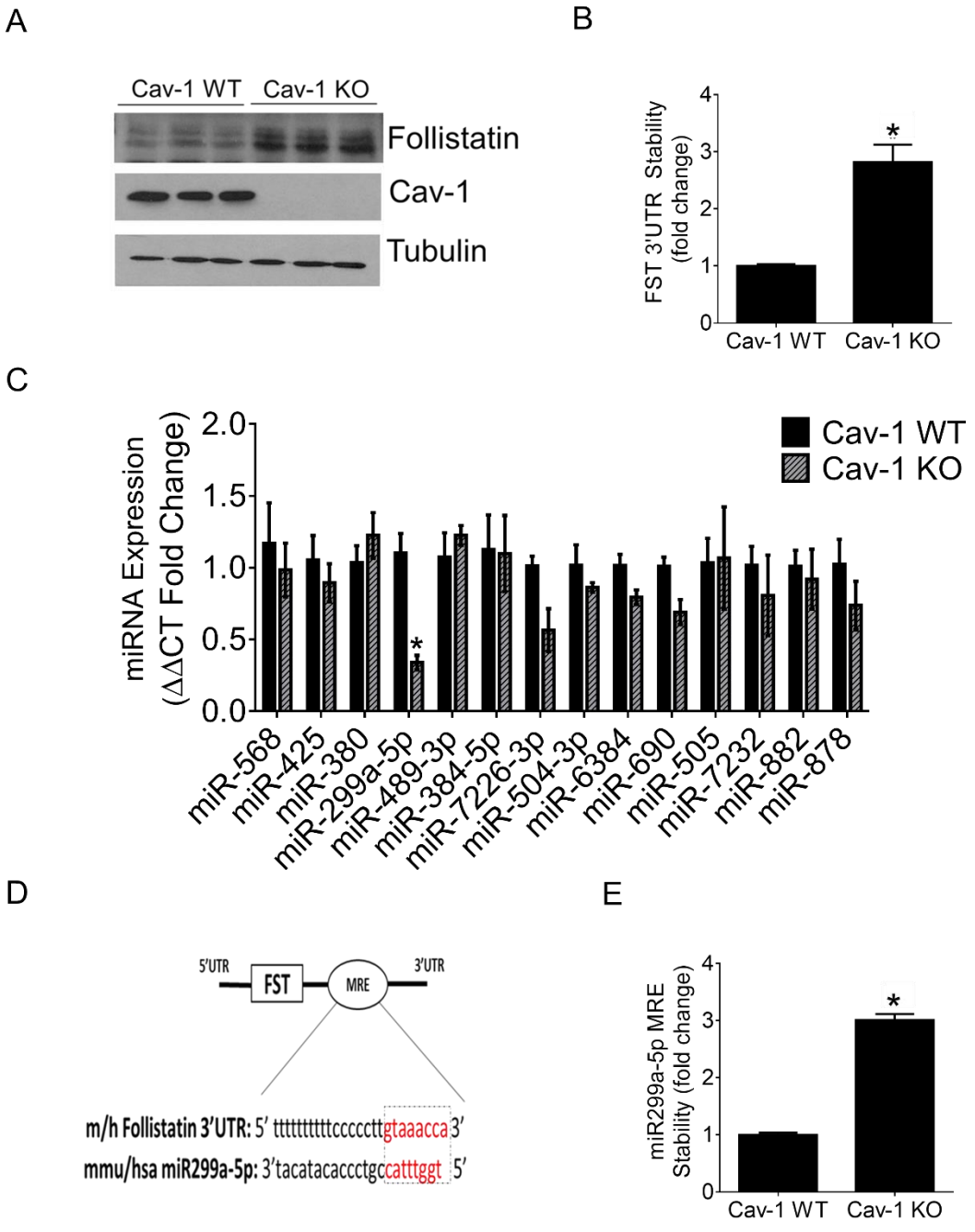
A
Cav-1 WT
Cav-1 KO
Follistatin
Cav-1
Tubulin
B
FST 3'UTR Stability (fold change)
Cav-1 WT
Cav-1 KO
C
miRNA Expression (ΔΔCT Fold Change)
Cav-1 WT
Cav-1 KO
miR-568
miR-425
miR-380
miR-299a-5p
miR-489-3p
miR-384-5p
miR-7226-3p
miR-504-3p
miR-6384
miR-690
miR-505
miR-7232
miR-882
miR-878
D
5'UTR
FST
MRE
3'UTR
m/h Follistatin 3'UTR: 5' ttttttttttccccctt gtaaacca 3'
mmu/hsa miR299a-5p: 3'tacatacaccctgc catttggt 5'
E
miR299a-5p MRE Stability (fold change)
Cav-1 WT
Cav-1 KO

Figure 4-1. Reduced miR299a-5p expression stabilizes the 3'UTR of FST in cav-1 KO MCs.

(A) FST protein was increased in cav-1 KO MC (n=9, *p<0.05). (B) Stability of the FST 3'UTR, as assessed by a luciferase reporter construct, was significantly enhanced in cav-1 KO vs WT MC (n=9, *p<0.05). (C) qRT-PCR analysis of the expression of miRNAs targeting FST showed significant depression of miR299a-5p in cav-1 KO MC (n=12, *p<0.05). (D) miR299a-5p is conserved in mice and humans and binds to an 8-mer miRNA regulatory element (MRE) within the 3'UTR of FST. (E) A luciferase reporter for mir299a-5p (MRE-luc) showed increased stability, reflecting lower miR299a-5p activity, in cav-1 KO vs WT MC(n=9, *p<0.05).

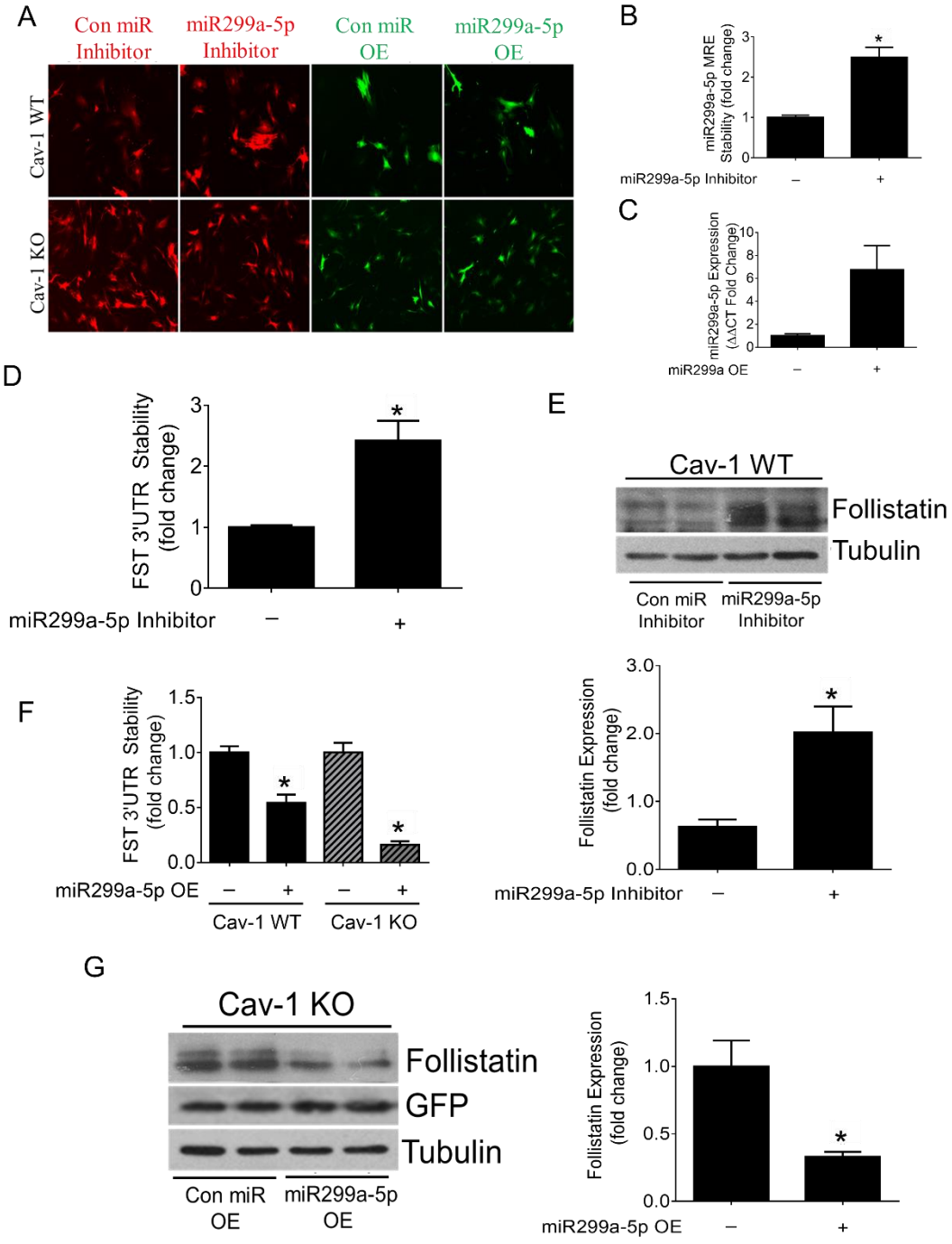
A
Con miR Inhibitor
miR299a-5p Inhibitor
Con miR OE
miR299a-5p OE
Cav-1 WT
Cav-1 KO
B
miR299a-5p MRE Stability (fold change)
miR299a-5p Inhibitor
C
miR299a-5p Expression (ΔΔCT Fold Change)
miR299a OE
D
FST 3'UTR Stability (fold change)
miR299a-5p Inhibitor
E
Cav-1 WT
Follistatin
Tubulin
Con miR Inhibitor
miR299a-5p Inhibitor
F
FST 3'UTR Stability (fold change)
miR299a-5p OE
Cav-1 WT
Cav-1 KO
Follistatin Expression (fold change)
miR299a-5p Inhibitor
G
Cav-1 KO
Follistatin
GFP
Tubulin
Con miR OE
miR299a-5p OE
Follistatin Expression (fold change)
miR299a-5p OE

Figure 4-2. miR299a-5p regulates the expression of FST through its 3'UTR.

(A) Cav-1 WT and KO MC were transfected with either the miR299a-5p inhibitor or precursor clones, or their respective controls, and effective transfection confirmed with mCherry and GFP immunofluorescence, respectively. (B) miR299a-5p inhibition significantly increased stability of the miR299a-5p MRE luciferase reporter in cav-1 WT MC (n=12, *$p<0.05$). (C) Overexpression of the miR299a-5p precursor increased miR-299a-5p levels, assessed using qRT-PCR (n=2). (D) An miR299a-5p inhibitor significantly enhanced stability of the FST 3'UTR in cav-1 WT MC (n=12, *$p<0.05$). (E) miR299a-5p inhibition significantly increased FST protein expression in cav-1 WT MC (n=5, *$p<0.05$). (F) Overexpression (OE) of an miR299a-5p precursor significantly repressed stability of the FST 3'UTR in cav-1 WT MC and KO MC (miR299a-5p overexpression is normalized to control transfection individually for cav-1 WT and cav-1 KO MC) (n=3, *vs control, $p<0.05$). (G) miR299a-5p OE in cav-1 KO MC significantly decreased FST protein expression (n=6, *$p<0.05$).

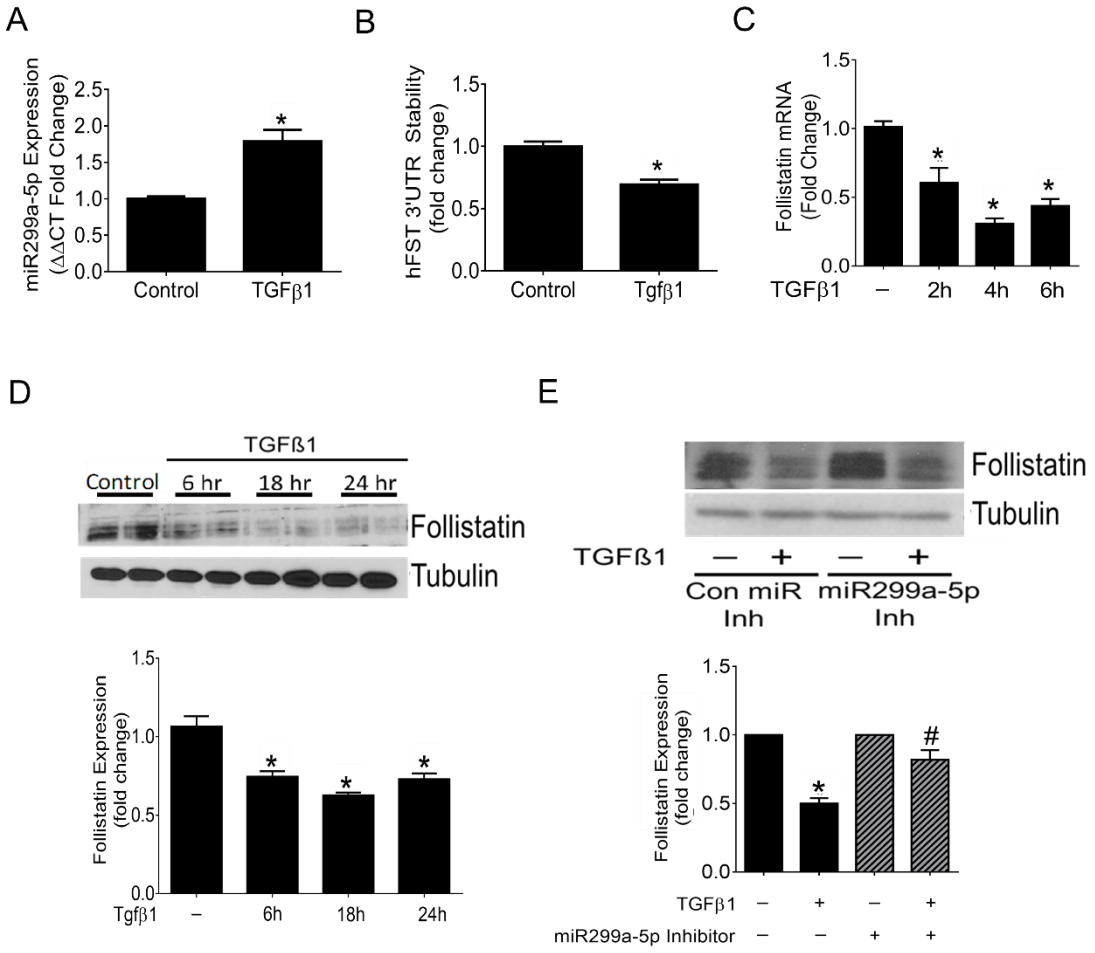
A
miR299a-5p Expression (ΔΔCT Fold Change)
2.5
2.0
1.5
1.0
0.5
0.0
*
Control
TGFβ1
B
hFST 3'UTR Stability (fold change)
1.5
1.0
0.5
0.0
*
Control
Tgfβ1
C
Follistatin mRNA (Fold Change)
1.5
1.0
0.5
0.0
*
*
*
TGFβ1 – 2h 4h 6h
D
TGFß1
Control 6 hr 18 hr 24 hr
Follistatin
Tubulin
Follistatin Expression (fold change)
1.5
1.0
0.5
0.0
*
*
*
Tgfβ1 – 6h 18h 24h
E
Follistatin
Tubulin
TGFß1 — + — +
Con miR Inh
miR299a-5p Inh
Follistatin Expression (fold change)
1.5
1.0
0.5
0.0
*
#
TGFβ1 – + – +
miR299a-5p Inhibitor – – + +

Figure 4-3.TFGβ1 represses FST through miR299a-5p up-regulation in cav-1 WT MC. (A) TGFβ1 (5ng, 24h) significantly increased the expression of miR299a-5p (n=4, *p<0.05). (B) TGFβ1 (5ng, 24h) significantly decreased stability of the FST 3'UTR (n=15, *p<0.05). (C) TGFβ1 (5ng) significantly reduced the FST mRNA transcript (n=8, *p<0.05). (D) TGFβ1 (5ng) significantly reduced FST protein expression (n=4, *p<0.05). (E) Inhibition of miR299a-5p significantly blunted the ability of TGFβ1 to reduce the FST protein expression (n=5, *vs con inh-con, #vs miR inh-con, p<0.05).

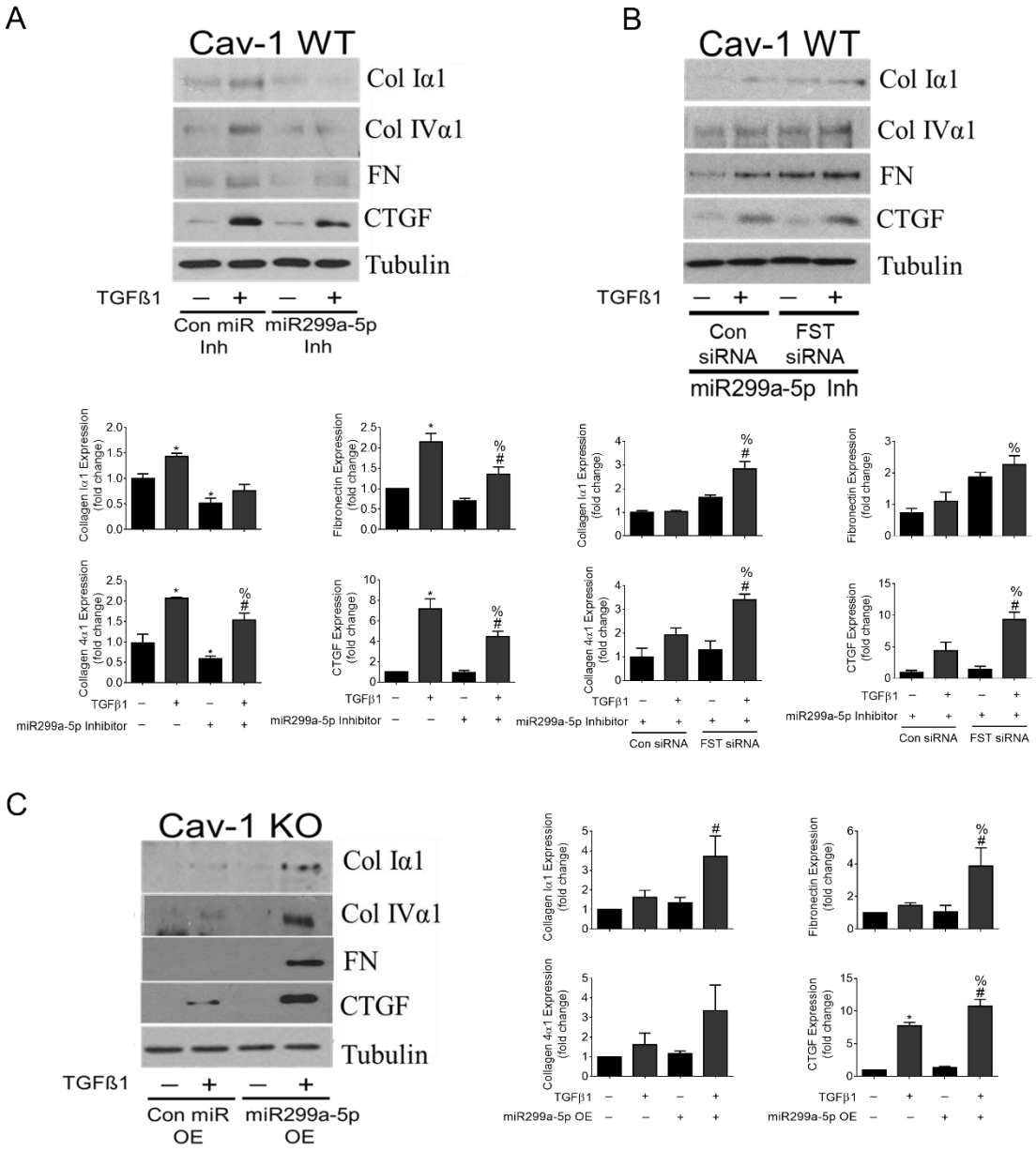
A
Cav-1 WT
Col Iα1
Col IVα1
FN
CTGF
Tubulin
TGFß1 – + – +
Con miR Inh
miR299a-5p Inh
B
Cav-1 WT
Col Iα1
Col IVα1
FN
CTGF
Tubulin
TGFß1 – + – +
Con siRNA
FST siRNA
miR299a-5p Inh
Collagen Iα1 Expression (fold change)
Fibronectin Expression (fold change)
Collagen 4α1 Expression (fold change)
CTGF Expression (fold change)
TGFβ1
miR299a-5p Inhibitor
Con siRNA
FST siRNA
C
Cav-1 KO
Col Iα1
Col IVα1
FN
CTGF
Tubulin
TGFß1 – + – +
Con miR OE
miR299a-5p OE
Collagen Iα1 Expression (fold change)
Fibronectin Expression (fold change)
Collagen 4α1 Expression (fold change)
CTGF Expression (fold change)
TGFβ1
miR299a-5p OE

Figure 4-4. TGFβ1 up-regulation of miR299a-5p enables ECM production through FST down-regulation.

(A) miR299a-5p inhibition significantly blunted basal ECM and CTGF expression and decreased TGFβ1 (0.5ng, 24h)-induced ECM and CTGF production in cav-1 WT MC (n=3, * vs con inh-con, #vs miR inh-con, %vs con inh-TGFβ1, $p<0.05$). (B) FST downregulation with siRNA attenuated the ability of an miR-299a-5p inhibitor to reduce the profibrotic response to TGFβ1 (0.5ng, 24h) (n=3, * vs con siRNA-con, #vs FST siRNA-con, %vs con siRNA-TGFβ1, $p<0.05$). (C) Overexpression (OE) of miR299a-5p significantly enhanced TGFβ1 (0.5ng, 24h)-induced production of ECM and CTGF (n=3, * vs con OE-con, #vs miR OE-con, %vs con OE-TGFβ1, $p<0.05$).

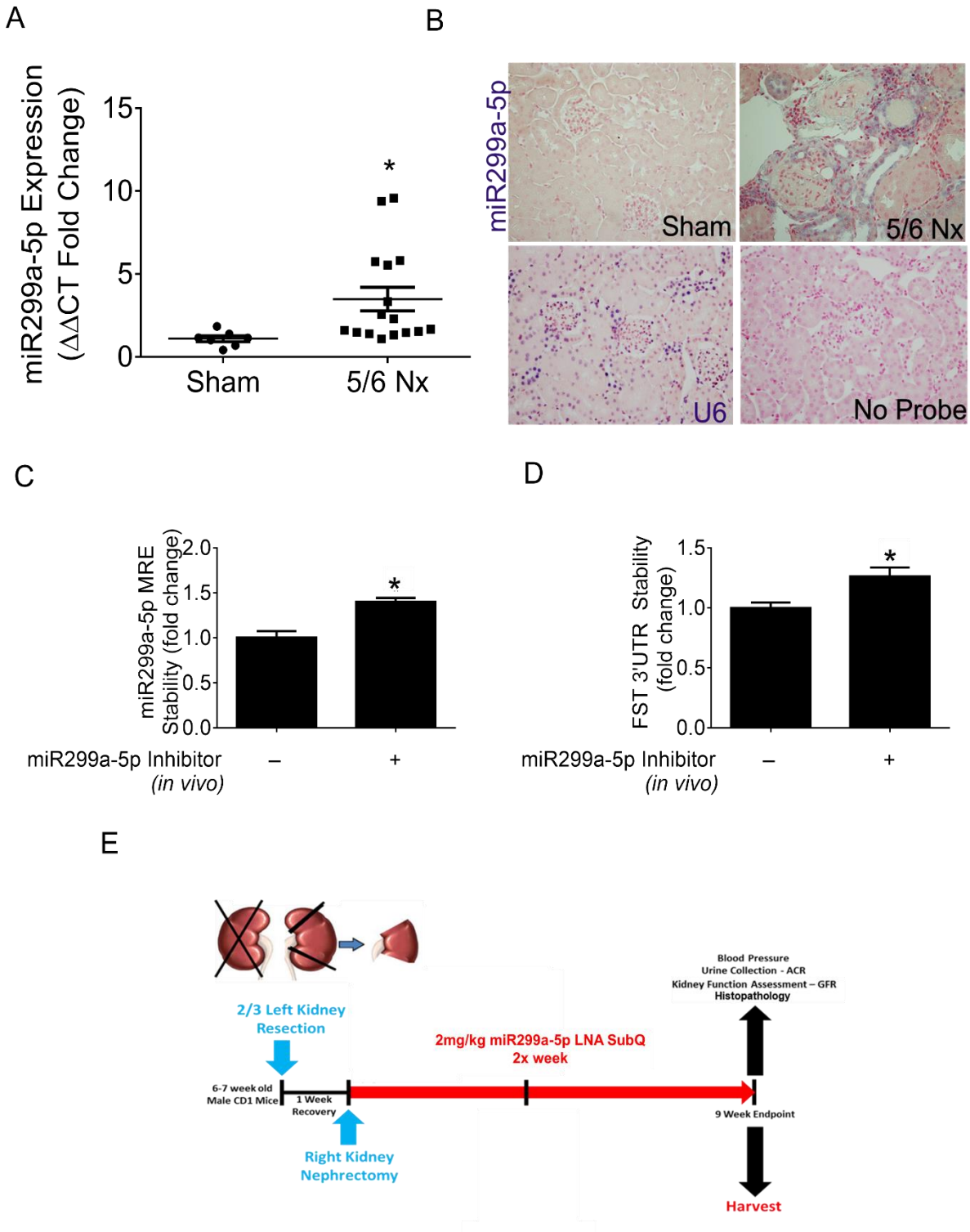
A
miR299a-5p Expression (ΔΔCT Fold Change)
15
10
5
0
*
Sham
5/6 Nx
B
miR299a-5p
Sham
5/6 Nx
U6
No Probe
C
miR299a-5p MRE Stability (fold change)
2.0
1.5
1.0
0.5
0.0
*
miR299a-5p Inhibitor (in vivo)
–
+
D
FST 3'UTR Stability (fold change)
1.5
1.0
0.5
0.0
*
miR299a-5p Inhibitor (in vivo)
–
+
E
2/3 Left Kidney Resection
6-7 week old Male CD1 Mice
1 Week Recovery
Right Kidney Nephrectomy
2mg/kg miR299a-5p LNA SubQ 2x week
Blood Pressure
Urine Collection - ACR
Kidney Function Assessment – GFR
Histopathology
9 Week Endpoint
Harvest

Figure 4-5. miR299a-5p expression is elevated in the kidneys of mice with CKD.
The expression of miR299a-5p was strongly elevated in the glomeruli and tubules of mice with the 5/6 nephrectomy model of CKD, as assessed through qRT-PCR (n-7-16 mice, *$p<0.05$) (A) and in-situ hybridization (ISH) (U6 snRNA was used as positive control to monitor hybridization efficiency) (B). (C) The in vivo miR299a-5p LNA inhibitor (100nM, 24h) stabilized the MRE-luciferase in cav-1 WT MC (n=3, *$p<0.05$), as well as FST3'UTR luciferase construct (D) (n=3, *$p<0.05$). (E) Flowchart of the timeline for in vivo assessment of the anti-fibrotic potential of miR299a-5p inhibition using an in vivo LNA inhibitor targeting miR299a-5p in mice with CKD (pre-Nx dose of miR299a-5p LNA is not shown in the diagram).

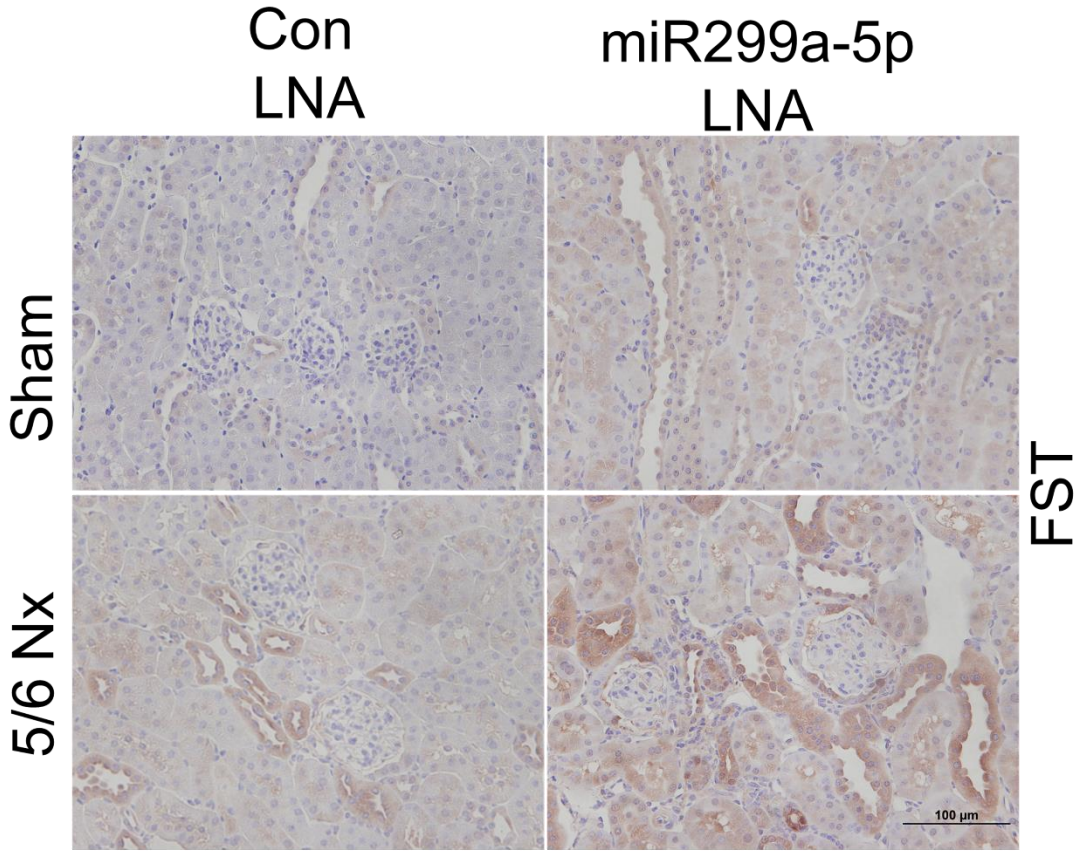
Con LNA
miR299a-5p LNA
Sham
5/6 Nx
FST
100 µm

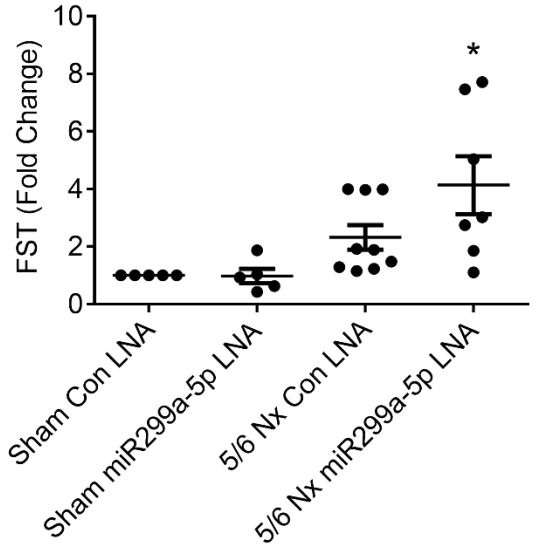
FST (Fold Change)
10
8
6
4
2
0
*
Sham Con LNA
Sham miR299a-5p LNA
5/6 Nx Con LNA
5/6 Nx miR299a-5p LNA

Figure 4-6. Effects of miR299a-5p LNA administration on the expression of FST in mice with CKD.

Systemic miR299a-5p LNA administration increased the expression of FST in the glomeruli and tubules of mice with CKD (n=5-9 mice, *vs Sham-Con-LNA, $p<0.05$, scale bar =100μm).

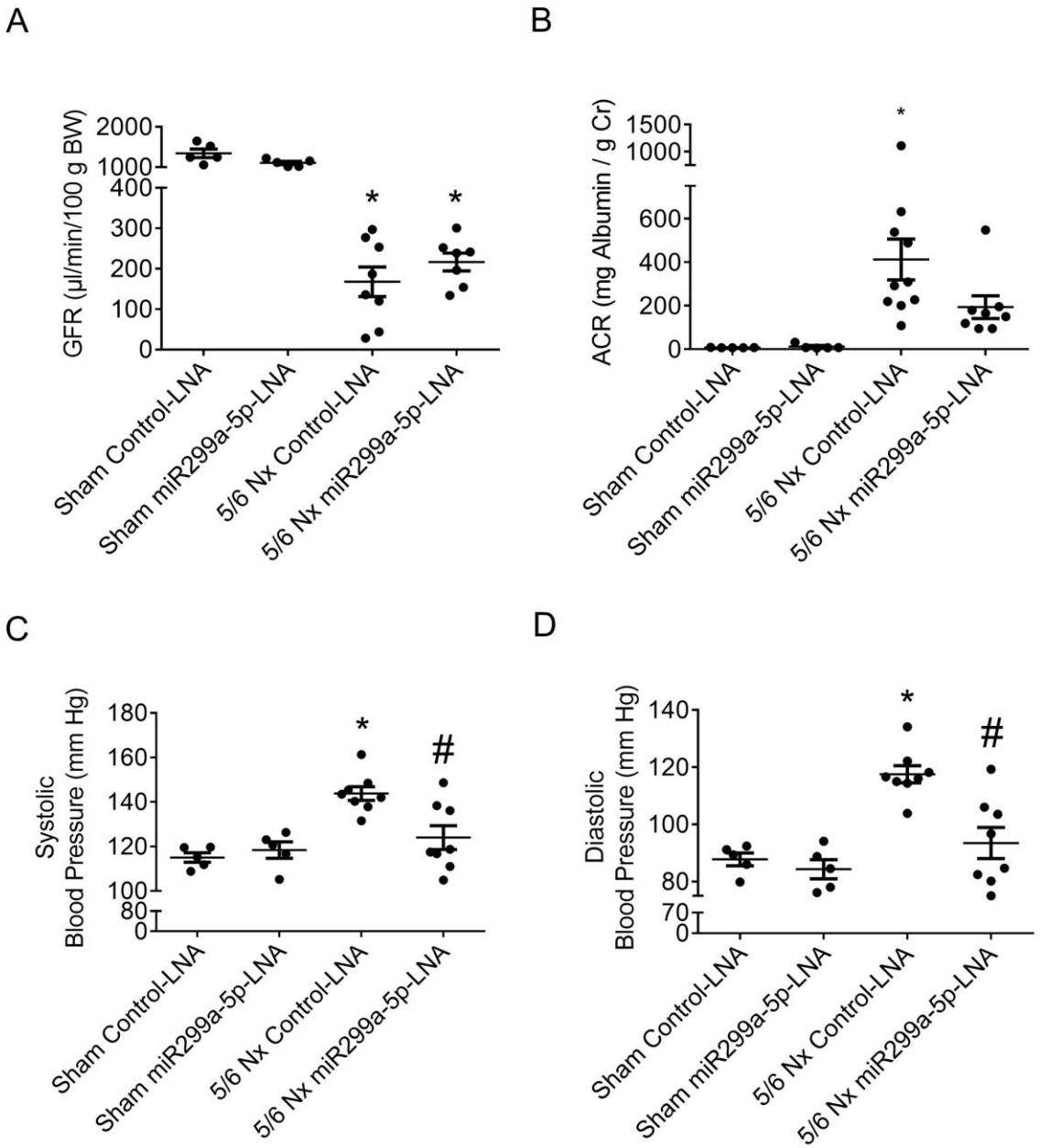
A
GFR (µl/min/100 g BW)
2000
1000
400
300
200
100
0
*
*
Sham Control-LNA
Sham miR299a-5p-LNA
5/6 Nx Control-LNA
5/6 Nx miR299a-5p-LNA
B
ACR (mg Albumin / g Cr)
1500
1000
600
400
200
0
*
Sham Control-LNA
Sham miR299a-5p-LNA
5/6 Nx Control-LNA
5/6 Nx miR299a-5p-LNA
C
Systolic Blood Pressure (mm Hg)
180
160
140
120
100
80
0
*
#
Sham Control-LNA
Sham miR299a-5p-LNA
5/6 Nx Control-LNA
5/6 Nx miR299a-5p-LNA
D
Diastolic Blood Pressure (mm Hg)
140
120
100
80
70
0
*
#
Sham Control-LNA
Sham miR299a-5p-LNA
5/6 Nx Control-LNA
5/6 Nx miR299a-5p-LNA

Figure 4-7. miR299a-5p inhibition improved kidney function in mice with CKD.
(A) The drastically diminished glomerular filtration rate (GFR) in CKD mice injected with control LNA was slightly improved by miR299a-5p LNA administration (n=5-9 mice, *vs Sham-Con-LNA $p<0.05$). (B) Albuminuria, as measured by the urinary albumin to creatinine ratio (ACR) was elevated in CKD mice and improved with miR299a-5p LNA administration (n=5-10 mice, *vs Sham-Veh, $p<0.05$). (C, D) High blood pressure, systolic (C) and diastolic (D) in mice with CKD was significantly improved by miR299a-5p LNA administration (n=5-8 mice, *vs Sham-Con-LNA, # vs 5/6 Nx- Con LNA $p<0.05$).

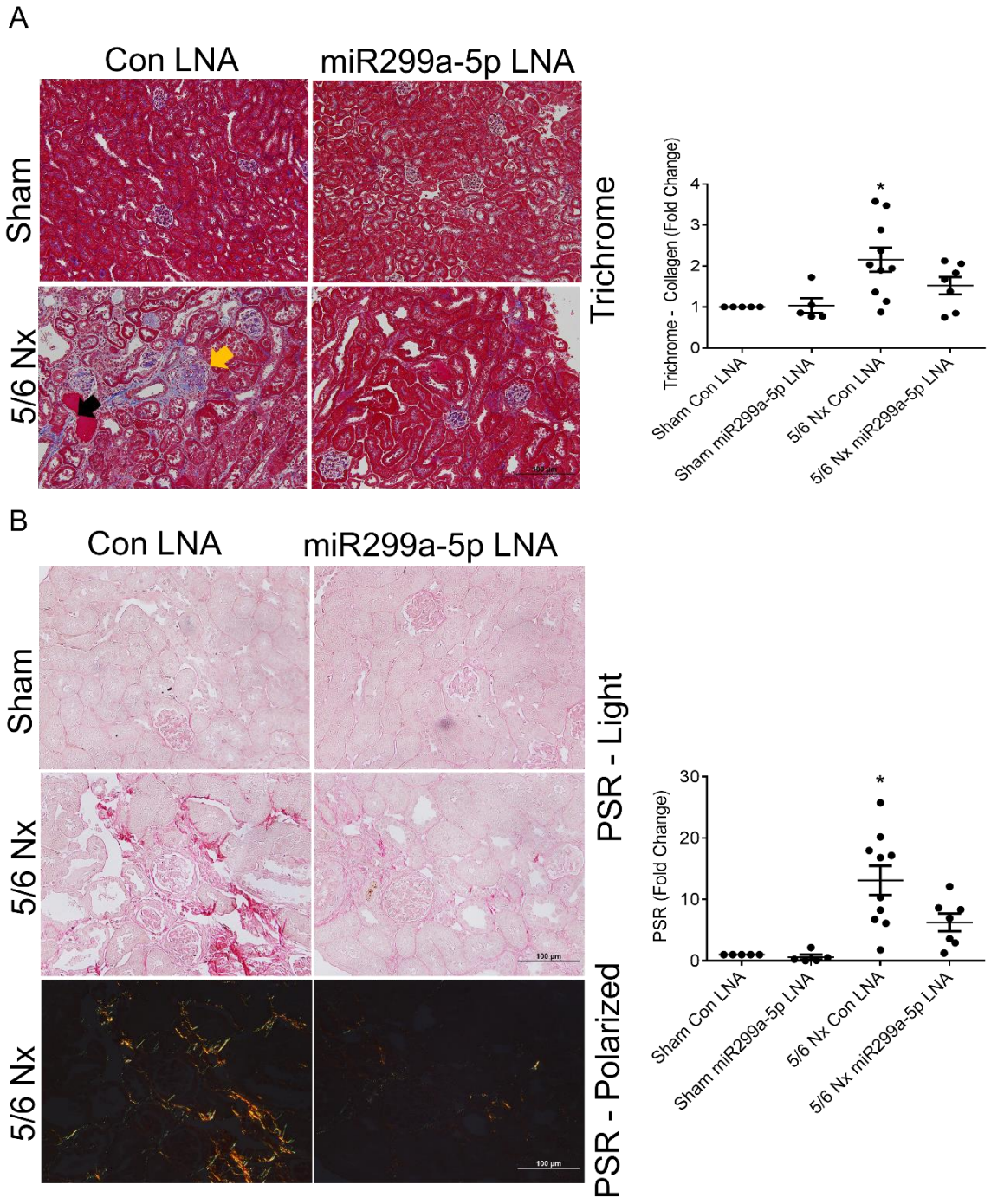
A
Con LNA
miR299a-5p LNA
Sham
5/6 Nx
Trichrome
Trichrome - Collagen (Fold Change)
Sham Con LNA
Sham miR299a-5p LNA
5/6 Nx Con LNA
5/6 Nx miR299a-5p LNA
B
Con LNA
miR299a-5p LNA
Sham
5/6 Nx
5/6 Nx
PSR - Light
PSR - Polarized
PSR (Fold Change)
Sham Con LNA
Sham miR299a-5p LNA
5/6 Nx Con LNA
5/6 Nx miR299a-5p LNA

Figure 4-8. miR299a-5p inhibition reduced renal fibrosis in mice with CKD.
CKD mice exhibited extensive glomerular sclerosis (yellow arrow) and tublulointerstitial fibrosis (black arrow), as assessed by trichrome (A) and PSR (B) staining, which was improved by miR299a-5p LNA administration (n=5-10 mice, *vs Sham-Con-LNA, $p<0.05$, scale bar =100μm).

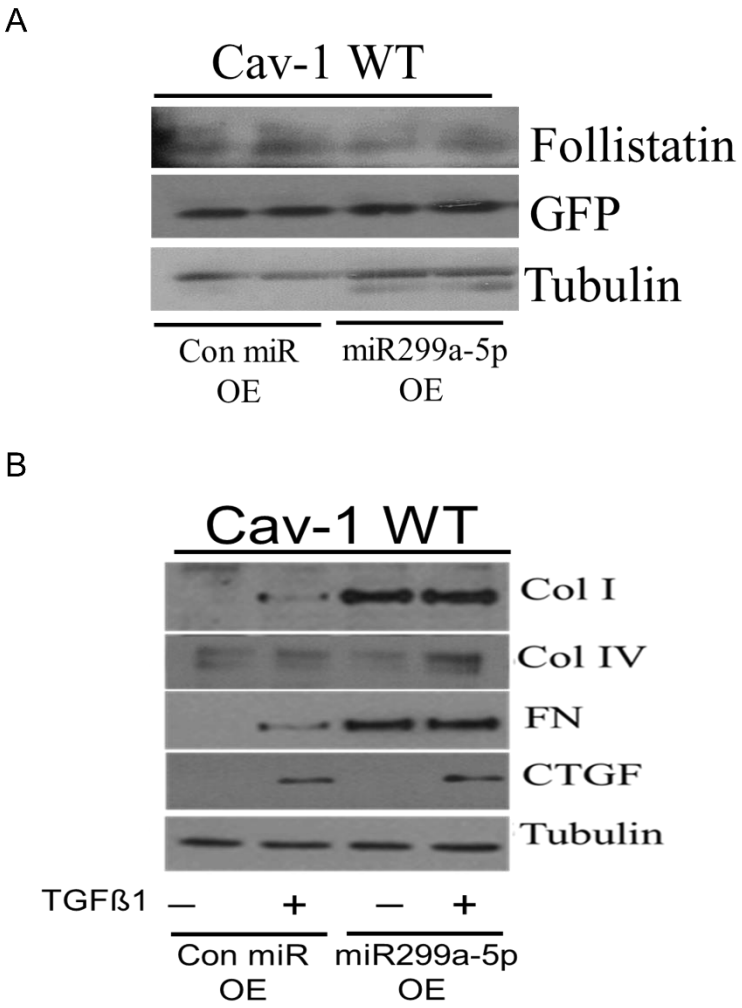

Figure 4-9. Supplemental Figure 1.

(A) miR299a-5p overexpression (OE) attenuated FST protein levels (n=2). (B) miR299a-5p overexpression increased basal expression of ECM and CTGF and augmented the ability of TGFβ1 (0.5ng, 24h) to promote their production (n=3, representative blots shown).

Table 4-1. Drugs and recombinant proteins.

Drugs and Recombinant Proteins	***Dilution/Amount***	***Source***
Recombinant Mouse TGFß1	0.5ng/ml-5ng/ml	R&D Systems
Recombinant Mouse Follistatin 244	1µg/ml	R&D Systems

Table 4-2. siRNA and miR LNA probes for ISH.

siRNA/LNA	***Application***	***Amount***	***Source***
Mouse Follistatin Silencer Select SiRNA	Transfection	50nM	Life Tech
Control Silencer Select SiRNA	Transfection	50nM	Life Tech
5'/3' DIG mmu-miR299a-5p miRCURY LNA detection probe	ISH	2.5pmol	Exiqon/Qiagen; YD00615334
5' DIG U6 miRCURY LNA detection probe, positive control	ISH	2.5pmol	Exiqon/Qiagen; YD00699002
In vivo LNA Inhibitor targeting mmu-miR299a-5p	Mice treatment (SQ)	2mg/kg (2x/week post Nx, 1 dose pre Nx)	Exiqon/Qiagen; 339203
In vivo LNA Inhibitor Scramble Control	Mice treatment (SQ)	2mg/kg (2x/week post Nx, 1 dose pre Nx)	Exiqon/Qiagen; 339203

Table 4-3. Plasmids.

Construct	***Source***
hFST 3´UTR Luciferase	Dr. Zhengping Xu
miR299a-5p precursor clone (GFP)	Genecopoeia; MmiR3388-MR04
miRNA scrambled precursor control clone (GFP)	Genecopoeia; CmiR0001-MR04
mir299a-5p MRE-Luc	Generated in Lab
miR299a-5p inhibitor clone (mCherry)	Genecopoeia; MmiR-AN0369-AM02
miRNA inhibitor scrambled control clone (mCherry)	Genecopoeia; CmiR-AN0001-AM02

Table 4-4. Antibodies.

Antibody/Probe	***Application***	***Dilution/Amount***	***Source***
Caveolin-1	WB	1:1,000	BD Biosciences; 610059
Follistatin (H-114)	WB	1:1,000	Santa Cruz; sc-30194
Follistatin	IHC	1:100	Proteintech; 60060-1-Ig
Fibronectin	WB	1:1000	BD Transduction; 610078
Collagen Iα1	WB	1:1000	Novus; NB600-408
Collagen IVα1	WB	1:1000	Novus; NB120-6586
CTGF(G-14)	WB	1:1000	Santa Cruz; sc-34772
GFP (4B10)	WB	1:1000	Cell Signaling; 2955
α-Tubulin	WB	1:10,000	Sigma; T6074
anti-Digoxigenin-AP Fab fragment	ISH	1:500	Roche; 11093274910

Table 4-5. qPCR Primers.

Primer	***Forward***	***Reverse***
mmu-miR-299a-5p	TGGTTTACCGTCCCACATACAT	Universal – Proprietary (Quanta)
mmu-miR-380-5p	ATGGTTGACCATAGAACATGCG	Universal – Proprietary (Quanta)
mmu-miR-384-5p	TGTAAACAATTCCTAGGCAATGT	Universal – Proprietary (Quanta)
mmu-miR-425-5p	AATGACACGATCACTCCCGTTGA	Universal – Proprietary (Quanta)
mmu-miR-489-3p	AATGACACCACATATATGGCAGC	Universal – Proprietary (Quanta)
mmu-miR-568	ATGTATAAATGTATACACAC	Universal – Proprietary (Quanta)
mmu-miR-504-3p	AGGGAGAGCAGGGCAGGGTTTC	Universal – Proprietary (Quanta)
mmu-miR-505-3p	CGTCAACACTTGCTGGTTTTCT	Universal – Proprietary (Quanta)
mmu-miR-6384	GCTTTCCTACTGTTTCCCTG	Universal – Proprietary (Quanta)
mmu-miR-690	AAAGGCTAGGCTCACAACCAAA	Universal – Proprietary (Quanta)
mmu-miR-7226-3p	TGACACAGCCATTCTCTGAGCAG	Universal – Proprietary (Quanta)
mmu-miR-7232-3p	TGGTTGAATTCGACTTTGGGGC	Universal – Proprietary (Quanta)
mmu-miR-878-3p	GCATGACACCACACTGGGTAGA	Universal – Proprietary (Quanta)
mmu-miR-882	AGGAGAGAGTTAGCGCATTAGT	Universal – Proprietary (Quanta)
Mouse U6 snRNA	TGGCCCCTGCGCAAGGATG	Universal – Proprietary (Quanta)
Mouse FST	AAAACCTACCGCAACGAATG	GGTCTGATCCACCACACAAG
Mouse 18S rRNA	GCCGCTAGAGGTGAAATTCTTG	CATTCTTGGCAAATGCTTTCG

Table 4-6. Synthesized oligonucleotide sequences for the cloning of mir299a-5p MRE-luc with ~60bp flanking the FST 3'UTR (highlighted in green) in PGL3 Control/ Vector (mir299a-5p 8mer MRE highlighted in yellow (P=phosphate).

miR299a-5p MRE Luciferase

Forward Strand/Sense	Reverse Strand/Anti-Sense
*P*ctagagttttttttttccccctt**gtaaacca**ttt**aagtccattcctcactat**gcacacccacctgtt	*P*ctagaacaggtgggtgtgcatagtgaggaatggac**ttaaatggtttac**aaggggggaaaaaaaaaact

Chapter 5: General Discussion and Conclusions

5.1 Rationale and General Summary

CKD is a major cause of morbidity and mortality, characterized by renal fibrosis that results in progressively worsening renal function [4–7]. Glomerular MC play a critical role in promoting renal fibrosis by producing fibrogenic matrix proteins such as fibronectin and collagen in response to profibrotic stimuli [35,79]. Our laboratory has previously determined that the ability of MC to promote matrix production is dependent on the expression and post-translational modification, through phosphorylation, of the caveolar membrane protein, cav-1 [77,78,226,227]. Increased cav-1 expression has been observed in several glomerular diseases in humans and in animal models of hypertensive CKD [81]. Furthermore, cav-1 knockout mice are protected against renal fibrosis, with no adverse side effects on blood pressure and renal function [77,81,130]. The role of cav-1 has been shown to be cell-type and organ specific [130,228,229]. Thus, ubiquitous repression of cav-1 in a clinical setting is not therapeutically viable due to the potential risks of adverse side effects. In addition, as of now, targeting cav-1 via therapeutic approaches specifically within MC in the kidneys is not technically feasible. In order to better understand why cav-1 deficient MC are protected against renal fibrosis, we carried out a microarray analysis, in which we identified FST as the most abundant gene in cav-1 deficient MC [22]. FST is a ubiquitously expressed glycoprotein that potently neutralizes several members of the TGFβ family, including ActA but not TGFβ1. TGFβ1 is highly upregulated in the injured kidney where it serves as a primary inducer of renal fibrosis [41,42,47,48]. While TGFβ1 inhibition is effective at halting the progression of renal fibrosis in a number of experimental kidney disease models, efforts to inhibit TGFβ1 in

clinical settings in patients with kidney disease have not been successful, due to various issues involving adverse side effects and/or the lack of any beneficial effects [41,51,52]. Hence, inhibition of alternative TGFβ members might be a more viable and effective therapeutic approach for the treatment of kidney fibrosis. To this end, we hypothesized ActA to be a likely candidate. Initially, ActA was identified to be important regulator of early developmental processes, including in the development of the kidneys [59–61]. ActA is not seen in healthy adult kidneys, but its expression is induced during the early stages of CKD in humans and in rodent models of kidney disease and injury [22,28,54,62–65]. Here, ActA has been shown to promote apoptosis and inhibit tubular cell regeneration and activate profibrotic pathways involved in the development of renal fibrosis [22,28,54,62–65]. Thus, we hypothesized that FST could be protective through its potent ability to specifically block ActA in the setting of kidney disease. No interventions as of now are able to inhibit and/or reverse the progression of CKD through ameliorating renal fibrosis. The primary objective of this thesis was to determine how FST is regulated at the molecular level in cav-1 deficient MC and determine whether its supplementation in the form of exogenous recombinant protein treatment or through genetic manipulation via miRNA silencing can protect against CKD. The overall findings of this thesis are presented in Figure 5-3.

5.2 Molecular Regulation of Follistatin by Caveolin-1

We have mechanistically established how the lack of cav-1 results in elevated FST expression at the mRNA and protein level in MC (Fig. 5-1). Our data show that cav-1 mediated regulation of FST occurs transcriptionally and post-transcriptionally by Sp1 and miR299a-5p, respectively (Fig. 5-1).

5.2.1 Transcriptional Regulation by Sp1

We show that cav-1 deficiency elevates Sp1 activity and binding to the FST promoter, resulting in increased FST promoter transcriptional activation and in turn increased FST mRNA and protein expression (Fig. 5-1). About 262 bp upstream of the translation start site of the FST promoter has been shown to be critical for the regulation of its expression in a manner that reflects endogenous mRNA expression [119]. In our studies, we identified two Sp1 bindings sites localized specifically within the 123 bp of the FST promoter that are important for its regulation. Sp1 has been noted as an important transcriptional factor that can activate the FST promoter in intestinal epithelial cells [121]. It is well known that Sp1 activity is under tight regulation via numerous post-translational modifications such as phosphorylation, acetylation, sumoylation, ubiquitylation, and glycosylation [122]. These post-translational modifications can positively or negatively influence the activity and binding of Sp1 [122]. Hence, it is likely that cav-1, a well-known regulator of a wide variety of intracellular signaling cascades, can lead to the activation and/or repression of a signaling protein that is involved in post-translationally

modifying Sp1. Our results show that cav-1 meditated regulation of the phosphorylation and activation of Sp1 is mediated through PI3K and PKCζ (Fig. 5-1). PI3K is a lipid kinase that is activated by a number of growth factors and takes part in the cascade of signal transduction events involved in cell growth and transformation [137,138]. PKCζ, classified as a downstream effector of PI3K, is an atypical serine/threonine kinase, which is activated without the need of calcium and/or diacylglycerol (DAG) [230]. PKCζ has been shown to be activated through secondary messengers generated through PI3K, such as PIP3 [147,230]. We have illustrated that cav-1 deficient MC exhibit basally elevated PI3K signaling. This elevation of PI3K signaling was associated with elevated PKCζ activation, which led to the phosphorylation and activation of Sp1. Overall, these results are the first showing a regulatory role of cav-1 in the post-translational regulation of Sp1 and in turn on the transcriptional regulation of FST in glomerular MC.

One of the major limitations of this study was that we were not able to establish how cav-1/caveolae regulate PI3K signaling. Future studies should examine how the lack of cav-1 result in increased PI3K activation. To this end, caveolae are highly enriched in signaling components, such as heterotrimeric G-proteins, Src kinases, EGF receptors, PDGF receptors, MAP kinases and the p85 subunit of PI3K [141]. Cav-1 within caveolae has been suggested to regulate PI3K/Akt signaling [141,231]. A recent study illustrated that cav-1 overexpression downregulates PI3K/Akt signaling in hepatoma CBRH7919 cells [141]. Phosphatase and tensin homolog (PTEN), through dephosphorylating PIP3, acts as the primary suppressor of PI3K activation [142]. A positive correlation between cav-1 and phosphatase and tensin homolog (PTEN) has been proposed [232].

Mechanistically, this has been hypothesized to occur through the cav-1 mediated translocation of PTEN from the cytoplasm to the cell membrane, where it is activated and in turn functions to inhibit PI3K [232]. These findings have been validated using cav-1 deficient mice which exhibit lower expression of PTEN at the cell surface [232]. These data support our findings and hint at a potential mechanism involving PTEN, through which the lack of cav-1 results in increased PI3K activation and in turn elevated FST expression in MC.

5.2.2 Post-transcriptional regulation by miR299a

In addition to identifying cav-1-mediated Sp1 regulation of FST at the transcriptional level, we have showed that the 3'UTR of FST is also differentially post-transcriptionally regulated by cav-1 (Fig. 5-1). miRNAs are short RNA sequences that bind to complimentary target sequences within the 3'UTR of a gene and in turn regulate post-transcriptional stability. Using bioinformatics tools, we identified numerous miRNAs that can target the FST 3'UTR. We determined that cav-1 deficiency is involved in downregulating the expression of some of these FST-targeting miRNAs, in particular miR299a-5p. miR299a-5p is localized to chromosome 14q32.31 cluster containing approximately 40 intergenic miRNAs, belonging to the miR-154 family [221,222]. miR299a-5p is predicted to target more than 150 genes involved in regulating a wide variety of cellular process and signaling pathways involving apoptosis, autophagy and fibrosis [221–223]. We have validated a functional role of miR299a-5p in binding the 8-mer MRE within the 3'UTR of FST and in-turn downregulating its transcript and protein

expression. Furthermore, we showed that miR299a-5p is induced by TGFß1. For the first time, we report that TGFβ1 inhibits FST expression in MC. While other groups have shown the ability of TGFβ1 to upregulate FST, TGFβ1-mediated depression of FST has not yet been described [225]. Our data suggest that TGFß1 downregulates FST through increasing miR299a-5p expression. With these results, we hypothesized that miR299a-5p augments TGFß1 signaling through the repression of FST. Unlike TGFß1, ActA was not found to repress FST expression (data not shown). How TGFß1 increases miR299a-5p and whether ActA also induces miR299-5p expression and activity needs to be assessed in future studies. There are two scenarios for consideration: 1) TGFß1 increases miR299a-5p at the transcriptional level and/or 2) TGFß1 increases miR299-5p through affecting miRNA processing and/or maturation. Potential strategies to assess these mechanisms involve examining the promoter of miR299a-5p to identify whether TGFß/smad responsive elements are important for TGFß1-mediated miR299a-5p upregulation. Unfortunately, this approach is technically challenging as promoter regions for miRNAs are not clearly defined and often overlap with and/or encompass several distinct miRNAs. Another approach would be to examine whether the maturation and/or processing of miR299a-5p is altered by TGFß1 by observing changes in the expression of miRNA processing and maturation enzymes, such as Drosha, Dicer and Argonaute.

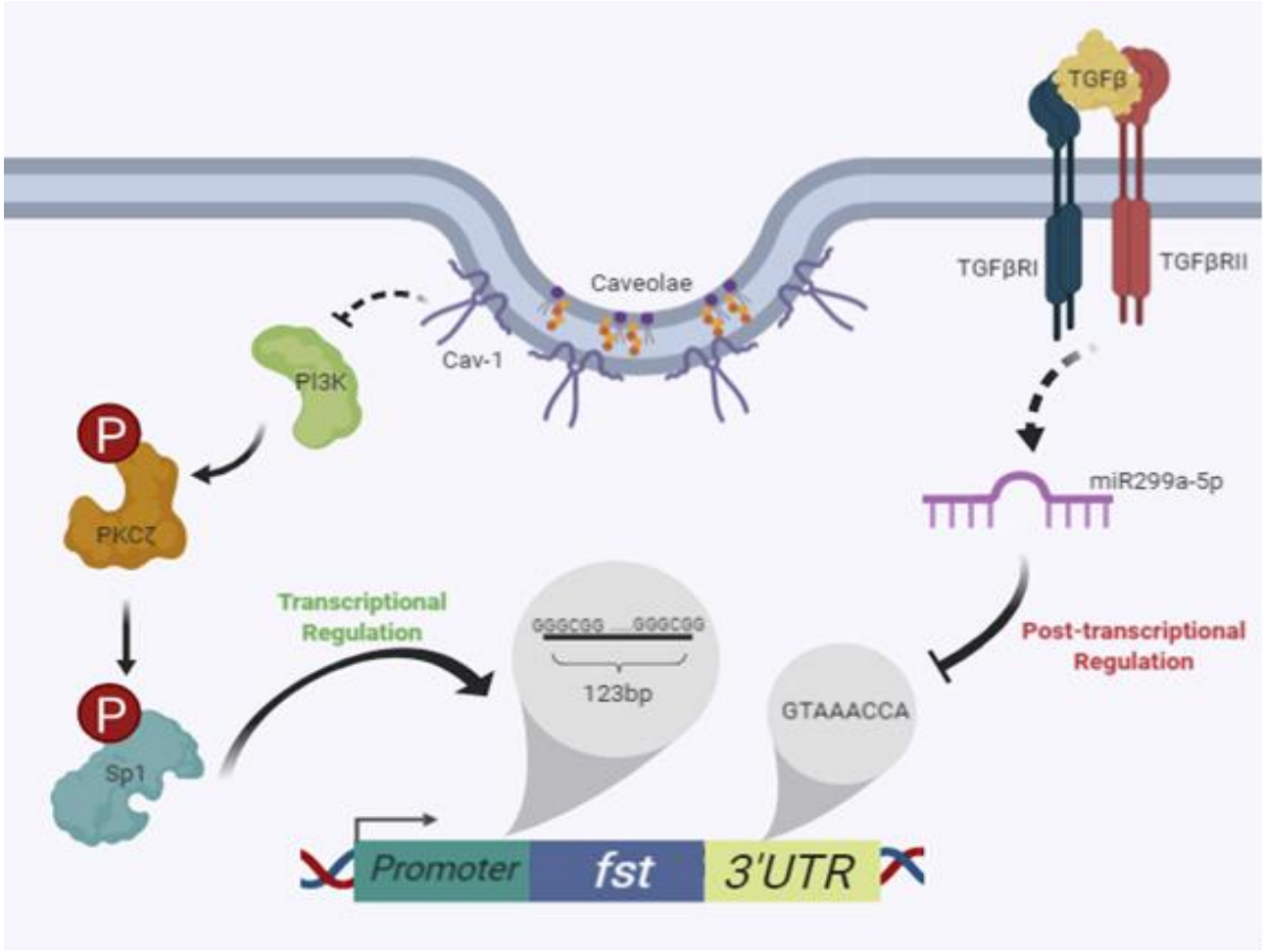

Figure 5-1. Molecular Regulation of FST.

Activation arrows (—›), *inhibition arrows* (——|), *unknown mechanism* (----). Cav-1 modulates the expression of FST through repressing the activation of PI3K signaling. Decreased PI3K signaling results in reduced PKCζ activation. PKCζ phosphorylates Sp1 resulting in its activation and nuclear translocation. Sp1 binds to the FST promoter resulting in its transcriptional activation and protein production. TGFß1 represses FST through inducing the expression of miR299a-5p. miR299a-5p post-transcriptionally represses FST expression through binding to its 3'UTR.

5.3 miR299a-5p in Renal Fibrosis and its Therapeutic Potential in CKD

Recent studies have implicated miR-154 and related family members, including miR299a-5p in the development pulmonary and cardiac fibrosis. miR154 and miR299a-5p are upregulated following myocardial infarction and cardiac fibrosis and are inversely correlated with cardiac function [223]. Therapeutic inhibition of miR-154 has protected against cardiac dysfunction and fibrosis [223]. Recent studies have also shown that the expression of miR299a-5p is increased in mouse models of pulmonary fibrosis and in patients with primary biliary cirrhosis [105,106,223]. A role for miR-154 family members generally, or miR-299a-5p specifically, in kidney fibrosis has not yet been investigated. Here, we first showed that miR299a-5p is upregulated in the glomeruli and tubules of mice with CKD. Consequently, we systemically inhibited miR299a-5p using subcutaneous administration of miR299a-5p targeting LNA oligonucleotide in mice with CKD. As expected, miR299a-5p inhibition protected against the development of renal fibrosis, improved kidney function and reduced albuminuria in mice with CKD. Sample size was a limitation in this study; these studies should be repeated to confirm results and obtain statistically significant readouts.

How miR299a-5p inhibition protects against renal fibrosis is not fully understood. In our studies, when miR299a-5p was inhibited, TGFß1 was not able to repress the expression of the antifibrotic protein FST, and consequently TGFß1-induced matrix production was blunted. Interestingly, when FST expression was downregulated, mir299a-5p inhibition was not able to repress the profibrotic actions of TGFß1. Similarly, upregulating the expression of miR299a-5p in cav-1 KO MC to the levels observed in

cav-1 WT MC was sufficient in restoring the ability of TGFß1 to promote matrix production in these cells. Furthermore, miR299a-5p inhibition, as expected, led to an increase in the expression of FST in cultured MC and in the glomeruli and tubules of mice with CKD. These results show that miR299a-5p through FST downregulation plays an important pathogenic role in promoting ECM production and that the protective effects of miR299a-5p inhibition are likely due to the enhanced expression of FST.

In addition to FST, several other mechanisms for the pathogenic effects of the miR-154 family have also been proposed. One of the primary pathways involves miRNA-mediated regulation of the profibrotic Wnt/ß-catenin signaling pathway [105,233]. Wnt/ß-catenin signaling is involved in the development of renal fibrosis [234] . However, in MC, miR-299a-5p did not affect ß-catenin transcriptional activity assay (data not shown). Another target of miR299a-5p, which we discovered and validated was Cripto-1 (data not shown). Cripto-1 also inhibits signaling of TGFß superfamily members, in particular through the neutralization of TGFß1 [235]. Thus, it is possible that miR299a-5p promotes fibrosis through the repression of both FST and Cripto-1. Future studies should examine the protective role of Cripto-1 in renal fibrosis and determine whether miR-299a promotes TGFß /activin signaling through its repression. Broader effects of miR299a-5p inhibition on gene expression should also be assessed using microarray analysis. These results could identify novel targets and deleterious signaling pathways that are regulated by this miRNA in a CKD setting.

5.4 Activin A in Kidney Fibrosis and Therapeutic Inhibition Strategies.

Even though TGFβ1 is a well-accepted driver of renal fibrosis, clinical studies testing the inhibition of this cytokine have not been successful [236]. Over the recent years, the TGFβ superfamily cytokine ActA has been hypothesized to be a potential alternative therapeutic target for the treatment of fibrosis. TGFβ1 has been shown to induce the expression and secretion of ActA in renal cells and non-renal cells [54,71,107]. ActA is also shown to be required for the profibrotic effects of TGFβ1 [54,71,107]. Overexpression of ActA has been noted in fibrotic process involved in the lung, pancreas, liver and skin [23,45,46,53,237]. In renal interstitial fibroblasts, tubular cells and mesangial cell, ActA has been shown to promote proliferation, differentiation and ECM production [22,54]. Systemic ActA was recently shown to be increased in patients with stage 2 CKD [65]. Circulating, renal and urinary ActA have been shown to be increased in several rodent models of kidney disease [22,25,26,28]. Surprisingly, we also observed elevation in the expression of renal FST in mice with CKD (data not shown). This increase in FST can be hypothesized to occur as a protective feedback mechanism in CKD. Here, it is possible that this endogenous increase in FST in response to CKD is not sufficient to counteract the elevation of activins and TGFβ1. Indeed, studies have suggested that an optimal FST to activin (F/A) ratio is required to observe protective effects. One study observed elevated levels of serum ActA and FST in patients with acute severe hepatitis and acute liver failure [238]. Here, a decreased F/A ratio was suggested to be a reliable indicator of the severity of acute liver injury and prognosis [238]. Similar effects were observed in cystic fibrosis patients, where a decrease in the F/A ratio was

associated with decreased physiological lung function [239]. Furthermore, supplemental FST given to mice with cystic fibrosis was found to inhibit ActA, skew the F/A ratio and improve survival and lung function [239]. Thus, it is likely that a decreased F/A ratio in mice kidneys with CKD results in exacerbated kidney function and pathology.

Given the ability of ActA to promote fibrosis, therapeutic ActA inhibition strategies have been investigated. ActA inhibition reduces TGFβ1-induced activity and matrix production in renal fibroblasts, fetal lung fibroblasts and hepatic and pancreatic stellate cells [71,107,237,240]. Our data suggest that ActA inhibition using exogenous FST supplementation is an effective therapeutic approach for blocking renal fibrosis [22]. Another ActA signaling inhibition strategy involves the use of a ligand trap in which the extracellular soluble domain of ActRII is fused to the Fc portion of IgG1. This fusion protein inhibits renal fibrosis, improve GFR and proteinuria in mice with CKD [25]. These ligand traps are also effective in improving anemia and bone mineral disorder associated with CKD [241–245]. They are also being tested in patients with various blood disorders and osteoporosis [246]. ActA and ActRII neutralization antibodies are also being developed and tested in sporadic inclusion body myositis patients (NCT02250443) and in overweight and obese patients with type 2 diabetes (NCT03005288). Figure 5-2 summaries theses ActA signaling inhibition strategies. These studies collectively suggest that ActA plays an important role in the development of renal fibrosis both directly and indirectly through TGFβ1 and that its inhibition is feasible and effective.

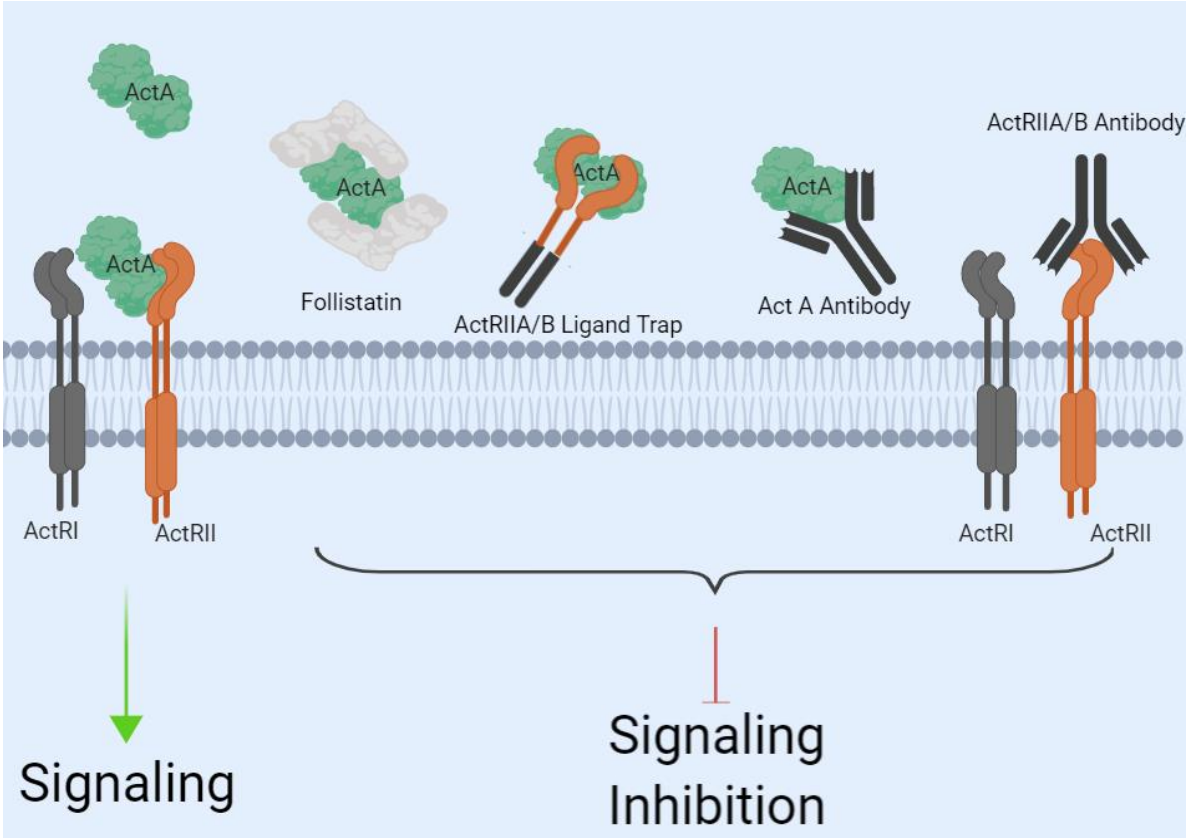

Figure 5-2. Activin A inhibition strategies.

Activin A exerts its biologic actions through binding to ActRII, which recruits, phosphorylates and activates ActRI, resulting in Smad 2 /3 activation, nuclear translocation and transcriptional activation. Follistatin is an endogenous inhibitor of activin A that binds to activin A and induces its internalization and lysosomal mediated degradation. ActRII ligand traps bind to and neutralize activin A and other TGFβ family ligands. They are formed by fusing the soluble extracellular domain of ActRII to an Fc portion of IgG1. Monoclonal neutralizing antibodies against activin A and/or ActRII block ligand access to the receptor.

5.5 Follistatin as an Antifibrotic Therapy

FST is as an endogenous activin inhibitor. Through alternative splicing, two main forms of follistatin are generated, FST288 and 315. FST315 is circulating, while FST288 is bound to surface heparan-sulfated proteoglycans through an heparin-binding site [46]. FST288 is more effective than FST315 in its ability to neutralize ActA [247]. Direct exogenous administration of FST has been shown to attenuate liver fibrosis, pulmonary fibrosis and tubulointerstitial fibrosis in a rat model of unilateral ureteral obstruction [23,107,109]. In a recent study, we treated diabetic mice with recombinant FST-288 and observed protective effects in terms of improving albuminuria and GFR while reducing glomerulosclerosis [22]. In this thesis, we determined the therapeutic efficacy of FST-288 in preventing the progression of renal fibrosis in a robust, clinically relevant 5/6 nephrectomy (Nx) renal mass reduction model of CKD. CKD mice treated with FST exhibited a significant improvement in kidney function (GFR) along with decreased albuminuria and renal fibrosis. This was associated with decreased activation of glomerular and interstitial fibroblasts along with decreased Smad3 signaling. Renal Smad3 signaling activation is primarily driven by TGFß1 [219]. However, activins also signal through Smad3 [57]. Since FST cannot directly target and neutralize TGFß1, the effects we observed in our studies are likely through the ability of FST to neutralize actA-induced profibrotic Smad3 signaling. Future studies should examine the specific contribution of ActA in the development of renal fibrosis and examine how FST influences TGFß1 signaling in a CKD setting in the presence or absence of ActA. Given the current uses of FST in humans in clinical gene transfer trials for muscle disorders and

based on its potent ability to block profibrotic responses in a wide variety of organs and cell types, it is a potential therapeutic candidate for renal fibrosis [22,23,46,248,249].

5.5.1 Follistatin in the regulation of Oxidative Stress in CKD.

Oxidative stress and apoptosis are critical components in the pathogenesis of kidney disease [83,84,188,250]. In our studies, exogenous FST was found to scavenge reactive oxygen species (ROS) and reduce renal oxidative stress *in vivo* in mice with CKD. Reductions in renal apoptosis and oxidative stress can be associated with improvements in kidney function along with reductions in renal fibrosis and inflammation. Direct evidence of the beneficial effects of reducing oxidative stress and apoptosis in CKD was presented in a recent study carried out in rats with adenine-induced CKD [251]. The use of curcumin, through its ability to increase an antioxidant transcriptional factor Nrf2, was able to protect against renal morphological damage, inflammation, fibrosis and apoptosis [251]. Thus, it is likely that repression of renal oxidative stress and apoptosis is another mechanism via which FST improves kidney function and decreases renal fibrosis in a CKD setting.

How FST prevents oxidative stress and cell death is not completely understood. Our *in vitro* studies suggest that the ability of FST to scavenge ROS and reduce oxidative stress is independent of ActA and/or ActB neutralization. FST has been characterized as a protective anti-apoptotic and anti-oxidative stress responsive protein through two distinct mechanisms involving extracellular TGFβ ligand neutralization and nuclear localization [97]. Our studies using over-expression of a mutant FST protein unable to enter the nucleus (FSTΔNLS) showed that the nuclear expression of FST is not required for its

ability to protect against oxidative stress generation and apoptosis. However, a limitation of this experiment was that the protective effects of endogenous nuclear FST protein could not be assessed and teased apart from the mutant FST protein. Secondly, our data suggest that ActA and ActB do not promote oxidative stress and apoptosis within MC. Interestingly, alternative TGFβ family members, such as BMP4 and myostatin, through Smad-dependent and independent signaling pathways, have been shown to promote ROS production and apoptosis in numerous cell types [94–96,193]. Thus, it is plausible that pro-oxidative cytokines such as BMP4 and myostatin are neutralized by FST in MC. This will need to be tested in future studies. ROS can also be directly produced within the mitochondria and cytoplasm by NAD(P)H oxidases (NOXs). We found that FST inhibits the expression of NOX4 in response to stress. Thus, NOX4 inhibition could be an alternative mechanism explaining the anti-oxidative effect of FST.

In addition to examining the protective role of FST involving nuclear retention, canonical TGFβ neutralization and NOX4 inhibition, we also directly tested the ability of FST to scavenge ROS. Here, we determined that FST does not possess intrinsic enzymatic peroxidase activity. Our data are the first showing that FST directly neutralizes reactive species such as H_2O_2, $ONOO^-$, HO, NO, ROO and SO. We hypothesized that the protein structure of FST might allow it to function as a ROS sink. Indeed, in accordance with the literature, we noted that methionine residues present within FST can be readily oxidized by H_2O_2 [207]. Future studies should assess the ability of mutant FST protein that lack these methionine residues. Based on our hypothesis, FST mutants lacking these reduced methionine residues should not be able to neutralize ROS. A limitation of this

study was that we were not able to fully explain why higher doses (10μg) of FST were not protected against renal fibrosis and CKD progression. Interestingly, we noted that CKD mice treated with high dose of FST exhibited a severe physiologic decrease in renal oxidative stress when compared to control sham-operated mice. Therefore, based on the hypothesis that basal expression of ROS is critical for cellular signaling and homeostasis, future studies should assess whether excessive ROS scavenging with high dose FST is responsible for negating the protective antifibrotic effects observed at lower doses of FST. To this end, a microarray screen of renal biopsies from CKD mice treated with several doses of FST ranging from 1μg to 10μg could help identify changes in oxidative stress markers and pathways that are differentially altered by higher doses of FST. These experiments will help establish a safe and effective therapeutic range of FST that is anti-oxidative and antifibrotic.

5.5.2 Follistatin in the regulation of blood pressure.

Hypertension is a prominent finding in CKD [111]. In our studies, exogenous recombinant FST supplementation (data not shown) and miR299a-5p inhibition (indirect FST elevation) decreased blood pressure in mice with CKD. How FST functions to lower blood pressures is not clearly understood. Some data suggest that the FST-targeted cytokines, such as ActA and BMP4 are correlated with elevated blood pressure. ActA and BMP4 have been shown to promote hypertension in preeclampsia and systemic, clinical and experimental models of pulmonary hypertension, respectively [252–255]. Thus, the blood pressure lowering effects of FST in CKD could be mediated through the

neutralization of ActA and/or BMP4. Impaired vascular reactivity has also been observed in hypertensive models of CKD [256,257]. The structural and functional vascular reactivity properties, including contractility and relaxation dynamics of small arteries are important for providing peripheral resistance and promoting systemic hypertension [258]. In rodents, the mesenteric vascular bed has been shown to be important for providing total peripheral resistance [259,260]. We observed that α_1-adrenergic receptor stimulated mesenteric contractions were significantly decreased while endothelium dependent, cholinergic mesenteric relaxations were improved in CKD mice treated with FST (data not shown). These vascular changes mediated by FST could be another mechanism via which blood pressure is improved in CKD. How FST functions to improve vascular reactivity of these resistant blood vessels is not known. Numerous cytokines, such as TNF-alpha, IL-1ß, and IL-6 have been shown to induce vasoconstriction, increase the response to vasoconstrictor agents or impair endothelium-dependent vasodilatation [261]. TGFβ1 has been shown to inhibit the production of vasodilators such as nitric oxide and stimulate the production of potent vasoconstrictors such as endothelin [262]. Whether ActA exerts similar vascular effects and whether FST plays a direct role in regulating vessel hemodynamics needs to be examined in future studies.

5.6 Conclusion

We have shown that the antifibrotic protein FST is transcriptionally upregulated in cav-1 deficient MC via augmentation of PI3K, PKCζ and Sp1 activity. Through increased FST expression, cav-1 deficient MC are protected against matrix production. Exogenous FST treatment inhibited TGFß-induced profibrotic Smad3 signaling and protected against the progression of renal fibrosis in mice with CKD. This protective phenotype was mediated through oxidative stress repression via scavenging of ROS. Cav-1 deficient MC were also found to exhibit decreased expression of a FST-targeting miRNA, miR299a-5p. TGFß1 led to upregulation of miR299a-5p, augmented ECM production and post-transcriptional inhibition of FST. Systemic mir299a-5p inhibition increased FST expression and decreased renal fibrosis in mice with CKD. In conclusion, given the lack effective treatments for halting or reversing the progression of CKD, our data collectively suggest that FST is a potential novel treatment for renal fibrosis that should be further characterized, validated and assessed in pre-clinical and clinical settings.

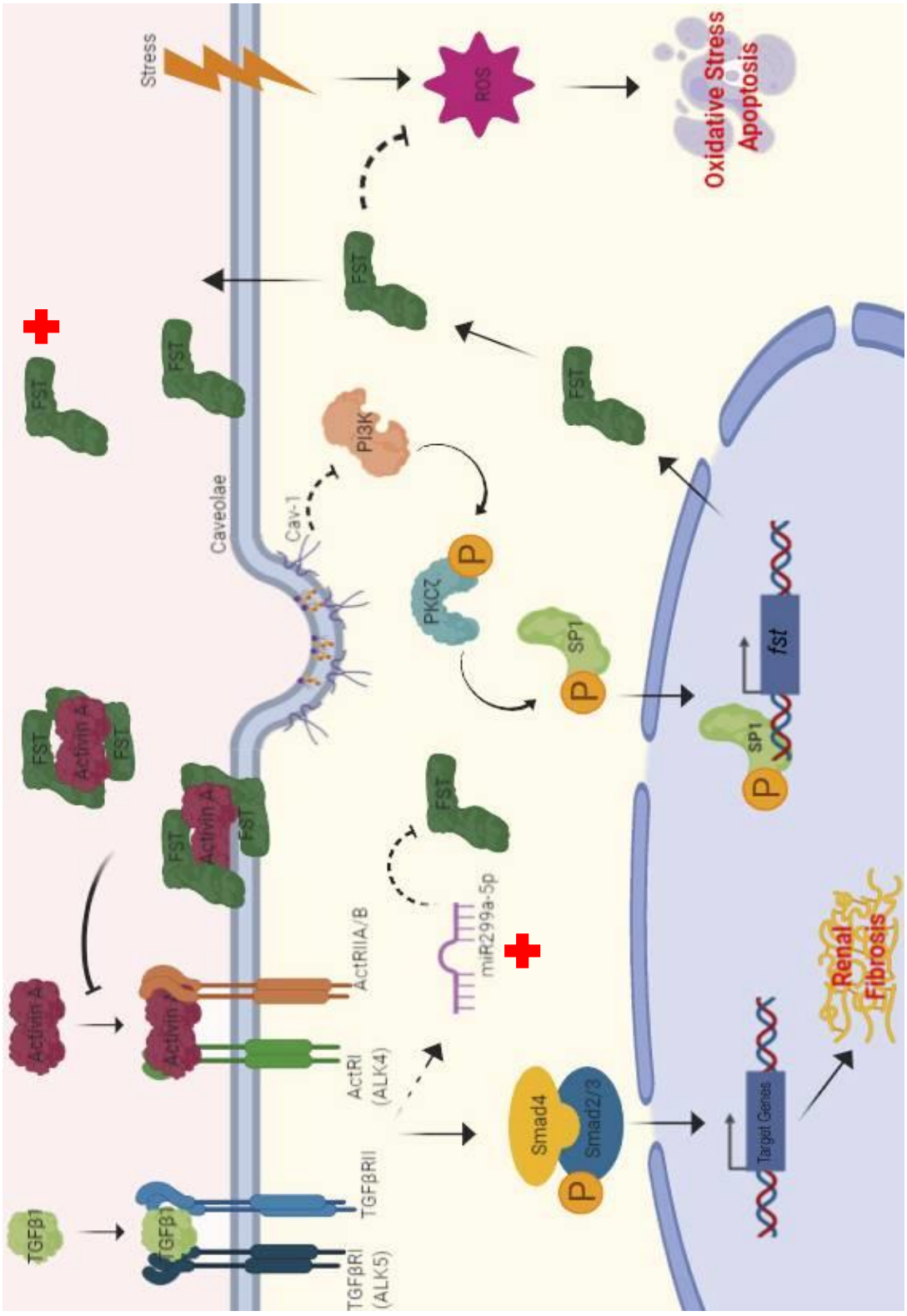
Stress
ROS
Oxidative Stress
Apoptosis
FST
Caveolae
Cav-1
PI3K
PKCζ
P
SP1
fst
Activin A
ActRIIA/B
ActRI
(ALK4)
TGFβRII
TGFβRI
(ALK5)
TGFβ1
miR299a-5p
Smad4
Smad2/3
Target Genes
Renal
Fibrosis

Figure 5-3. Summary of research findings.

Activation arrows (—›), *inhibition arrows* (——|), *unknown mechanism* (----), *therapeutic intervention* (+). Cav-1 modulates the expression of FST through repressing the activation of PI3K-PKCζ-Sp1 signaling. FST acts as a ROS scavenger. FST is secreted and acts to neutralize the actions of TGFß cytokines, primarily ActA but not TGFß1. ActA and TGFß1 both signal via Smad2/3 to drive fibrotic signaling. ActA is required for the profibrotic effects of TGFß1. FST bound at the cell surface (FST 288) and circulating FST (FST 315) act to scavenge activins and inhibit downstream fibrotic signaling. Exogenous recombinant FST treatment alleviated renal oxidative stress, reduced renal fibrosis and albuminuria while improving kidney function in mice with CKD. miR299a-5p is elevated in CKD. Systemic miR299a-5p inhibition ameliorated renal fibrosis.

References

[1] H.G. Preuss, Basics of renal anatomy and physiology., Clin. Lab. Med. 13 (1993) 1–11. http://www.ncbi.nlm.nih.gov/pubmed/8462252 (accessed May 22, 2019).

[2] W. Kriz, B. Kaissling, Structural Organization of the Mammalian Kidney, in: Seldin and Giebisch's The Kidney, Elsevier, 2013: pp. 595–691. doi:10.1016/B978-0-12-381462-3.00020-3.

[3] J.H. Miner, The glomerular basement membrane., Exp. Cell Res. 318 (2012) 973–8. doi:10.1016/j.yexcr.2012.02.031.

[4] F. AB, Mechanisms of progression of chronic kidney disease, Pediatr. Nephrol. 39 (2010) 511–516. doi:10.1007/s00467-007-0524-0.

[5] W. Metcalfe, How does early chronic kidney disease progress ?, (2007) 26–30. doi:10.1093/ndt/gfm446.

[6] V. Jha, G. Garcia-Garcia, K. Iseki, Z. Li, S. Naicker, B. Plattner, R. Saran, A.Y.-M. Wang, C.-W. Yang, Chronic kidney disease: global dimension and perspectives., Lancet. 382 (2013) 260–72. doi:10.1016/S0140-6736(13)60687-X.

[7] D. Campbell, M.R. Weir, Defining, Treating, and Understanding Chronic Kidney Disease-A Complex Disorder, J. Clin. Hypertens. 17 (2015) 514–527. doi:10.1111/jch.12560.

[8] R.M. Perkins, I.D. Bucaloiu, H.L. Kirchner, N. Ashouian, J.E. Hartle, T. Yahya, GFR decline and mortality risk among patients with chronic kidney disease., Clin. J. Am. Soc. Nephrol. 6 (2011) 1879–86. doi:10.2215/CJN.00470111.

[9] F. Ward, J. Holian, P.T. Murray, Drug therapies to delay the progression of chronic kidney disease., Clin. Med. 15 (2015) 550–7. doi:10.7861/clinmedicine.15-6-550.

[10] R. Saran, B. Robinson, K.C. Abbott, L.Y.C. Agodoa, P. Albertus, J. Ayanian, R. Balkrishnan, J. Bragg-Gresham, J. Cao, J.L.T. Chen, E. Cope, S. Dharmarajan, X. Dietrich, A. Eckard, P.W. Eggers, C. Gaber, D. Gillen, D. Gipson, H. Gu, S.M. Hailpern, Y.N. Hall, Y. Han, K. He, P. Hebert, M. Helmuth, W. Herman, M. Heung, D. Hutton, S.J. Jacobsen, N. Ji, Y. Jin, K. Kalantar-Zadeh, A. Kapke, R. Katz, C.P. Kovesdy, V. Kurtz, D. Lavalee, Y. Li, Y. Lu, K. McCullough, M.Z. Molnar, M. Montez-Rath, H. Morgenstern, Q. Mu, P. Mukhopadhyay, B. Nallamothu, D. V Nguyen, K.C. Norris, A.M. O'Hare, Y. Obi, J. Pearson, R. Pisoni, B. Plattner, F.K. Port, P. Potukuchi, P. Rao, K. Ratkowiak, V. Ravel, D. Ray, C.M. Rhee, D.E. Schaubel, D.T. Selewski, S. Shaw, J. Shi, M. Shieu, J.J. Sim, P. Song, M. Soohoo, D. Steffick, E. Streja, M.K. Tamura, F. Tentori, A. Tilea, L. Tong, M. Turf, D. Wang, M. Wang, K. Woodside, A. Wyncott, X. Xin, W. Zang, L. Zepel, S. Zhang, H. Zho, R.A. Hirth, V. Shahinian, US Renal Data System 2016 Annual Data Report: Epidemiology of Kidney Disease in the United States., Am. J.

Kidney Dis. 69 (2017) A7–A8. doi:10.1053/j.ajkd.2016.12.004.

[11] Y. Liu, Renal fibrosis: new insights into the pathogenesis and therapeutics, Kidney Int. 69 (2006) 213–217. doi:10.1038/sj.ki.5000054.

[12] G.J. Becker, T.D. Hewitson, The role of tubulointerstitial injury in chronic renal failure., Curr. Opin. Nephrol. Hypertens. 9 (2000) 133–8. http://www.ncbi.nlm.nih.gov/pubmed/10757217.

[13] K.S. Hodgkins, H.W. Schnaper, Tubulointerstitial injury and the progression of chronic kidney disease, Pediatr. Nephrol. 27 (2012) 901–909. doi:10.1007/s00467-011-1992-9.

[14] Y. Liu, Cellular and molecular mechanisms of renal fibrosis., Nat. Rev. Nephrol. 7 (2011) 684–96. doi:10.1038/nrneph.2011.149.

[15] T.W. Meyer, S. Anderson, H.G. Rennke, B.M. Brenner, Reversing glomerular hypertension stabilizes established glomerular injury., Kidney Int. 31 (1987) 752–9. doi:10.1038/ki.1987.62.

[16] A.M. El Nahas, Glomerulosclerosis : intrinsic and extrinsic pathways, Am. J. Pathol. (1996) 773–777.

[17] X. Meng, D.J. Nikolic-paterson, H.Y. Lan, Inflammatory processes in renal fibrosis, Nat. Publ. Gr. 10 (2014) 493–503. doi:10.1038/nrneph.2014.114.

[18] C. Kurts, U. Panzer, H.-J. Anders, A.J. Rees, The immune system and kidney disease: basic concepts and clinical implications., Nat. Rev. Immunol. 13 (2013) 738–53. doi:10.1038/nri3523.

[19] R.J. Johnson, J. Floege, A. Yoshimura, H. Iida, W.G. Couser, C.E. Alpers, The activated mesangial cell: a glomerular “myofibroblast”?, J. Am. Soc. Nephrol. 2 (1992) S190-7.

[20] D. Schlöndorff, B. Banas, The mesangial cell revisited: no cell is an island., J. Am. Soc. Nephrol. 20 (2009) 1179–1187. doi:10.1681/ASN.2008050549.

[21] D. Schlöndorff, The glomerular mesangial cell: an expanding role for a specialized pericyte., FASEB J. 1 (1987) 272–281.

[22] D. Zhang, A.L. Gava, R. Van Krieken, N. Mehta, R. Li, B. Gao, E.M. Desjardins, G.R. Steinberg, T. Hawke, J.C. Krepinsky, The caveolin-1 regulated protein follistatin protects against diabetic kidney disease, Kidney Int. (2019). doi:10.1016/J.KINT.2019.05.032.

[23] A. Maeshima, K. Mishima, S. Yamashita, M. Nakasatomi, M. Miya, N. Sakurai, T. Sakairi, H. Ikeuchi, K. Hiromura, Y. Hasegawa, I. Kojima, Y. Nojima, Follistatin, an activin antagonist, ameliorates renal interstitial fibrosis in a rat model of unilateral ureteral obstruction, Biomed Res. Int. 2014 (2014).

doi:10.1155/2014/376191.

[24] D.Y.P.P. Fang, B. Lu, S. Hayward, D.M. de Kretser, P.J. Cowan, K.M. Dwyer, The Role of Activin A and B and the Benefit of Follistatin Treatment in Renal Ischemia-Reperfusion Injury in Mice, Transplant. Direct. 2 (2016) e87. doi:10.1097/TXD.0000000000000601.

[25] O.A. Agapova, Y. Fang, T. Sugatani, M.E. Seifert, K.A. Hruska, Ligand trap for the activin type IIA receptor protects against vascular disease and renal fibrosis in mice with chronic kidney disease, Kidney Int. 89 (2016) 1231–1243. doi:10.1016/j.kint.2016.02.002.

[26] M.J. Williams, T. Sugatani, O.A. Agapova, Y. Fang, J.P. Gaut, M.-C. Faugere, H.H. Malluche, K.A. Hruska, The activin receptor is stimulated in the skeleton, vasculature, heart, and kidney during chronic kidney disease, Kidney Int. 93 (2018) 147–158. doi:10.1016/j.kint.2017.06.016.

[27] W.N. Leonhard, S.J. Kunnen, A.J. Plugge, A. Pasternack, S.B.T. Jianu, K. Veraar, F. El Bouazzaoui, W.M.H. Hoogaars, P. Ten Dijke, M.H. Breuning, E. De Heer, O. Ritvos, D.J.M. Peters, Inhibition of Activin Signaling Slows Progression of Polycystic Kidney Disease., J. Am. Soc. Nephrol. 27 (2016) 3589–3599. doi:10.1681/ASN.2015030287.

[28] X.J. Ren, G.J. Guan, G.H.G. Liu, T. Zhang, G.H.G. Liu, Effect of activin A on tubulointerstitial fibrosis in diabetic nephropathy, Nephrology. 14 (2009) 311–320. doi:10.1111/j.1440-1797.2008.01059.x.

[29] T.D. Hewitson, Fibrosis in the kidney: is a problem shared a problem halved?, Fibrogenesis Tissue Repair. 5 (2012) S14. doi:10.1186/1755-1536-5-S1-S14.

[30] A.F. Michael, W.F. Keane, L. Raij, R.L. Vernier, S. Michael Mauer, The glomerular mesangium, 1980. doi:10.1038/ki.1980.18.

[31] D. Schlöndorff, Roles of the mesangium in glomerular function., Kidney Int. 49 (1996) 1583–1585. doi:10.1038/ki.1996.229.

[32] M.E. Choi, E.G. Kim, Q. Huang, B.J. Ballermann, Rat mesangial cell hypertrophy in response to transforming growth factor-beta 1, Kidney Int. 44 (1993) 948–958. doi:10.1038/ki.1993.336.

[33] D. Drenckhahn, H. Schnittler, R. Nobiling, W. Kriz, Ultrastructural organization of contractile proteins in rat glomerular mesangial cells., Am. J. Pathol. 137 (1990) 1343–51. http://www.pubmedcentral.nih.gov/articlerender.fcgi?artid=1877732&tool=pmcentrez&rendertype=abstract.

[34] J.C. Krepinsky, Y. Li, D. Tang, L. Liu, J. Scholey, A.J. Ingram, Stretch-induced Raf-1 activation in mesangial cells requires actin cytoskeletal integrity, Cell. Signal. 17 (2005) 311–320. doi:10.1016/j.cellsig.2004.07.010.

[35] B.L. Riser, P. Cortes, X. Zhao, J. Bernstein, F. Dumler, R.G. Narins, Intraglomerular pressure and mesangial stretching stimulate extracellular matrix formation in the rat, J. Clin. Invest. 90 (1992) 1932–1943. doi:10.1172/JCI116071.

[36] L. Buschhausen, S. Seibold, O. Gross, T. Matthaeus, M. Weber, E. Schulze-Lohoff, Regulation of mesangial cell function by vasodilatory signaling molecules, Cardiovasc. Res. 51 (2001) 463–469. doi:10.1016/S0008-6363(01)00340-6.

[37] H. Sugiyama, N. Kashihara, H. Makino, Y. Yamasaki, Z. Ota, Reactive Oxygen Species Induce Apoptosis in Cultures Human Mesangial Cells, J Am Soc Nephrol. 7 (1997) 2357–2363.

[38] M.S. Sundaram, S. Nagarajan, A. Jagdeeshwaran, M.A. Devi, Chronic Kidney Disease — Effect of Oxidative Stress, Chinese J. Biol. 2014 (2014) 1–6.

[39] M.M. Kiefer, M.J. Ryan, Primary Care of the Patient with Chronic Kidney Disease, Med. Clin. North Am. 99 (2015) 935–952. doi:10.1016/J.MCNA.2015.05.003.

[40] H.L. Heerspink, D. de Zeeuw, Novel drugs and intervention strategies for the treatment of chronic kidney disease, Br. J. Clin. Pharmacol. 76 (2013) n/a-n/a. doi:10.1111/bcp.12195.

[41] X.-M. Meng, P.M.-K. Tang, J. Li, H.Y. Lan, TGF-β/Smad signaling in renal fibrosis., Front. Physiol. 6 (2015) 82. doi:10.3389/fphys.2015.00082.

[42] L.-N.J. López-Hernández FJ1, Role of TGFb in chronic kidney disease: An integration of tubular, glomerular and vascular effects, Cell Tissue Res. 347 (2012) 141–154. doi:10.1007/s00441-011-1275-6.

[43] A. Leask, D.J. Abraham, TGF-beta signaling and the fibrotic response., FASEB J. 18 (2004) 816–27. doi:10.1096/fj.03-1273rev.

[44] R. Schulz, T. Vogel, R. Dressel, K. Krieglstein, TGF-beta superfamily members, ActivinA and TGF-beta 1, induce apoptosis in oligodendrocytes by different pathways, Cell Tissue Res. 334 (2008) 327–338. doi:10.1007/s00441-008-0714-5.

[45] M. Antsiferova, S. Werner, The bright and the dark sides of activin in wound healing and cancer, J. Cell Sci. 125 (2012) 3929–3937. doi:10.1242/jcs.094789.

[46] M.P. Hedger, D.M. De Kretser, The activins and their binding protein, follistatin-Diagnostic and therapeutic targets in inflammatory disease and fibrosis, Cytokine Growth Factor Rev. 24 (2013) 285–295. doi:10.1016/j.cytogfr.2013.03.003.

[47] H.W. Schnaper, S. Jandeska, C.E. Runyan, S.C. Hubchak, R.K. Basu, J.F. Curley, R.D. Smith, T. Hayashida, TGF-beta signal transduction in chronic kidney disease., Front. Biosci. (Landmark Ed. 14 (2009) 2448–65. doi:10.2741/3389.

[48] K. Tamaki, S. Okuda, T. Ando, T. Iwamoto, M. Nakayama, M. Fujishima, TGF-beta 1 in glomerulosclerosis and interstitial fibrosis of adriamycin nephropathy,

Kidney Int. 45 (1994) 525–536. doi:10.1038/ki.1994.68.

[49] Y.E. Zhang, Non-Smad pathways in TGF-beta signaling., Cell Res. 19 (2009) 128–39. doi:10.1038/cr.2008.328.

[50] L. Gewin, The many talents of transforming growth factor- b in the kidney, (2019) 203–210. doi:10.1097/MNH.0000000000000490.

[51] F. Vincenti, F.C. Fervenza, K.N. Campbell, M. Diaz, L. Gesualdo, P. Nelson, M. Praga, J. Radhakrishnan, L. Sellin, A. Singh, D. Thornley-Brown, F.V. Veronese, B. Accomando, S. Engstrand, S. Ledbetter, J. Lin, J. Neylan, J. Tumlin, A Phase 2, Double-Blind, Placebo-Controlled, Randomized Study of Fresolimumab in Patients With Steroid-Resistant Primary Focal Segmental Glomerulosclerosis, Kidney Int. Reports. 2 (2017) 800–810. doi:10.1016/j.ekir.2017.03.011.

[52] J. Voelker, P.H. Berg, M. Sheetz, K. Duffin, T. Shen, B. Moser, T. Greene, S.S. Blumenthal, I. Rychlik, Y. Yagil, P. Zaoui, J.B. Lewis, Anti–TGF- β 1 Antibody Therapy in Patients with Diabetic Nephropathy, J. Am. Soc. Nephrol. 28 (2017) 953–962. doi:10.1681/ASN.2015111230.

[53] M. Myllärniemi, J. Tikkanen, J.J. Hulmi, A. Pasternack, E. Sutinen, M. Rönty, O. Leppäranta, H. Ma, O. Ritvos, K. Koli, Upregulation of activin-B and follistatin in pulmonary fibrosis - a translational study using human biopsies and a specific inhibitor in mouse fibrosis models., BMC Pulm. Med. 14 (2014) 170. doi:10.1186/1471-2466-14-170.

[54] S. Yamashita, A. Maeshima, I. Kojima, Y. Nojima, Activin A Is a Potent Activator of Renal Interstitial Fibroblasts, J. Am. Soc. Nephrol. 15 (2004) 91–101. doi:10.1097/01.ASN.0000103225.68136.E6.

[55] E. Kreidl, D. Oztürk, T. Metzner, W. Berger, M. Grusch, Activins and follistatins: Emerging roles in liver physiology and cancer., World J. Hepatol. 1 (2009) 17–27. doi:10.4254/wjh.v1.i1.17.

[56] W. Vale, J. Rivier, J. Vaughan, R. McClintock, A. Corrigan, W. Woo, D. Karr, J. Spiess, Purification and characterization of an FSH releasing protein from porcine ovarian follicular fluid, Nature. 321 (1986) 776–779. doi:10.1038/321776a0.

[57] D.M. de Kretser, R.E. O'Hehir, C.L. Hardy, M.P. Hedger, The roles of activin A and its binding protein, follistatin, in inflammation and tissue repair, Mol. Cell. Endocrinol. 359 (2012) 101–106. doi:10.1016/j.mce.2011.10.009.

[58] N. Ling, S.-Y. Ying, N. Ueno, S. Shimasaki, F. Esch, M. Hotta, R. Guillemin, Pituitary FSH is released by a heterodimer of the β-subunits from the two forms of inhibin, Nature. 321 (1986) 779–782. doi:10.1038/321779a0.

[59] A. Maeshima, Y.-Q. Zhang, M. Furukawa, T. Naruse, I. Kojima, Hepatocyte growth factor induces branching tubulogenesis in MDCK cells by modulating the activin-follistatin system, Kidney Int. 58 (2000) 1511–1522. doi:10.1046/j.1523-

1755.2000.00313.x.

[60] T. Tuuri, M. Erämaa, K. Hildén, O. Ritvos, The tissue distribution of activin beta A- and beta B-subunit and follistatin messenger ribonucleic acids suggests multiple sites of action for the activin-follistatin system during human development., J. Clin. Endocrinol. Metab. 78 (1994) 1521–1524. doi:10.1210/jcem.78.6.8200957.

[61] O. Ritvos, T. Tuuri, M. Erämaa, K. Sainio, K. Hildén, L. Saxén, S.F. Gilbert, Activin disrupts epithelial branching morphogenesis in developing glandular organs of the mouse., Mech. Dev. 50 (1995) 229–45. http://www.ncbi.nlm.nih.gov/pubmed/7619733 (accessed July 3, 2019).

[62] A. Maeshima, Y.Q. Zhang, Y. Nojima, T. Naruse, I. Kojima, Involvement of the activin-follistatin system in tubular regeneration after renal ischemia in rats., J. Am. Soc. Nephrol. 12 (2001) 1685–1695. http://www.ncbi.nlm.nih.gov/pubmed/11461941 (accessed July 2, 2019).

[63] S. Takahashi, M. Nakasatomi, Y. Takei, H. Ikeuchi, T. Sakairi, Y. Kaneko, K. Hiromura, Y. Nojima, A. Maeshima, Identification of Urinary Activin A as a Novel Biomarker Reflecting the Severity of Acute Kidney Injury, Sci. Rep. 8 (2018) 5176. doi:10.1038/s41598-018-23564-3.

[64] A. Nordholm, S. Egstrand, E. Gravesen, M.L. Mace, M. Morevati, K. Olgaard, E. Lewin, Circadian rhythm of activin A and related parameters of mineral metabolism in normal and uremic rats, Pflügers Arch. - Eur. J. Physiol. (2019) 1–16. doi:10.1007/s00424-019-02291-2.

[65] F. Lima, H. Mawad, A.A. El-Husseini, D.L. Davenport, H.H. Malluche, Serum bone markers in ROD patients across the spectrum of decreases in GFR: Activin A increases before all other markers, Clin. Nephrol. 91 (2019) 222–230. doi:10.5414/CN109650.

[66] A.T. Kadiombo, A. Maeshima, K. Kayakabe, H. Ikeuchi, T. Sakairi, Y. Kaneko, K. Hiromura, Y. Nojima, Involvement of infiltrating macrophage-derived activin A in the progression of renal damage in MRL- *lpr* mice, Am. J. Physiol. Physiol. 312 (2017) F297–F304. doi:10.1152/ajprenal.00191.2016.

[67] K.S. Famulski, D. Kayser, G. Einecke, K. Allanach, D. Badr, J. Venner, B. Sis, P.F. Halloran, Alternative Macrophage Activation-Associated Transcripts in T-Cell-Mediated Rejection of Mouse Kidney Allografts, Am. J. Transplant. 10 (2010) 490–497. doi:10.1111/j.1600-6143.2009.02983.x.

[68] K.S. Famulski, B. Sis, L. Billesberger, P.F. Halloran, Interferon-γ and Donor MHC Class I Control Alternative Macrophage Activation and Activin Expression in Rejecting Kidney Allografts: A Shift in the Th1-Th2 Paradigm, Am. J. Transplant. 8 (2008) 547–556. doi:10.1111/j.1600-6143.2007.02118.x.

[69] K.L. Jones, A. Mansell, S. Patella, B.J. Scott, M.P. Hedger, D.M. de Kretser, D.J.

Phillips, Activin A is a critical component of the inflammatory response, and its binding protein, follistatin, reduces mortality in endotoxemia., Proc. Natl. Acad. Sci. U. S. A. 104 (2007) 16239–44. doi:10.1073/pnas.0705971104.

[70] N. Yamashita, T. Nakajima, H. Takahashi, H. Kaneoka, Y. Mizushima, T. Sakane, Effects of activin A on IgE synthesis and cytokine production by human peripheral mononuclear cells., Clin. Exp. Immunol. 94 (1993) 214–9. doi:10.1111/j.1365-2249.1993.tb06003.x.

[71] W. Wada, H. Kuwano, Y. Hasegawa, I. Kojima, The dependence of transforming growth factor-beta-induced collagen production on autocrine factor activin A in hepatic stellate cells., Endocrinology. 145 (2004) 2753–9. doi:10.1210/en.2003-1663.

[72] M.A. Borahay, A. Al-Hendy, G.S. Kilic, D. Boehning, Signaling Pathways in Leiomyoma: Understanding Pathobiology and Implications for Therapy, Mol. Med. 21 (2015) 242–256. doi:10.2119/molmed.2014.00053.

[73] F.S. Machado, N.E. Rodriguez, D. Adesse, L.R. Garzoni, M.P. Lisanti, R.D. Burk, C. Albanese, K. Van, L.M. Weiss, F. Nagajyothi, J.D. Nosanchuk, E. Mary, Caveolins and Caveolae, 729 (2012) 65–82. doi:10.1007/978-1-4614-1222-9.

[74] H.N. Fridolfsson, D.M. Roth, P.A. Insel, H.H. Patel, Regulation of intracellular signaling and function by caveolin, FASEB J. 28 (2014) 3823–3831. doi:10.1096/fj.14-252320.

[75] R. van Krieken, J.C. Krepinsky, Caveolin-1 in the Pathogenesis of Diabetic Nephropathy: Potential Therapeutic Target?, Curr. Diab. Rep. 17 (2017). doi:10.1007/s11892-017-0844-9.

[76] S. Chand, Caveolin-1 in renal disease, Sci. J. Genet. Gene Ther. 4 (2018) 7–14.

[77] T.H. Guan, G. Chen, B. Gao, M.R. Janssen, L. Uttarwar, a J. Ingram, J.C. Krepinsky, Caveolin-1 deficiency protects against mesangial matrix expansion in a mouse model of type 1 diabetic nephropathy., Diabetologia. 56 (2013) 2068–77. doi:10.1007/s00125-013-2968-z.

[78] B. Zhang, F. Peng, D. Wu, A.J. Ingram, B. Gao, J.C. Krepinsky, Caveolin-1 phosphorylation is required for stretch-induced EGFR and Akt activation in mesangial cells, Cell. Signal. 19 (2007) 1690–1700. doi:10.1016/j.cellsig.2007.03.005.

[79] F. Peng, B. Zhang, D. Wu, A.J. Ingram, B. Gao, J.C. Krepinsky, TGFbeta-induced RhoA activation and fibronectin production in mesangial cells require caveolae., Am. J. Physiol. Renal Physiol. 295 (2008) F153-64. doi:10.1152/ajprenal.00419.2007.

[80] T. Guan, B. Gao, G. Chen, X. Chen, M. Janssen, L. Uttarwar, A.J. Ingram, J.C. Krepinsky, Colchicine attenuates renal injury in a model of hypertensive chronic

kidney disease., Am. J. Physiol. Renal Physiol. 305 (2013) F1466-76. doi:10.1152/ajprenal.00057.2013.

[81] R.K. Sindhu, A. Ehdaie, N.D. Vaziri, C.K. Roberts, Effects of chronic renal failure on caveolin-1, guanylate cyclase and AKT protein expression., Biochim. Biophys. Acta. 1690 (2004) 231–7. doi:10.1016/j.bbadis.2004.06.013.

[82] T.B. Thompson, T.F. Lerch, R.W. Cook, T.K. Woodruff, T.S. Jardetzky, The structure of the follistatin:activin complex reveals antagonism of both type I and type II receptor binding., Dev. Cell. 9 (2005) 535–43. doi:10.1016/j.devcel.2005.09.008.

[83] A.B. Sanz, B. Santamaria, M. Ruiz-Ortega, J. Egido, A. Ortiz, Mechanisms of Renal Apoptosis in Health and Disease, J. Am. Soc. Nephrol. 19 (2008) 1634–1642. doi:10.1681/ASN.2007121336.

[84] J.C. Jha, C. Banal, B.S.M. Chow, M.E. Cooper, K. Jandeleit-Dahm, Diabetes and Kidney Disease: Role of Oxidative Stress, Antioxid. Redox Signal. 25 (2016) 657–684. doi:10.1089/ars.2016.6664.

[85] I. Burlaka, L.M. Nilsson, L. Scott, U. Holtbäck, A.C. Eklöf, A.B. Fogo, H. Brismar, A. Aperia, Prevention of apoptosis averts glomerular tubular disconnection and podocyte loss in proteinuric kidney disease, Kidney Int. 90 (2016) 135–148. doi:10.1016/j.kint.2016.03.026.

[86] J.G. Dickhout, J.C. Krepinsky, Endoplasmic reticulum stress and renal disease, Antioxid Redox Signal. 11 (2009) 2341–2352. doi:10.1089/ARS.2009.2705.

[87] V. Yum, R.E. Carlisle, C. Lu, E. Brimble, J. Chahal, C. Upagupta, K. Ask, J.G. Dickhout, Endoplasmic reticulum stress inhibition limits the progression of chronic kidney disease in the Dahl salt-sensitive rat, Am. J. Physiol. Physiol. 312 (2017) F230–F244. doi:10.1152/ajprenal.00119.2016.

[88] Z. Mohammed-Ali, C. Lu, M.K. Marway, R.E. Carlisle, K. Ask, D. Lukic, J.C. Krepinsky, J.G. Dickhout, Endoplasmic reticulum stress inhibition attenuates hypertensive chronic kidney disease through reduction in proteinuria, Sci. Rep. 7 (2017) 1–14. doi:10.1038/srep41572.

[89] H. Saleh, E. Schlatter, D. Lang, H.G. Pauels, S. Heidenreich, Regulation of mesangial cell apoptosis and proliferation by intracellular Ca(2+) signals., Kidney Int. 58 (2000) 1876–84. doi:10.1111/j.1523-1755.2000.00359.x.

[90] C. Wang, T. Li, S. Tang, D. Zhao, C. Zhang, S. Zhang, S. Deng, Y. Zhou, X. Xiao, Thapsigargin induces apoptosis when autophagy is inhibited in HepG2 cells and both processes are regulated by ROS-dependent pathway, Environ. Toxicol. Pharmacol. 41 (2016) 167–179. doi:10.1016/j.etap.2015.11.020.

[91] Z. Ma, C. Fan, Y. Yang, S. Di, W. Hu, T. Li, Y. Zhu, J. Han, Z. Xin, G. Wu, J. Zhao, X. Li, X. Yan, Thapsigargin sensitizes human esophageal cancer to TRAIL-

induced apoptosis via AMPK activation, Sci. Rep. 6 (2016) 35196. doi:10.1038/srep35196.

[92] L. Li, G. Hu, Pink1 protects cortical neurons from thapsigargin-induced oxidative stress and neuronal apoptosis., Biosci. Rep. 35 (2015) 1–8. doi:10.1042/BSR20140104.

[93] B.P.S. Kang, S. Frencher, V. Reddy, A. Kessler, A. Malhotra, L.G. Meggs, High glucose promotes mesangial cell apoptosis by oxidant-dependent mechanism, Am. J. Physiol. Physiol. 284 (2003) F455–F466. doi:10.1152/ajprenal.00137.2002.

[94] W. Chen, T.K. Woodruff, K.E. Mayo, Activin A-induced HepG2 liver cell apoptosis: Involvement of activin receptors and Smad proteins, Endocrinology. 141 (2000) 1263–1272. doi:10.1210/en.141.3.1263.

[95] H. Valderrama-Carvajal, E. Cocolakis, A. Lacerte, E.H. Lee, G. Krystal, S. Ali, J.J. Lebrun, Activin/TGF-β induce apoptosis through Smad-dependent expression of the lipid phosphatase SHIP, Nat. Cell Biol. 4 (2002) 963–969. doi:10.1038/ncb885.

[96] Y. Qi, J. Ge, C. Ma, N. Wu, X. Cui, Z. Liu, Activin A regulates activation of mouse neutrophils by Smad3 signalling, Open Biol. 7 (2017) 160342. doi:10.1098/rsob.160342.

[97] L. Zhang, K. Liu, B. Han, Z. Xu, X. Gao, The emerging role of follistatin under stresses and its implications in diseases, Gene. 639 (2018) 111–116. doi:10.1016/j.gene.2017.10.017.

[98] W. Filipowicz, S.N. Bhattacharyya, N. Sonenberg, Mechanisms of post-transcriptional regulation by microRNAs: are the answers in sight?, Nat. Rev. Genet. 9 (2008) 102–14. doi:10.1038/nrg2290.

[99] E. Matoulkova, E. Michalova, B. Vojtesek, R. Hrstka, The role of the 3' untranslated region in post-transcriptional regulation of protein expression in mammalian cells., RNA Biol. 9 (2012) 563–76. doi:10.4161/rna.20231.

[100] P. Trionfini, A. Benigni, G. Remuzzi, MicroRNAs in kidney physiology and disease, Nat. Rev. Nephrol. 11 (2015) 23–33. doi:10.1038/nrneph.2014.202.

[101] I.G. Gomez, N. Nakagawa, J.S. Duffield, MicroRNAs as novel therapeutic targets to treat kidney injury and fibrosis, Am. J. Physiol. - Ren. Physiol. (2016) ajprenal.00523.2015. doi:10.1152/ajprenal.00523.2015.

[102] A.C.K. Chung, H.Y. Lan, MicroRNAs in renal fibrosis, Front. Physiol. 6 (2015) 1–9. doi:10.3389/fphys.2015.00050.

[103] J.A. Broderick, P.D. Zamore, MicroRNA therapeutics., Gene Ther. 18 (2011) 1104–10. doi:10.1038/gt.2011.50.

[104] P. Trionfini, A. Benigni, MicroRNAs as Master Regulators of Glomerular Function

in Health and Disease, J. Am. Soc. Nephrol. 28 (2017) 1686–1696. doi:10.1681/ASN.2016101117.

[105] J. Milosevic, K. Pandit, M. Magister, E. Rabinovich, D.C. Ellwanger, G. Yu, L.J. Vuga, B. Weksler, P. V. Benos, K.F. Gibson, M. McMillan, M. Kahn, N. Kaminski, Profibrotic role of miR-154 in pulmonary fibrosis, Am. J. Respir. Cell Mol. Biol. 47 (2012) 879–887. doi:10.1165/rcmb.2011-0377OC.

[106] K.A. Padgett, R.Y. Lan, P.C. Leung, A. Lleo, K. Dawson, T.K. Mao, R.L. Coppel, A.A. Ansari, M.E. Gershwin, A. Manuscript, Primary Biliary Cirrhosis is Associated With Altered Hepatic microRNA Expression, Ambio. 32 (2010) 246–253. doi:10.1016/j.jaut.2009.02.022.Primary.

[107] F. Aoki, M. Kurabayashi, Y. Hasegawa, I. Kojima, Attenuation of bleomycin-induced pulmonary fibrosis by follistatin., Am. J. Respir. Crit. Care Med. 172 (2005) 713–20. doi:10.1164/rccm.200412-1620OC.

[108] C. Karagiannidis, G. Hense, C. Martin, M. Epstein, B. Rückert, P.-Y. Mantel, G. Menz, S. Uhlig, K. Blaser, C.B. Schmidt-Weber, Activin A is an acute allergen-responsive cytokine and provides a link to TGF-beta-mediated airway remodeling in asthma., J. Allergy Clin. Immunol. 117 (2006) 111–8. doi:10.1016/j.jaci.2005.09.017.

[109] S. Patella, D.J. Phillips, J. Tchongue, D.M. de Kretser, W. Sievert, Follistatin attenuates early liver fibrosis: effects on hepatic stellate cell activation and hepatocyte apoptosis., Am. J. Physiol. Gastrointest. Liver Physiol. 290 (2006) G137-44. doi:10.1152/ajpgi.00080.2005.

[110] A.L. Gava, F.P. Freitas, C.M. Balarini, E.C. Vasquez, S.S. Meyrelles, Effects of 5/6 nephrectomy on renal function and blood pressure in mice., Int. J. Physiol. Pathophysiol. Pharmacol. 4 (2012) 167–73. http://www.pubmedcentral.nih.gov/articlerender.fcgi?artid=3466491&tool=pmcentrez&rendertype=abstract (accessed April 18, 2016).

[111] A. Leelahavanichkul, Q. Yan, X. Hu, C. Eisner, Y. Huang, R. Chen, D. Mizel, H. Zhou, E.C. Wright, J.B. Kopp, J. Schnermann, P.S.T. Yuen, R.A. Star, Angiotensin II overcomes strain-dependent resistance of rapid CKD progression in a new remnant kidney mouse model., Kidney Int. 78 (2010) 1136–53. doi:10.1038/ki.2010.287.

[112] J. Floege, H.R. Radeke, R.J. Johnson, Glomerular cells in vitro versus the glomerulus in vivo., Kidney Int. 45 (1994) 360–368. doi:10.1038/ki.1994.46.

[113] R. Li, T. Wang, K. Walia, B. Gao, J.C. Krepinsky, Regulation of profibrotic responses by ADAM17 activation in high glucose requires its C-terminus and FAK, J. Cell Sci. 131 (2018) jcs208629. doi:10.1242/jcs.208629.

[114] P.R.O. Neill, V. Kalyanaraman, N. Gautam, S. Louis, Subcellular optogenetic

activation of Cdc42 controls local and distal signaling to drive immune cell migration, (2016) 1442–1450. doi:10.1091/mbc.E15-12-0832.

[115] L.W. Evans, S. Muttukrishna, N.P. Groome, Development, validation and application of an ultra-sensitive two-site enzyme immunoassay for human follistatin, J. Endocrinol. 156 (1998) 275–282. doi:10.1677/joe.0.1560275.

[116] S. Saito, Y. Sidis, A. Mukherjee, Y. Xia, A. Schneyer, Differential biosynthesis and intracellular transport of follistatin isoforms and follistatin-like-3., Endocrinology. 146 (2005) 5052–5062. doi:10.1210/en.2005-0833.

[117] K. Suginos, N. Kurosawas, T. Nakamuras, K. Takios, N. Lingll, K. Titanill, Molecular Heterogeneity of Follistatin, an Activin-binding Protein, J. Biol. Chem. 268 (1993) 15579–15587.

[118] D.M. de Kretser, M.P. Hedger, K.L. Loveland, D.J. Phillips, Inhibins, activins and follistatin in reproduction, Hum. Reprod. Update. 8 (2002) 529–541. doi:10.1093/humupd/8.6.529.

[119] E. De Groot, J. Veltmaat, A. Caricasole, L. Defize, A. Van Den Eijnden-van Raaij, Cloning and analysis of the mouse follistatin promoter, Mol. Biol. Rep. 27 (2000) 129–139. doi:10.1023/A:1007159031000.

[120] X. Messeguer, R. Escudero, D. Farré, O. Núñez, J. Martínez, M.M. Albà, PROMO: detection of known transcription regulatory elements using species-tailored searches., Bioinformatics. 18 (2002) 333–4. http://www.ncbi.nlm.nih.gov/pubmed/11847087 (accessed April 11, 2016).

[121] B.M. Necela, W. Su, E.A. Thompson, Peroxisome proliferator-activated receptor gamma down-regulates follistatin in intestinal epithelial cells through Sp1, J. Biol. Chem. 283 (2008) 29784–29794. doi:10.1074/jbc.M804481200.

[122] N.Y. Tan, L.M. Khachigian, Sp1 phosphorylation and its regulation of gene transcription., Mol. Cell. Biol. 29 (2009) 2483–2488. doi:10.1128/MCB.01828-08.

[123] Y. Zhang, M. Liao, M.L. Dufau, Phosphatidylinositol 3-kinase/protein kinase Czeta-induced phosphorylation of Sp1 and p107 repressor release have a critical role in histone deacetylase inhibitor-mediated derepression of transcription of the luteinizing hormone receptor gene., Mol. Cell. Biol. 26 (2006) 6748–6761. doi:10.1128/MCB.00560-06.

[124] E.H. Walker, M.E. Pacold, O. Perisic, L. Stephens, P.T. Hawkins, M.P. Wymann, R.L. Williams, Structural determinants of phosphoinositide 3-kinase inhibition by wortmannin, LY294002, quercetin, myricetin, and staurosporine., Mol. Cell. 6 (2000) 909–19. http://www.ncbi.nlm.nih.gov/pubmed/11090628 (accessed March 26, 2019).

[125] J.S.L. Yu, W. Cui, Proliferation, survival and metabolism: the role of PI3K/AKT/mTOR signalling in pluripotency and cell fate determination,

Development. 143 (2016) 3050–3060. doi:10.1242/dev.137075.

[126] M.M. Chou, W. Hou, J. Johnson, L.K. Graham, M.H. Lee, C.-S. Chen, A.C. Newton, B.S. Schaffhausen, A. Toker, Regulation of protein kinase C ζ by PI 3-kinase and PDK-1, Curr. Biol. 8 (1998) 1069–1078. doi:10.1016/S0960-9822(98)70444-0.

[127] T. Moriyama, Y. Tsuruta, A. Shimizu, M. Itabashi, T. Takei, S. Horita, K. Uchida, K. Nitta, The significance of caveolae in the glomeruli in glomerular disease., J. Clin. Pathol. 64 (2011) 504–9. doi:10.1136/jcp.2010.087023.

[128] O. Tamai, N. Oka, T. Kikuchi, Y. Koda, M. Soejima, Y. Wada, M. Fujisawa, K. Tamaki, H. Kawachi, F. Shimizu, H. Kimura, T. Imaizumi, S. Okuda, Caveolae in mesangial cells and caveolin expression in mesangial proliferative glomerulonephritis, Kidney Int. 59 (2001) 471–480. doi:10.1046/J.1523-1755.2001.059002471.X.

[129] R. Komers, W.E. Schutzer, J.F. Reed, J.N. Lindsley, T.T. Oyama, D.C. Buck, S.L. Mader, S. Anderson, Altered Endothelial Nitric Oxide Synthase Targeting and Conformation and Caveolin-1 Expression in the Diabetic Kidney, Diabetes. 55 (2006) 1651–1659. doi:10.2337/db05-1595.

[130] S. Kim, Y. Lee, J.E. Seo, K.H. Cho, J.H. Chung, Caveolin-1 increases basal and TGF-β1-induced expression of type I procollagen through PI-3 kinase/Akt/mTOR pathway in human dermal fibroblasts, Cell. Signal. 20 (2008) 1313–1319. doi:10.1016/j.cellsig.2008.02.020.

[131] X. Wang, L. Shi, Z. Han, B. Liu, Follistatin-like 3 suppresses cell proliferation and fibronectin expression via p38MAPK pathway in rat mesangial cells cultured under high glucose, Int. J. Clin. Exp. Med. 8 (2015) 15214–15221.

[132] Y. Sidis, D. V. Tortoriello, W.E. Holmes, Y. Pan, H.T. Keutmann, A.L. Schneyer, Follistatin-Related Protein and Follistatin Differentially Neutralize Endogenous *vs.* Exogenous Activin, Endocrinology. 143 (2002) 1613–1624. doi:10.1210/endo.143.5.8805.

[133] K. Tsuchida, K.Y. Arai, Y. Kuramoto, N. Yamakawa, Y. Hasegawa, H. Sugino, Identification and Characterization of a Novel Follistatin-like Protein as a Binding Protein for the TGF-β Family, J. Biol. Chem. 275 (2000) 40788–40796. doi:10.1074/jbc.M006114200.

[134] J. Willert, M. Epping, J.R. Pollack, P.O. Brown, R. Nusse, A transcriptional response to Wnt protein in human embryonic carcinoma cells., BMC Dev. Biol. 2 (2002) 8. http://www.ncbi.nlm.nih.gov/pubmed/12095419 (accessed November 29, 2018).

[135] R.R. Bartholin L, Maguer-Satta V, Hayette S, Martel S, Gadoux M, Corbo L, Magaud JP, Transcription activation of FLRG and follistatin by activin A, through

Smad proteins, participates in a negative feedback loop to modulate activin A function, Oncogene. 21 (2002) 2227–35. doi:10.1038/sj.onc.1205294.

[136] K. Miyanaga, S. Shimasaki, Structural and functional characterization of the rat follistatin (activin-binding protein) gene promoter., Mol. Cell. Endocrinol. 92 (1993) 99–109. http://www.ncbi.nlm.nih.gov/pubmed/8472873 (accessed November 29, 2018).

[137] J.Á.F. Vara, E. Casado, J. de Castro, P. Cejas, C. Belda-Iniesta, M. González-Barón, PI3K/Akt signalling pathway and cancer, Cancer Treat. Rev. 30 (2004) 193–204. doi:10.1016/j.ctrv.2003.07.007.

[138] D.A. Fruman, H. Chiu, B.D. Hopkins, S. Bagrodia, L.C. Cantley, R.T. Abraham, The PI3K Pathway in Human Disease., Cell. 170 (2017) 605–635. doi:10.1016/j.cell.2017.07.029.

[139] S. Shack, X.-T. Wang, G.C. Kokkonen, M. Gorospe, D.L. Longo, N.J. Holbrook, Caveolin-induced activation of the phosphatidylinositol 3-kinase/Akt pathway increases arsenite cytotoxicity., Mol. Cell. Biol. 23 (2003) 2407–14. http://www.ncbi.nlm.nih.gov/pubmed/12640124 (accessed December 21, 2018).

[140] W. Zundel, L.M. Swiersz, A. Giaccia, Caveolin 1-mediated regulation of receptor tyrosine kinase-associated phosphatidylinositol 3-kinase activity by ceramide., Mol. Cell. Biol. 20 (2000) 1507–14. http://www.ncbi.nlm.nih.gov/pubmed/10669728 (accessed December 21, 2018).

[141] Y. Zhan, L. Wang, J. Liu, K. Ma, C. Liu, Y. Zhang, W. Zou, Choline Plasmalogens Isolated from Swine Liver Inhibit Hepatoma Cell Proliferation Associated with Caveolin-1/Akt Signaling, PLoS One. 8 (2013). doi:10.1371/journal.pone.0077387.

[142] N. Chalhoub, S.J. Baker, PTEN and the PI3-kinase pathway in cancer., Annu. Rev. Pathol. 4 (2009) 127–50. doi:10.1146/annurev.pathol.4.110807.092311.

[143] H. Xia, W. Khalil, J. Kahm, J. Jessurun, J. Kleidon, C.A. Henke, Pathologic Caveolin-1 Regulation of PTEN in Idiopathic Pulmonary Fibrosis, Am. J. Pathol. 176 (2010) 2626–2637. doi:10.2353/ajpath.2010.091117.

[144] N.Y. Tan, V.C. Midgley, M.M. Kavurma, F.S. Santiago, X. Luo, R. Peden, R.G. Fahmy, M.C. Berndt, M.P. Molloy, L.M. Khachigian, Angiotensin II–Inducible Platelet-Derived Growth Factor-D Transcription Requires Specific Ser/Thr Residues in the Second Zinc Finger Region of Sp1, Circ. Res. 102 (2008) e38-51. doi:10.1161/CIRCRESAHA.107.167395.

[145] S. Pal, K.P. Claffey, H.T. Cohen, D. Mukhopadhyay, Activation of Sp1-mediated vascular permeability factor/vascular endothelial growth factor transcription requires specific interaction with protein kinase C zeta., J. Biol. Chem. 273 (1998) 26277–80. doi:10.1074/JBC.273.41.26277.

[146] T. Hirai, K. Chida, Protein kinase Cζ (PKCζ): Activation mechanisms and cellular

functions, J. Biochem. 133 (2003) 1–7. doi:10.1093/jb/mvg017.

[147] M.L. Standaert, G. Bandyopadhyay, Y. Kanoh, M.P. Sajan, R. V Farese, Insulin and PIP3 activate PKC-zeta by mechanisms that are both dependent and independent of phosphorylation of activation loop (T410) and autophosphorylation (T560) sites., Biochemistry. 40 (2001) 249–55. http://www.ncbi.nlm.nih.gov/pubmed/11141077 (accessed July 31, 2018).

[148] N. Oka, M. Yamamoto, C. Schwencke, J.I. Kawabe, T. Ebina, S. Ohno, J. Couet, M.P. Lisanti, Y. Ishikawa, Caveolin interaction with protein kinase C. Isoenzyme-dependent regulation of kinase activity by the caveolin scaffolding domain peptide, J. Biol. Chem. 272 (1997) 33416–33421. doi:10.1074/jbc.272.52.33416.

[149] J. Couet, S. Li, T. Okamoto, T. Ikezu, M.P. Lisanti, Identification of peptide and protein ligands for the caveolin-scaffolding domain. Implications for the interaction of caveolin with caveolae-associated proteins., J. Biol. Chem. 272 (1997) 6525–33. doi:10.1074/JBC.272.10.6525.

[150] J. Chun, T. Kwon, E.J. Lee, S. Hyun, S.-K. Hong, S.S. Kang, The subcellular localization of 3-phosphoinositide-dependent protein kinase is controlled by caveolin-1 binding, Biochem. Biophys. Res. Commun. 326 (2004) 136–146. doi:10.1016/j.bbrc.2004.10.208.

[151] T.E. Fox, K.L. Houck, S.M. O'Neill, M. Nagarajan, T.C. Stover, P.T. Pomianowski, O. Unal, J.K. Yun, S.J. Naides, M. Kester, Ceramide recruits and activates protein kinase C ζ (PKCζ) within structured membrane microdomains, J. Biol. Chem. 282 (2007) 12450–12457. doi:10.1074/jbc.M700082200.

[152] W.-C. Huang, Y.-S. Lin, C.-Y. Wang, C.-C. Tsai, H.-C. Tseng, C.-L. Chen, P.-J. Lu, P.-S. Chen, L. Qian, J.-S. Hong, C.-F. Lin, Glycogen synthase kinase-3 negatively regulates anti-inflammatory interleukin-10 for lipopolysaccharide-induced iNOS/NO biosynthesis and RANTES production in microglial cells., Immunology. 128 (2009) e275-86. doi:10.1111/j.1365-2567.2008.02959.x.

[153] J.-S. Kim, Z.-Y. Park, Y.-J. Yoo, S.-S. Yu, J.-S. Chun, p38 kinase mediates nitric oxide-induced apoptosis of chondrocytes through the inhibition of protein kinase C ζ by blocking autophosphorylation, Cell Death Differ. 12 (2005) 201–212. doi:10.1038/sj.cdd.4401511.

[154] J. Wu, S. Zhao, Q. Tang, F. Zheng, Y. Chen, L. Yang, X. Yang, L. Li, W. Wu, S.S. Hann, Activation of SAPK/JNK mediated the inhibition and reciprocal interaction of DNA methyltransferase 1 and EZH2 by ursolic acid in human lung cancer cells, J. Exp. Clin. Cancer Res. 34 (2015) 99. doi:10.1186/s13046-015-0215-9.

[155] S. Chu, T.J. Ferro, Identification of a hydrogen peroxide-induced PP1-JNK1-Sp1 signaling pathway for gene regulation, Am. J. Physiol. Cell. Mol. Physiol. 291 (2006) L983–L992. doi:10.1152/ajplung.00454.2005.

[156] H. Xiao, X.-H. Bai, Y. Wang, H. Kim, A.S. Mak, M. Liu, MEK/ERK pathway mediates PKC activation-induced recruitment of PKCζ and MMP-9 to podosomes, J. Cell. Physiol. 228 (2013) 416–427. doi:10.1002/jcp.24146.

[157] M. Motojima, T. Ando, T. Yoshioka, Sp1-like activity mediates angiotensin-II-induced plasminogen-activator inhibitor type-1 (PAI-1) gene expression in mesangial cells., Biochem. J. 349 (2000) 435–41. http://www.ncbi.nlm.nih.gov/pubmed/10880342 (accessed December 21, 2018).

[158] R. Kikkawa, M. Haneda, T. Uzu, D. Koya, T. Sugimoto, Y. Shigeta, Translocation of protein kinase C alpha and zeta in rat glomerular mesangial cells cultured under high glucose conditions., Diabetologia. 37 (1994) 838–41. http://www.ncbi.nlm.nih.gov/pubmed/7988787 (accessed December 21, 2018).

[159] L. Xia, H. Wang, S. Munk, J. Kwan, H.J. Goldberg, I.G. Fantus, C.I. Whiteside, High glucose activates PKC-ζ and NADPH oxidase through autocrine TGF-β_1 signaling in mesangial cells, Am. J. Physiol. Physiol. 295 (2008) F1705–F1714. doi:10.1152/ajprenal.00043.2008.

[160] H. Chen, Y. Zhou, K.Q. Chen, G. An, S.Y. Ji, Q.K. Chen, Anti-fibrotic Effects via Regulation of Transcription Factor Sp1 on Hepatic Stellate Cells, Cell. Physiol. Biochem. 29 (2012) 51–60. doi:10.1159/000337586.

[161] Y.-S. Kum, K.-H. Kim, T.-I. Park, I.-S. Suh, H.-K. Oh, C.-H. Cho, J.-B. Park, Y.-C. Chang, J.-H. Park, K.-G. Lee, K.-K. Park, Antifibrotic effect via the regulation of transcription factor Sp1 in lung fibrosis, Biochem. Biophys. Res. Commun. 363 (2007) 368–374. doi:10.1016/J.BBRC.2007.08.176.

[162] J.H. Kang, Y.-M. Chae, K.-K. Park, C.-H. Kim, I.-S. Lee, Y.-C. Chang, Suppression of mesangial cell proliferation and extracellular matrix production in streptozotocin-induced diabetic rats by Sp1 decoy oligodeoxynucleotide in vitro and in vivo, J. Cell. Biochem. 103 (2008) 663–674. doi:10.1002/jcb.21440.

[163] A.C. Poncelet, H.W. Schnaper, Sp1 and Smad proteins cooperate to mediate transforming growth factor-beta 1-induced alpha 2(I) collagen expression in human glomerular mesangial cells., J. Biol. Chem. 276 (2001) 6983–92. doi:10.1074/jbc.M006442200.

[164] Y.-M. Chae, K.-K. Park, I.-K. Lee, J.-K. Kim, C.-H. Kim, Y.-C. Chang, Ring-Sp1 decoy oligonucleotide effectively suppresses extracellular matrix gene expression and fibrosis of rat kidney induced by unilateral ureteral obstruction, Gene Ther. 13 (2006) 430–439. doi:10.1038/sj.gt.3302696.

[165] G. Brodin, A. Åhgren, P. ten Dijke, C.-H. Heldin, R. Heuchel, Efficient TGF-β Induction of the Smad7 Gene Requires Cooperation between AP-1, Sp1, and Smad Proteins on the Mouse Smad7 Promoter, J. Biol. Chem. 275 (2000) 29023–29030. doi:10.1074/jbc.M002815200.

[166] W. Dröge, Free Radicals in the Physiological Control of Cell Function, Physiol. Rev. 82 (2002) 47–95. doi:10.1152/physrev.00018.2001.

[167] V.J. Thannickal, B.L. Fanburg, Reactive oxygen species in cell signaling, Am. J. Physiol. Cell. Mol. Physiol. 279 (2000) L1005–L1028. doi:10.1152/ajplung.2000.279.6.L1005.

[168] H. Sies, Oxidative stress: From basic research to clinical application, Am. J. Med. 91 (1991) S31–S38. doi:10.1016/0002-9343(91)90281-2.

[169] H. Nasri, Antioxidant therapy to ameliorate chronic kidney disease induced by oxidative stress ; an updated mini-review, J. Prev. Epidemiol. 2 (2017) 22–25.

[170] J. Lyttonsg, M. Westlins, M.R. Hanleyll, Thapsigargin Inhibits the Sarcoplasmic or Endoplasmic Reticulum Ca-ATPase Family of Calcium Pumps, J. Biol. Chem. 266 (1991) 17067–17071. http://www.jbc.org/content/266/26/17067.full.pdf (accessed September 18, 2018).

[171] X. Gao, S. Wei, K. Lai, J. Sheng, J. Su, J. Zhu, H. Dong, H. Hu, Z. Xu, Nucleolar follistatin promotes cancer cell survival under glucose-deprived conditions through inhibiting cellular rRNA synthesis, J. Biol. Chem. 285 (2010) 36857–36864. doi:10.1074/jbc.M110.144477.

[172] Z. Chong, P. Dong, H. Riaz, L. Shi, X. Yu, Y. Cheng, L. Yang, Disruption of follistatin by RNAi increases apoptosis, arrests S-phase of cell cycle and decreases estradiol production in bovine granulosa cells, Anim. Reprod. Sci. 155 (2015) 80–88. doi:10.1016/j.anireprosci.2015.02.003.

[173] C.M. Oslowski, F. Urano, Measuring ER stress and the unfolded protein response using mammalian tissue culture system, Methods Enzymol. 490 (2013) 71–92. doi:10.1016/B978-0-12-385114-7.00004-0.Measuring.

[174] Y.A.. & S.F.. Simon H.U, Role of reactive oxygen species (ROS) in apoptosis induction, Apoptosis. 5 (2000) 415–418.

[175] Y. Zhang, J. Liu, X.Y. Tian, W.T. Wong, Y. Chen, L. Wang, J. Luo, W.S. Cheang, C.W. Lau, K.M. Kwan, N. Wang, X. Yao, Y. Huang, Inhibition of bone morphogenic protein 4 restores endothelial function in db/db diabetic mice, Arterioscler. Thromb. Vasc. Biol. 34 (2014) 152–159. doi:10.1161/ATVBAHA.113.302696.

[176] C. Lin, X. Zhao, D. Sun, L. Zhang, W. Fang, T. Zhu, Q. Wang, B. Liu, S. Wei, G. Chen, Z. Xu, X. Gao, Transcriptional activation of follistatin by Nrf2 protects pulmonary epithelial cells against silica nanoparticle-induced oxidative stress., Sci. Rep. 6 (2016) 21133. doi:10.1038/srep21133.

[177] S. Haridoss, M.I. Yovchev, H. Schweizer, S. Megherhi, M. Beecher, J. Locker, M. Oertel, Activin A is a prominent autocrine regulator of hepatocyte growth arrest, Hepatol. Commun. 1 (2017) 852–870. doi:10.1002/hep4.1106.

[178] M. Liu, C. Mao, J. Li, F. Han, P. Yang, Effects of the Activin A–Follistatin System on Myocardial Cell Apoptosis through the Endoplasmic Reticulum Stress Pathway in Heart Failure, Int. J. Mol. Sci. 18 (2017) 374. doi:10.3390/ijms18020374.

[179] L.M. Coutinho, E.L. Vieira, C. Dela Cruz, M. Casalechi, A.L. Teixeira, H.L. Del Puerto, F.M. Reis, Apoptosis modulation by activin A and follistatin in human endometrial stromal cells., Gynecol. Endocrinol. 32 (2016) 161–5. doi:10.3109/09513590.2015.1103222.

[180] L. Allen, D.H. Dockrell, T. Pattery, D.G. Lee, P. Cornelis, P.G. Hellewell, M.K.B. Whyte, Pyocyanin Production by Pseudomonas aeruginosa Induces Neutrophil Apoptosis and Impairs Neutrophil-Mediated Host Defenses In Vivo, J. Immunol. 174 (2005) 3643–3649. doi:10.4049/jimmunol.174.6.3643.

[181] Y. Wang, R. Branicky, A. Noë, S. Hekimi, Superoxide dismutases: Dual roles in controlling ROS damage and regulating ROS signaling, J. Cell Biol. 217 (2018) 1915–1928. doi:10.1083/jcb.201708007.

[182] O. Hashimoto, T. Nakamura, H. Shoji, S. Shimasaki, Y. Hayashi, H. Sugino, O. Hashimoto, T. Nakamura, H. Shoji, S. Shimasaki, Y. Hayashi, H. Sugino, A novel role of follistatin, an activin-binding protein, in the inhibition of activin action in rat pituitary cells: Endocytotic degradation of activin and its acceleration by Follistatin associated with cell-surface heparan sulfate, J. Biol. Chem. 272 (1997) 13835–13842. doi:10.1074/jbc.272.21.13835.

[183] Y. Gorin, K. Block, J. Hernandez, B. Bhandari, B. Wagner, J.L. Barnes, H.E. Abboud, Nox4 NAD(P)H Oxidase Mediates Hypertrophy and Fibronectin Expression in the Diabetic Kidney, 280 (2005) 39616–39626. doi:10.1074/jbc.M502412200.

[184] K.T. Kuroda J, Ago T, Nishimura A, Nakamura K, Matsuo R, Wakisaka Y, Kamouchi M, Nox4 Is a Major Source of Superoxide Production in Human Brain Pericytes, 8582 (2015) 429–438. doi:10.1159/000369930.

[185] N.Y. Hakami, H. Wong, M.H. Shah, G.J. Dusting, F. Jiang, H.M. Peshavariya, Smad-independent pathway involved in transforming growth factor β1-induced Nox4 expression and proliferation of endothelial cells, Naunyn. Schmiedebergs. Arch. Pharmacol. 388 (2015) 319–326. doi:10.1007/s00210-014-1070-5.

[186] Y. Liu, Y. Wang, W. Ding, Y. Wang, Mito-TEMPO Alleviates Renal Fibrosis by Reducing Inflammation , Mitochondrial Dysfunction , and Endoplasmic Reticulum Stress, Oxid. Med. Cell. Longev. Article ID (2018) 1–13. doi:10.1155/2018/5828120.

[187] K. Richter, T. Kietzmann, Reactive oxygen species and fibrosis: further evidence of a significant liaison, Cell Tissue Res. 365 (2016) 591–605. doi:10.1007/s00441-016-2445-3.

[188] S. Ruiz, P.E. Pergola, R.A. Zager, N.D. Vaziri, Targeting the transcription factor Nrf2 to ameliorate oxidative stress and inflammation in chronic kidney disease, Kidney Int. 83 (2013) 1029–1041. doi:10.1038/ki.2012.439.

[189] N. Sahni, K.L. Gupta, Dietary antioxidents and oxidative stress in predialysis chronic kidney disease patients, J. Nephropathol. 1 (2012) 134–142. doi:10.5812/nephropathol.8108.

[190] H. Makino, H. Sugiyama, N. Kashihara, Apoptosis and extracellular matrix–cell interactions in kidney disease, Kidney Int. 58 (2000) S67–S75. doi:10.1046/J.1523-1755.2000.07711.X.

[191] X. Gao, H. Dong, C. Lin, J. Sheng, F. Zhang, J. Su, Z. Xu, Reduction of AUF1-mediated follistatin mRNA decay during glucose starvation protects cells from apoptosis, Nucleic Acids Res. 42 (2014) 10720–10730. doi:10.1093/nar/gku778.

[192] R.V.M. Manalo, P.M.B. Medina, The endoplasmic reticulum stress response in disease pathogenesis and pathophysiology, Egypt. J. Med. Hum. Genet. 19 (2018) 77–81. doi:10.1016/j.ejmhg.2017.07.004.

[193] S. Sriram, S. Subramanian, D. Sathiakumar, R. Venkatesh, M.S. Salerno, C.D. Mcfarlane, R. Kambadur, M. Sharma, Modulation of reactive oxygen species in skeletal muscle by myostatin is mediated through NF-κB, Aging Cell. 10 (2011) 931–948. doi:10.1111/j.1474-9726.2011.00734.x.

[194] J.R. Hully, L. Chang, R.H. Schwall, H.R. Widmer, T.G. Terrell, N.A. Gillett, Induction of apoptosis in the murine liver with recombinant human activin A., Hepatology. 20 (1994) 854–62. http://www.ncbi.nlm.nih.gov/pubmed/7927226 (accessed August 16, 2018).

[195] R.H. Schwall, K. Robbins, P. Jardieu, L. Chang, C. Lai, T.G. Terrell, Activin induces cell death in hepatocytes in vivo and in vitro., Hepatology. 18 (1993) 347–56. http://www.ncbi.nlm.nih.gov/pubmed/8340063 (accessed August 16, 2018).

[196] Y. Zhang, Y. Qi, Y. Zhao, H. Sun, J. Ge, Z. Liu, Activin A induces apoptosis of mouse myeloma cells via the mitochondrial pathway, Oncol. Lett. 15 (2017) 2590–2594. doi:10.3892/ol.2017.7584.

[197] T. Nishihara, N. Okahashi, N. Ueda, Activin A induces apoptotic cell death, Biochem Biophys Res Commun. 197 (1993) 985–991. doi:10.1006/bbrc.1993.2576.

[198] M. Jiang, W.Y. Ku, Z. Zhou, E.S. Dellon, G.W. Falk, H. Nakagawa, M.L. Wang, K. Liu, J. Wang, D.A. Katzka, J.H. Peters, X. Lan, J. Que, BMP-driven NRF2 activation in esophageal basal cell differentiation and eosinophilic esophagitis, J. Clin. Invest. 125 (2015) 1557–1568. doi:10.1172/JCI78850.

[199] R. Lim, R. Acharya, P. Delpachitra, S. Hobson, C.G. Sobey, G.R. Drummond, E.M. Wallace, Activin and NADPH-oxidase in preeclampsia: insights from in vitro

and murine studies, Am. J. Obstet. Gynecol. 212 (2015) 86.e1-86.e12. doi:10.1016/j.ajog.2014.07.021.

[200] W. Lv, G.W. Booz, F. Fan, Y. Wang, R.J. Roman, Oxidative stress and renal fibrosis: Recent insights for the development of novel therapeutic strategies, Front. Physiol. 9 (2018) 1–11. doi:10.3389/fphys.2018.00105.

[201] Q. Yang, F. Wu, J. Wang, L. Gao, L. Jiang, H.-D. Li, Q. Ma, X. Liu, B. Wei, L. Zhou, J. Wen, T. tao Ma, J. Li, X. Meng, Nox4 in renal diseases: An update, Free Radic. Biol. Med. 124 (2018) 466–472. doi:10.1016/J.FREERADBIOMED.2018.06.042.

[202] C.D. Bondi, N. Manickam, D.Y. Lee, K. Block, Y. Gorin, H.E. Abboud, J.L. Barnes, NAD(P)H Oxidase Mediates TGF-beta 1-Induced Activation of Kidney Myofibroblasts, J. Am. Soc. Nephrol. 21 (2010) 93–102. doi:10.1681/ASN.2009020146.

[203] R.J. Tan, D. Zhou, L. Xiao, L. Zhou, Y. Li, S.I. Bastacky, T.D. Oury, Y. Liu, Extracellular Superoxide Dismutase Protects against Proteinuric Kidney Disease., J. Am. Soc. Nephrol. 26 (2015) 2447–59. doi:10.1681/ASN.2014060613.

[204] R.L. Levine, L. Mosoni, B.S. Berlett, E.R. Stadtman, Methionine residues as endogenous antioxidants in proteins., Proc. Natl. Acad. Sci. U. S. A. 93 (1996) 15036–40. http://www.ncbi.nlm.nih.gov/pubmed/8986759 (accessed August 1, 2018).

[205] S. Luo, R.L. Levine, Methionine in proteins defends against oxidative stress., FASEB J. 23 (2009) 464–72. doi:10.1096/fj.08-118414.

[206] M. Roche, P. Rondeau, N.R. Singh, E. Tarnus, E. Bourdon, The antioxidant properties of serum albumin, FEBS Lett. 582 (2008) 1783–1787. doi:10.1016/j.febslet.2008.04.057.

[207] Y. Sidis, A.L. Schneyer, P.M. Sluss, L.N. Johnson, H.T. Keutmann, Follistatin: Essential Role for the N-terminal Domain in Activin Binding and Neutralization, J. Biol. Chem. 276 (2001) 17718–17726. doi:10.1074/jbc.M100736200.

[208] Q. Wang, H.T. Keutmann, A.L. Schneyer, P.M. Sluss, Analysis of Human Follistatin Structure: Identification of Two Discontinuous N-Terminal Sequences Coding for Activin A Binding and Structural Consequences of Activin Binding to Native Proteins, Endocrinology. 141 (2000) 3183–3193. doi:10.1210/endo.141.9.7675.

[209] B.Y. Jeong, H.Y. Lee, C.G. Park, J. Kang, S.L. Yu, D.R. Choi, S.Y. Han, M.H. Park, S. Cho, S.Y. Lee, W.M. Hwang, S.R. Yun, H.M. Ryu, E.J. Oh, S.H. Park, Y.L. Kim, S.H. Yoon, Oxidative stress caused by activation of NADPH oxidase 4 promotes contrast-induced acute kidney injury, PLoS One. 13 (2018) e0191034. doi:10.1371/journal.pone.0191034 [doi].

[210] A.K. Salahudeen, E.C. Clark, K.A. Nath, Hydrogen peroxide-induced renal injury. A protective role for pyruvate in vitro and in vivo., J. Clin. Invest. 88 (1991) 1886–1893. doi:10.1172/JCI115511.

[211] M.C. Iglesias-de la Cruz, P. Ruiz-Torres, J. Alcamí, L. Díez-Marqués, R. Ortega-Velázquez, S. Chen, M. Rodríguez-Puyol, F.N. Ziyadeh, D. Rodríguez-Puyol, Hydrogen peroxide increases extracellular matrix mRNA through TGF-β in human mesangial cells, Kidney Int. 59 (2001) 87–95. doi:10.1046/j.1523-1755.2001.00469.x.

[212] Z.L. Li, Y. Shi, G. Le, Y. Ding, Q. Zhao, 24-Week Exposure to Oxidized Tyrosine Induces Hepatic Fibrosis Involving Activation of the MAPK/TGF-β1 Signaling Pathway in Sprague-Dawley Rats Model, Oxid. Med. Cell. Longev. 2016 (2016) 1–12. doi:10.1155/2016/3123294.

[213] X. Bai, X. Li, J. Tian, L. Xu, J. Wan, Y. Liu, A new model of diabetic nephropathy in C57BL/6 mice challenged with advanced oxidation protein products, Free Radic. Biol. Med. 118 (2018) 71–84. doi:10.1016/J.FREERADBIOMED.2018.02.020.

[214] N. Mehta, D. Zhang, R. Li, T. Wang, A. Gava, P. Parthasarathy, B. Gao, J.C. Krepinsky, Caveolin-1 regulation of Sp1 controls production of the antifibrotic protein follistatin in kidney mesangial cells, Cell Commun. Signal. 17 (2019) 37. doi:10.1186/s12964-019-0351-5.

[215] S. Kreth, M. Hübner, L.C. Hinske, MicroRNAs as clinical biomarkers and therapeutic tools in perioperative medicine, Anesth. Analg. 126 (2018) 670–681. doi:10.1213/ANE.0000000000002444.

[216] C. Chakraborty, A.R. Sharma, G. Sharma, C.G.P. Doss, S.-S. Lee, Therapeutic miRNA and siRNA: Moving from Bench to Clinic as Next Generation Medicine., Mol. Ther. Nucleic Acids. 8 (2017) 132–143. doi:10.1016/j.omtn.2017.06.005.

[217] A.J. Kriegel, M. Liang, MicroRNA In situ Hybridization for Formalin Fixed Kidney Tissues, J Vis Exp. 30 (2013) 1–6. doi:10.3791/50785.

[218] F. Mignone, C. Gissi, S. Liuni, G. Pesole, Untranslated regions of mRNAs., Genome Biol. 3 (2002) REVIEWS0004. http://www.pubmedcentral.nih.gov/articlerender.fcgi?artid=139023&tool=pmcentrez&rendertype=abstract (accessed March 5, 2016).

[219] L. Chen, T. Yang, D.-W. Lu, H. Zhao, Y.-L. Feng, H. Chen, D.-Q. Chen, N.D. Vaziri, Y.-Y. Zhao, Central role of dysregulation of TGF-β/Smad in CKD progression and potential targets of its treatment, Biomed. Pharmacother. 101 (2018) 670–681. doi:10.1016/j.biopha.2018.02.090.

[220] I. Loeffler, G. Wolf, Transforming growth factor-β and the progression of renal disease, Nephrol. Dial. Transplant. 29 (2014) i37–i45. doi:10.1093/ndt/gft267.

[221] Y. Zhang, C. Liu, J. Wang, Q. Li, H. Ping, S. Gao, P. Wang, MiR-299-5p regulates

apoptosis through autophagy in neurons and ameliorates cognitive capacity in APPswe/PS1dE9 mice., Sci. Rep. 6 (2016) 24566. doi:10.1038/srep24566.

[222] A. Formosa, E.K. Markert, A.M. Lena, D. Italiano, E. Finazzi-Agro', A.J. Levine, S. Bernardini, A. V Garabadgiu, G. Melino, E. Candi, MicroRNAs, miR-154, miR-299-5p, miR-376a, miR-376c, miR-377, miR-381, miR-487b, miR-485-3p, miR-495 and miR-654-3p, mapped to the 14q32.31 locus, regulate proliferation, apoptosis, migration and invasion in metastatic prostate cancer cells, Oncogene. 33 (2014) 5173–5182. doi:10.1038/onc.2013.451.

[223] B.C. Bernardo, S.S. Nguyen, X.M. Gao, Y.K. Tham, J.Y.Y. Ooi, N.L. Patterson, H. Kiriazis, Y. Su, C.J. Thomas, R.C.Y. Lin, X.J. Du, J.R. McMullen, Inhibition of miR-154 Protects Against Cardiac Dysfunction and Fibrosis in a Mouse Model of Pressure Overload, Sci. Rep. 6 (2016) 1–12. doi:10.1038/srep22442.

[224] N. Mehta, A.L. Gava, D. Zhang, B. Gao, J. Krepinsky, Follistatin Protects against Glomerular Mesangial Cell Apoptosis and Oxidative Stress to Ameliorate Chronic Kidney Disease, Antioxid. Redox Signal. (2019) ars.2018.7684. doi:10.1089/ars.2018.7684.

[225] M. Fazzini, G. Vallejo, A. Colman-Lerner, R. Trigo, S. Campo, J.L.S. Barañao, P.E. Saragüeta, Transforming growth factor beta1 regulates follistatin mRNA expression during in vitro bovine granulosa cell differentiation., J. Cell. Physiol. 207 (2006) 40–8. doi:10.1002/jcp.20533.

[226] F. Peng, D. Wu, A.J. Ingram, B. Zhang, B. Gao, J.C. Krepinsky, RhoA activation in mesangial cells by mechanical strain depends on caveolae and caveolin-1 interaction., J. Am. Soc. Nephrol. 18 (2007) 189–198. doi:10.1681/ASN.2006050498.

[227] Y. Zhang, F. Peng, B. Gao, A.J. Ingram, J.C. Krepinsky, High glucose-induced RhoA activation requires caveolae and PKC 1-mediated ROS generation, AJP Ren. Physiol. 302 (2012) F159–F172. doi:10.1152/ajprenal.00749.2010.

[228] P. Shivshankar, C. Brampton, S. Miyasato, M. Kasper, V.J. Thannickal, C.J. Le Saux, Caveolin-1 deficiency protects from pulmonary fibrosis by modulating epithelial cell senescence in mice., Am. J. Respir. Cell Mol. Biol. 47 (2012) 28–36. doi:10.1165/rcmb.2011-0349OC.

[229] X.M. Wang, Y. Zhang, H.P. Kim, Z. Zhou, C.A. Feghali-Bostwick, F. Liu, E. Ifedigbo, X. Xu, T.D. Oury, N. Kaminski, A.M.K. Choi, Caveolin-1: a critical regulator of lung fibrosis in idiopathic pulmonary fibrosis., J. Exp. Med. 203 (2006) 2895–906. doi:10.1084/jem.20061536.

[230] S. Lee, E.G. Lynn, J.-A. Kim, M.J. Quon, Protein kinase C-zeta phosphorylates insulin receptor substrate-1, -3, and -4 but not -2: isoform specific determinants of specificity in insulin signaling., Endocrinology. 149 (2008) 2451–8. doi:10.1210/en.2007-1595.

[231] T.A. Yap, M.D. Garrett, M.I. Walton, F. Raynaud, J.S. de Bono, P. Workman, Targeting the PI3K–AKT–mTOR pathway: progress, pitfalls, and promises, Curr. Opin. Pharmacol. 8 (2008) 393–412. doi:10.1016/J.COPH.2008.08.004.

[232] W.A. Shihata, M.R.A. Putra, J.P.F. Chin-Dusting, Is There a Potential Therapeutic Role for Caveolin-1 in Fibrosis?, Front. Pharmacol. 8 (2017) 567. doi:10.3389/fphar.2017.00567.

[233] L.Y. Sun, Z.D. Bie, C.H. Zhang, H. Li, L.D. Li, J. Yang, MiR-154 directly suppresses DKK2 to activate Wnt signaling pathway and enhance activation of cardiac fibroblasts, Cell Biol. Int. 40 (2016) 1271–1279. doi:10.1002/cbin.10655.

[234] R.J. Tan, D. Zhou, L. Zhou, Y. Liu, Wnt/β-catenin signaling and kidney fibrosis., Kidney Int. Suppl. 4 (2014) 84–90. doi:10.1038/kisup.2014.16.

[235] P.C. Gray, G. Shani, K. Aung, J. Kelber, W. Vale, Cripto Binds Transforming Growth Factor beta (TGF-β) and Inhibits TGFβ Signaling, Mol. Cell. Biol. 28 (2008) 7260–7260. doi:10.1128/mcb.01609-08.

[236] M. Yanagita, Inhibitors/antagonists of TGF-β system in kidney fibrosis., Nephrol. Dial. Transplant. 27 (2012) 3686–91. doi:10.1093/ndt/gfs381.

[237] S. Yamashita, Activin A Is a Potent Activator of Renal Interstitial Fibroblasts, J. Am. Soc. Nephrol. 15 (2004) 91–101. doi:10.1097/01.ASN.0000103225.68136.E6.

[238] S. DE Lin, T. KAWAKAMI, A. Ushio, A. SATO, S.-I.I. SATO, M. IWAI, R. Endo, Y. TAKIKAWA, K. Suzuki, Ratio of circulating follistatin and activin A reflects the severity of acute liver injury and prognosis in patients with acute liver failure, 21 (2006) 374–380. doi:10.1111/j.1440-1746.2005.04036.x.

[239] C.L. Hardy, S.J. King, N.A. Mifsud, M.P. Hedger, D.J. Phillips, F. Mackay, D.M. de Kretser, J.W. Wilson, J.M. Rolland, R.E. O'Hehir, The activin A antagonist follistatin inhibits cystic fibrosis-like lung inflammation and pathology, Immunol. Cell Biol. 93 (2015) 567–574. doi:10.1038/icb.2015.7.

[240] N. Ohnishi, T. Miyata, H. Ohnishi, H. Yasuda, K. Tamada, N. Ueda, H. Mashima, K. Sugano, Activin A is an autocrine activator of rat pancreatic stellate cells: potential therapeutic role of follistatin for pancreatic fibrosis., Gut. 52 (2003) 1487–93. http://www.pubmedcentral.nih.gov/articlerender.fcgi?artid=1773818&tool=pmcentrez&rendertype=abstract (accessed April 14, 2016).

[241] R.N.V.S. Suragani, S.M. Cadena, S.M. Cawley, D. Sako, D. Mitchell, R. Li, M. V Davies, M.J. Alexander, M. Devine, K.S. Loveday, K.W. Underwood, A. V Grinberg, J.D. Quisel, R. Chopra, R.S. Pearsall, J. Seehra, R. Kumar, Transforming growth factor-β superfamily ligand trap ACE-536 corrects anemia by promoting late-stage erythropoiesis, Nat. Med. 20 (2014) 408–414. doi:10.1038/nm.3512.

[242] R.N. Suragani, S.M. Cadena, D. Mitchell, D. Sako, M. Davies, K. Tomkinson, M.

Devine, J. Ucran, A. Grinberg, K. Underwood, R.S. Pearsall, J. Seehra, R. Kumar, ACE-536, a Modified Type II Activin Receptor Increases Red Blood Cells In Vivo by Promoting Maturation of Late Stage Erythroblasts, Blood. 116 (2010). http://www.bloodjournal.org/content/116/21/4236?sso-checked=true (accessed July 16, 2019).

[243] W. Jelkmann, Activin receptor ligand traps in chronic kidney disease, Curr. Opin. Nephrol. Hypertens. 27 (2018) 351–357. doi:10.1097/MNH.0000000000000433.

[244] T. Sugatani, Systemic Activation of Activin A Signaling Causes Chronic Kidney Disease-Mineral Bone Disorder, Int. J. Mol. Sci. 19 (2018) 2490. doi:10.3390/ijms19092490.

[245] O.A. Agapova, Y. Fang, T. Sugatani, M.E. Seifert, K.A. Hruska, D.A. Galloway, L.A. Laimins, B. Division, F. Hutchinson, Ligand trap for the activin type IIA receptor protects against vascular disease and renal fibrosis in mice with chronic kidney disease, Kidney Int. 89 (2016) 1231–1243. doi:10.1016/j.kint.2016.02.002.

[246] P. Fenaux, J.J. Kiladjian, U. Platzbecker, Luspatercept for the treatment of anemia in myelodysplastic syndromes and primary myelofibrosis, Blood. 133 (2019) 790–794. doi:10.1182/blood-2018-11-876888.

[247] O. Hashimoto, N. Kawasaki, K. Tsuchida, S. Shimasaki, T. Hayakawa, H. Sugino, Difference between follistatin isoforms in the inhibition of activin signalling: activin neutralizing activity of follistatin isoforms is dependent on their affinity for activin., Cell. Signal. 12 (2000) 565–71. http://www.ncbi.nlm.nih.gov/pubmed/11027950 (accessed July 25, 2019).

[248] L.R. Rodino-Klapac, A.M. Haidet, J. Kota, C. Handy, B.K. Kaspar, J.R. Mendell, Inhibition of myostatin with emphasis on follistatin as a therapy for muscle disease., Muscle Nerve. 39 (2009) 283–96. doi:10.1002/mus.21244.

[249] J.R. Mendell, Z. Sahenk, V. Malik, A.M. Gomez, K.M. Flanigan, L.P. Lowes, L.N. Alfano, K. Berry, E. Meadows, S. Lewis, L. Braun, K. Shontz, M. Rouhana, K.R. Clark, X.Q. Rosales, S. Al-Zaidy, A. Govoni, L.R. Rodino-Klapac, M.J. Hogan, B.K. Kaspar, A phase 1/2a follistatin gene therapy trial for becker muscular dystrophy., Mol. Ther. 23 (2015) 192–201. doi:10.1038/mt.2014.200.

[250] S. Sifuentes-Franco, D.E. Padilla-Tejeda, S. Carrillo-Ibarra, A.G. Miranda-Díaz, Oxidative Stress, Apoptosis, and Mitochondrial Function in Diabetic Nephropathy, Int. J. Endocrinol. 2018 (2018) 1–13. doi:10.1155/2018/1875870.

[251] B.H. Ali, S. Al-Salam, Y. Al Suleimani, J. Al Kalbani, S. Al Bahlani, M. Ashique, P. Manoj, B. Al Dhahli, N. Al Abri, H.T. Naser, J. Yasin, A. Nemmar, M. Al Za'abi, C. Hartmann, N. Schupp, Curcumin Ameliorates Kidney Function and Oxidative Stress in Experimental Chronic Kidney Disease, Basic Clin. Pharmacol. Toxicol. 122 (2018) 65–73. doi:10.1111/bcpt.12817.

[252] A. Yndestad, K.-O. Larsen, E. Øie, T. Ueland, C. Smith, B. Halvorsen, I. Sjaastad, O.H. Skjønsberg, T.M. Pedersen, O.-G. Anfinsen, J.K. Damås, G. Christensen, P. Aukrust, A.K. Andreassen, Elevated levels of activin A in clinical and experimental pulmonary hypertension, J. Appl. Physiol. 106 (2009) 1356–1364. doi:10.1152/japplphysiol.90719.2008.

[253] Y.-L. Tsai, C.-C. Chang, L.-K. Liu, P.-H. Huang, L.-K. Chen, S.-J. Lin, The Association Between Serum Activin A Levels and Hypertension in the Elderly: A Cross-Sectional Analysis From I-Lan Longitudinal Aging Study, Am. J. Hypertens. 31 (2018) 369–374. doi:10.1093/ajh/hpx185.

[254] F. Petraglia, L. Aguzzoli, A. Gallinelli, P. Florio, M. Zonca, C. Benedetto, K. Woodruff, Hypertension in pregnancy: changes in activin A maternal serum concentration., Placenta. 16 (1995) 447–54. doi:10.1016/0143-4004(95)90102-7.

[255] D.B. Frank, A. Abtahi, D.J. Yamaguchi, S. Manning, Y. Shyr, A. Pozzi, H.S. Baldwin, J.E. Johnson, M.P. De Caestecker, Bone morphogenetic protein 4 promotes pulmonary vascular remodeling in hypoxic pulmonary hypertension, Circ. Res. 97 (2005) 496–504. doi:10.1161/01.RES.0000181152.65534.07.

[256] P. Vavrinec, R.P.E. Van Dokkum, M. Goris, H. Buikema, R.H. Henning, Losartan protects mesenteric arteries from ROS-associated decrease in myogenic constriction following 5/6 nephrectomy, JRAAS - J. Renin-Angiotensin-Aldosterone Syst. 12 (2011) 184–194. doi:10.1177/1470320310391328.

[257] S. Benchetrit, A. Mandelbaum, J. Bernheim, E. Podjarny, J. Green, Altered vascular reactivity following partial nephrectomy in the rat : a possible mechanism of the blood-pressure-lowering e ff ect of heparin, Nephrol. Dial. Transplant. (1999) 64–69.

[258] E.L. Schiffrin, Reactivity of small blood vessels in hypertension: relation with structural changes. State of the art lecture., Hypertension. 19 (1992) II1-9. doi:10.1161/01.HYP.19.2_Suppl.II1-a.

[259] K.L. Christensen, M.J. Mulvany, Mesenteric arcade arteries contribute substantially to vascular resistance in conscious rats., J. Vasc. Res. 30 (1993) 73–9. doi:10.1159/000158978.

[260] Y. Naito, H. Yoshida, C. Konishi, N. Ohara, Differences in responses to norepinephrine and adenosine triphosphate in isolated, perfused mesenteric vascular beds between normotensive and spontaneously hypertensive rats., J. Cardiovasc. Pharmacol. 32 (1998) 807–18. http://www.ncbi.nlm.nih.gov/pubmed/9821856 (accessed July 29, 2018).

[261] E. Vila, M. Salaices, Cytokines and vascular reactivity in resistance arteries, Am. J. Physiol. Circ. Physiol. 288 (2005) H1016–H1021. doi:10.1152/ajpheart.00779.2004.

[262] M.A. Perrella, M.K. Jain, M.E. Lee, Role of TGF-beta in vascular development and vascular reactivity., Miner. Electrolyte Metab. 24 (1998) 136–43. http://www.ncbi.nlm.nih.gov/pubmed/9525696 (accessed August 2, 2018).

Copyright Licenses

Fig 1-11

OXFORD UNIVERSITY PRESS LICENSE TERMS AND CONDITIONS

Jul 06, 2019

This Agreement between Mr. Neel Mehta ("You") and Oxford University Press ("Oxford University Press") consists of your license details and the terms and conditions provided by Oxford University Press and Copyright Clearance Center.

License Number	4623370754282
License date	Jul 06, 2019
Licensed content publisher	Oxford University Press
Licensed content publication	Endocrinology
Licensed content title	The Dependence of Transforming Growth Factor-β-Induced Collagen Production on Autocrine Factor Activin A in Hepatic Stellate Cells
Licensed content author	Wada, Wataru; Kuwano, Hiroyuki
Licensed content date	Jun 1, 2004
Type of Use	Thesis/Dissertation
Institution name	
Title of your work	THE THERAPUTIC ROLE OF FOLLISTATIN IN CHRONIC KIDNEY DISEASE
Publisher of your work	McMaster University
Expected publication date	Sep 2019
Permissions cost	0.00 CAD
Value added tax	0.00 CAD
Total	0.00 CAD
Title	THE THERAPUTIC ROLE OF FOLLISTATIN IN CHRONIC KIDNEY DISEASE
Institution name	McMaster University
Expected presentation date	Sep 2019
Portions	Figure 6
Requestor Location	Mr. Neel Mehta 82 Dewside Dr Brampton, ON L6R0X5 Canada Attn: Mr. Neel Mehta
Publisher Tax ID	GB125506730
Total	0.00 CAD
Terms and Conditions	